

# Energy Optimization of Smart Water Systems using UAV Enabled Zero-Power Wireless Communication Networks



**Varsha Radhakrishnan**

Supervisors: Prof Wenyan Wu and Dr Waheb Abdullah

School of Engineering and The Built Environment

Faculty of Computing, Engineering and the Built Environment

Birmingham City University

This thesis is submitted for the degree of

*Doctor of Philosophy*

June 2023




Dedicated to my daughter, husband, parents and friends for their constant support and love.



## Declaration

I, (Varsha Radhakrishnan), hereby declare that all the information submitted by me in the thesis is correct, true and valid. I will present the supporting documents as and when required.

Signed:   
\_\_\_\_\_

Date: 13.06.2023  
\_\_\_\_\_

**Varsha Radhakrishnan**

June 2023

## **ACKNOWLEDGEMENTS**

Firstly, I would like to thank God almighty for showering his blessings and giving me the strength to complete this work.

I would like to express my sincere gratitude to my project supervisor, as Director of Studies Prof. Wenyan Wu for her valuable time, suggestions, help and strong encouragement. I also would like to thank her for funding my PhD research project; without her support, I would never have been able to pursue this goal. Her valuable suggestions at all times fuelled my confidence to come up with new findings. I would also like to thank my second supervisor Waheb Abdullah for his immense support at the final stages of the research, and that of our research group all the supporting staffs for their constant support and willingness to help.

I would really like to thank my daughter, husband and parents who encouraged me to study abroad. Their constant motivation and support helped me during difficult times. Next, I would sincerely like to thank all the research students in the School of Engineering in Birmingham City University for their camaraderie and help through meetings and discussions. I sincerely thank my friend, Sujith Surendran who was a constant support by way of suggestions and constructive criticism.

## ABSTRACT

Real-time energy consumption is a crucial consideration when assessing the effectiveness and efficiency of communication using energy hungry devices. Utilizing new technologies such as UAV-enabled wireless powered communication networks (WPCN) and 3D beamforming, and then a combination of static and dynamic optimization methodologies are combined to improve energy usage in water distribution systems (WDS).

A proposed static optimization technique termed the Dome packing method and dynamic optimization methods such as extremum seeking are employed to generate optimum placement and trajectories of the UAV with respect to the ground nodes (GN) in a WDS.

In this thesis, a wireless communication network powered by a UAV serves as a hybrid access point to manage many GNs in WDS. The GNs are water quality sensors that collect radio frequency (RF) energy from the RF signals delivered by the UAV and utilise this energy to relay information via an uplink. Optimum strategies are demonstrated to efficiently handle this process as part of a zero-power system: removing the need for manual battery charging of devices, while at the same time optimizing energy and data transfer over WPCN.

Since static optimization does not account for the UAV's dynamics, dynamic optimization techniques are also necessary. By developing an efficient trajectory, the suggested technique also reduces the overall flying duration and, therefore, the UAV's energy consumption. This combination of techniques also drastically reduces the complexity and calculation overhead of purely high order static optimizations.

To test and validate the efficacy of the extremum seeking implementation, comparison with the optimal sliding mode technique is also undertaken. These approaches are applied to ten distinct case studies by randomly relocating the GNs to various positions. The findings from a random sample of four of these is presented, which reveal that the proposed strategy reduces the UAV's energy usage significantly by about 16 percent compared to existing methods.

The (hybrid) static and dynamic zero-power optimization strategies demonstrated here are readily extendable to the control of water quality and pollution in natural freshwater resources and this will be discussed at the end of this thesis.

## TABLE OF CONTENTS

DECLARATIONS.....	iii
ACKNOWLEDGEMENTS.....	iv
ABSTRACT.....	v
LIST OF TABLES.....	x
LIST OF FIGURES .....	xi
LIST OF ABBREVIATIONS .....	xiv
CHAPTER 1 INTRODUCTION .....	1
1.1 INTELLIGENT MONITORING IN WDS.....	1
1.2 RADIO FREQUENCY ENERGY TRANSMISSION .....	5
1.3 RESEARCH MOTIVATIONS AND PROBLEM STATEMENT	7
.....	
1.4 AIM AND OBJECTIVES.....	7
1.4.1 AIM.....	7
1.4.2 OBJECTIVES .....	8
1.5 RESEARCH SCOPE .....	9
1.6 RESEARCH CONTRIBUTIONS.....	11
1.7 THESIS ORGANIZATION.....	12
CHAPTER 2 LITERATURE REVIEW .....	13
2.1 INTRODUCTION .....	13
2.2 SMART WATER SYSTEMS.....	13
2.2.1 SENSING AND CONTROL .....	15
2.2.2 DATA COLLECTION AND COMMUNICATION .....	16



2.2.3 WIRELESS ENERGY TRANSFER FOR SMART WATER SYSTEMS.....	19
2.2.3.1 TECHNIQUES USED FOR WIRELESS ENERGY TRANSFER .....	20
2.2.3.1 ISSUES IN WET.....	22
2.3 ENERGY MANAGEMENT IN UAV ENABLED WPCN .....	22
2.3.1 WIRELESS POWERED COMMUNICATION NETWORK.....	23
2.3.2 UAV ENABLED WIRELESS ENERGY TRANSFER .....	23
2.3.2.1 APPROACHES USED IN UAV ENABLED ENERGY TRANSFER .....	25
2.3.2.2 OPTIMIZATION ALGORITHMS FOR ENERGY MANAGEMENT IN WIRELESS COMMUNICATION .....	26
2.4 NAVIGATION OPTIMIZATION OF THE UAV USING WPCN .....	27
2.4.1 PATH PLANNING CHALLENGES.....	29
2.4.2 OPTIMIZATION ALGORITHMS AND TECHNIQUES USED FOR TRAJECTORY DESIGN .....	29
2.4.2.1 MATHEMATICAL MODEL-BASED ALGORITHMS.....	30
2.4.2.2 BIOINSPIRED ALGORITHMS .....	30
2.4.2.3 MACHINE LEARNING ALGORITHMS.....	31
2.4.2.4 NODE BASED ALGORITHMS .....	32
2.4.3 PATH PLANNING CONSTRAINTS .....	34
2.5 RESEARCH GAPS.....	35
2.6 SUMMARY .....	36
CHAPTER 3 RESEARCH METHODOLOGY .....	37
3.1 INTRODUCTION .....	37
3.2 SYSTEM MODEL CONCEPTUAL DESIGN.....	38

3.2.1 DOWNLINK COMMUNICATION DESIGN .....	41
3.2.2 UPLINK COMMUNICATION DESIGN.....	45
3.3 STATIC ENERGY FUNCTION FORMULATION.....	48
3.3.1 PLACEMENT OF THE GROUND NODES.....	48
3.3.2 3D CLUSTERING .....	48
3.3.2.1 3D K-MEANS.....	49
3.3.3 ENERGY FUNCTION FORMULATION INCLUDING UAV DYNAMICS .....	50
3.4 DYNAMIC OPTIMIZATION MODELS FOR OPTIMAL TRAJECTORY DESIGN .....	52
3.4.1 EXTREMUM SEEKING OPTIMAL TRAJECTORY .....	52
3.4.2 SLIDING MODE OPTIMAL TRAJECTORY .....	54
3.5 PARAMETERS AND SYSTEM SPECIFICATIONS.....	57
3.6 SUMMARY .....	58
CHAPTER 4 DOME PACKING METHOD FOR ENERGY OPTIMIZATION OF THE GROUND NODES AND UAV IN THE WPCN	60
4.1 INTRODUCTION .....	60
4.2 DOME PACKING METHOD FOR OPTIMAL ENERGY TRANSFER .....	60
4.2.1 IMPLEMENTATION OF 3D K MEANS .....	61
4.2.2 IMPLEMENTING 3D ENERGY BEAMFORMING .....	63
4.3 ANALYSIS AND DISCUSSION OF THE SIMULATION RESULTS .....	64
4.3.1 EVALUATING THE DOME PACKING METHOD .....	69
4.4 SUMMARY .....	72
CHAPTER 5 OPTIMAL TRAJECTORY DESIGN FOR THE UAV IN THE WPCN.....	73

5.1 INTRODUCTION .....	73
5.2 STATIC OPTIMIZATION FOR THE TRAJECTORY DESIGN .....	73
5.3 DYNAMIC OPTIMIZATION FOR THE OPTIMAL HEIGHT OF THE UAV .....	79
5.3.1 DYNAMIC MODEL OF THE UAV .....	79
5.3.1 EXTREMUM SEEKING OPTIMAL TRAJECTORY .....	81
5.3.2 SLIDING MODE OPTIMAL TRAJECTORY .....	86
5.4 SUMMARY .....	89
CHAPTER 6 ANALYSIS AND DISCUSSION OF SIMULATION RESULTS USING CASE STUDY .....	90
6.1 INTRODUCTION .....	90
6.2 CASE STUDY DESIGN .....	90
6.3 ANALYSIS AND DISCUSSION .....	93
6.4 SUMMARY .....	100
CHAPTER 7 CONCLUSION AND FUTURE WORK .....	101
7.1 THEORETICAL JUSTIFICATION AND ACHIEVEMENTS ...	102
7.1.1 SIGNIFICANCE OF THE STUDY .....	104
7.2 FUTURE WORKS .....	104
REFERENCES .....	107
APPENDIX A PUBLICATIONS .....	117
APPENDIX B THE IMPLEMENTATION SOURCE CODE .....	132
APPENDIX C .....	147

## LIST OF TABLES

Table 2.1:	Commercially available water quality sensors and measuring parameters.....	15
Table 2.2:	Comparison of commonly used protocols based on cost, energy use, and data rate.....	17
Table 2.3:	Analysis of protocols based on their benefits and drawbacks.....	18
Table 2.4:	Comparison of current methods and its shortcomings.....	27
Table 2.5:	Comparison of methods for path planning using UAV.....	33
Table 3.1:	Outputs of 3D beam analysis.....	44
Table 3.2:	Assumed simulation values for LoRa data transmission.....	47
Table 3.3:	Referenced and author defined parameters.....	47
Table 3.4:	Variables defined in Energy function formulation.....	51
Table 3.5:	Parameter set up for the simulation of UAV enabled WPCN.....	58
Table 5.1:	Height of the UAV at each cluster centroid.....	78
Table 5.2:	Parameter set up for dynamic optimization.....	81
Table 6.1:	Height of the UAV at each cluster centroid using Dome packing ...	97
Table 6.2:	Optimized heights (m) of the UAV using extremum seeking.....	98
Table 6.3:	Real time convergence (s) of the UAV to reach optimum using extremum seeking.....	98
Table 6.4:	Optimized heights (m) of the UAV using sliding mode.....	99

## LIST OF FIGURES

Figure 1.1:	Applications of IoT .....	2
Figure 1.2:	Wireless powered communication architecture .....	6
Figure 1.3:	Research Design.....	11
Figure 2.1:	A layered view of the Smart Water Architecture. Source: Dr Qi Wang, (2018) .....	14
Figure 2.2:	Categorizing wireless power transfer techniques.....	20
Figure 2.3:	n-element phased array transmitter. Source: Natarajan, (2005) ..	21
Figure 2.4:	UAV enabled WPCN .....	24
Figure 3.1:	A system of a UAV-enabled WPCN incorporating 3D beaming	38
Figure 3.2:	Application scenario of monitoring water quality with UAV-enabled WPCN.....	39
Figure 3.3:	Proposed Conceptual Diagram for Energy optimized Navigation Model .....	40
Figure 3.4:	A Constructed 3D beam pattern.....	43
Figure 3.5:	LoRa packet format.....	46
Figure 3.6:	Placement of GN's on uneven 3D surface .....	48
Figure 3.7:	Elbow method. Source: Chunhui and Haitao, (2019) .....	49
Figure 3.8a:	Cost function E.....	53
Figure 3.8b:	Block diagram of Extremum seeking control .....	54
Figure 3.8c:	Optimal equilibrium.....	54
Figure 3.9:	Block diagram of Extremum seeking sliding control .....	56

Figure 3.10a:	Modified Block diagram of optimal sliding mode control .....	59
Figure 3.10b:	Extremum Sliding Mode Control & Response .....	59
Figure 4.1:	Simulation results of calculating the centroids using 3D dome packing method .....	65
Figure 4.2:	Power consumption vs height of the UAV .....	66
Figure 4.3:	UAV power consumption vs clusters.....	66
Figure 4.4:	Power harvested depending on height $h_{uav}$ using N=24 antenna modules .....	67
Figure 4.5:	Energy harvested by the GT nodes based on clusters and its received power .....	68
Figure 4.6:	KxP matrix .....	69
Figure 4.7:	Performance of Dome packing method .....	70
Figure 4.8:	Computation time using Dome packing method.....	71
Figure 4.9:	Comparison of power consumption with and without Dome packing .....	72
Figure 5.1:	The trajectory of the UAV on a 3D plane.....	75
Figure 5.2:	The optimized routing path of the UAV with power consumption .....	75
Figure 5.3:	Power consumption of the UAV based on flight time and height	77
Figure 5.4:	Throughput of the GN's based on clusters.....	78
Figure 5.5:	Schematic of the UAV .....	79
Figure 5.6:	Simulink model for optimum seeking of height .....	82
Figure 5.7:	Optimized height using Extremum seeking for initial condition $h_0$ at 46.4073 m.....	82
Figure 5.8:	Power used by UAV when reaching the optimal height.....	83
Figure 5.9:	Optimized height using Extremum seeking after modifying perturbation .....	83

Figure 5.10:	Modified perturbation power used by UAV when reaching the optimal height .....	84
Figure 5.11:	Simulink model for optimum seeking of height including static power.....	84
Figure 5.12:	Optimized height using Extremum seeking with static power ....	85
Figure 5.13:	Modified perturbation power used by UAV including static power.....	85
Figure 5.14:	New optimized trajectory using extremum seeking model.....	85
Figure 5.15:	Simulink model for optimum height using sliding mode .....	86
Figure 5.16:	Optimized height value using sliding mode.....	87
Figure 5.17:	Simulink model for sliding mode optimization including static power.....	87
Figure 5.18:	Optimized height using sliding mode with static power.....	87
Figure 5.19:	Zero power for reaching the optimal height with static power ....	88
Figure 5.20:	New optimized trajectory using sliding mode optimization model.....	88
Figure 6.1:	Selected GN locations for application of the proposed approaches.....	91
Figure 6.2:	UAV trajectories calculated for selected case studies .....	92
Figure 6.3:	The throughput of the system for the proposed Dome packing method.....	94
Figure 6.4:	Energy consumed by the UAV with existing and proposed methods .....	95
Figure 6.5:	Comparison of wireless power transfer from UAV to GN's .....	95
Figure 6.6:	Comparison of UAV power consumption based on cluster.....	96
Figure 6.7:	Comparison of UAV power consumption based on the flight time.....	96

## NOMENCLATURE

### Abbreviations / Acronyms

AI	Artificial Intelligence
AMI	Advanced Metering Infrastructure
ANN	Artificial Neural Network
BLE	Bluetooth Low Energy
BOD	Biochemical Oxygen Demand
BTX	Benzene Toluene and Xylene
COD	Chemical Oxygen Demand
C-NOMA	Clustered Nonorthogonal Multiple Access
CR	Coding Rate
DO	Dissolved Oxygen
DMA	District Metered Area
DQL	Deep Q Learning
DRL	Deep Reinforcement Learning
DT	Delaunay Triangulation
EH	Energy Harvesting
EMF	Electromagnetic Field



ESOT	Extremums Seeking Optimal Trajectory
FL	Fuzzy Logic
GN	Ground Nodes
GSM	Global System for Mobile Communication
GPS	Global Positioning Systems
gPROMS	General-purpose Modelling System
GT	Ground Terminal
HAP	Hybrid Access Point
HPBW	Half Power Beamwidth
IoT	Internet of Things
ILP	Integer Linear Programming
LoRaWAN	Low Power Wide Area Network
LoS	Line of Sight
LQR	Linear Quadratic Regulator
LZT	lead Zirconate Titanate
MDP	Markov Decision Process
MEMS	Micro-Electromechanical Systems
MILP	Mixed Integer Linear Programming
NB-IoT	Narrow Band Internet of Things
NLoS	Non-Line of Sight

O3	Oxygen
ORP	Oxidation-Reduction Potential
PSO	Particle Swarm Optimization
QL	Q Learning
QTC	Quality Threshold Clustering
RF	Radio Frequency
RFID	Radio Frequency Identifier
RL	Reinforcement Learning
SAGIN	Space–Air-Ground Integrated Network
SARSA	State-Action-Reward-State-Action
SCA	Sequential Convex Approximation
SCADA	Supervisory Controller and Data Acquisition
SDSS	Smart Decision Support System
SF	Spreading Factor
SINR	Signal-to-Interference Noise Ratio
SMOT	Sliding Mode Optimal Trajectory
SWAN	Smart Water Network Forum
SWMS	Sewage Wastewater Monitoring System
SWIPT	Simultaneous Wireless Information and Power Transfer
TSP	Travelling Salesman Problem

UAV	Unmanned Aerial Vehicle
UHF	Ultra High Frequency
URA	Uniform Rectangular Array
USV	Unmanned Surface Vehicle
UV	Ultraviolet
VHF	Very High Frequency
WDS	Water Distribution Systems
WDSS	Wireless Decision Support System
WHO	World Health Organization
WIT	Wireless Information Transfer
WSN	Wireless Sensor Network
WET	Wireless Energy Transfer
WDT	Wireless Data Transfer
WDSS	Wireless Decision Support System
WPCN	Wireless Powered Communication Network
XPS	X-ray Photoelectron Spectroscopy

# CHAPTER 1

## INTRODUCTION

Climate change and its impact on sustainability has been, and is likely to remain most keenly felt in the distribution, refinement and availability of clean water resources, which are key to human health, food production as well as environmental life cycles. Sophisticated management and control of this resource is therefore also of great geopolitical significance. A pre-requisite of its management is effective monitoring of the flow and quality of water, viz: levels of acidity (pH), Dissolved Oxygen (DO), Biological/Chemical Oxygen Demand (B/COD), etc.

This chapter provides a brief overview of the technological background of water monitoring and distribution systems along with the key motivations for undertaking research into their energy management. The problem statement, aim, objectives, outline methodology, research contributions and thesis organisation are formalised at the end of this chapter.

### **1.1 Intelligent Monitoring in Water Distribution Systems (WDS)**

Intelligent monitoring is described as a technique used to monitor, regulate, manage, and optimise networks using various computational techniques that will provide users with pertinent resources and data (Xu et al., 2014). Intelligent monitoring, which connects people and things via wireless sensor technology, includes the Internet of Things (IoT) as a basic component by utilising the underlying technologies such as embedded systems, internet protocols, communication technologies, software platforms, etc. (Al-Fuqaha et al., 2015). This allows things or devices to ‘see’, ‘think’, and communicate autonomously, as well as provide outcomes using various decision-making algorithms based on historical data. It is a rapidly expanding field of application for the military, energy management, healthcare, and many other fields, and some of these are represented in Figure 1.1. In 1999, Kevin Ashton coined the term IoT. Later, it was used to connect a collection of devices (Zhou et al., 2011). By this means, information may be sent across various electronic devices equipped with cutting-edge technology.

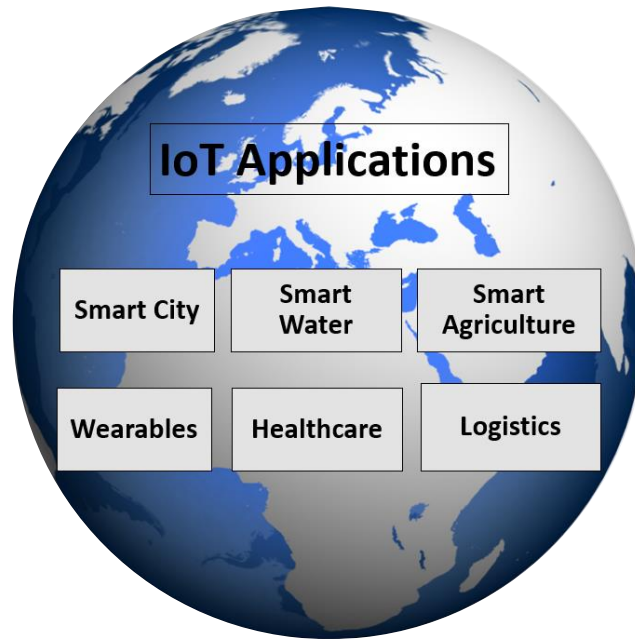


Figure 1.1 Applications of IoT

One of the most important things that needs to be undertaken for environmental monitoring is dealing with the growing problem of water-borne infections, which are a potentially catastrophic health risk. Consequently, guaranteeing the water's quality is essential to the maintenance of a stable living environment for everyone. The increase in biological and non-biological components, as well as a change in the water's colour and odour seriously affects water quality (Lehtola et al., 2004). Bacteria and viruses would be considered biological pollutants, whereas changes in the concentration of chlorine, salt, ammonia, etc. would be considered as non-biological contaminants. The entire water ecology is seriously threatened by all these toxins. Consequently, it is necessary to monitor and safeguard the water using a system that is both affordable and effective (Zulkifli and Noor, 2017). The suitability of water for a given purpose, taking into account both its biotic (e.g., bacteria, fungus, etc) and abiotic (B.O.D., D.O., pH) features, is how its quality may be evaluated. Detecting components and evaluating them in relation to predetermined benchmark criteria and ranges is an essential part of water quality monitoring. In most cases, determining the quality of water requires conforming to certain requirements based on the water's intended use. For an analysis that is both more accurate and more dependable, additional samples need to be gathered.

When compared to real-time monitoring for early warning and prompt action against water pollution, manual techniques are seen as inefficient. The monitoring of daily activities in the WDS is made easier by communication and cognitive technologies included in IoT. Huan et al. (2020) developed automated solutions with the use of Narrow Band Internet of Things (NB-IoT) technology in order to monitor the water quality at aquaculture farms. Using this technology, automatic collection, storage, and processing of water quality information such as pH, dissolved oxygen (DO), and other similar information may be sent to the cloud for decision making, which helps in making emergency decisions and promotes breeding in ponds.

Nie et al. (2020) suggest using IoT and big data-based supervisory controller and data acquisition (SCADA) systems for monitoring water quality as well as notifying water suppliers regarding any leaks for the purpose of underwater management so that issues can be resolved in a significantly shorter amount of time.

A combination of hardware and software was described by Cao et al. (2020) in order to monitor the water quality in open water sources such as rivers, lakes, and other similar bodies of water. They introduce the intelligent cruise unmanned surface vehicle (USV), which is equipped with a solar panel for power, global positioning system (GPS), and communication antennas, as well as a water quality detecting module that contains data-gathering water quality sensors. The method of ensemble learning is then applied in order to get an understanding of how the patterns of water vary and facilitate rapid measurements.

On the other hand, Kumar and Hong, (2022) implemented an IoT-based surveillance system called the Sewage Wastewater Monitoring System (SWMS) in order to monitor the treatment of wastewater and enhance water quality. In this system, the data is delivered from devices such as sensors to a system that is running intelligent analytic software along the course of a wireless sensor network via a secure networking protocol. The sewage system will then collect and treat any impurities that it finds in order to produce effluent. These effluents can then be applied to or recovered directly from the water source with the least amount of environmental impact. In addition to measuring water flow dynamics throughout the treatment process, the IoT-enabled smart water sensor measures water temperature, quality, and pressure. Furthermore, the method evaluates the plant's efficiency in treating wastewater and ensures that chemical emissions remain within allowable limits.

Water quality monitoring for smart farming is used by Said Mohamed et al. (2021), Viani et al. (2017) and Lambrinos (2019) to increase agricultural production while reducing food demand. Mohamed et al. (2021) use UAV and robots to support farming methods such as irrigation, harvesting, control pesticides in real time by using a smart decision support system (SDSS) that combines IoT, machine learning (ML), deep learning (DL) and artificial intelligence (AI) methods. Viani et al. (2017) recommended using a wireless decision support system (WDSS) as the basis for a decision support system (DSS) in order to optimise agricultural irrigation and reduce the amount of water that is wasted. The management of the farming operation is made easier with the help of this system, which makes use of a wireless sensor and actuation network to collect a variety of different biological parameters. It also uses a fuzzy logic (FL) method to provide a realistic experience for farmers, allowing them to examine the impacts of irrigation and climate on the soil and plants, and to suggest actions that would improve crop yields as well as improving water quality and prevent environmental damage. On the other hand, Lambrinos (2019) proposed a DSS that would improve smart farming by collecting data on crops and weather from a variety of sensors connected to a LoRaWAN network. This would allow for more intelligent decision-making. In terms of integrating data from a wide variety of sources, it employs a technique known as "data fusion". On the basis of the information gathered, recommendations for irrigation guidance are provided in order to guarantee that crops are efficiently watered while also conserving water in situations where this is possible. In addition, farmers should have the ability to protect their crops from unfavourable weather conditions by employing a method that provides alerts.

Security, standardization of the protocols and privacy are some of the main challenges in IoT. Kamalinejad et al. (2015) and Nordrum (2016) predicted that the extensive use of IoT devices will result in a significant rise in energy use around 2022, which will have an impact on the effectiveness of wireless network monitoring. The management of energy in wireless networks must therefore become a bigger research priority. Using energy harvesting methods, which are ways of gathering energy from natural sources like light, vibration, pressure, etc., makes energy management feasible (Sun et al., 2019; Jushi et al., 2016; He et al., 2018). IoT is made possible by the integration of several technologies, including wireless sensor networks (WSN), radio frequency identification (RFID), energy harvesting (EH), and AI.

## 1.2 Radio Frequency Energy Transmission

EH entered the market at a time when the majority of IoT devices were battery-focused and required battery life extension. Energy harvesting equipment becomes more sustainable when disposable batteries are replaced with rechargeable batteries and super capacitors. Many features of energy harvesting techniques are attracting greater research attention currently. The new energy harvesting methods and their desirable properties such as low cost, efficiency, availability and high robustness could benefit water management (Bhatti et al., 2016). An energy harvesting module is a piece of technology that produces energy and controls it for the attached sensors, processors, and communication components (Kosunalp, 2016). The EH gadget gathers energy from the application environment, such as light, vibrations, radio frequency waves, etc., and transforms it into electrical energy for its operations (Alshattnawi, 2017). Over the past several years, wireless energy transfer (WET) has drawn greater interest, particularly for use in charging mobile devices and implanted medical devices in patients within a limited range of a few centimetres. Since the gadget used magnetic resonant coupling, its range proved to be a significant problem. To deliver energy across very long distances, radio frequency (RF) enabled WETs employ electromagnetic waves. In RF energy harvesting, RF waves are originated from a transmitter and use fixed frequency bands such as UHF, VHF etc. through which they propagate and reach the receiver for long distance communications. For integrating into application devices, RF energy receivers are less expensive and more compact (Bi et al., 2015). The problem of attenuation over long distances is why RF is used only for energy constrained devices such as sensors. Recent advancements in antenna arrays and communications protocols enable for more energy-efficient power transfer in far-field communications (Bevacqua et al., 2021).



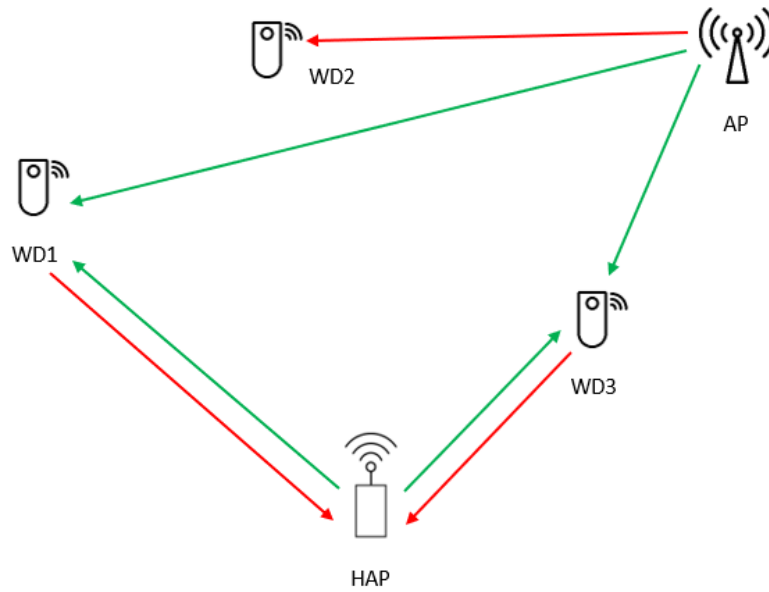


Fig 1.2 Wireless powered communication architecture

The WET technologies use a technique called simultaneous wireless information and power transfer (SWIPT) to send information and power over the same wireless signal. In SWIPT, the information received from the same signal was encoded using energy that the receivers were receiving. The wireless powered communication network (WPCN) architecture in Figure 1.2, which uses the signal energy received to transmit information to the sender, is a new technique being employed, which is similar to SWIPT, attracting attention of researchers.

WPCN, EH utilizing RF and AI could all work together to promote the wider implementation of IoT (Zhou et al., 2011).

The advancement of aforementioned technologies has aided the creation of effective strategies to address several pressing problems in real time. IoT, a related technology that has gained significant attention because of its connectedness and intelligence. IoT helps to link all devices to form a network, including machines and sensors and the WPCN helps to transmit both information uplink (GN's to the HAP) and downlink (HAP to the GN's) communication. By allowing relays to utilise the RF signal of the HAP for transmitting both energy and information transmission during communication by making use of the SWIPT concept in WPCN. Only a small number of water distribution applications have been adapted for this relatively new technology. Most approaches in WDS have focused more on network data management than on energy management.

### **1.3 Research Motivations and Problem Statement**

The most significant issue with wireless devices water distribution systems (WDS) is limited battery life, which necessitates battery replacement or recharging after a predetermined period with a large number of energy constrained IoT devices in need of innovative wireless energy charging techniques to alleviate this issue. The same can be said of manned and unmanned aerial vehicles.

The majority of research work focuses on data management and transmissions during communication within WPCN by taking into account only uplink communications (Wang et al., 2021; Xu et al., 2018). The adaptable and effective wireless communication solutions of UAVs have garnered significant attention from researchers and industries equally. Companies such as Facebook and Google have utilised this technology to provide internet connectivity to remote areas, while Amazon has employed it for the purpose of charging electric vehicles (Fotouhi et al., 2019; Karagianni, Rigas and Bassiliades, 2022). But a very little of the current research takes into consideration the energy management of the combined uplink and downlink communication using charging over air, a UAV as a HAP in a WPCN within a WDS. Additionally, the UAV's on-board energy is limited and must be allocated for communication, moving, hovering, and other activities. These are therefore the major motivations for the research. The main challenge using WPCN within WDS is energy optimization during communication. By optimizing the UAV's trajectory and calculating an optimum height for the UAV, the overall energy efficiency, including for communication could be improved. This should reduce the total flight time and energy needed throughout the flight. Since water quality must be examined, often due to several problems including leaks, floods, and other concerns, results in significant data overhead that can impact the energy consumption during communication. Therefore, this thesis focuses on filling this research gap.

### **1.4 Aim and Objectives**

#### **1.4.1 Aim**

The main aim of the thesis is to develop an energy optimization (zero-power) method for near real time monitoring (due to the delay in the signal processing to and from the base station) in water distribution system. The zero-power is defined instruments that require no batteries or manual charging mechanism. To achieve this goal, the current sensor technologies, various

energy harvesting methods and other relevant technologies are taken into account and applied. Since the smart water monitoring system includes different levels in the architecture, the sensing and communication requirements are also part of this discussion. More specifically, investigating the methods that could be adopted to optimize energy usage during both charging and communication in a real time water monitoring system.

### **1.4.2 Objectives**

To achieve the aim above, the thesis objectives can be identified as:

1. Review energy harvesting methods and select a method suitable for water distribution system (WDS) to produce sufficient energy.
2. Propose and design a zero-power system using both static and dynamic optimization methods to manage energy usage and improve performance of the wireless powered communication network (WPCN).
3. Evaluate the energy management scheme in comparison with existing schemes and demonstrate its efficacy and feasibility.

To achieve the aim and objectives above, inclusion of an unmanned aerial vehicle (UAV) is to be investigated that serves as a flying base station for the uplink and downlink communication between the base station and the ground nodes (GNs) in order to meet the goal of efficient energy transfer and optimization.

There is currently a drive among the research community to optimize energy usage of both unmanned and manned aerial vehicles to reduce fuel consumption and emissions. However, achievement of this has become illusive, especially using a single technology or technique. This thesis will primarily address this research gap by using a variety of optimization techniques, both static and dynamic, implementable in real time with zero-power performance.

Random clustering of GNs is unlikely to be an optimum strategy for the purposes of optimizing position and energy usage of a UAV. Alternatively, using a 3D dome packing approach to construct an ideal charging path along which the UAV navigates while energising the GN's and collecting data, the overall energy consumption of the UAV may be lowered. It is further contended that by using static optimization to establish a static initial condition, the dynamics of the UAV could be included in the reckoning of overall energy usage during a flight. Then, the UAV's energy use, total flight time and recycling time can all be optimized under combined

static and dynamic optimization strategies (The time difference between each of the UAV's hovering positions is known as the recycle time).

## **1.5 Research Scope**

A detailed literature review, as a first step, aims to identify the most appropriate energy harvesting, data collection and sensor technologies for WDS. The criteria of steady state energy generated by each published approach is used to evaluate effectiveness.

The second step aims to evaluate the various remote technologies applied in WPCN for energy management in WDS.

Once the appropriate sensor and network technologies have been identified, a static simulation of the system can be undertaken by arranging the GNs at different positions in 3D space to determine the amount of energy utilised by a UAV enabling a WPCN. To achieve the objective of energy optimization, the UAV would act as a flying base station for the uplink and downlink communication between the base station and the GNs. In this process, the total energy consumption of the UAV is to be calculated and then optimized by using a proposed 3D dome packing method to create an optimal charging path through which the UAV navigates by energizing the GNs while gathering data. This is to be achieved by calculating the centroid of a cluster of GNs, rather than position the UAV randomly. This position is to be adjusted for the practicality of beaming range. As a result, the energy consumption of the UAV, the total flight time and recycling time can then be minimized. Several configurations of different positions of the GNs are proposed to test the feasibility of the method.

The optimized heights obtained by the 3D dome packing method can further become initial conditions for a dynamic state model developed to provide a more realistic calculation of the total energy usage by including UAV dynamics. The total energy consumption of the system could then be optimized based on a cost function, which includes terms from both the static and dynamic parts of the overall trajectory. Energy usage terms for data transmission and charging may also be included. Dynamic optimization schemes are then to be developed, and extensive MATLAB and Simulink model simulations used to evaluate the proposed static and dynamic methods.

For clarity, thesis development is structured as follows:

1. To undertake a comprehensive review of published literature of the existing technologies and methods used in WDS.
2. Determination of a static energy cost (objective) function to include charging and communication between GN's and a UAV.
3. Optimization of the static energy cost function using 3D dome packing.
4. Derivation of a physical (dynamic) model of the UAV suitable for dynamic optimization.
5. Determination of a dynamic cost function to include UAV dynamics.
6. Optimization of the dynamic cost function using extremum seeking methods and optimal sliding modes.
7. Combined static and dynamic optimization of overall cost function.
8. Parametric study of the robustness of the overall strategy over different GN topologies.

The aforementioned structure is depicted in Figure 1.3. This diagram shows how the research process begins with the identification of research gaps, followed by the disclosure of existing sensors in WDS and the technologies, such as UAV-enabled WPCN, that could be integrated. It is then followed by a conceptual design and mathematical formulation of the scenario employing GNs, UAVs, and water quality sensors, and how this is developed in the following chapters of the thesis is detailed here: First, a static optimization technique is developed by incorporating the latest technologies; next, a dynamic optimization method is implemented, which will include the dynamics of the system. The optimization of energy is carried out by constructing an ideal trajectory for the UAV, which is accomplished by calculating an optimal height for the UAV. This optimal height would utilise the best route, and as a result, the energy consumption and total flight duration of the UAV are both to be optimized. In conclusion, to determine whether or not the suggested approach is successful, it will be assessed by a number of case studies.

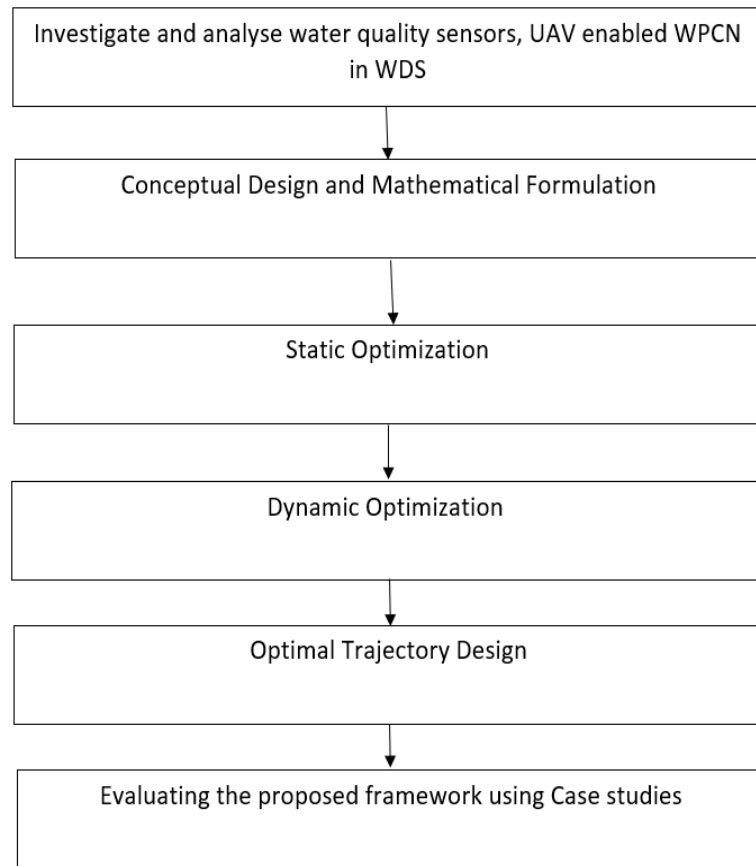


Figure 1.3 Research Design

## 1.6 Research Contributions

Even though there are many advancements in RF based charging methods, there is still much opportunity for the optimization of UAV energy and data transfer, particularly as UAVs are known to have limitations of flight time and power, while flying without replenishment of their own battery state of charge. This work addresses the following in this regard:

1. Identifying sensors, communication technologies and harvesting methods which can be used for the implementation of UAV enabled WPCN in WDS, through which the UAV can optimally complete its mission with zero-power performance.
2. Development of a new static optimization (Dome packing) method applied to the packing of sensors / GN's in the WDS, focusing on optimizing the energy during communication with beamforming.
3. Design of optimal trajectories based on a dynamic model of the UAV using novel dynamic optimization methods.

4. Application of hybrid static and dynamic energy optimization techniques to construct a trajectory that maximises the UAV's energy efficiency and minimizes flight duration over an exhaustive range of different GN topologies.

## **1.7 Thesis Organization**

The subsequent chapters will provide a more in-depth analysis of each approach, as well as an explanation of the findings. The rest of the thesis is organized as follows:

**Chapter 2** provides a background of the smart water system and a detailed discussion of WPCN, UAV enabled data acquisition and how the energy is sub-optimized in the existing literature.

**Chapter 3** develops methodologies for the conceptual design of the system and how the proposed methods will be mathematically formulated utilising static and dynamic optimization techniques to be applied in the WDS.

**Chapter 4** presents the simulation results of the proposed system that optimizes the energy and mission completion time of the UAV for optimal energy transfer / emergency-based charging using Dome packing, a static optimization approach. This comprises of 3D clustering and beamforming.

**Chapter 5** provides an optimal trajectory design for the UAV using both the static methods of Chapter 4 and dynamic optimization methods such as extremum seeking and optimal sliding mode algorithms.

**Chapter 6** analyses and discusses the findings of the simulation results. Additionally, case studies are exhaustively applied across a range of topologies to verify the convergence of the algorithms used and evaluate outcomes in context of past research.

**Chapter 7** summarises the thesis, highlighting the contributions made to the field of study, as well as provide some prospective future research directions for applying the work to regulation of water quality monitoring.

# **CHAPTER 2**

## **LITERATURE REVIEW**

### **2.1 Introduction**

The water sector is facing many issues when it comes to long term management of urban water systems. Climate change, drought, and rising population all necessitate a greater focus on developing sustainable water management systems. The water distribution system (WDS) is an essential field of research that has an impact on the world's economic development. As a result of the aforementioned, people's health and safety are compromised. Water loss due to leaks, water quality management, enhanced service quality, and operational efficiency are some of the factors that are now being considered for WDS. According to a 2020 WHO report, over 2 billion people across the globe lack access to safe drinking water. As a result, advanced communication technologies must be integrated into the WDS to ensure water quality and reduce water loss. The cost of operating a water distribution system and conducting water quality control tests consume a significant amount of energy, which varies depending on the location. As a result, a cost-effective water quality monitoring system is required to monitor and preserve water (Zulkifli and Noor, 2017). As the world's population grows, so does the demand for clean water, necessitating the need for technological improvements in water management.

### **2.2 Smart Water Systems**

Water pipeline monitoring, water quality in open water sources, smart water meter reading, IoT security for smart water systems (SWS), and other smart water applications are among smart water applications. A structure and methodology were designed to secure the integrity of client information, the security of devices, and the integrity of data transported via the network (Pacheco et al., 2017). Pipe leakage detection is an application that has emerged as a result of IoT expansion. Because a significant volume of water was leaking from pipes, various IoT devices, WSNs, and cloud services are employed to detect and warn the user about leaks (Wu et al., 2017). The amount of leakage is largely dependent on the flow pressure, and it is difficult to quantify the precise volume of water loss in a specific location. To address this problem, water distributors devised the District Metered Area (DMA) mechanism, which



applies a divide-and-conquer strategy in which the complicated water distribution system (WDS) is partitioned into independent regulated sub networks. As a result, leaks are quickly identified, water pressure is regulated during emergency circumstances, and accidental contamination is reduced. Another application that was developed utilising IoT devices was water quality monitoring of open water sources. It uses low-cost devices and network virtualization to effectively maintain water quality and safeguard the economy's health (Prasad et al., 2016; Menon et al., 2017).

A five-layer smart water architecture was developed by the Smart Water Network Forum (SWAN) to address the problems with water management (Cahn, 2014) as in Figure 2.1. The physical assets consist of pipes, valves, reservoirs etc that help in collecting data from the SWS using different sensors attached to it. The data will be transferred from one point to another or a central data server using the collection and communication layer. The collected data will be managed and presented meaningfully to utility companies or end users. The last layer is the data fusion and analysis consisting of tools that help in integrating data analytics and intelligent algorithms to manage operations such as water quality monitoring, leak detection and respond in real time. As a result of how significant they are to the thesis's work, the layers 2 and 3, which are the sensing and control, and the collection and communication layers, are taken further in the following sub sections:

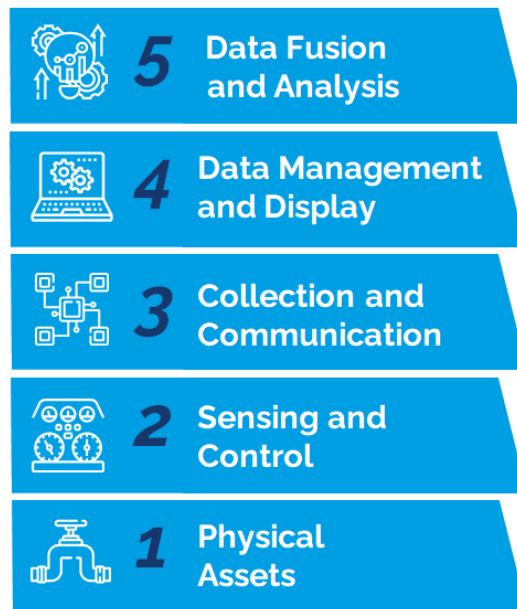


Figure 2.1 A layered view of the Smart Water Architecture Source: Dr Qi Wang, (2018)

### 2.2.1 Sensing and Control

The sensing and control layer's main function is to connect devices of the IoT network with the data servers of the operator. When applied to WDS, this layer consists of sensors, EH devices and remotely controlled devices such as pumps and valves. A smart pipeline is one among the smart components used in SWS designed to condition monitor the pipe which helps in the real time monitoring of the flow, pressure, vibration, corrosion, water quality and leaks, without affecting the operations of the pipeline. The smart meter is another technological device that can measure, analyse, store and transmit the amount of water consumed by an individual/company so that the supplier can keep track of any water loss, damaged meters or illegal water use. The customer can also keep track of the water usage. The monitoring of this data necessitates the installation of advanced metering infrastructure (AMI) by water providers to increase hydraulic and energy efficiency, as well as leakage control and illegitimate water connections. Some of the relevant commercially available devices are tabulated below:

Table 2.1. Commercially available water quality sensors and measuring parameters

Source	Sensor	Water quality parameter
Broeke(2005)	Spectro::lyser	Turbidity, temperature, pressure, colour, dissolved ions, UV254
O'Flyrm et al., 2007	SmartCoast	pH, dissolved oxygen(DO), conductivity, temperature, turbidity, phosphate, water level
Mcdougale et al., 2012	Kapta 3000 AC4	Chlorine, temperature, pressure, conductivity
Libelium(2014)	Smart water(Libelium)	pH, dissolved oxygen(DO), conductivity, temperature, oxidation-reduction potential(ORP), turbidity, dissolved ions
Tsopela et al., 2016	Lab-on-chip	Any specific bio-chemical
S::can(2017)	I::scan	Colour, turbidity, UV254

In SWS, there are different commercially accessible sensors also called nodes of various kinds that are used for real-time water monitoring as represented in Table 2.1 and discussed further in (Radhakrishnan and Wu, 2019). The Smart Water Solution by Libelium, Kaptia 3000 AC4, electrochemical optical sensors and Spectro::lyser are some of the sensing devices used widely for collecting water quality data (Abirami and Karlmarx, 2013). The data includes information such as temperature, pressure, conductivity, water flow, chlorine, pH, turbidity, COD, BTX, O3 and other toxins etc. The cost, effectiveness, and choice of water quality variables influence the sensor's selection (Miao Wu et al., 2010; Philipp Hohenblum, 2014). Batteries are necessary for the operation of each and every one of these nodes but, maintaining and managing their energy consumption is always problematic and expensive.

### **2.2.2 Data Collection and Communication**

Data must be gathered and transmitted to the higher layers via the collection and communication layer. The sensors utilise the data they gather from various remote places and send it to base station to analyse and process data for the SWS. In these levels, there is interpersonal communication that allows information to be transmitted as well as decisions to be made depending on the data analysis, carried out by the top layers. Communication techniques are selected based on the distance over which the data is being carried, the cost, the standards, the level of technical development, and the topology (Azhar et al, 2020).

The cellular technology enables a two-way mobile communication between the controller and applications group, since it will be located further away from the site. When long-distance transmission is necessary, such as 2G, 3G, 4G or 5G, this technology is employed. Other long-distance transmission technologies include GSM and GPRS. It necessitates higher power consumption, making them unsuitable for WDN. Short-range protocols such as Zigbee, 6lowpan, and RFID are examples of protocols that might be used between sensors and controllers. RFID is a data collection system that employs an electronically programmed tag (Farook et al., 2015). It is unreliable to use for measurement since it requires a programmed static tag. The 6lowpan protocol is an IP-based protocol that can connect to the next IP network without using gateways. Its cheap cost and power usage are further advantages. It supports both star and mesh topology. LoRa (Low Power Wide Area Network) is another protocol that has received a lot of attention because of its cheap power consumption, low cost, and high data rate when used in IoT, and it employs a star topology. Zigbee is a popular low-power wireless technology that offers low-cost and secure communication. It also supports topologies such as

star, mesh, and tree (Sarawi et al., 2017). The benefits of 6lowpan, LoRa, and Zigbee make them the best candidates for WDS, out of which LoRa has been selected here, since the data is to be transmitted to longer distances with very low energy consumption and low communication cost based on Table 2.2 and Table 2.3 as has been discussed in (Radhakrishnan and Wu, 2019; Mutiara, Herman and Mohd, 2020).

Table 2.2. Comparison of commonly used protocols based on cost, energy use, and data rate

<b>Protocol</b>	<b>Energy consumption</b>	<b>Cost</b>	<b>Data Rate</b>
Zigbee	Low	Low	40-250 kbps
6lowpan (IPv6)	Low	High	20-250 kbps
BLE	Very Low	Low	100-230 kbps
NB-Iot (4G)	Medium	Very High	200-240 kbps
LoRa	Very Low	Low	0.3-50Kbps

Table 2.3. Analysis of protocols based on their benefits and drawbacks

<b>Protocol</b>	<b>Advantage</b>	<b>Disadvantage</b>
GSM	Cost effective, self-calibrating	More power consumption, attenuation
GPRS	Communication range	More power consumption, Performance issues (Speed)
BLE	Very low power, cost and more security compared to Wi-Fi	Limited amount of data transfer
Low power Wi-Fi	Longer range	Less data range
Zigbee	Low power, cost and provide security	Less range
6lowpan (IPv6)	Low cost & power consumption	Security of data
RFID	All types of data can be transferred	Need of a programmed static tag makes it unreliable to use for measurement and limited range
LoRa	Very low power consumption & high data rate	Security issues and high cost

### 2.2.3 Wireless Energy Transfer for Smart Water Systems

The management of energy in the sensor network and the sensor nodes may be divided into two parts for the purpose of energy distribution. The project in SWS requires a lot of energy since it aims to monitor activities in close to real time, especially for data transfer and communication. For all forms of processing and data analysis, this produced data must be sent to the base station. Furthermore, the current sensors are more battery-reliant, requiring more power to detect and transmit data. Therefore the need for extra power for the sensor nodes to transmit data is one of the key issues with wireless networks. A viable solution to this issue is to transmit power to/between the sensor nodes. According to Bhatti et al. (2016), a thorough investigation of the various energy transfer methods such as mechanical waves, magnetic fields and electromagnetic radiations were employed in wireless networks for various applications. Power transmission utilising a magnetic or thermal field will be acceptable since the current thesis is focused on analysing the water quality in pipelines. A wireless power transmission protocol developed by Nikolettseas et al. (2017) and an energy-efficient scheduling strategy for power transfer by Ejaz et al. (2016) were two recent advancements for this issue. The wireless power transfer protocol consists of two protocols: one checks the energy balance, and the other determines if each sensor node has enough power to send energy. Reduced energy consumption of the transmitters in software defined wireless sensor networks is the goal of the scheduling study of Ejaz et al. (2016). A multipoint scheduling approach was created to enhance network output in a related study by Xiao et al. (2015). The utilization of network resources such as sensors, base stations, software's, data etc., which uses more energy and cost, is another issue in wireless communication networks.

To address the existing energy management problems, a fresh perspective is offered by the energy management of sensor nodes. The study by Dial et al. (2016) serves as an introduction to concentrate on the individual sensor nodes rather than the network. By applying online reinforcement learning, the work offers an adaptive sampling approach where real-time data is gathered using a sampling interval and an adaptive algorithm is utilised to pick out the sampling data of high quality. The study by Dias et al. was able to show that node lifespan increased but was unable to address the issue of enhancing sensor node storage. The author also suggested that cloud computing services that use machine learning techniques would be able to address this problem. Since the actual deployment instructions of the project weren't present as the research was conducted in a simulated setting which makes it difficult to verify this method. To reduce the number of transmissions, Borgne et al. (2017) apply prediction

algorithms in the sensor node and gateway to detect future measurements. The management of energy and memory for storing and processing data in the sensor was a challenge for all the aforementioned techniques.

### 2.2.3.1 Techniques used for Wireless Energy Transfer

According to how distant GNs can be from the power source, the technologies utilised for wireless energy transmission are divided into two categories: near field communication and far field communication as represented in Figure 2.2. Near field communication is used in applications like wireless charging, electric automobiles, tiny robots, etc. to wirelessly transfer power to the receiver using electric and magnetic fields using inductive and capacitive coupling (Lu et al., 2016). Far field radiation, on the other hand, is made up of electromagnetic waves that travel at the speed of light. The nondirective RF power transfer is mainly used in Radio frequency identification (RFID) applications where non-line of sight communication is established. The RFID system employs a tag that is electronically configured to capture data (Farooq et al., 2016; Bevacqua et al., 2021). To employ RFIDs, the distance between the source and the receiver has to be relatively short. To charge sensors and gather data, the UAV with RFID must have up and down motions and as a result, the majority of the energy is lost. Thus it is unreliable for measurement since a programmed static tag is required .

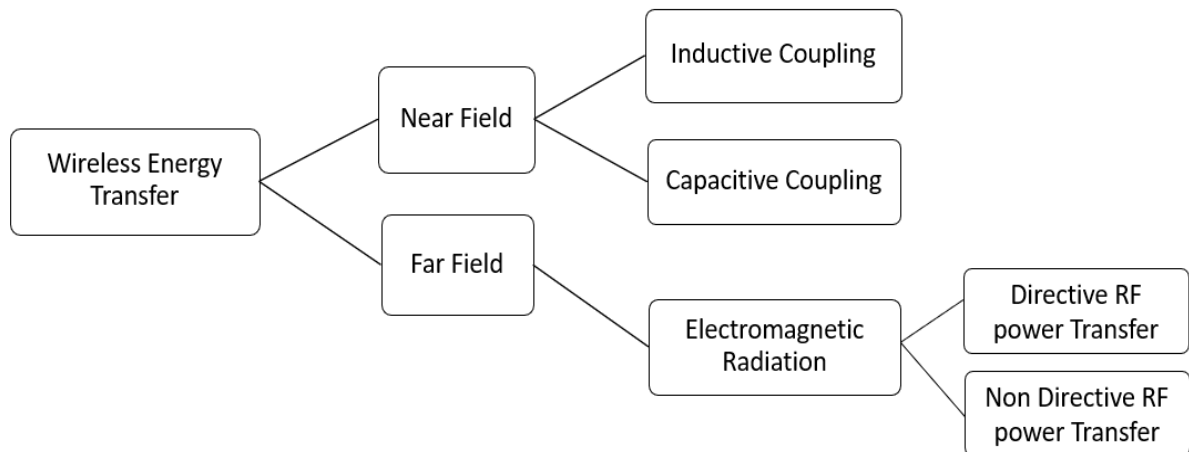


Figure 2.2 Categorizing wireless power transfer techniques

In directional RF power transfer, the radio waves are emitted isotropically for broadcasting applications or in a specified direction for node-to-node transmissions. In wireless communication, beamforming is used to guide a signal or beam to the target recipient using

antenna arrays. In order to vary the direction of the active main lobe of the beam, the depiction of an n-element phased array transmitter will be used and is shown as in Figure 2-3.

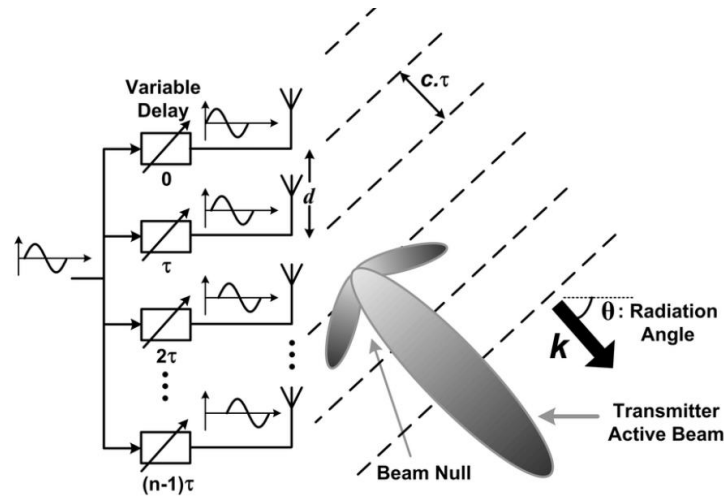


Figure 2.3: n-element phased array transmitter. Source: Natarajan, (2005).

The directional antennas may be combined with the UAV to use the beamforming technique, which will increase communication coverage and effectiveness. Beamforming is a technique that makes use of a number of antennas to concentrate the waveform in a particular direction. This method helps to reduce issues relating to coverage as well as interference. For example, if a laptop that is connected to a beamforming router is relocated from one area to another, the beam will be recalculated and travel along with the laptop. Beamforming in energy-harvesting wireless networks has been the subject of research into its underlying principles, topologies, and a variety of application-specific approaches (Alsaba et al., 2018). In full-duplex wireless powered communication, this technology has been utilised to reduce self-interference and increase user data rates (Wang et al., 2018).

The advancement of water management research has been enhanced by the combination of various technologies as discussed above. And the challenges with the water distribution system's energy management could be addressed by integrating energy harvesting with IoT technology. To improve the smart water system, the sensing and control layer might be integrated with solar cell, piezoelectric, electromagnetic or thermoelectric harvesting techniques. Research on micro-electro-mechanical systems (MEMS) such as piezoelectric nanowires, lead zirconate titanate (PZT) films, multi-parameter sensor chips employing iridium oxide film, and X-ray photoelectron spectroscopy (XPS) analysis is now underway



and might advance water research (Zhou et al., 2017). The integration of these new technologies would also help to improve factors such as maximizing coverage, energy management etc.

### **2.2.3.2 Issues in WET**

#### **Maximizing Coverage**

Maximizing the coverage is one of the major optimization issues in all wireless networks. The distance between the source and the ground nodes in a wireless network determines how far signals may travel to reach them. This distance is referred to as the network's coverage. One of the ways to increase operation, performance, and coverage is the development of UAVs that are capable of operating as flying base stations.

#### **Energy Management**

The power transmission between sensor nodes is an important technical innovation that was implemented using IoT to manage energy consumption. An electromagnetic field will be appropriate for wireless power transmission if it is determined that the water quality in the pipes must be assessed. The solutions to the WET issues are further discussed through the literature review in the following sections.

## **2.3 Energy Management in UAV enabled WPCN**

The components used in SWS are currently powered by batteries, however research in WPCN is opening new opportunities for energy management and harvesting as a result of charging through air as opposed to the traditional battery charging scheme. Its lack of battery replacement difficulties leads to minimal operational costs and an improvement in performance.

The WET has achieved more attention over the recent years especially in charging mobile devices and embedded medical device in patients for collecting data within a specific range within few centimetres. The range of the device was a major issue as it uses magnetic resonant coupling. The RF enabled WET uses electromagnetic waves to transfer energy over much longer distances. The RF energy receivers are cheaper and compatible for integration into the application devices (Bi et al., 2015). Simultaneous wireless information and power transfer (SWIPT) is a method used in WET is to transmit both energy and information using the same signal. In SWIPT the receivers use the received energy to encode the information received

from the same signal. An upcoming method used like SWIPT which attain the researchers focus is the wireless powered communication network (WPCN) architecture where the energy received from the signal is used to transmit information to the sender.

### **2.3.1 Wireless Powered Communication Network**

The WPCN architecture, which uses the energy received from the signal to transfer information to the sender, is a possible approach such as utilised by SWIPT that has attracted the attention of researchers. When compared to the traditional battery charging technology, research in the domain of WPCN is leading to new techniques in energy harvesting and management owing to charging over air. Consequently, it does not require battery replacement, resulting in lower operating costs and improved performance. Another benefit of WPCN is that it provides a consistent and controllable power supply under a variety of needs and physical situations, making it ideal for low-power IoT devices. WPCN is a preferable alternative for wireless energy transmission because of its cheap operational cost, increased range, and tiny form factor (Bi et al., 2016). The design of resource allocation schemes, interference management, and other factors are carefully considered when extending WPCN into IoT. (Ramezani and Jamalipour, 2017; Olatinwo et al., 2018). The communications used in SWS are currently powered by batteries, however research in WPCN is opening new opportunities for energy management and harvesting because of charging through air, as opposed to the traditional battery charging scheme.

In cellular communication using WPCN, fixed base stations transmit energy to the receivers, allowing for the collection and transmission of data. Since the base stations are fixed, there is a "double near-far" issue since users at greater distances get less energy and demand more energy to transmit data. Using the UAV as a mobile base station in the WDS should help alleviate the near-far problem caused by LOS problems with fixed antennas (Bi et al., 2015, Cho et al., 2018)

### **2.3.2 UAV Enabled Wireless Energy Transfer**

UAVs have been under development for decades. They were primarily intended for military use as well as emergency scenarios such as floods. Maintenance, resources, and network costs were high in typical numerous stationary base stations, leading to the deployment of UAVs as flying base stations to gather data. Since the advent of advancements in electronics, such as sensors and microprocessors, UAVs have become quite popular and are deployed commercially. The UAV may operate as a flying base station to boost coverage, performance,

and operation, which is appropriate for the application scenario shown in Figure 2.4. The study of how to save energy by focusing on throughput has received a lot of attention. The deployment of UAVs in 2D space (level terrain), the best altitude for improved coverage, and the minimizing number of drones were all investigated (Lyu et al., 2017; Kalantari et al., 2016).

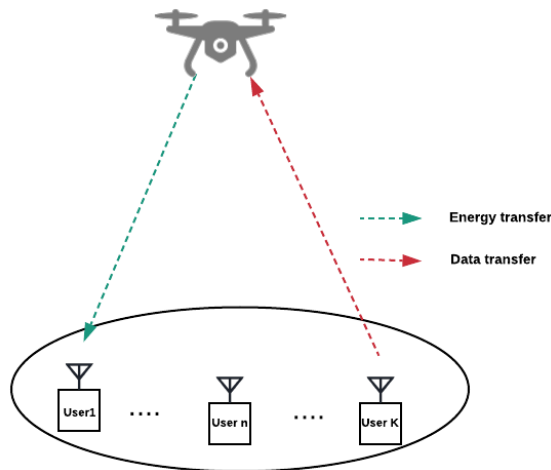


Figure 2.4: UAV enabled WPCN

An investigation into the use of beamforming in energy-harvesting wireless networks included compiling a list of the several conceptual frameworks, physical implementations, and operational procedures that were discovered during the course of the research (Alsaba et al., 2018). In full-duplex wireless powered communication, this method has been utilised to reduce self-interference and improve data rate among users (Wang et al., 2018). Beamforming is also employed in one of the studies where a high UAV uplink throughput is attained on board the UAV. This offers a variety of benefits, including the following: (Tomasz et al., 2020; Yamen et al., 2018; Angeletti and Lisi, 2014).

- i. Broader coverage: The beam is concentrated on a particular spot, the same frequency may be reused, which allows for an increased number of users and greater coverage.
- ii. Higher data rate and quality of service: The beam is concentrated on a single receiver, the signal-to-interference noise ratio (SINR) is increased, which results in an increase in efficiency.
- iii. Improved security: It offers a higher level of protection and safety due to the fact that the beams are not disseminated in all directions.

iv. Less interference: Instead of broadcasting in all directions, which might result in interference, beamforming makes use of directional antennas to help guide the beam in the desired direction.

### **2.3.2.1 Approaches used in UAV enabled energy transfer**

There are primarily two approaches that may be taken to extend the amount of time an UAV can remain in the airspace, which in turn extends the capability of both energy transfer and communication. An initial approach might be to expand the size of the battery; however, this will result in greater costs and will make the UAV heavier to fly, which will result in increased fuel consumption. It is better however, to obtain power for the UAV from intermittent sources. These sources could employ wireless power transfer technologies like electromagnetic field (EMF) or non-electromagnetic field transmissions (non-EMF) (Lu et al., 2018).

In the EMF based method, high voltage power lines are used to recharge the UAV's using the electromagnetic field from the lines. Adjusting coupling coefficients between the power line and the UAV and managing the frequency within the onboard UAV makes it practically difficult to apply it in real life (Choi et al., 2015; Bi et al., 2016). Non-EMF consists of different methods such as PV arrays, laser beaming, dynamic soaring etc. In PV arrays, the UAV will be integrated with PV arrays which use solar radiation to charge the battery and store the energy for the night-time. But this method had some limitations as it is completely depending on the solar radiation which is not the constant source of energy required for communication (Safyanu et al., 2019). In laser beaming, an external source feeds the laser source to create a strong laser beam that is used to charge the UAV, but the difficulties in the practical implementation of having a moving charge source are that the UAV should remain close to the charging station (Achtelik et al., 2011).

Currently, researchers are encouraged to combine Beamforming in antenna design with applications such as satellite, energy harvesting, wireless communication, and so on (Angeletti and Lisi, 2014). Beamforming has been utilised to boost the capacity of the uplink for on-board UAVs in various studies (Alsaba et al., 2018; Izydorczyk et al., 2020). Because the beam is focused on a single receiver, it provides more coverage, security, and quality of service, as well as a higher data rate with little interference. Aquilina et al. (2019) and Yang et al. (2019) utilised iterative algorithms in UAV enabled sensor networks to optimise the energy transfer and therefore increase the energy efficiency, while Zhan et al. (2018) and Yang et al. (2018)

used iterative (static) algorithms in UAV enabled sensor networks to optimise the energy transfer and thus increase the energy efficiency.

### **2.3.2.2 Optimization Algorithms for Energy Management in Wireless Communication**

There are several benefits of employing a UAV as an airborne base station, such as the flexibility to move about and deploy fast, as well as a greater line of sight (LoS) (Mozaffari et al., 2017) for data collection, though some still prefer to use ground-based stations. UAVs provide a variety of significant technological challenges, including interference, battery life, energy management, trajectory planning, and deploying in three dimensions, despite the fact that they offer a number of considerable benefits. The deployment is the key problem, and its success is dependent on energy consumption.

The development of a wireless power transfer protocol and an energy-efficient power transfer scheduling approach are some recent examples of improvements in energy management (Nikoletseas et al., 2017). The wireless power transfer protocol is comprised of two protocols: one protocol checks the power of each sensor node to determine whether or not it can transmit energy, and the second protocol determines whether or not there is a balance of energy. In a software-defined wireless sensor network, energy transmitters are activated by the process of scheduling and thereby reducing the amount of energy consumed by the transmitters by requesting power transfer, energy transfer activation optimization and confirmation. At network layer, energy management in water distribution systems might be handled by deploying this technology (Ejaz et al., 2016).

During real-time deployment of wireless powered networks, energy efficiency was still an important consideration. Some of the authors anticipated that the UAV would have sufficient energy to operate, and they employ techniques such as sequential convex approximation (SCA), scheduling and energy harvesting to control the UAV's energy consumption. Table 2.4 provide a comparison of the approaches that are currently in use as well as their deficiencies.

Table 2.4. Comparison of current methods and its shortcomings

<b>Ref.</b>	<b>Method</b>	<b>Limitations</b>
(Yang et al., 2018; Zhan et al., 2018)	Utilize iterative algorithms to maximize the transmission of energy.	It is not implemented in WPCN.
(Izydorczyk et al., 2020; Alsaba et al., 2018)	Beaming to enhance uplink wireless data transmission (WDT).	The UAV's energy consumption is not considered.
(Bi et al., 2015; Cho et al., 2018)	To reduce completion time, use the bisection search technique with the sub gradient algorithm.	The sensors are presumptively on an even plane with the UAV's fixed height and RF charging mechanism.
(Ejaz et al., 2016; Nikolettseas et al., 2017)	Scheduling Wireless power transfer protocol combined with scheduling.	Not applied in WPCN for WDS
(Chen et al., 2020)	Convex approximation is being used in an iterative process to maximize transmit power.	Achieved using sophisticated mathematical techniques, and the height of the UAV is fixed.
(Zeng et al., 2020; Mozaffari et al., 2017)	Power distribution, path planning, user scheduling, and bandwidth all interact together to maximize energy efficiency.	Implemented exclusively in mobile communication networks.
(Mozaffari et al., 2017; Kalantari et al., 2016)	Reduce overall flying duration by cell partitioning.	Mainly implemented in telecommunications; Not applied in WPCN

## 2.4 Navigation optimization of the UAV using WPCN

The UAV is effective in keeping a constant level of service, and numerous approaches and designs have been created to increase the efficiency of energy harvesting by optimising the trajectory path. Xu et al. (2018) adopted a trajectory based on time discretized technique with an estimated mission completion time in order to optimise the minimum amount of energy that was harvested. Wang et al. (2018) on the other hand, used this technique in order to maximise both the average and the minimum throughput to all devices. With a single ground user and a UAV at constant speed, a framework for optimising the trajectory in two-dimensional space has been introduced (Zeng and Zhang, 2017). The ground users, on the

other hand, were treated evenly in a one-dimensional plane for simplicity's sake, however this has an impact on applicability throughout implementation. An iterative method of sub slot allocation and UAV trajectory design was presented by (Xu et al., 2018) to maximise the mean information rate of IoT devices in the communication service.

Additionally, a clustered non-orthogonal multiple access system was taken into consideration. During the time that the UAV is either collecting data or energy, the tangential line method is used to establish the trajectory route that it will take. The research carried out by Tang et al. (2020) uses the tangential line technique for path planning and 'broadcasting' energy to the ground nodes. The trajectory departs from the starting point and avoids the obstacles by using the circle's tangent line approach. The sub-paths are common tangents connecting adjacent obstacle circles. This approach could provide the shortest collision-free route by joining the arcs between tangent points on the same obstacle circle and contrasting the lengths of several paths from the starting point to the concluding point. This is implemented with the goal of achieving the highest possible minimum throughput. In contrast, Zeng and Zhang (2017) employs the technique for trajectory planning and optimization. The UAV consumes a significant amount of its available energy to ascend to higher altitudes in order to collect data, and then it descends to a lower level in order to be closer to the sensors so that it may transmit energy to them. Beamforming offers the potential to significantly cut down on the loss of both time and energy.

In wireless mobile communication, when the UAV serves as an airborne base station, the power distribution, trajectory, user scheduling, and bandwidth may be optimised to produce the highest possible level of energy efficiency (Yang et al., 2018). The majority of unmanned aerial vehicle (UAV) communication systems include either trajectory, routing, or route optimization as a way to improve energy economy, performance, and throughput. (Zeng et al., 2020; Zhan et al., 2018) proposed an energy efficiency model and design based on a fixed wing UAV's trajectory, speed, and duration. (Sun et al., 2019) utilised a three-dimensional trajectory and resource allocation for the purpose of overall throughput optimization in solar-powered UAV communication. The vast majority of the currently available research concentrates on the optimization of energy consumption on a horizontal plane, with the assumption that the height of the UAV remains unchanged. According to the studies that have already been conducted, there has not been a large amount of study conducted on minimising the overall energy that a UAV consumes when operating in an uneven terrain.

### **2.4.1 Path Planning Challenges**

There are a number of challenges associated with UAV technology, such as those associated with channel estimates, resource allocation, path planning, privacy and security concerns, interference, etc. and that there is a significant investment of both time and money involved in finding an optimum path to finish the mission in the WDS. The challenges associated with path planning will be the key concern in this work. The following list provides a full analysis of the many obstacles that the UAV must overcome while choosing its flying path (Majeed and Oun Hwang, 2022; Ait Saadi et al., 2022):

**Flight path length:** The measure of the distance that must be travelled by the UAV between its point of departure and its destination in order to successfully complete the mission in an optimal way.

**Energy efficiency:** The process of making the most efficient use of the energy that the UAV has by reducing the amount of fuel consumed, the amount of battery power used, and any other operations that use up the energy that is on board the UAV.

**Time efficiency:** This refers to how long it takes the UAV to complete the mission while using the route that has the least amount of travel time. It also depends on the distance travelled and the total amount of time that must be invested in order to accomplish the task at hand.

**Cost efficiency:** It comprises the total cost of the operations of the UAV, which includes computational cost, fuel usage, communication costs between sensor nodes or access points, expenditures for battery recharge and maintenance costs. It has a direct relationship to both the total amount of time and energy that the UAV consumes.

**Optimality:** The solution to a problem that requires the least amount of money, effort, and time to implement the best option. The solutions may also be non-optimal, in which case they provide a solution without taking into account any of the limitations, or they may be suboptimal, in which case they provide a solution that does not satisfy any of the criteria.

### **2.4.2 Optimization algorithms and techniques used for Trajectory Design**

There are different 3D trajectory planning algorithms have been developed throughout the course of time for use in a variety of various rural and urban applications. Due to the fact that its design is both effective and easy to understand, it is frequently utilised in real-time UAV applications. The algorithms are broken down into four primary categories: those that are mathematical model-based, those that are bioinspired, those that are machine learning-based,



and those that are node-based. (Liang Yang et al., 2014; Majeed and Oun Hwang, 2022). The algorithm/techniques to be used are determined by the application and its environment.

#### **2.4.2.1 Mathematical model-based algorithms**

Based on computational complexity and design strategy, this method, which employs several mathematical functions and equations for an optimal path planning of the UAV focusing on minimizing cost, time and energy. Specifically, this focuses on minimising the cost of the mission while also reducing its flight time. Control theory, metaheuristics, linear programming, mixed integer linear programming, and nonlinear programming are some of the examples of algorithms that belong to this area.

For example, much of the research has provided evidence focusing on obstacle avoidance for path planning of a UAV using Integer linear programming (ILP) and mixed integer linear programming (MILP) in linear programming method (Waen et al., 2017; Almutairi et al., 2022), whereas some authors used Markov decision process (MDP) algorithms such as state-action-reward-state-action (SARSA) (Zhang et al., 2021; Zhao et al., 2019). But the energy efficiency of the UAV/communication is not considered. By taking a different approach, some of the probabilistic models such as an improved ant colony optimization with penalty strategy, were used to find the trajectory path focusing on obstacle avoidance which provide efficient result, but energy utilisation during the communication were not considered (Yue and Chen, 2019; Li et al., 2020).

#### **2.4.2.2 Bioinspired algorithms**

Bio-inspired problem-solving entails exploiting biological behaviours to tackle problem inspired by the environment. This strategy for route planning eliminates the requirement for complicated environment models and replace them with timesaving search procedures in order to get the best possible answer. To address these difficulties, evolutionary algorithms like particle swarm optimization (PSO), adaptive multi-objective differential algorithms, and neural network algorithms are utilised. These algorithms analyse the problem at several distinct levels.

Several publications have acknowledged the potential of evolutionary algorithms for use in path planning with UAVs, such as the genetic algorithm coupled with sequential convex approximation, in which the trajectory was optimised by significantly reducing the amount of time it took for the UAV to complete its mission (Pi and Zhou, 2021). ANN and A\* algorithms

were used by Sanna et al.(2021) to address the problem of coverage, path planning and to determine a path that would avoid collisions and congestion.

### **2.4.2.3 Machine learning algorithms**

Machine learning algorithms are a subset of AI techniques in which the system make decisions independently without any external interference. It incorporates many approaches that were used to train the system and detect certain patterns. It is mainly classified into supervised, unsupervised and reinforcement learning based on how the data is arranged.

For instance, the literature of Yoo et al. (2017) emphasis on contrasting the effectiveness of applying Kalman and Gaussian filters, both of which were used to reduce the problems of noise and probability of collision during communication. The model recognises a pattern in the way that networked elements influence UAV motion, learns and improves its estimation precision through the use of Gaussian techniques, which fall under the category of supervised learning. Despite the fact that it produces superior outcomes, the error rate was not particularly high while utilising this strategy. The unsupervised method consists of clustering algorithms such as quality threshold clustering (QTC), K-means etc. For instance, the research conducted on implementing clustering leads to clustered nonorthogonal multiple access (C-NOMA) and density-based clustering for trajectory designing of the UAV (Chen et al., 2021; Na et al., 2021). The above strategy also focuses on improving the achievable uplink throughput whereas Shen et al.(2022) used greedy learning clustering to group the machines and an energy map to identify an optimal hovering position for better throughput. The research of optimizing the path planning by applying further methods leads to Reinforcement learning (RL) (Kosunalp, 2016), Q learning (QL)(Wang et al., 2021b; Alam and Moh, 2022) and Deep Q learning (DQL) (Tang et al., 2020; Jo et al., 2022). Since maximizing minimum throughput by planning the trajectory and optimizing the time is a non-convex problem, Tang et al. (2020) applied multi agent Deep Q learning using a penalty and reward scheme. Alam and Moh, (2022) provided a survey of the different QL based position aware routing protocols and its future research directions which include precise energy consumption of the UAV, space-air-ground integrated network (SAGIN) routing for mobile communications to improve the coverage and the need of HAP's and accurate channel models whereas Wang et al. (2021b) used iterative hybrid algorithm using Q learning to reduce the position errors and correct it for energy efficient navigation. The research of Dong and Liu, (2021) focussed on coverage

route planning with UAV cameras under a two-dimensional plane with constrained power integrating deep reinforcement learning merged with double Q learning and clustering.

#### **2.4.2.4 Node based algorithms**

To build a route based on a set of nodes such as sensors, node-based optimization methods are utilised. It searches through a collection of nodes that have precalculated sensing, placement, and processing. This is a dynamic programming approach that generates a cost function and explores all accessible nodes in the graph or map to find the shortest path (Liang Yang et al., 2014; Al-Janabi and Al-Raweshidy, 2017).

To create an optimal trajectory for data collection, Tong et al. (2019) used affinity propagation (AP) method to find the hovering points or collection points of the UAV and a dynamic programming approach is used to create an optimal trajectory by selecting the shortest path whereas Wu et al. (2022) used TSP and dynamic programming. A comparison of path algorithms such as Dijkstra and heuristic algorithms are employed for an efficient path planning, and Dijkstra outperforms heuristic methods based on the simulation results (Danancier et al., 2019) whereas the famous searching algorithms such as Dijkstra, A\* dynamic and D\* were compared to explore the recent technologies for path planning in multi robot systems (Madridano et al., 2021). An adaptive lazy theta\* algorithm is developed for the purpose of calculating an ideal path in three-dimensional space in real time. In this approach, the three-dimensional space is subdivided into multiple levels in order to filter successor nodes that are unsuitable due to the limitations of the UAV. Additionally, dynamic heuristics are utilised in order to enhance the precision of the computed route (Wu et al., 2020). Mandloi et al. (2021) performed a comparative analysis of the A\*, slow theta\*, and theta\* algorithms in two-dimensional and three-dimensional space with the goal of determining the most efficient route for the UAV to take from its origin to its destination. Table 2.5 provides a comparison of the algorithms that are most commonly used as well as the restrictions associated with each method throughout the process of path planning for the UAV.

Table 2.5. Comparison of methods for path planning using UAV

<b>Ref.</b>	<b>Method</b>	<b>Limitations</b>
(Pi and Zhou, 2021; Sanna et al., 2021)	Genetic Algorithm combined Sequential convex approximation, ANN	Minimum completion time by resource allocation and trajectory optimization. Nodes are deployed only in 2D space. Energy consumption of the UAV is not considered.
(Zhan et al., 2018; Wu et al., 2018)	Successive convex approximation	Consider only uplink communication scenario. Focus only on minimize energy consumption of sensor nodes
(Hua et al., 2017; Sun et al., 2019; Tang et al., 2020)	Maximizing of the sum throughput using convex optimization.	Design of the trajectory and the energy consumption model are not considered.
(Waen et al., 2017; Almutairi et al., 2022)	Integer Linear Programming (ILP); Mixed Integer Linear Programming (MILP)	Total service time of the UAV is minimized while energy efficiency is not considered. Focus only on obstacle avoidance.
(Yue and Chen, 2019; Li et al., 2020)	Ant colony optimization with penalty strategy, Modified Ant colony optimization	2D space with obstacle avoidance is considered. Real time trajectory planning is not considered.
(Zhang et al., 2021; Zhao et al., 2019)	Markov decision process (MDP); SARSA	Focus only on obstacle avoidance in real time. Energy consumption of UAV is not considered.
(Miller et al., 2011)	Delaunay Triangulation DT(P) combined with Polynomial approximation.	Energy efficiency of the UAV is not considered.
(Mandloi et al., 2021; Mandow and de La Cruz, 2010; Hossein Motlagh et al., 2016)	Graph search algorithm (NAMOA*), A* algorithm	Survey on the standardization, safety, collision avoidance and obstacle detection.
(Jo et al., 2022; Tang et al., 2020; Kosunalp, 2016)	Deep Reinforced Learning, DQL based power control algorithm, Q Learning	Only transmit power is taken into account for optimization.

According to the disclosure of several optimization methods for UAV-enabled WPCN, the implementation of each strategy resulted in a number of constraints, which are detailed in Table 2.5. Some of the approaches only take into consideration a two-dimensional view of the situation, which prevents them from providing a real-time implementation of the solution. On the other hand, methods such as DT(P), ANN, Genetic algorithm with convex approximation doesn't take energy efficiency into account at all as its focus was on obstacle avoidance. Since, the consumption of energy is such a significant aspect in the WDS which takes into account of sensor nodes and communication systems that require a lot of power. At this point in the project, combinatorial and clustering optimizations, integrated with technologies such as beamforming, will be used.

### **2.4.3 Path Planning Constraints**

There are different constraints that need to be taken in to account while planning the trajectory of the UAV (Ait Saadi et al., 2022; Aggarwal and Kumar, 2020).

- **Altitude:** The altitude of the UAV is measured in metres. The low flying height of the UAV causes it to come into contact with a number of obstacles as it travels along its path. When flying at a high altitude, on the other hand, there is a greater demand placed on the UAV's energy supply as well as concerns regarding coverage.
- **Energy consumption:** It is the total amount of energy that the unmanned aerial vehicle (UAV) consumes in order to communicate, move, hover, and do other computational activities. It is dependent on the time, altitude, path length, and environment with which the UAV interacts.
- **Obstacles/threats:** It is anything that interferes with the UAV's normal flight path, and it might be static obstacles like buildings or mountains, or dynamic threats like other drones or objects that are in motion. It is possible that the UAV may be destroyed or damaged by it, which would result in a considerable increase in the costs associated with maintaining it.
- **Velocity:** It is crucial for both the planning of the UAV's flight route and the control of its flight. A lower velocity has an immediate influence on the amount of fuel that is used, in contrast to a higher velocity which makes flying the UAV more difficult but speeds up the task. Because of this, a fair average velocity is always selected in order to save both time and energy.

In this thesis, the navigation of the UAV takes into consideration energy consumption, altitude, and obstructions; however, velocity is assumed to be a constant other than during the hovering process (when it approaches zero at constant height).

## **2.5 Research Gaps**

As described in the background section 1.1, intelligent water monitoring is a sophisticated technique that integrates computing, engineering, and environmental elements to ensure water quality and thereby maintain the water ecosystem. The literature review in this study assesses the diverse contributions made by researchers in smart water distribution systems in sensing, collection and communication, and WET. It reveals some of the new water quality sensors and protocols that could be integrated with wireless energy transfer methods to resolve issues such as coverage and energy management in WDS. The recent advancement of WPCN, UAV and EH technologies has aided in water monitoring by lowering costs and boosting efficiency in determining water quality.

However, while the use of a UAV alleviates the doubly near far problem (where the nearby nodes receive sufficient energy whereas the far away nodes starve) because it is mobile, it still uses energy to travel close to GNs in order to either supply energy or facilitate communication, the problem of minimizing its travel remains to be addressed. This will be a key focus of the work.

The literature research also exposes, however, current challenges in data and energy management in WDS, as a proliferation of energy hungry sensors are used during monitoring and communication.

The problem is compounded by inadequate solutions to the problem of maintaining both unmanned and manned aerial vehicles in flight for an adequate amount of time due to finite battery charge and onboard devices draining it. It is clear that no one solution has been able to resolve this problem and is unlikely to in the foreseeable future. It is inevitable that any solution to this problem will necessitate zero-power performance of the devices utilized including the UAV itself.

This thesis proposes a solution by integrating advanced technologies such as WPCN, beamforming with the UAV along with optimization methods in wireless communication. It is evident that there is a significant paucity of research on energy management of the UAV

enabled technologies to wirelessly charge the GNs and collect data. Most of the study therefore focuses on energy management of the UAV to enable data management and monitoring of water quality using wireless networks and WPCN.

The navigation optimization of the UAV for path planning using different algorithms such as mathematical/machine learning was also considered to satisfy different constraints and analyse the advantages and limitations of each method. It is observed that some of the studies focus only on energy optimization on an even plane, with the height of the UAV considered to be constant, as discussed above. According to Table 2.4, there has been little research in minimising the overall energy of the UAV over uneven terrain. The thesis is therefore mainly focussing on resolving this research gap by optimizing the energy and height of the UAV using 3-dimensional beamforming in UAV enabled WPCN and dynamic optimization methods for energy management.

## **2.6 Summary**

The discussion in this chapter starts with the layered view of smart water systems to identify the current sensors and new technologies that could be used in WDS. This thesis focuses on the communication and sensing layer in the WDS. In this layer, energy usage was the focus as there are large number of GNs in the WDS and battery life limitation was always a major concern. Using the literature study, different wireless communication methods were taken into consideration to review and identify the method compatible with WDS. For battery recharging issues, the doubly near far problem of the UAV was raised and is to be resolved using a UAV enabled WPCN. This chapter discusses how it could be applied. It also reviews different energy harvesting methods/technologies used in WDS and identifies a research gap in the need for energy optimization in WDS and how it could be effectively implemented with new technologies such as UAV enabled WPCN and beamforming. In order to focus on this, energy management strategies and navigation optimization methods were considered which could optimize the energy of the UAV by constructing an optimal trajectory with respect to charging, communication and UAV dynamics.

# CHAPTER 3

## RESEARCH METHODOLOGY

### 3.1. Introduction

This chapter not only provides a more in-depth description of the WPCN that is enabled for UAVs and been deployed for WDS but also introduces the optimization algorithms and techniques to be used for their energy management. When reaching an optimum hovering point, the UAV which is part of the communication environment serves as a hybrid access point in the WPCN and will be able to send energy and gather data on the water quality. Some of the contributions made in this chapter have been presented in Radhakrishnan et al. (2021).

In order to focus the radio frequency (RF) signals that are transmitted to GNs, the UAV makes use of a technology known as three-dimensional beamforming. The energy that can be harvested from these energy signals by the GNs is then utilised for the transmission of data. An equal time is assigned for both energy and data transmission during the communication. Information ( $I = -p \log_2 p$ ) is optimized at  $dI/dp = 0$ . Thus  $\log_2 p \cdot dp/dp + p(1/p) = 0$ . Hence  $\log_2 p = -1$  or  $p = 1/2$ . Therefore, equal transmission and charging probabilities and rates are required for optimal energy and data transmission.

In current cellular communication schemes, the WPCN is deployed with the help of fixed base stations that broadcast energy to recipients for the purposes of data gathering and transmission. Since the base stations have been fixed, users who are further away receive less energy and demand more energy for data transmission. This scenario is known as the doubly near-far problem. Due to issues regarding line of sight (LoS) with fixed-based stations, the double near-far problem will be resolved in this thesis by deploying a UAV as a flying base station but, its deviation from a centroid of GN clusters is also optimized with respect to beam strength.



### 3.2. System Conceptual Design

A system model is presented to optimise the position of the UAV in order to reduce the amount of time and energy required for the flight, as shown in Figure 3.1. The WPCN system used in this model consists of rotary-winged UAVs that can communicate through line of sight (LoS) with GNs that are equipped with rechargeable batteries. To generate a three-dimensional perspective of the GN points, the GNs must first be positioned using Cartesian coordinates of a point in 3D is  $x$ ,  $y$ , and  $z$  and in this thesis height ( $h$ ) is used instead of  $z$ . The UAV receives power from an RF energy charging station, and then it beamforms the power to the GNs using the WET components that are on board. The location of the ground sensors are positioned inside an ellipse with radius  $R_c$ . Since both the UAV and the GNs are observed from a three-dimensional viewpoint, a dome is an effective shape to use when attempting to portray how the GNs are clustered together in the terrain region.

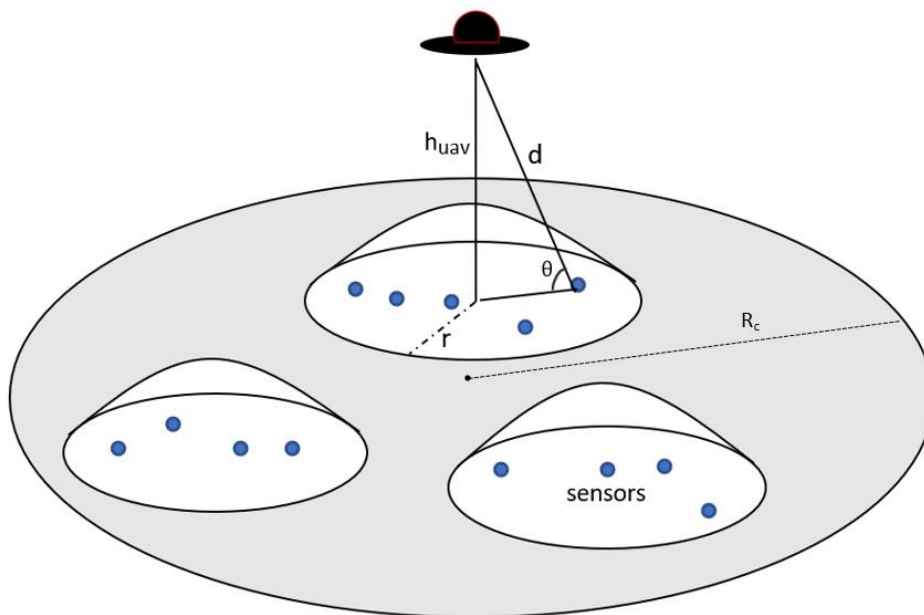


Figure 3.1: A system perspective of a UAV-enabled WPCN incorporating 3D beaming

The radius of the clusters is denoted by the notation ' $r$ ' in this context. The starting location of the UAV will be determined by utilising a 3D K-means clustering method in combination with the GN points ( $x_n$ ,  $y_n$ , and  $h_n$ ) to estimate the centroids of the clusters. It is anticipated that the nodes involved in beamforming will also receive energy, since they are located in the same line of sight as the nodes that are involved in charging. This task will be completed using a rotary wing UAV that is equipped with beamforming due to the requirement for hovering as

well as flying motions. A downlink channel model will make use of a 3D perspective of the ground nodes, which will be viewed as being on an uneven plane, as opposed to being limited by a 2D perspective of fixed base stations (as is assumed for even terrain).

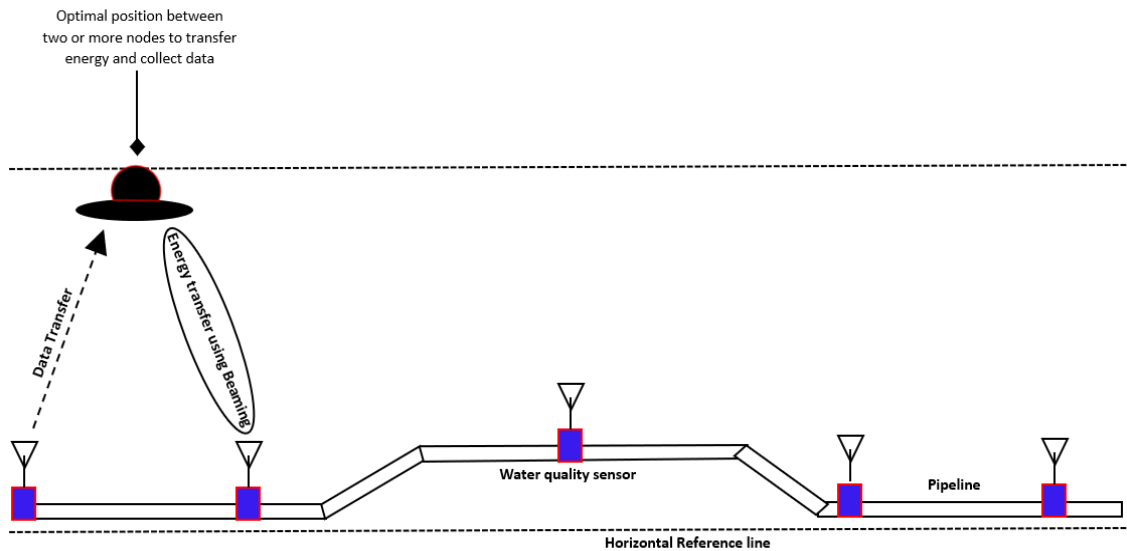


Figure 3.2: Application scenario of monitoring water quality with UAV-enabled WPCN

The implementation of UAV enabled WPCN in a water quality monitoring scenario is illustrated in Figure 3.2 which offers a detailed picture of one among the cluster nodes. In this scenario, the GNs are distributed at random along a water pipeline at various points that are designated by a horizontal reference line and are positioned at variable heights above the ground. A UAV that can function as a flying base station is capable of sending RF energy signals through beamforming while simultaneously collecting data on water quality. Matlab is used to perform simulations and analysis of antenna signals by using the research of COMSOL (n.d.), which allows the beamforming concept to be integrated with the onboard functionality of the UAV. During the communication, the UAV will be hovering in an optimal position with respect to the amount of energy it uses and the overall amount of flying time it needs to complete the mission. The implementation of dynamic optimization methods in conjunction with the suggested ‘Dome packing’ method will be used to arrive at the ideal location. These methods will be formulated in subsequent sections of this and later chapters.

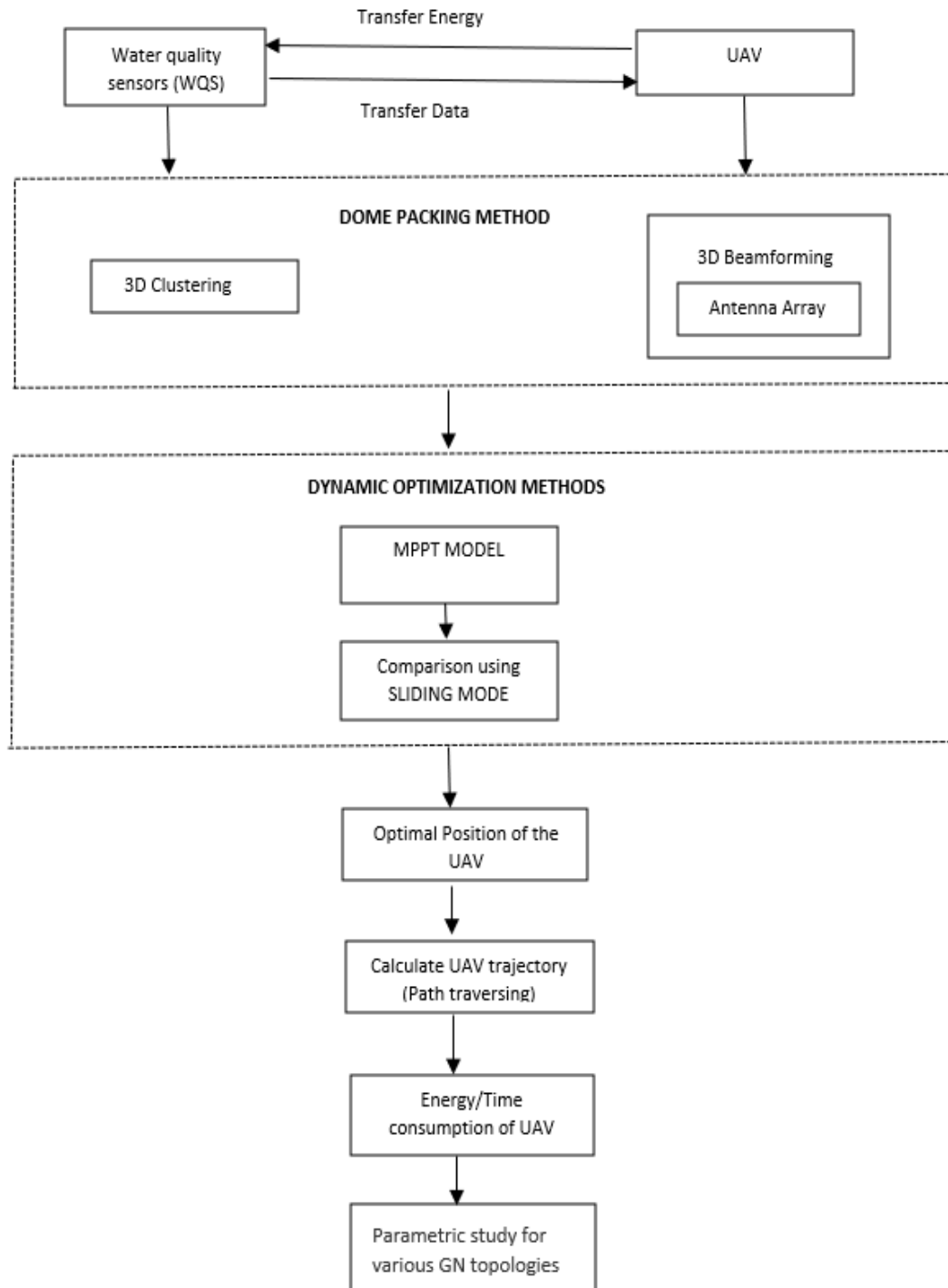


Figure 3.3 Proposed Conceptual Diagram for Energy optimized Navigation Model

The concept could suitably be deployed in emergency scenarios, such as when a water pipeline bursts, when water is contaminated by outside sources, or any other situation in which urgent information on water quality is to be gathered. In the proposed conceptual diagram in Figure 3.3, a proposed dome packing method will be used to provide an energy optimized trajectory design for the WDS. In this approach, a 3D clustering algorithm will be implemented to pack

the sensors in a specified region, which in this case is a water pipeline structure. In other words, the water pipeline will serve as the location of the sensors. The LoRa protocol is employed for data collecting, and a 3D beamforming technology is used to charge the water quality sensors that are installed in the water pipeline. The suggested technique allows for the calculation of the best possible location for the UAV, which in turn allows for the design of the trajectory.

The energy consumption of the UAV as well as the energy received by the GNs is firstly calculated using the dome packing method. The energy time graph of the UAV and the GNs are generated with  $n$  rounds of iteration and a comparison made with the non-dome packing approach. After the implementation of the proposed dome packing approach, dynamic optimization methods are developed to integrate the dynamics of the UAV with the proposed dome packing method to increase overall optimality of the system. Utilizing two distinct algorithms for dynamic optimization allows this optimization approach to be reviewed and validated.

### 3.2.1 Downlink Communication Design

The UAV is equipped with a uniform rectangular antenna array (URA) with  $N$  radiating elements, and the horizontal position at each time  $t$  is  $u(t) = (x(t), y(t))$  and it could be identified using global positioning system (GPS) integrated in UAV. The GN's have fixed positions on the ground  $g_n = (x_n, y_n, h_n)$  and are mounted with two omnidirectional antennas for WIT and WET. The distance formula may be used to determine the distance between the UAV and the GNs ( $d$ ) at any given time (Wang et al., 2021a):

$$d = \sqrt{(u(t) - g_n(t))^2 + h_{uav}^2} \quad (3.1)$$

where  $h_{uav}$  denotes the UAV's flight altitude. A theoretical path loss model could be integrated with this model using a vector  $l \in \mathbb{C}^{N \times 1}$  used to compute the communication link power loss between the UAV and GNs, where  $\mathbb{C}^{N \times 1}$  represents an  $N$  element transmitter with the space of  $N \times 1$  complex matrices (Zeng et al., 2019).

$$l = \sqrt{I_0} l_1 a(N, \theta, \phi) \quad (3.2)$$

The steering vector is represented as  $a(N, \theta, \phi)$  triple, while the elevation and azimuth angles of the LoS/NLoS route between the UAV and the ground node are denoted as  $\theta, \phi$  and range

of  $\theta$  from  $-90$  to  $90$ ,  $\phi$  from  $-180$  to  $180$  for NLoS. The large-scale and small-scale fading variables are  $l_0$  and  $l_1$ , respectively, where  $l_1 \in \mathbb{C}^{N \times 1}$  and  $l_0$  rely on the LoS and NLoS connectivity between the transmitter and the receiver (Zeng et al., 2019).

$$l_0 = 10^{-\left(\frac{\text{Pr}_{\text{LoS}} \text{PL}_{\text{LoS}} + \text{Pr}_{\text{NLoS}} \text{PL}_{\text{NLoS}}}{10}\right)} \quad (3.3)$$

$$\text{PL}_{\text{LoS}} = \text{PL}_{\text{FS}}(d_0) + 10 \mathcal{E}_{\text{LoS}} \log(d) \quad \text{and} \quad \text{PL}_{\text{NLoS}} = \text{PL}_{\text{FS}}(d_0) + 10 \mathcal{E}_{\text{NLoS}} \log(d) \quad (3.4)$$

$$\text{where } \text{PL}_{\text{FS}} = 20 \log\left(d_0 f \frac{4\pi}{c}\right) - G_t - G_r \quad (3.5)$$

and

$d_0$  is the reference distance which equates to 1 metre

PL stands for propagation loss

$\text{Pr}_{\text{LoS}}$  is the probability of LoS,  $\text{Pr}_{\text{LoS}} + \text{Pr}_{\text{NLoS}} = 1$

FS stands for free space path loss

$c$  is the speed of light

$f$  is frequency.

The environmental-dependent path loss exponents for LoS and NLoS communication are  $\mathcal{E}_{\text{LoS}}$  and  $\mathcal{E}_{\text{NLoS}}$ , while the transmitter and reception antenna gains are  $G_t$  and  $G_r$  (Radhakrishnan and Wu, 2019).

In this thesis, pathloss factors are not considered as the focus is on optimizing energy consumption of the UAV during charging and communication than considering the whole communication. If the pathloss were considered, it could have resulted in some amount of energy lost during communication.

To study, analyse and implement the beamforming technique, different tools were considered at the initial phases of the research which included Ansys, Matlab etc. Matlab was selected to implement the scenario as the Ansys tool is mainly focussed on antenna design and it is beyond the scope of this thesis to integrate this with sensor placement and optimization methods. On the other hand, Matlab enables the construction and analysis of common sensor array configurations.

Initially, the 3D beam is constructed and analysed in Matlab R2022a as part of the research using the sensorArrayAnalyzer toolbox. Phased Array System Toolbox is a Matlab-based tool which is a subset of Sensor Array Analyzer. This package includes functions for designing and simulating beamforming and sensor arrays for wireless communication in 2D and 3D. Active and passive arrays, including subarrays can be modelled and analysed. These arrays enable the transmission and reception of simulated signals for the development of beamforming methods. The array types include uniform arrays such as rectangular, linear, circular or concentric, spherical etc and element type include choices such as custom, isotropic or cosine antennas. By analysing the beam formation using different arrays, rectangular array provided the required beam strength for the work. Figure 3.4 depicts the outcome of an 8x6 uniform rectangular array antenna pattern using custom antenna type study at a frequency of 1GHz followed by the analysis of the 3D beam represented as in Table 2.3. A 1GHz frequency is used as the waves with higher frequency carries more energy and with lower frequencies, charging the sensors in WDS would be difficult. Different frequencies were used during this simulation and 1GHz were the optimized one for the thesis as in appendix C.4. The different parameter value selections were based on the strength (half power beam width) and array directivity of the beam provided by Sensor Array Analyzer during analysis. In this project, antenna design is not considered, and the Matlab tool is actually used to analyse the strength and directivity of the beam.

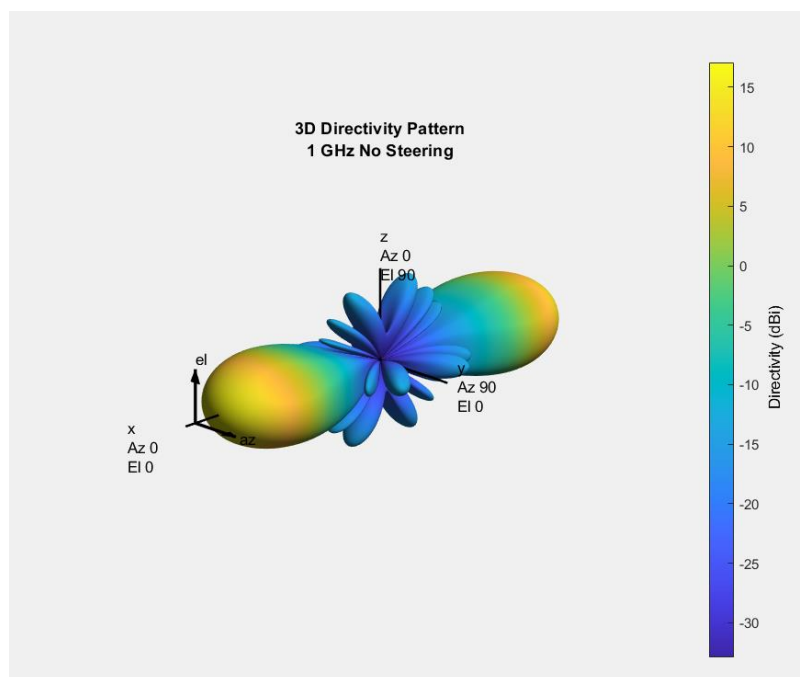


Figure 3.4: A Constructed 3D beam pattern

Table 3.1: Outputs of 3D beam analysis

Parameters	Value
Array Directivity	17.18 dBi at Az; 0 El
Array Span	X=0 m y=750 mm z=1.05 m
Number of Elements	48
HPBW	22.04° Az / 18.00° El
FPBW	61.19° Az / 44.00° El
SLL	30.00 dB Az / 30.01 dB El

Formulations to create antenna radiation patterns (beamwidth) pointing at the GN's have been provided by Balanis (2016). These are summarized in equations (3.6 - 3.8) below in which the antenna gains created in horizontal and vertical planes ( $A_H, A_V$ ) are calculated as follows:

$$A(\theta, \phi) = A_H(\theta) + A_V(\phi) \quad (3.6)$$

$$A_H(\theta) = \min\left[12\left(\frac{\theta}{\theta_{3dB}}\right)^2, A_m\right] \quad (3.7)$$

$$A_V(\phi) = \min\left[12\left(\frac{\phi - \phi_{tilt}}{\phi_{3dB}}\right)^2, A_m\right] \quad (3.8)$$

where  $A_m$  is the side lobe level attenuation of the generated beam,  $\phi_{tilt}$  is the beam tilting angle required by the UAV to reach GN, and  $\theta_{3dB}$  and  $\phi_{3dB}$  represent the 3dB beamwidth of the horizontal and vertical patterns of the beam, respectively (M Series Mobile, 2017). The distances (horizontal and vertical) from the cluster centre to the ground terminal node,  $d$  and  $H$ , are used to compute the angle,  $\tan^{-1}(H/d)$ , to guide the beam in the direction of the GN. The range of the beam  $d\sin(\alpha)$ , where  $\alpha$  is the beamwidth, is also determined by calculating the half power beamwidth (HPBW). To construct a beamforming energy signal ( $S$ ), equation (3.9) will be used (Zhang and Ho, 2013).

$$S = P_T \mathbf{w} \text{ HPBW} \quad (3.9)$$

where  $P_T$  is the transmitted power from the antenna array, and  $\mathbf{w}$  is the beamforming vector of the energy signal. The formula for the beamforming vector is  $\mathbf{w} = \mathbf{v}_1 / \|\mathbf{v}_1\|$ , in which  $\mathbf{v}_1$  is an eigenvector determined by taking the largest eigen value ( $E_i$ ) from matrix  $L$ , where  $L = \mathbf{H}^H \mathbf{H}$  and  $H$  is the conjugate transpose of matrix  $L$ . The power spectrum density of each sub band should be less than or equal to the square of the Euclidean norms of the beaming signal, and hence  $\|\mathbf{w}\|_2^2 = 1$  can be assumed (Liu et al., 2020; Timotheou et al., 2014).

In this case, an assumption is made that the energy received will be mostly utilised by the GNs for data transmission apart from activities such as activating sensors etc. Let  $T_{\text{tot}}$  be the overall time necessary for energy transfer and information transmission. Then according to probability,  $(1-X)T_{\text{tot}}$  be the time needed for data transfer and let  $XT_{\text{tot}}$  be the time needed for energy transfer and  $X$  is the fraction of probability for data and energy transfer. As explained in the introduction (3.1), it is expected that data transmission and energy transfer are assigned equal amounts of time.

The harvested power ( $P_{\text{EH}}$ ) ought to be higher than the threshold ( $P_{\text{TH}}$ ) value of the GNs, which can be considered constant while  $P_T$  varies with transmission distance. Therefore,  $P_{\text{EH}}$  depends on  $P_T/d^2$ , where  $d$  is the distance between the GN's and the UAV:

$$P_{\text{EH}} = \eta XT_{\text{tot}} P_T E_i / d^2 \geq P_{\text{TH}} \quad (3.10)$$

where the efficiency of energy conversion, also considered as constant is denoted as  $\eta$  and  $E_i = 1 / \|\mathbf{v}_1\|^2$  where  $\|\mathbf{v}_1\|^2$  is the norm of the eigen vector. Similarly, the UAV's energy consumption for WET is  $E_{\text{ET}}$  and given by: (Wang et al., 2021; Radhakrishnan and Wu, 2022).

$$E_{\text{ET}} = P_T XT_{\text{tot}} \quad (3.11)$$

### 3.2.2 Uplink Communication Design

The amount of energy utilised ( $E_{\text{DT}}$ ) during data transfer depends on the harvested power of the GNs as (3.12)

$$E_{\text{DT}} = P_{\text{EH}} (1-X) T_{\text{tot}} \quad (3.12)$$

The LoRa protocol will be used to implement data transmission due to its low power consumption, cost and high data rate when applied in IoT and assuming that the UAV acts as a LoRaWAN gateway to receive the packets that has been sent by the GNs. Therefore, LoRa



protocol is used in this thesis along with the findings from literature review, Table 2.2 and Table 2.3 for data transmission from the GNs to the UAV. In this thesis the LoRa is implemented using the packet format as the focus is on optimizing the energy consumption of the UAV. The LoRa packet format is represented in Figure 3.5 where ‘Preamble’ is used for synchronisation of the information between the transmitter and the receiver. Payload is where the message is encoded and followed by cyclic redundancy check (CRC) whereas the header provides information about the payload length, spreading factor (SF), coding rate (CR) etc. ‘Whitening’ is used in this simulation by adding a known sequence to the payload to reduce the redundancy during transmission. LoRa is also compatible with the advanced water quality sensors such as libellium based on the reveal in the Table 2.1 (Libellium, 2015).

<b>Preamble</b> 0–65535 symbols SF No coding	<b>Sync</b> 4.25 symbols SF No coding	<b>Header (if explicit)</b> 0–3 bytes SF–2 CR4	<b>Payload</b> 0–255 bytes SF CR	<b>Uplink CRC</b> 0–2 bytes SF CR
---	--	---	---	--

Figure 3.5: LoRa packet format

The data transfer rate R will be calculated in bits per second (bps) using the formula as below: (Pukrongta and Kumkhet, 2019).

$$R = SF * \frac{4}{2^{SF}} * 1000 \quad (3.13)$$

Where BW is the bandwidth used for communication. In the simulation, the following values are used as in Table 3.2. The control of congestion in the SF (Spreading Factor) plays a crucial role in optimizing communication networks. By adjusting the transmission range, a smaller value of SF can effectively reduce congestion and improve the overall efficiency of data transmission. In this context, a higher value of 7 is assumed, ensuring a larger transmission range that can accommodate more devices. On the other hand, (CR) is employed to eliminate interferences, a lower value of CR (4 is chosen) is preferable as it minimizes transmission delays within the communication system. This ensures smoother and more reliable data transfers, which ultimately enhances the overall performance of the network.

Table 3.2: Assumed simulation values for LoRa data transmission

Parameter	Value
Bandwidth	50 KHz
SF	7
CR	4

The data transfer time ( $T_{DT}$ ) will be proportional to the data transmission rate multiplied by the size of data delivered ( $Sz$ ) (Zeng and Zhang, 2017; Hua et al., 2017). Therefore,

$$T_{DT} = Sz / (1-X) R \quad (3.14)$$

Finally, the total energy consumed by the UAV through each communication cycle, i.e., the amount of energy needed by the UAV for the movement and WET, is calculated.

$$E_{Tot} = E_{UAV} + E_{DT} + E_{ET} \quad (3.15)$$

where  $E_{UAV}$  stands for the propulsion energy that the UAV uses to move and hover, which will be calculated in the next section.

Table 3.3: Referenced and author defined parameters

Referenced Parameter	Author defined parameters
Energy conversion efficiency ( $\eta$ ) (Wang et al., 2021)	Transmit Power ( $P_T$ )
Norm of Eigen vector ( $E_i$ ) (Wang et al., 2021)	Harvested Power ( $P_{EH}$ )
Data transfer rate ( $R$ ) Pukrongta and Kumkhet, 2019	Threshold Power ( $P_{TH}$ )
Size of data delivered ( $Sz$ ) Zeng and Zhang, 2017; Hua et al., 2017	Energy consumption of UAV for WET ( $E_{ET}$ )
	Energy utilized by GN's during data transfer ( $E_{DT}$ )
	Data transfer time ( $T_{DT}$ )
	Total energy consumed by UAV ( $E_{Tot}$ )
	Propulsion energy ( $E_{UAV}$ )

### 3.3. Static Energy Function Formulation

#### 3.3.1 Placement of the Ground Nodes

The placement of GNs or sensor nodes in the WDS has been addressed in the literature by, Shahra and Wu (2020) and others such as Geelen et al. (2021). The actual placement of the sensor nodes in the WDS is not explored in this thesis, the emphasis is on optimising energy and time during communication. The nodes are arranged in a 3D for an uneven surface using Matlab by calculating x, y and z quadrants where these x, y axes are measured in kilometres and z is in metres. The UAV's maximum flying height is restricted to 122 metres while the minimum is limited to 30 m by the UK Civil Aviation Authority (2019). It can be assumed that the GNs are arranged in a random order over the 3D plane as illustrated in Figure 3.6.

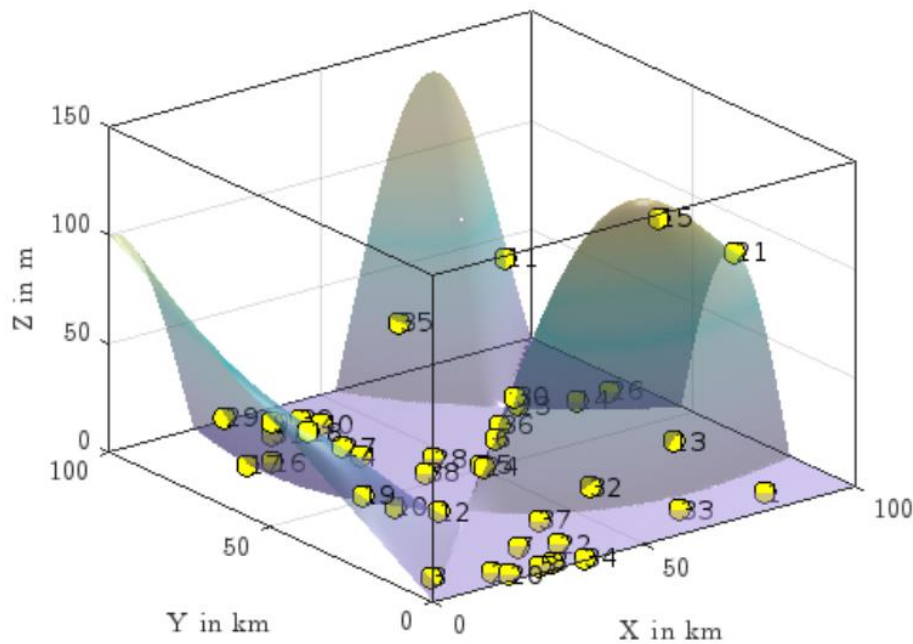


Figure 3.6: Placement of GNs on uneven 3D surface

#### 3.3.2 3D Clustering

Clustering is a process of grouping data into different clusters according to the similarity in their behaviour or properties. It is mainly performed by calculating the distance between the points or objects from the origin and groups are created based on these distances. There are

different types of clustering methods such as K-means, hierarchical etc. The selection of the clustering method depends on the application.

### 3.3.2.1 3D K-means

K-means is the simplest and one of the most efficient clustering methods that have been used for more than 50 years. In the three-dimensional (3D) K-means method, the data points which lie in 3D space are divided into different clusters and a cluster centre is assigned to each. To find the three-dimensional distance, the horizontal, vertical and diagonal distances are calculated. The number of cluster centres can be defined by the user, if the user is able to identify based on the different categories of behaviour from the data. Otherwise, the elbow method is used to automatically identify the number of cluster centres. To find the optimal number of clusters, the method minimizes the sum of squared error of distances with respect to the number of clusters. To then determine the optimal point, the selection of the elbow point where there is minimum number of clusters and minimum square error is identified. This point corresponds to the number of cluster centres for implementing K-means in order to obtain the centroid. A graph with the elbow method is shown in Figure 3.7, which indicates that a value of  $k = 3$  is optimal as the change in distortion values are small after  $k = 3$  (Chunhui and Haitao, 2019; Lakhmi et al., 2014).

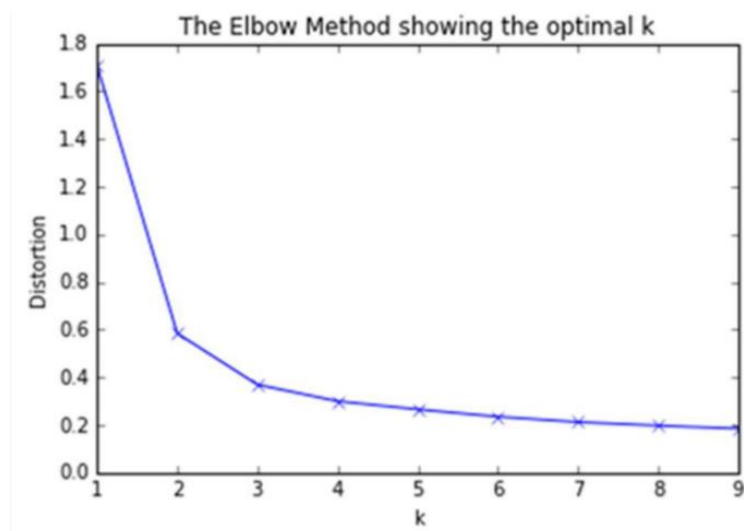


Figure 3.7: Elbow method. Source: Chunhui and Haitao, (2019).

In this thesis, clustering is used to group the water quality nodes based on the distance so that the nodes with similar distances to each other are grouped into the same clusters. A cluster

centre is calculated for each cluster by finding the centroid and then the beamforming technique is applied. After node placement at fixed sites, a dome packing method will be implemented that will be covered in the later chapters.

### 3.3.3 Energy Function Formulation including UAV Dynamics

A UAV's energy consumption and utilisation have always been a problem in WPCN. This issue could be alleviated by reducing the overall energy consumption and flight execution time of the UAV during communication and energy transfer in the WDS. A cost function can be computed to determine the UAV's ideal energy usage. This includes:

Kinetic energy  $T = \frac{1}{2}mv^2$ ,

Potential energy  $V = mgh$ ,

Transmitted energy  $E_{ET}$ ,

associated with the UAV.

Based on Lagrange's formulation  $L = V - T$ , an extended Lagrangian,  $L = V - T + E_{Tot}$  is proposed and consequently, the energy function,  $E$ , can be formulated as follows:

$$E = mgh - \frac{1}{2}mv_{uav}^2 + E_{Tot}(h_{uav}) \quad (3.16a)$$

$$\text{Or } E = mgh_{uav} - \frac{1}{2}ma^2h_{uav}^2 + E_{Tot}(h_{uav}) \quad (3.16b)$$

where  $m$  is the UAV mass and the (vertical) dynamics of the UAV are represented by the UAV state model (see section 5.3.1 for further details) in terms of UAV altitude,  $h$ :

$$v_{uav} = \dot{h} = -ah_{uav} \quad (3.17)$$

where  $a$  is the reciprocal of the time constant,  $\tau = c/m$  where  $c$  is viscous coefficient of air.

Accordingly,

$$\text{The problem is stated as follows: } \min_{h_{uav}} E \quad (3.18)$$

$$\text{Subject to constraint 1: } v_{uav} = v_{max} \quad (3.19)$$

$$\text{constraint 2: } u(0) = u_I, u(T) = u_F \quad (3.20)$$

$$\text{constraint 3: } E_{ET}(h_{uav}) \geq E_{TH} d^2 \quad (3.21)$$

The problem constraints may be restated as:

$E_{ET}(h_{uav})$  should be larger than the threshold energy ( $E_{TH}$ ) of the GNs times  $d^2$  for it to be detectable, which is  $h^2/\sin^2\theta$  where  $\theta$  is the elevation of the UAV (3.21), due to inverse square law of power transmission.

The velocity is presumed to be maximal (3.19), and the starting and ending positions of the UAV to finish the mission are  $u_I$  and  $u_F$  (3.20).

If the energy function is quadratic and the state equation is linear, this combination may be solved with the help of Matlab using a linear quadratic regulator design. The design calculates the UAV's range/position  $h$  where the Energy function is at its optimum. However, these assumptions are not necessary for the purposes of this thesis.

The following Table 3.4 lists the variables defined in this section for ease of reference.

Table 3.4: Variables defined in Energy function formulation

<b>Constants and Variables</b>	<b>Definition</b>
$m$	UAV mass
$c$	Viscous friction of air
$h, h_{uav}$	UAV altitudes
$\dot{h}, v, v_{uav}, v_{max}$	UAV velocities
$\tau = 1/a$	Time constant = $c/m$
$E, E_{TH}, E_{Tot}$	Energy function, Threshold energy, Total of charging and transmission energies
$L$	Lagrangian
$T$	Kinetic energy
$V$	Potential energy

### 3.4. Dynamic Optimization Models for Optimal Trajectory Design

There are many different engineering disciplines that experience challenges of optimization. In many cases, they are vulnerable to non-linear differential and algebraic models as well as other process restrictions. It is necessary to have an efficient and adaptable implementation of numerical algorithms for their solution and for their formulation to be suitable for the usage of methods that are based on dynamic optimization. The process of constructing intelligent strategies for the purposes of result prediction with the use of mathematical models of differential and algebraic equations is referred to as dynamic optimization. In order to undertake this kind of process, one may choose from a large number of different tools and techniques (Caspari et al., 2019). However, most if not all physical and other systems are based on a linear physical model and a quadratic cost or energy function and such is the case in this thesis. Solutions to this kind of problem are well rehearsed in the literature and standard methodologies relating to linear quadratic regulation (LQR) are well established. Nevertheless, the methods described below such as extremum seeking and optimum sliding mode are also applicable to non-linear state models and cost/energy functions that are not necessarily quadratic. These methodologies applied here will also work for non-linear systems and cost functions of any order, provided that an optimum exists.

Matlab Simulink is used in this thesis to simulate solutions for the dynamic optimization techniques used since it was readily accessible and compactible with the aforementioned methodology and implementation in section 3.3.

#### 3.4.1 Extremum Seeking Optimal Trajectory

Extremum seeking control is underpinned by the Theorem of Averages, which states that a T-periodic signal can be represented by its average value over the period T, i.e.:

$$\dot{h} = f(h, u, t) \quad (3.22)$$

is proportional to its 'average' value to within  $O(\epsilon)$ , where  $\epsilon > 0$ ,

$$\dot{h}_{eq} = \frac{1}{T} \int_0^T f(h, u, t) dt \quad (3.23)$$

Note that this is the state equation that represents the physical-dynamic system and it is not necessarily linear. In the case of the UAV, if this is also the input signal  $u$  that is fed to the

developed Simulink model in Figure 3.8 then the system is linear and system dynamics of the UAV are simply represented by an integrator.

In a Taylor series, the input to the integrator ( $E(h) + a \sin \omega t$ ) in Figure 3.8 can be expanded as follows:

$$\dot{h}_{\text{eq}} = \left( E(h) + a \sin \omega t \cdot \frac{\partial E}{\partial h} + \frac{1}{2} a^2 \sin^2 \omega t \cdot \frac{\partial^2 E}{\partial h^2} + O(a^3) \right) a \sin \omega t \quad (3.24)$$

Using the Theorem of Averages, it follows by integration that:

$$\dot{h}_{\text{eq}} = \frac{\omega a^2}{2} \frac{\partial E}{\partial h} \quad (3.25)$$

As a result, the stationary point of  $E$  is an equilibrium point of the system, as demonstrated in (3.25) and can be proven to be stable (Lehman and Weibel, 1999; Krstić and Wang, 2000) if  $\frac{\partial^2 E}{\partial h^2} < 0$ , the criterion for a maximum, is met. The greater the perturbation, the sooner the maximum is achieved. The block diagram of the extremum seeking control is represented in Figure 3.8b; Note that there is no requirement for  $E$  to be quadratic. In the example below,  $E$  is the cubic function

$$E(h) = 250 h^3 - 250 h^2 + 70h - 8$$

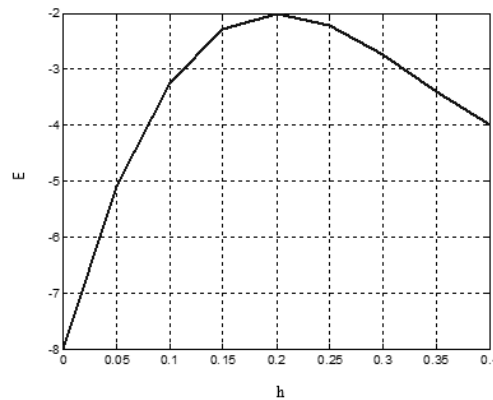


Figure 3.8a: Cost function  $E$



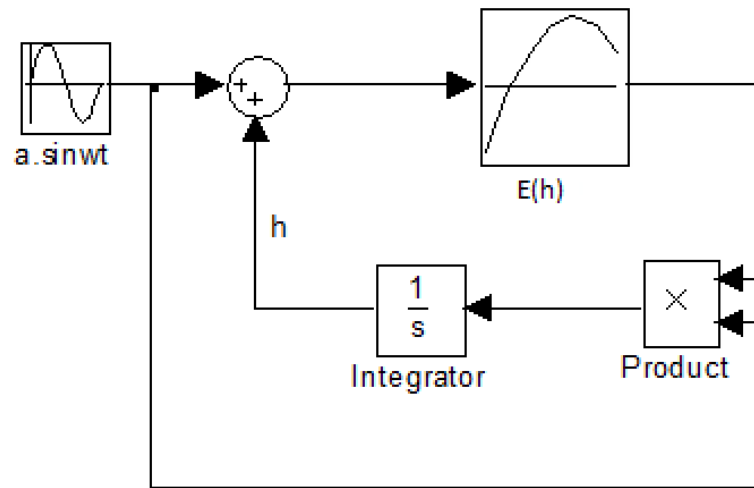


Figure 3.8b: Block diagram of Extremum seeking control

The results of the optimization are shown below, clearly reaching a maximum of  $E$  clearly at  $h = 0.2$

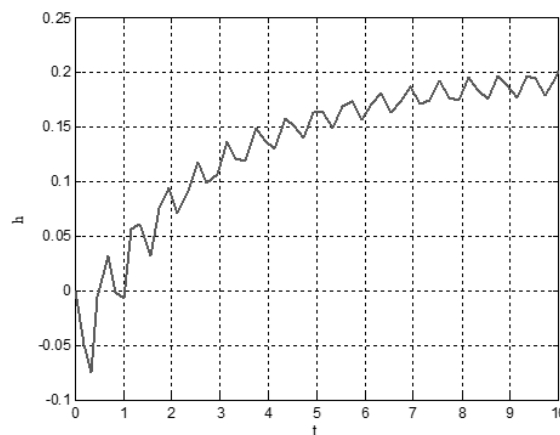


Figure 3.8c: Optimal equilibrium

### 3.4.2 Sliding Mode Optimal Trajectory

A more robust convergence to the optimum may be possible by adopting sliding modes (Aarsnes et al., 2019; Sbarciog et al., 2020), in which the necessity for perturbation of the state  $h$  and input  $u$  is partially eliminated by switching.

Recognizing that  $E(h)$  is independent of inputs and is at the optimum when it resembles a monotonically increasing function of time alone, or a ramp  $r(t)$ , allows one to build an optimal

sliding mode towards which the energy can be made to converge. Thus, the definition of a potential sliding-mode is as follows:

$$s = E - r = 0 \quad (3.26)$$

A switching control could then direct the system performance parameter  $E$  towards  $r(t)$ . Here, the switching gain  $k$  is used to force this outcome for a state model simplified to an integrator as in the example above;

$$u = -k \operatorname{sgn}(E - r) \quad (3.27)$$

$$\dot{h} = u \quad (3.28)$$

By defining the Lyapunov function  $V$  as the energy of the sliding mode and replacing (3.26), (3.27), and (3.28), the sliding mode existence requirements are as follows:

$$V = \frac{1}{2} s^2 \quad (3.29)$$

For the sliding-mode to be stable, this energy function must always be decreasing. Thus:

$$\therefore \dot{V} < 0 \quad (3.30)$$

$$\therefore s \dot{s} < 0 \quad (3.31)$$

$$s \dot{s} = s(\dot{E} - \dot{r}) < 0 \quad (3.32)$$

$$s(E_h \dot{h} - \dot{r}) < 0 \quad (3.33)$$

$$s(E_h u - \dot{r}) < 0 \quad (3.34)$$

$$u > \dot{r} / E_h \quad (3.35)$$

$$\text{Thus, } k > \left| \frac{\dot{r}}{\frac{\partial E}{\partial h}} \right| \quad (3.36)$$

The partial derivative of  $E$  is also forced to be positive since a monotonically increasing function  $r(t)$  is being followed. Equation 3.36 establishes a condition on the switching gain  $k$

to maintain a stable optimal sliding mode. This solution is depicted in the block diagram of Figure 3.9:

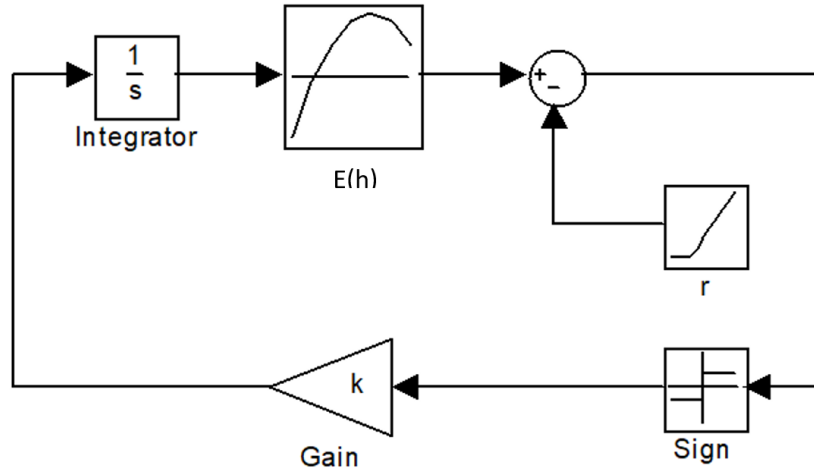


Figure 3.9: Block diagram of Extremum seeking sliding control

The optimal sliding algorithm can be modified by constraining the sliding mode sinusoidally and updating the system input as follows:

$$u = -k \operatorname{sgn} \sin \beta s \quad (3.37)$$

Substituting  $\sin \beta s$  for sigma ( $\sigma = \sin \beta s$ ), the Lyapunov function (3.29) is modified as

$$V = \frac{1}{2} \sigma^2 \quad (3.38)$$

Similarly, the stability criteria will be updated as below:

$$\dot{V} = \sigma \dot{\sigma} < 0 \quad (3.39)$$

$$\beta \sin \beta s \cos \beta s \dot{s} < 0 \quad (3.40)$$

$$\frac{\beta}{2} \sin 2\beta s \dot{s} < 0 \quad (3.41)$$

$$\approx \frac{\beta}{2} 2\beta s \dot{s} < 0, \text{ for } s \approx 0 \quad (3.42)$$

$$\text{or } \beta^2 s \dot{s} < 0 \quad (3.43)$$

This results in the same conditions (3.31-3.36). The solution is demonstrated in Figure 3.10b below, where  $\beta s$  and  $\beta \dot{s}$  effectively replace  $s$  and  $\dot{s}$  in the Lyapunov function. This further results in a scaling of time, enabling easier tuning of the algorithm. Note that  $\beta = 2\pi/\alpha$ , where  $\alpha$  is a small positive tuneable parameter  $< 1$ , in this case 0.1.

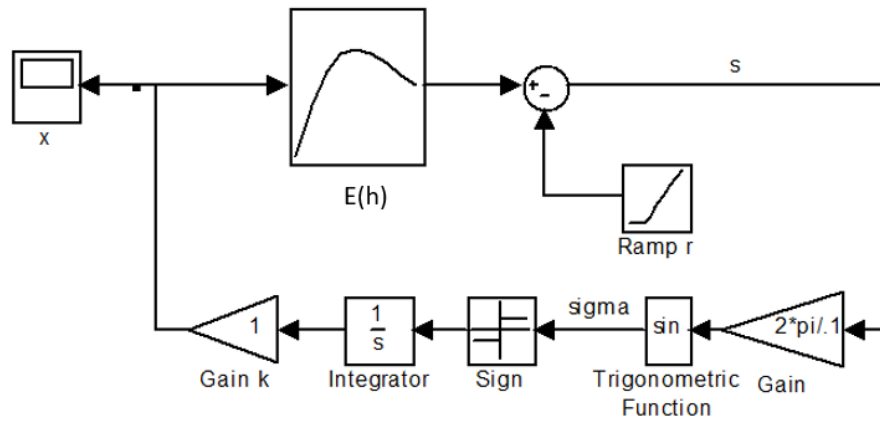


Figure 3.10a: Modified Block diagram of optimal sliding mode control

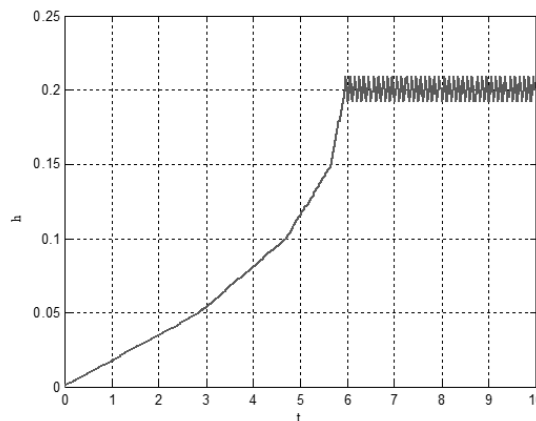


Figure 3.10b: Extremum Sliding Mode Control & Response

The optimum seeking sliding control will be implemented using a modified version of the model shown in Figure 3.10a in chapter 5 to understand the logic of the method.

### 3.5. Parameters and System Specifications

To implement the proposed optimisations to achieve the UAV's up, down, and hovering motion requirements, rotary wing beamforming on board UAV will be employed. Additionally, a three-dimensional view of the users on the ground as well as the UAV's

trajectory in an uneven plane is adopted. Libellium water quality sensors were tested and characterised in case of the need for simulation using Matlab. Similarly, the frequency ( $f$ ) selection and antenna design to implement beamforming is analysed and simulated using Matlab equations and sensorArrayAnalyzer toolbox as mentioned in section 3.2.1. All the parameters used for the implementation of the simulated model are tabulated in Table 3.5. The speed of the UAV ( $v$ ) will be set at a maximum based on the research of Yang et al. (2020) and power coefficient ( $PCoeff$ ) value is set to a maximum of 10 for the energy conversion efficiency in an ideal environment. The required power ( $ReqPower$ ) and data transmission power ( $P_{DT}$ ) of the GN's were setup based on the literature work using Libellium water quality sensors (Libellium.com, 2022).

Table 3.5: Parameter set up for the simulation of UAV enabled WPCN

<b>Parameters</b>	<b>Values</b>
No. of GN's	40
Speed of light ( $c$ )	$3 \times 10^8$ m/s
Speed of UAV ( $v$ )	30 m/s
Frequency ( $f$ )	1.5 GHz
Power coefficient of the UAV ( $PCoeff$ )	10
Transmit Power of UAV ( $P_T$ )	10 W
Required Power of GN ( $ReqPower$ )	5 mW
Data Transmission Power ( $P_{DT}$ )	0.5 mW

### 3.6. Summary

In this chapter, a system model design of the application scenario is introduced in section 3.1 for a WDS in a WPCN which make use of the concept of 3D beamforming to focus the energy signals to the terminal GNs in a terrain. The GN's use this energy to transmit data to the uplink by implementing the Lora protocol. The doubly near far problem of using the fixed base stations is resolved using a UAV which acts as a flying base station in this model. A

mathematical design of the uplink and downlink communication model followed by the problem formulation is presented in section 3.2. In section 3.3, the methodology to address the static optimization problem is proposed, whereas two separate strategies for solving the dynamic optimization subject to the constraints of the UAV physical model were demonstrated in section 3.4. All system parameters and specifications have been addressed and tabulated in section 3.5.

## CHAPTER 4

### THE DOME PACKING METHOD FOR ENERGY

### OPTIMIZATION OF GROUND NODES AND UAV IN WPCN

#### 4.1. Introduction

According to the literature review of Chapter 2, the proliferation of IoT devices in the WDS consumes a significant amount of the total energy for wireless communication. The previous Chapter 3 outlines the proposed optimization strategies, their mathematical formulation and design methodologies to be utilized to address this issue. It also informed how the WPCN's energy-efficient communication system was to be developed. The implementation of the proposed dome packing method will now be covered in detail in this chapter. By hovering at an optimal position to maximise the energy throughput, the communication between the UAV and the GNs offer both a method of charging and also data transmission to and from the GNs. This method could be suitable for emergency charging and data collection in critical situations such as sudden spread of water illness, contamination owing to leakage and flooding or other scenarios in which the WDS becomes inaccessible.

#### 4.2. Dome Packing Method for Optimal Energy Transfer

The Dome packing method consists of implementing 3D clustering to pack the GN sensors as discussed in section 3.3.1 and calculating the optimal number of clusters at  $k = 6$  using elbow method discussed in 3.3.2.1 and applying a 3D beamforming method to charge the GNs using the downlink communication design, as discussed in section 3.2.1. These two methods are combined to develop the Dome packing method.

The dome packing method involves fitting  $M$  domes into a simulated space with a radius of  $R_c$  to achieve the highest possible packing density as represented in Figure 3.2. These domes do not intersect one another throughout the packing process. This enhanced 3D K-means method also organises the GNs into a uniform pattern based on the detectivity of the beam by

the sensors.. In addition to packing and grouping the GNs and the 3D K-means technique also predict the cluster centroids at which the UAV (one UAV in this thesis) might be positioned in order to perform beaming. The following is the developed algorithm that is used to implement this dome packing approach.

---

**Algorithm 4.1:** Algorithm to implement Dome packing method (DPM)

---

1: Initialize the system parameter values  $u(t)$ ,  $g_n(t)$ ,  $h_{uav}$

2: Repeat **for**  $n=1:k$  Perform 3D k means clustering of the GN's and calculate the clusters and its cluster centroids ( $c1 \dots cx$ )

3: **end**

4: **Repeat**  $n= c1:cx$ , Position the UAV at the cluster centroid

5: Calculate beamforming range based on the antenna array to find  $h_{uav}$  from the cluster centroids

6: **If** GN's are unreachable **then**, calculate  $\Delta (u_{\Delta x}, u_{\Delta y}, u_{\Delta z})$  which will be the change in position and the UAV will be repositioned until a LoS is established.

7: **else**

8: **goto** step 4

9: **end**

---

#### 4.2.1 Implementation of 3D K-means

The three-dimensional clustering using the K-means algorithm of 3D coordinates is required to group the GNs in order to implement the 3D Beamforming technique. The horizontal position of the UAV at time  $t$ , the fixed positions of the GNs, and the height of the UAV are represented in algorithm 1 by the variables  $u(t)$ ,  $g_n(t)$  and  $h_{uav}$  respectively. The following is the detailed procedure for applying the K-means method:



---

**Algorithm 4.1a:** Algorithm to implement 3D K means

---

1. Choose  $k$  data points from  $g_n(t)$  as initial centroids.
  2. **for** each data point, compute the distance to each centroid  $C_n$  using Euclidean norm  
$$\text{dist}_n = (\sum_{i=1}^n |g_n(t) - C_n|^2)^{1/2}$$
  3. Calculate the index and values of the nearest centroid
  4. **end**
  5. Recompute centroids using current cluster memberships
  6. **for**  $i=1: C_n$
  7. find the points in each of the existing clusters and compute row-wise mean to calculate the new centroid  $Ce_n$
  8. **end**
  9. **if** UAV's minimum height ( $h_{\text{uav}}$ ) is not above 30 m to earth centroid value
  10. **then**,  $Ce_n(z) = Ce_n(z) + 30$  where  $z$  represents the height coordinates of the new cluster centroid.
- 

In Algorithm 4.1a, the 3D clustering using K-means is applied to find an initial optimal position of the UAV for downlink communication to charge the GNs. By considering each of the data points, the Euclidian distance from each of the initial centroids is calculated to compute the nearest centroid for each GN. Based on the newly calculated cluster, the centroids are recomputed. Since it is an iterative method, a maximum of 1000 iterations are used during the simulation. This algorithm takes into account the assumption that the UAV should be at a minimum flying height of 30 m in order to provide people with safety while also reducing the risk of obstacles and damage and that is the reason to add it along with the centroid value ( $Ce_n(z)$ ).

## 4.2.2 Implementing 3D Energy Beamforming

---

**Algorithm 4.1b:** Algorithm to implement 3D Beamforming and find beam range

---

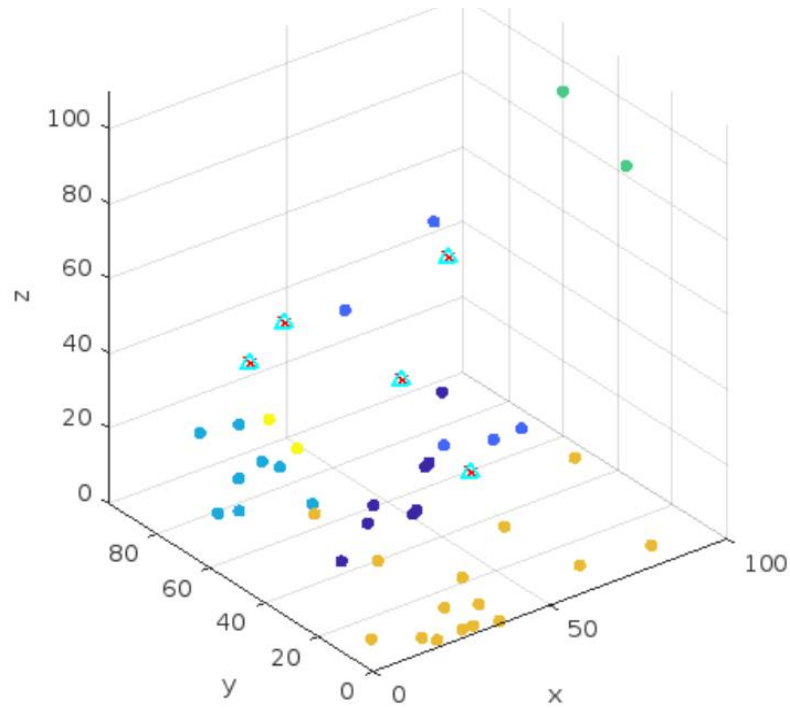
1. Compute the horizontal (H), vertical (V) and diagonal (d) distances using  $Ce_n$  and  $g_n(t)$ .
  2. **Then**, calculate  $\theta \leftarrow \cos^{-1}\left(\frac{V}{d}\right)$ ,  $\phi \leftarrow \tan^{-1}\left(\frac{H}{V}\right)$
  3. Assign the constants  $\theta_{3dB}$ ,  $\phi_{3dB}$  and  $A_m$
  4. **function** Powercompute (H,V, d,  $\theta$ ,  $\phi$ ,  $\theta_{3dB}$ ,  $\phi_{3dB}$ ,  $A_m$ )
  5.  $\phi_{tilt} \leftarrow \tan^{-1}\left(\frac{H}{d}\right)$
  6.  $A(\theta, \phi) \leftarrow A_H(\theta) + A_V(\phi)$  calculate the beamwidth
  7.  $\alpha \leftarrow A(\theta, \phi)/2$
  8.  $HP\_BeamW \leftarrow d\sin(\alpha)$  range of the beam
  9. **return** HP\_BeamW
  10. **end function**
  11. **if** HP\_BeamW < -30
  12. **goto** step 6 algorithm1
  13. **else**
  14. TotalbeamStrength  $\leftarrow$  TotalbeamStrength+HP\_BeamW \*  $P_T$
  15. fligtime\_unit = ReqPower. / (HP\_BeamW \*  $P_T$ )
- 

The implementation of 3D Beamforming of step 5 is explained and formulated in 3.2.1 and the 3dB bandwidth of the horizontal and vertical patterns  $\theta_{3dB}$  and  $\phi_{3dB}$  are assigned to be -30dB and side lobe level attenuation  $A_m$  to 1000 for simulation purposes. All these values are selected based on the beam analysis performed and optimized as discussed in 3.2.1 using sensorArrayanalyser toolbox. The cluster centroids calculated using the algorithm 1b is used to calculate the half power beamwidth (HPBW) for Beamforming using  $A(\theta, \phi)$  which is the beaming angle directed towards the GN using equations (3.7) and (3.8). The UAV needs to realign its position if any of the GNs cannot be reached or if the power generated from the beam is less than -30 dB (1 microwatts) (a stronger beam requires less charging time) which

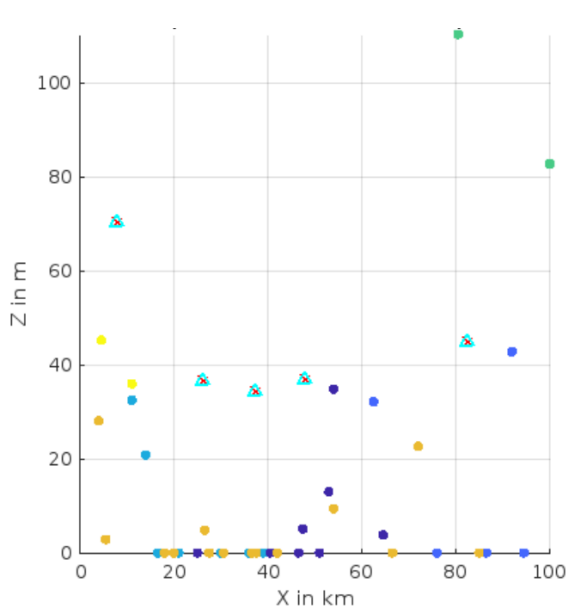
will be the checking a condition to verify whether a centroid is valid or not. The change in  $\Delta x$ ,  $\Delta y$  and  $\Delta h$  will be taken into account until a line of sight is established with the GNs when calculating the UAV's new location ( $\Delta x$ ,  $\Delta y$ ,  $\Delta h$ ) and is estimated based on the position of the GN and the area covered by the beam. Otherwise, the total beam strength will be calculated using HPBW and transmit power ( $P_T$ ), and `fligttime_unit` calculates how many time units will be required to charge each GN using the required power of the GN's (`ReqPower`), which make use of the parameters set in Table 3.2.

### **4.3. Analysis and Discussion of the Simulation Results**

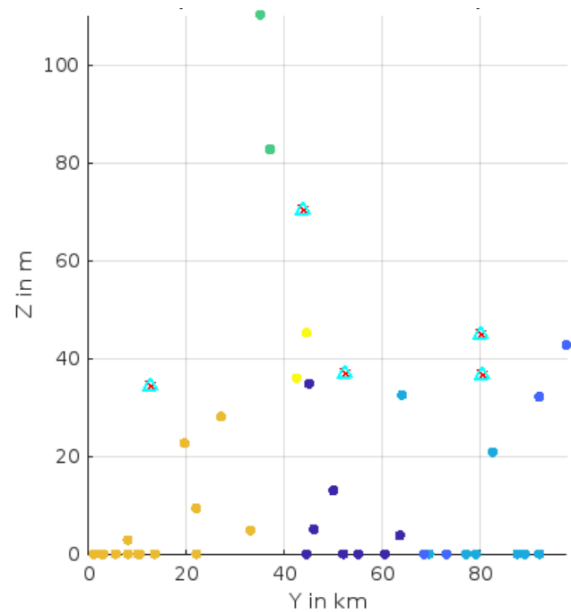
In this section, the implementation of the dome packing method to optimize the energy consumption of the UAV and the GN's will be discussed. Figure 4.1a illustrates the output that is produced as a result of implementing the proposed dome packing method for calculating the optimal position of the cluster centroids which establish the optimized hovering position through which the UAV will be navigating. In this illustration, 40 nodes that are situated in 3D space are clustered together using a 3D clustering approach. Each cluster is visualized as a collection of dots that are filled with different colours for each, and a cluster centroid in the form of a blue triangle marked with red cross. Figures 4.1b and c are visualisations depicting different perspectives of the clusters and their centroids in the  $xz$  and  $yz$  planes, respectively. The amount of time it takes to compute the implementation of the proposed method with the help of 3D K-means and the beamforming algorithm is less than 0.37 seconds. If the method has executed longer, which would have made impossible to implement the project in real time This demonstrates that the performance of the suggested method could be carried out within a time frame that is acceptable.



a) 3D view of the cluster and its centroids



b) Representation of clusters and centroids in XZ plane



c) Representation of clusters and centroids in YZ plane

Figure 4.1: Simulation results of calculating the centroids using 3D dome packing method

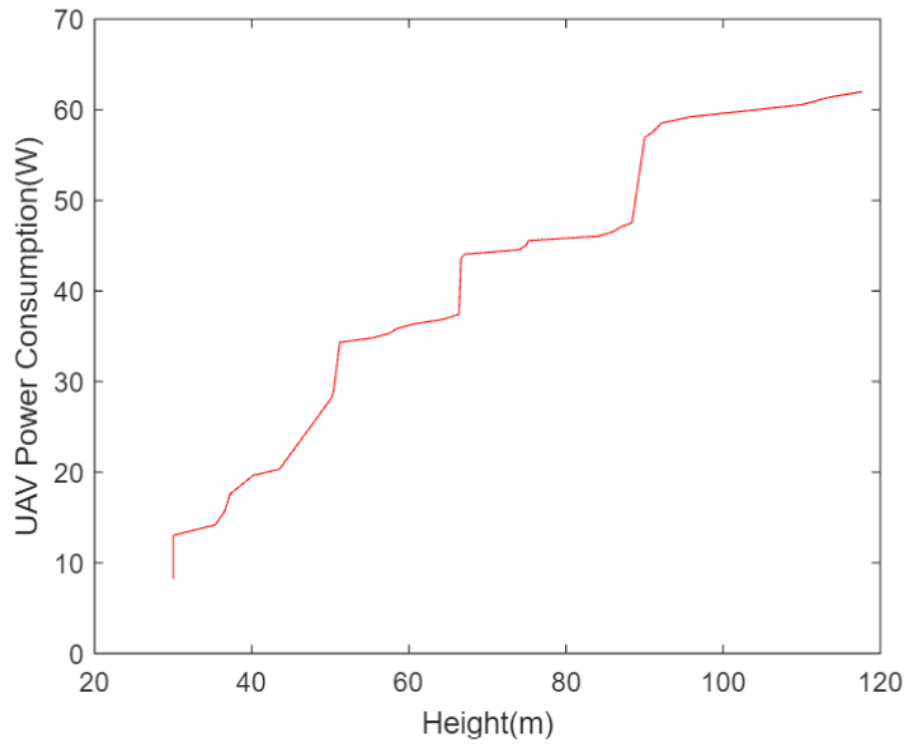


Figure 4.2: Power consumption vs height of the UAV

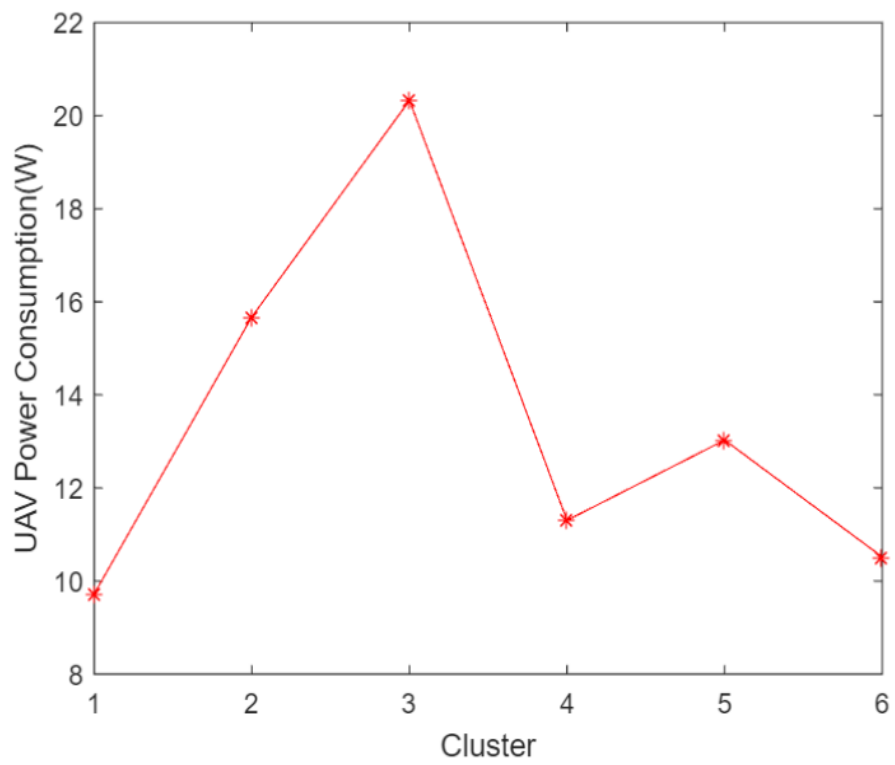


Figure 4.3: UAV power consumption vs clusters

The results of the simulation shown in Figs. 4.2 and 4.3 offer a clearer picture of how the energy consumption of the UAV fluctuates depending on the change in height and also dependent on whether or not it is servicing various clusters as it is travelling along its flight route. It can be seen in Figure 4.2 that the amount of energy that the UAV uses up throughout the flight has a direct impact on the change in height that the UAV experiences during the mission. On the other hand, beginning at Figure 4.3, the amount of energy that is used by the UAV shifts at various clusters since it is dependent on the number of GNs that are being served by the UAV. It is possible to conclude from Figure 4.3 that the number of GNs found in cluster 3 is higher compared to other clusters. The GNs were randomly positioned as the placement of nodes is not a part of this research, thereby executing the proposed method, which determines the number of nodes in each cluster.

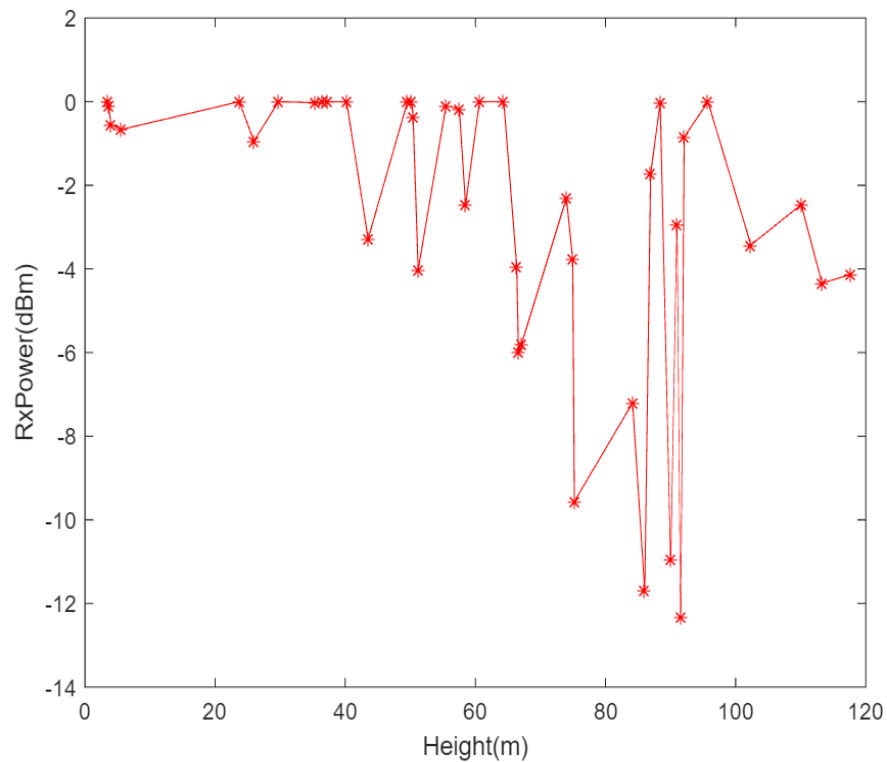


Figure 4.4: Power harvested depending on height  $h_{uav}$  using  $N = 24$  antenna modules

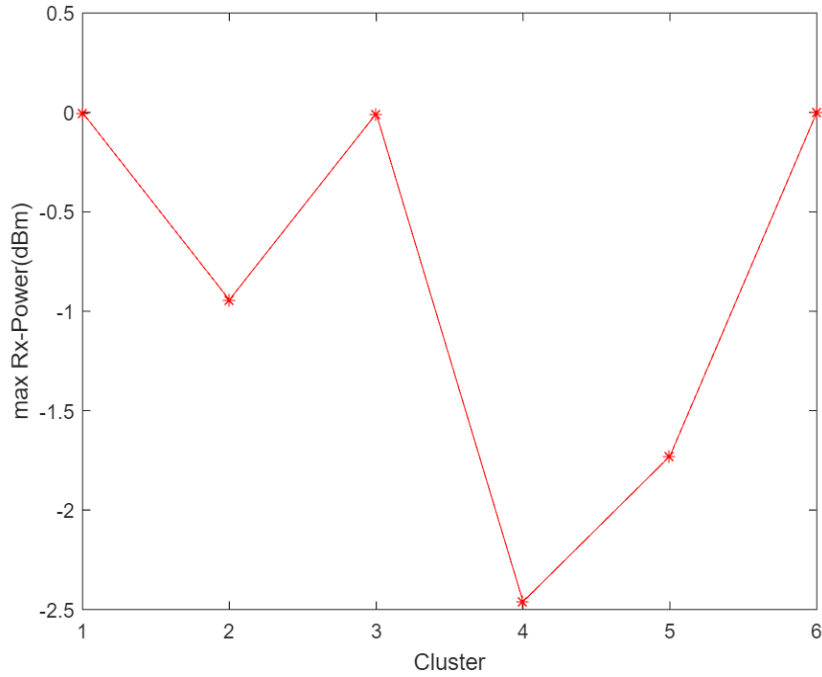


Figure 4.5: Energy harvested by the GT nodes based on clusters and its received power

Figure 4.4 is a visualization of the quantity of harvested power that is gathered by the GNs at a height  $h_{uav}$  from the UAV with  $N = 24$  antenna components analysed using Matlab's Sensor Array Analyser as discussed in section 3.2.1. It also shows that the energy harvested during the mission has a direct impact on the flying height of the UAV as well as the number of GNs in that cluster. The output power is measured in decibels-mW, and hence the term "decibel-milliwatt". Every 3 dBm increase in output power approximately doubles power, and every 10 dBm increase in output power amplifies by ten times the power. Similarly, a power level of 0 dBm is equivalent to 1 mW of power (Downey, 2013). As a result, clusters 1, 3 and 6 receive around 1mW of power during beaming, whereas the other clusters receive less power around 0.6 mW. Both Figure 4.4 and Figure 4.5 illustrates how the amount of energy that can be gathered by beaming to each of the GN clusters at time  $t$  seconds, varies dependent upon the clusters and height measured in metres. The RxPower variation in Figure 4.4 between 65 and 95 m is due to the less number of nodes in that cluster and the same can be observed at cluster 4 in Figure 4.5. The following section evaluates the proposed dome packing method by making use of the F1 score, precision and computation time.

### 4.3.1 Evaluating the Dome Packing Method

In order to evaluate the dome packing method, a machine learning method is used which works by calculating Precision, Recall and F score, the first requirement is to calculate the clusters and classes used in the simulation. As the elbow method is being used, the number of clusters is optimised to 6 as discussed in Chapter 3. A class is the position of GN's based on how it is classified and to calculate the classes, the region where the GN's are located is equally divided into regions  $x = [0 \ 33]$ ,  $y = [0 \ 33]$ ,  $x_1 = [34 \ 66]$ ,  $y_1 = [34 \ 66]$ ,  $x_2 = [67 \ 100]$ ,  $y_2 = [67 \ 100]$ , such that the cluster result table will be a KxP matrix, where K is the number of clusters and P is the number of classes, as represented in Figure 4.6.

Classes  $\longrightarrow$

Clusters $\downarrow$		$P_1$	$P_2$	.....	$P_p$
	$K_1$	$a_{11}$	$a_{12}$	.....	$a_{1p}$
	$K_2$	$a_{21}$	$a_{22}$	.....	$a_{2p}$
	.....			.....	
	$K_k$	$a_{k1}$	$a_{k2}$	.....	$a_{kp}$

Figure 4.6: KxP matrix

The term "akp" refers to the total number of GNs that have been grouped into the kth cluster and P are intervals or classes in this context. Now, in order to assess how effective the suggested dome packing technique is, the KxP matrix together with the following criteria are being used in the simulation analysis: Precision, recall, and the F1 score are the requirements that must be met. Precision determines, for each cluster, the class that has the most objects that have been assigned to it or how correct classification of instances are measured . After that, the GNs in each cluster are added together, and the total is then divided by the total number of objects that are clustered (Mallawaarachchi, 2020). The calculation is as follows:

$$\text{Precision} = \frac{\sum_k \max_p \{ a_{kp} \}}{\sum_k \sum_p a_{kp}} \quad (4.1)$$

The cluster that has been assigned the most GNs for each class is identified as the one to use in the calculation of Recall. The total number of clustered and unclustered nodes is then



summed up, and the result is added to the maximum number of nodes for each class, which is then divided by that total. It also provides a calculation of any non-classified instances in the matrix.

$$\text{Recall} = \frac{\sum_p \max_k \{ a_{kp} \}}{\sum_k \sum_p a_{kp} + U} \quad (4.2)$$

where U will be the number of unclustered GN's in the simulation graph.

The harmonic mean of Recall and Precision is the F-score which is calculated using the equation (4.3).

$$\text{Fscore} = 2 \times \frac{\text{Precision} \times \text{Recall}}{\text{Precision} + \text{Recall}} \quad (4.3)$$

In the process of determining the overall efficiency of the approach, F-score is required, and for this, the precision and recall values need to be calculated. A good Fscore should provide at least an average of precision and recall. The evaluation of the dome packing method is presented in Figure 4.7.

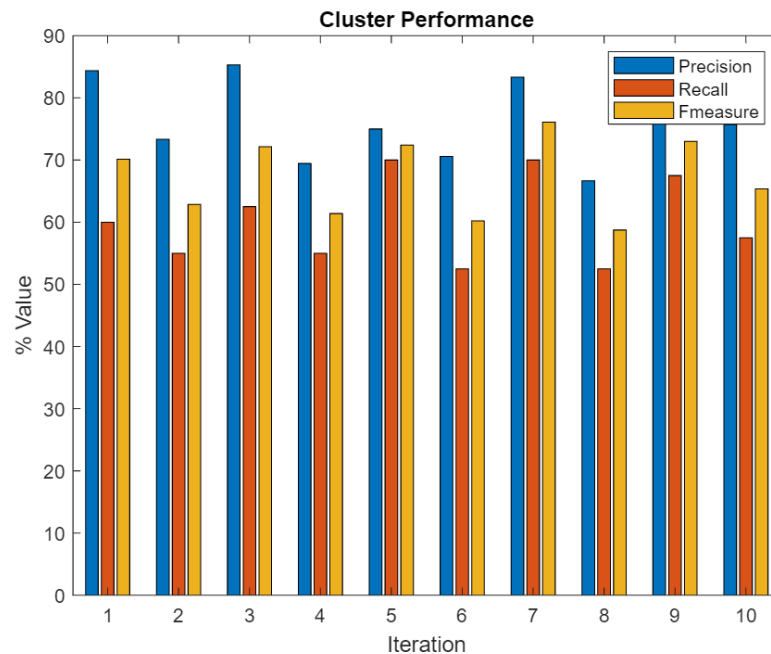


Figure 4.7: Performance of Dome packing method

In Figure 4.7, the Precision reaches a maximum of 88% with higher intra-cluster similarity and maximum Recall and F scores are 70% and 75%, respectively based on 10 case studies.

The average of Precision and Recall calculates to 73% which is around 75%, the value that were calculated separately. Furthermore, it shows that a cluster's characteristics are more comparable to one another than to those of other clusters. Therefore, the algorithm seems to plausibly implement a static optimization solution based on the simulation. The algorithm performs 1000 iterations with different recalculated centroid points to calculate an optimal centroid point of the clusters. Using this analysis method, the number of clusters predicted using the proposed technique causes the overall accuracy to rise while recall falls. The Figure 4.8 supports the efficiency of the proposed dome packing algorithm with a computation time of 0.47 seconds.

```
Command Window
-----
3D k-Means will run with 6 clusters and 40 data points.
Domepacking used 1000 iterations of changing centroids.
Computation time for Domepacking: 4.715990e-01 seconds.
>>
```

Figure 4.8: Computation time using Dome packing method

By contrasting the proposed method with a solution that does not use the dome packing method i.e., without implementing 3D clustering and beamforming, Figure 4.9 illustrates the extent to which the proposed method is plausible. As can be observed from figure, the power consumption of the suggested method is significantly more efficient than that of the non-dome packing approach.

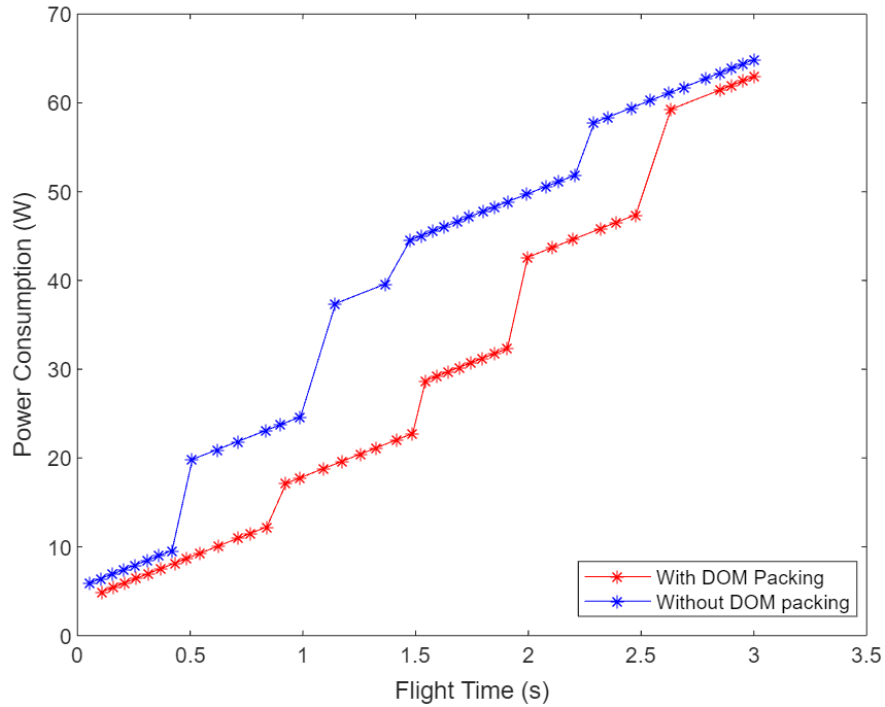


Figure 4.9: Comparison of UAV power consumption with and without Dome packing

#### 4.4. Summary

Communication using 5G networks relies heavily on a technology called beamforming. Beamforming allows an array of antennas to dynamically modify the direction and down-tilt towards receivers by rotating the antenna pattern. This is accomplished by tilting the array. Moreover, in order to perform the processing, communication, and decision making, the WDS's IoT devices require a significant amount of power. Based on this, the primary objective of this simulation is to come up with a strategy that will enable minimization of the energy during communication. In this chapter, a dome packing method that combines positioning of a UAV with respect to 3D clustering using beamforming is used to optimise the energy consumption of the UAV by optimally packing the sensors or GNs and finding an ideal hovering position for the UAV to reduce energy consumption while minimising the total flight time. The proposed method was evaluated using an F score based on Precision and Recall clustering criteria.

## CHAPTER 5

# OPTIMAL TRAJECTORY DESIGN FOR THE UAV IN THE WPCN

### 5.1. Introduction

In this chapter, the trajectory is designed initially by using the static optimization methods, where the approaches and formulation were discussed in Section 3.3. Then the algorithms developed using extremum seeking and sliding mode methods are used to dynamically optimize hovering points. Finally, both static and dynamic methods are combined for overall optimization of the trajectory, with respect to energy cost functions.

### 5.2. Static Optimization for the Trajectory Design

This method of optimization minimizes the distance from the GNs and cluster centroids and will be used to build an optimised trajectory using the computed ideal hovering points calculated and simulated in Chapter 4. Thereafter, the recycle time of the UAV will be optimised in a manner that is analogous to the Traveling Salesman Problem (TSP). The total flying time is determined from the recycle time, which takes into account the delays that occur between the several rounds flown by the UAV before the mission is complete. This contributes to keeping the flying time as short as possible without any complications such as power loss, data loss etc.

The Algorithm 5.1 provides a precise outline of the procedures that must be undertaken in order to optimize the recycle time and, as a result, reduce the cost of the UAV's route. This approach uses the  $distF$  variable, which has an initial value set to  $\alpha$ , to determine the optimal distance. The value of the loop variable in 'iv' in Algorithm 5.1 is initially set to 1. Using the loop conditions, over 1000 iterations, a random permutation sequences for the six cluster centroids (C) are created with the shortest amount of flight time (bestseq). Following this, step 6 will be used to determine the shortest distance, with the locations of the GNs and the cluster centroids serving as inputs. If the value that is computed for  $dist$  is smaller than the value that is calculated for ' $distF$ ', then the new optimum distance is set as ' $distF$ ', and the best sequence that may be used by the UAV to produce an optimal trajectory is saved. This

approach, which is based on finding the minimum distance travelled, is used to optimise the amount of energy that the UAV consumes.

---

**Algorithm 5.1: Algorithm to optimize recycle time**

---

1. Initialize distF variable to  $\sigma$  and a loop variable iv set to 1.
  2. **while** iv < 1000
  3. Set a random sequence (seq) using randperm(k) function
  4. **for** ic = 0 : k
  5. **if** ic == 0
  6. dist = dist +  $(\sum_{i=1}^n |g_n(t) - C(\text{seq}(ic + 1))|^2)^{1/2}$
  7. **else if** ic == k
  8. dist = dist +  $(\sum_{i=1}^n |C(\text{seq}(ic)) - g_n(t)|^2)^{1/2}$
  9. **else**
  10. dist = dist +  $(\sum_{i=1}^n |C(\text{seq}(ic)) - C(\text{seq}(ic + 1))|^2)^{1/2}$
  11. **end**
  12. **end**
  13. **if** dist < distF
  14. **then**, distF = dist
  15. bestseq = seq
  16. **end**
  17. increment iv
  18. **end**
-

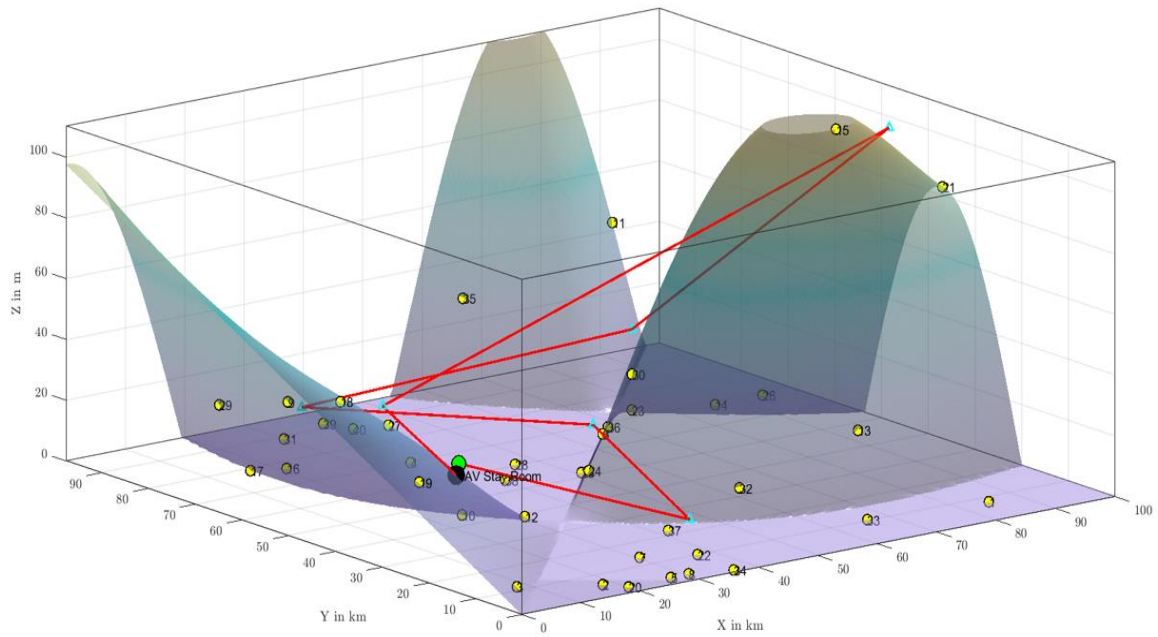


Figure 5.1: The optimized trajectory of the UAV on a 3D plane

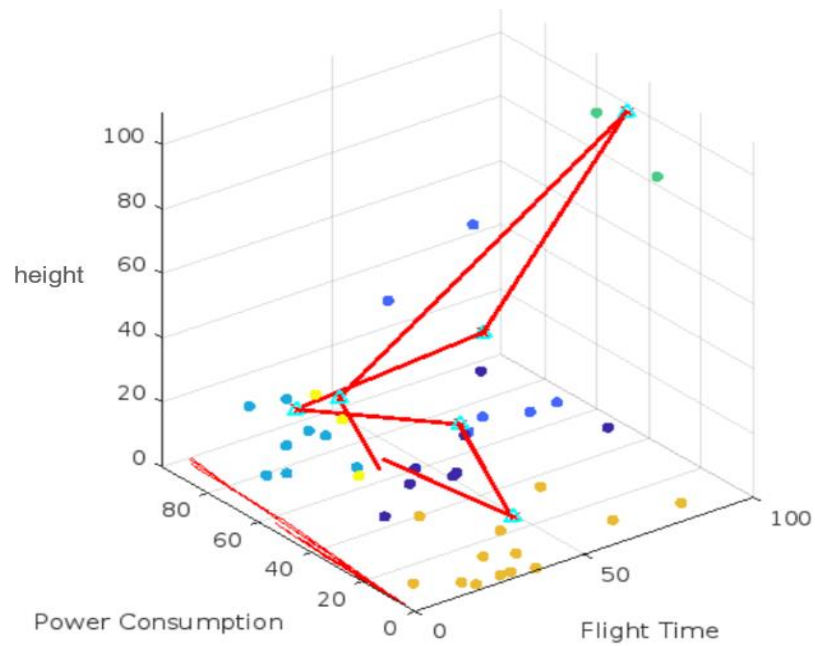


Figure 5.2: The optimized routing path of the UAV with power consumption

After utilising the aforementioned technique to calculate the optimum distances, the trajectory of the UAV is illustrated in Figure 5.1 as it travels through 3D space to reach its destination. The routing pathway that the UAV will take through these cluster centroids is determined by calculating the best sequential path. Figure 5.2 shows how the UAV's optimized trajectory is determined based on its height and how the power consumption is related to the flight time.

Based on this figure, it is also possible to compare the power consumption of optimized trajectory with other trajectories.

The overall flight time of the UAV may be determined with the use of Algorithm 5.2 below. The power coefficient value is set to 10 in this approach to calculate the power consumption of the UAV via the best efficient sequence of the trajectory. The goal of this calculation is to determine how much power the UAV uses.

In a similar fashion, both the power and ‘flighttime’ variables start off with a value of zero. In step 2, the loop will iterate the specified number of times, ‘numel’ = 6, which will determine the total number of elements in the array (bestseq).

Having determined the clusters using algorithm 1a described in Section 4.2, the following step is to compute the index of the best sequential order path using those determined clusters. In step 5, the distance (dist) from the sequential cluster centroids is determined by using the best sequential paths.

In step 6, the power consumption of the UAV is determined by utilising the computed distance (dist). In step 9, a loop is used to iterate and determine the power of the UAV, as well as its flying time and hovering time, when all of the indices of the sequential route will have been calculated.

In the following phases, the value that is returned by the function ‘flighttime\_unit’ is the number of time units that will be required to charge each GN in accordance with the energy specification requirement that it has. For instance, if each GN needs 5J for its functioning and the UAV can act as a beaming source and can supply 1J for 1 second, the UAV needs five flighttime\_units to fully charge a single GN that is part of a cluster. The computation of the flighttime\_unit has previously been covered in Algorithm 5.2 in Section 4.2.2. It is dependent on the charging time for the GN's, which in turn relies on the beaming strength of the UAV.

---

**Algorithm 5.2: Algorithm to calculate the total flight time**

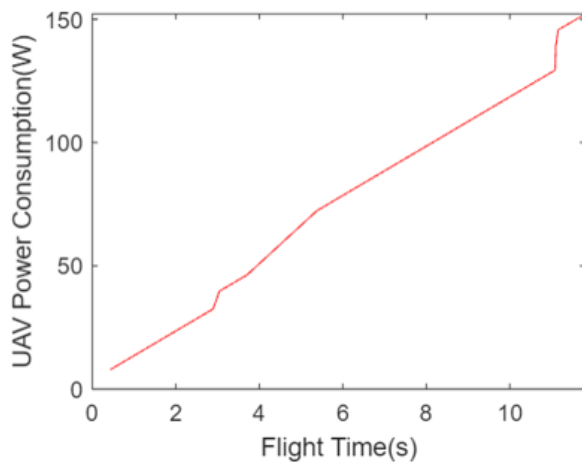
---

1. Initialize powercoeff to 10 and Power and flighttime to 0.
2. **for** ij = 1: numel(bestseq)
3. Find the index of the bestseq from the calculated cluster to variable ind
4. **if** ij < numel(bestseq)
5.  $dist = (\sum_{i=1}^n |C(bestseq(ij)) - C(bestseq(ij + 1))|^2)^{1/2}$

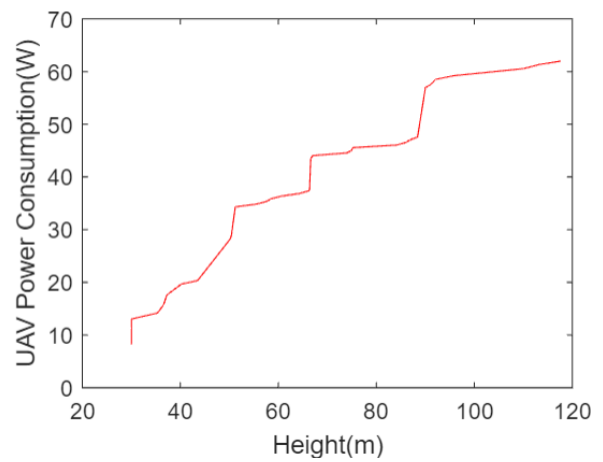
```

6. Power = Power + dist. * powercoeff / 100
7. end for
8. if (~isempty(ind))
9. for k = 1: numel(bestseq)
10. Power = Power + flighttime_unit(ind(k)). * powercoeff
11. flighttime = flighttime + flighttime_unit(ind(k))
12. hoveringtime = flighttime_unit(ind(k))
13. end for
14. end if
15. end

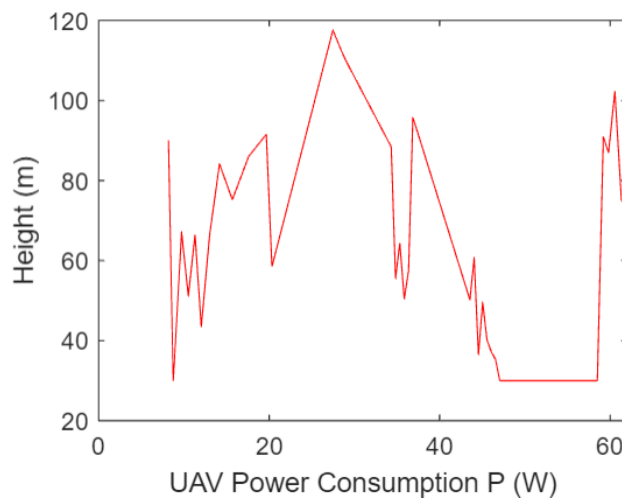
```



a) UAV power consumption vs flight time



b) UAV power consumption vs height



c) UAV power consumption based on clusters vs height

Figure 5.3: Power consumption of the UAV based on flight time and height



The rise in the amount of power required by the UAV as a function of flight duration and altitude is shown in this Figure 5.3. The power consumption of the UAV with respect to the flight duration and height while applying the algorithms is represented in Figures. 5.3 a & b. Figure 5.3c further illustrates how the amount of energy used by the UAV at each cluster with the number of nodes and how it varies when the height of the UAV is modified. The heights calculated for each cluster centroid using this method is represented as  $h_0$  in Table 5.1 and the values obtained are as follows:

Table 5.1: Height of the UAV at each cluster centroid

<b><math>h_0</math></b>	19.4345	23.1136	16.6705	106.5611	11.3139	46.4073
-------------------------	---------	---------	---------	----------	---------	---------

The throughput of the GNs based on the clusters is shown in Figure 5.4. As mentioned in Section 3.2.1, the purpose of the illustration is to offer an example of the quantity of data that will be provided to the UAV from each of the clusters by making use of the LoRa protocol.

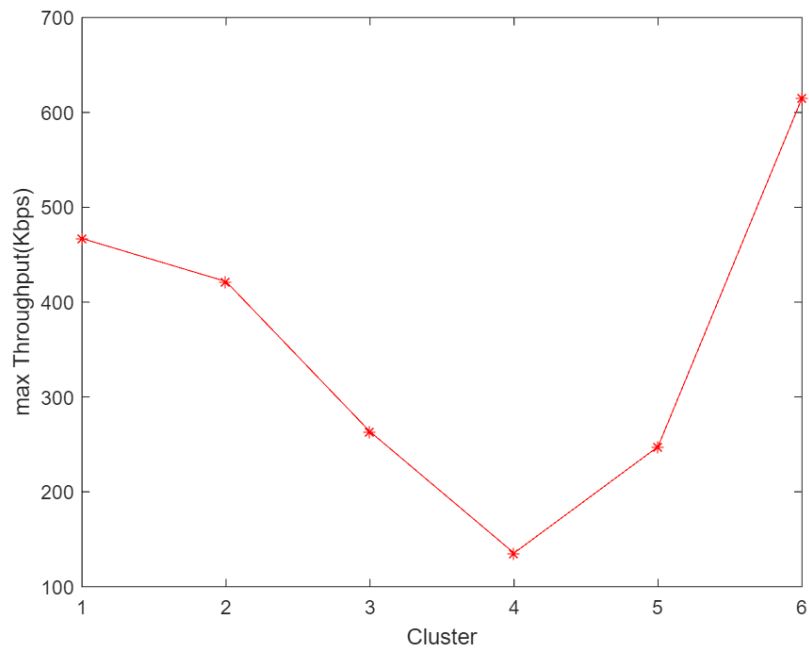


Figure 5.4: Throughput of the GN's based on clusters

### 5.3. Dynamic Optimization for the Optimal Height of the UAV

Dynamic optimization is performed by taking into account the UAV dynamics, which are not included in the static optimization discussed so far in this chapter. In this approach, the optimal height of the UAV is calculated based on both the output of the static optimization (which is the initial condition input to the dynamic optimization process) as well as the dynamics of the UAV. The UAV will then hover about a point calculated using dynamic optimization methods with the aim of optimizing the energy/power usage. The methodology of these dynamic optimization methods, i.e., extremum seeking and optimum sliding mode, have already been formulated in section 3.4. Before this can be applied, a dynamic model of the UAV itself must be formulated.

#### 5.3.1 Dynamic Model of the UAV

The physical state model of the UAV may be formulated as follows:

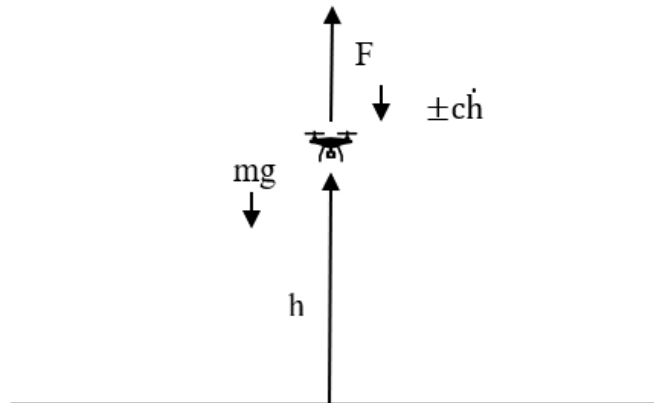


Figure 5.5: Schematic of the UAV

Figure 5.5 represents the dynamic model of the system. According to Newton's second law:

$$m\ddot{h} = F - c\dot{h} - mg \quad (5.1)$$

where  $m$  is the mass of the UAV,  $F$  is the force acting upwards,  $c$  is the viscous friction coefficient,  $\dot{h}$  the speed,  $\ddot{h}$  the acceleration,  $g$  is the gravitational constant and  $h$  is the height of the UAV, all of which are illustrated in Figure 5.5. Since  $c\dot{h}$  and  $mg$  act in the direction opposite to the force acted upon the UAV by its motor, they are of negative sign.

$$\text{Equilibrium condition: } F = mg, \ddot{h} = -\frac{c}{m} \dot{h} \quad (5.2)$$

$$\text{Therefore, } \dot{h} = -\frac{c}{m} h, \text{ and } h = -\frac{m}{c} \dot{h} \quad (5.3)$$

$$\text{Motor power, } P = F\dot{h}, \text{ so } F = \frac{P}{\dot{h}} = mg \quad (5.4)$$

$$P = mg\dot{h}$$

$$\dot{h} = \frac{P}{mg} \quad (5.5)$$

$$\text{Total power (} P_T \text{)} = P + P_{\text{(STATIC)}} \quad (5.6)$$

where  $P_{\text{STATIC}}$  is the power used by the UAV calculated from the static optimization methods.

### 5.3.1a Alternative model with the UAV's power rating

$$\text{Power, } P = F_m \dot{h} \quad (5.7)$$

$F_m$  is the UAV motor force, obtained from rotor radius and motor torque,

$$T_m = \frac{\text{Rated Power}}{\text{Rated Speed}} \quad (5.8)$$

$$\text{Or model input, } u = P \text{ instead of } F_m \quad (5.9)$$

The alternative model uses the power of the UAV as input rather than the traction force.

$$\text{Since } P = \frac{dE}{dt} = \frac{dE}{dh} \frac{dh}{dt} \rightarrow 0 \quad (5.10)$$

Simultaneously optimizing  $E$  and obtaining equilibrium equates to zero power. These are precisely the goals that were sought to be achieved by the extremum seeking controller introduced in chapter 3. Additionally,  $P$  may replace the sliding mode  $s = 0$ , also formulated later in that chapter.

Table 5.2 contains all the parameters that are now utilised to create the dynamic model to compute the optimum height and, therefore, the trajectory of the UAV. For the state model of

the UAV,  $h$  and  $\dot{h}$  are the designated states and  $A$  is the state matrix,  $B$ , is the input matrix and matrices  $C$  and  $D$  are unity and zero matrices in the state block.

Table 5.2: Parameter set up for dynamic optimization

Parameters	Values
Mass of UAV (m)	1 kg
Drag coefficient (c)	$1.5 \times 10^{-5}$
State model and values $\dot{x} = Ax + Bu$ $y = Cx + Du$ for A: $x = [h, \dot{h}]'$ , $\dot{x} = [\dot{h}, \ddot{h}]$ , $\ddot{h} = -\frac{c}{m}\dot{h}$ for B: $u = F_m \dot{h}$ , $F_m$ nominally 1 due to k for C: $y = h$	
A	$\begin{bmatrix} 0 & 1 \\ 0 & -c/m \end{bmatrix}$
B	$\begin{bmatrix} 0 \\ 1 \end{bmatrix}$
C	$[1 \ 0]$
D	$[0]$

### 5.3.2 Extremum Seeking Optimal Trajectory

The extremum seeking optimal trajectory (ESOT) was discussed in the methodology Section 3.4.1. The modifications described in the previous section, i.e., replacement of the integrator with the UAV dynamics state model and the input to this model by Power (Equation 5.10), simulate the optimal height of the UAV as in Figure 5.6.

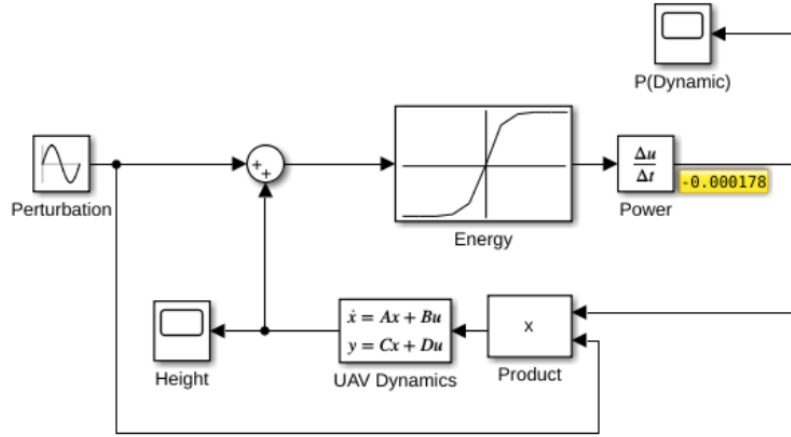


Figure 5.6: Simulink model for optimum seeking of height

The energy graph is a look up table constructed from the energy consumption of the UAV as represented as follows in equation 5.11.

$$\Delta E = mg\Delta h - \frac{1}{2}ma^2\Delta h^2 + E_{\text{Tot}}(h_{\text{uav}}) \quad (5.11a)$$

$$\Delta E = mg(h_{\text{uav}} - h_0) - \frac{1}{2}ma^2(h_{\text{uav}} - h_0)^2 + E_{\text{Tot}}(h_{\text{uav}}) \quad (5.11b)$$

Where  $h_0$  is the height of the cluster centroids calculated from the static optimization in Table 5.1. To compute the power output, the energy that is produced must first be differentiated. The result of the calculation in equation 5.10 is then applied to the product block together with a perturbation, which is also an additive input as per the algorithm described in Section 3.4. The optimum height is determined from an initial condition of  $h_0 = 46.4073$  m as in Figure 5.7. (Additional simulations for the other initial conditions of Table 5.1 may be found in Appendix C).

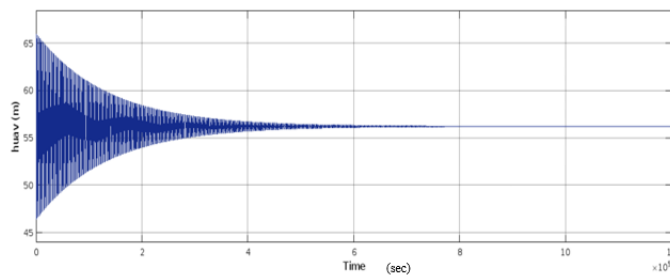


Figure 5.7: Optimized height using Extremum seeking for initial condition  $h_0 = 46.4073$  m

The simulation shows that an optimal height of 56.2 m is calculated about which the UAV hovers before remaining in that position and thereby optimize the energy consumption of the

UAV before completing the mission. This calculation would take a few seconds offline after which the UAV could fly directly to this position.

The zero-power performance of the system is illustrated in Figure 5.8 below where the power is optimizing to zero when the UAV is at an optimal position confirming a zero-power system.

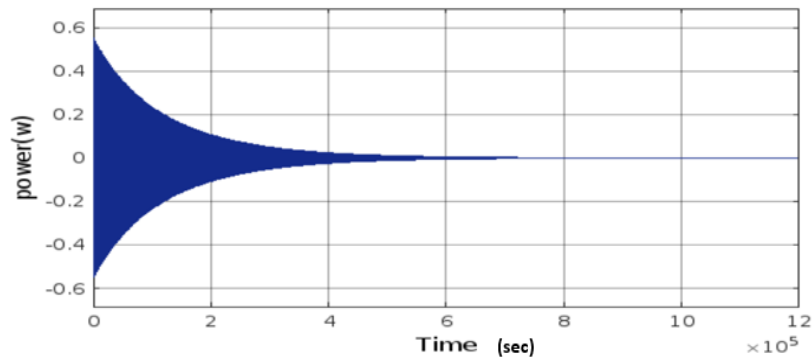


Figure 5.8: Power used by UAV when reaching the optimal height

Retuning of the perturbation parameters such as amplitude, frequency etc., however, affords the possibility of the dynamic algorithm operating in real time. The simulation in Figure 5.9 was undertaken with a perturbation amplitude of 0.05 and perturbation frequency of 100 rad/s. If these are changed to 0.5 and 10 rad/s, respectively, the following simulation is obtained for the same initial condition:

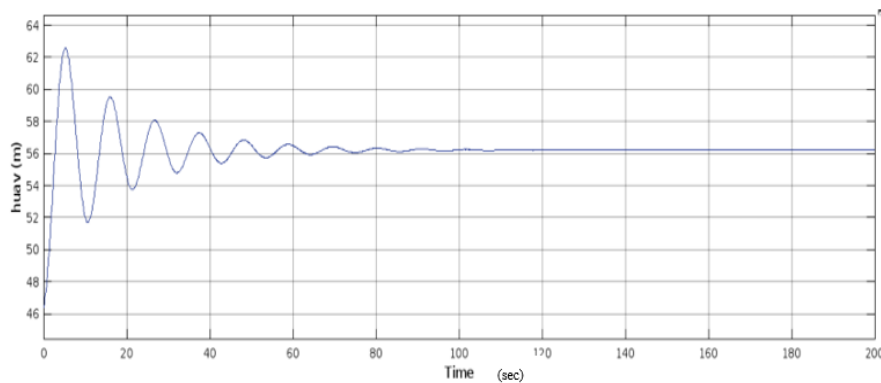


Figure 5.9: Optimized height using Extremum seeking after modifying perturbation

The zero-power performance is maintained as shown below:

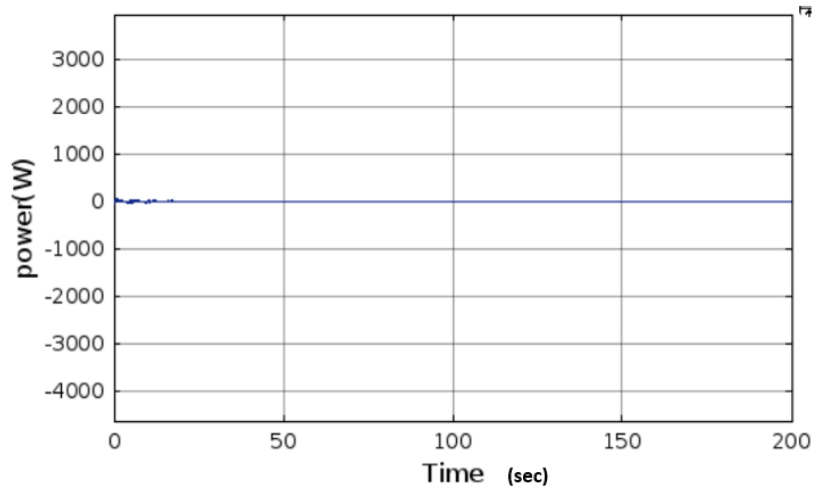


Figure 5.10: Modified perturbation power used by UAV when reaching the optimal height

The algorithm converges to optimum height in about 1min, which is approximately how long it might reasonably take for the UAV to fly to the new optimum in any case. Therefore, it has been possible to find a set of perturbation parameters for the algorithm to be implementable in real time. Further tuning may yet be possible to improve convergence time.

Another reason for switching from energy to power in the formulation of the control algorithm is so that the static power calculated previously can be added to the dynamic power calculation above. This is achieved in the block diagram of Figure 5.11 below.

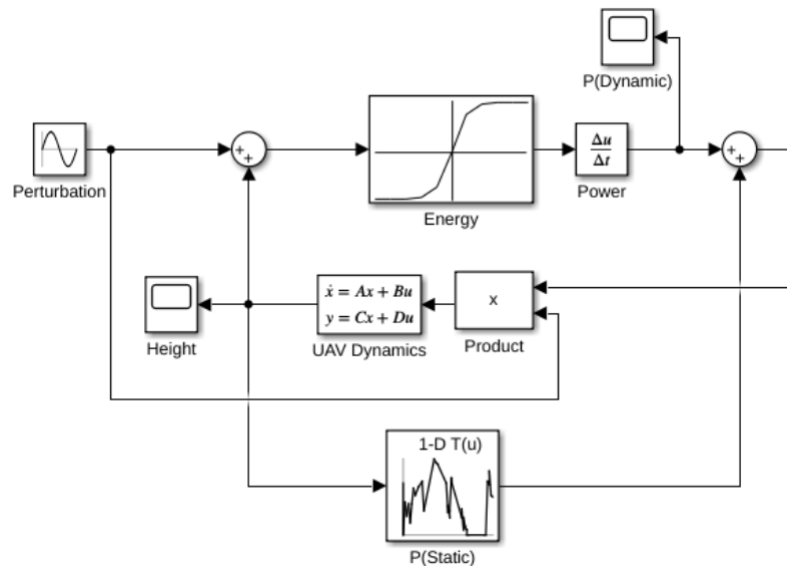


Figure 5.11: Simulink model for optimum seeking of height including static power

Inclusion of the static power term modifies the convergence time to nearer 2 mins as shown in Figure 5.12 and zero-power performance is also confirmed in Figure 5.13.

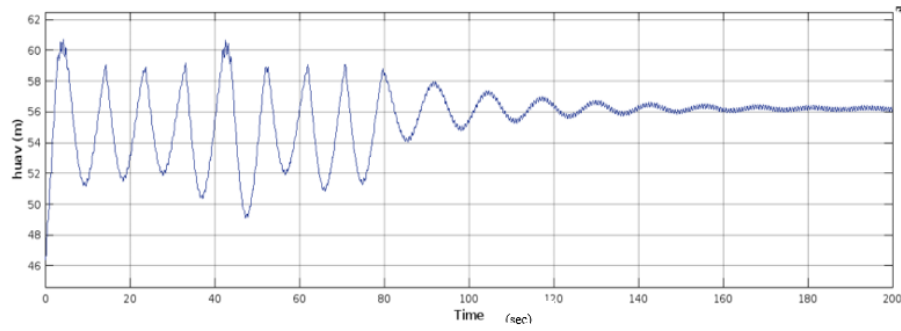


Figure 5.12: Optimized height using Extremum seeking with static power

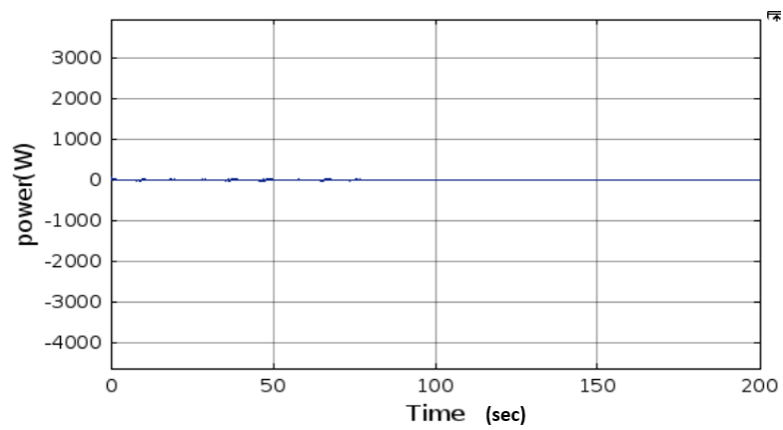


Figure 5.13: Modified perturbation power used by UAV including static power

Over all of the initial conditions of Table 5.1, a new trajectory path is derived as in Figure 5.14.

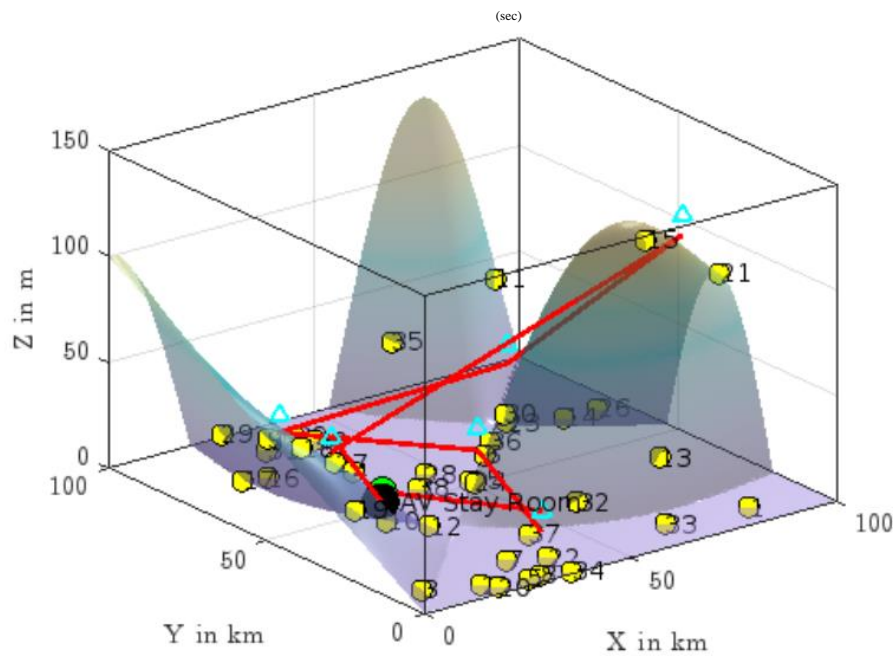


Figure 5.14: New optimized trajectory using extremum seeking model



### 5.3.3 Sliding Mode Optimal Trajectory

The sliding mode optimal trajectory (SMOT) method uses a similar, but not identical formulation to that discussed in the previous section and in Chapter 3, Section 3.4. The extremum seeking controller uses the Theorem of Averages to derive an optimization algorithm, whereas optimal sliding modes minimize a Lyapunov function representing the energy of the sliding mode. In this application, the sliding mode becomes the power derived from the energy function, as formulated in Equation 5.10.

The acceleration input (gain  $k$ ) to the state model is switched according to control law (3.27), where the sliding mode,  $s$ , is dynamic power ( $P_{\text{Dynamic}}$ ).

A state model, UAV dynamics, of Section 5.3.1 is utilised.

The optimization scheme for finding the optimal height using sliding mode is depicted in Figure 5.15:

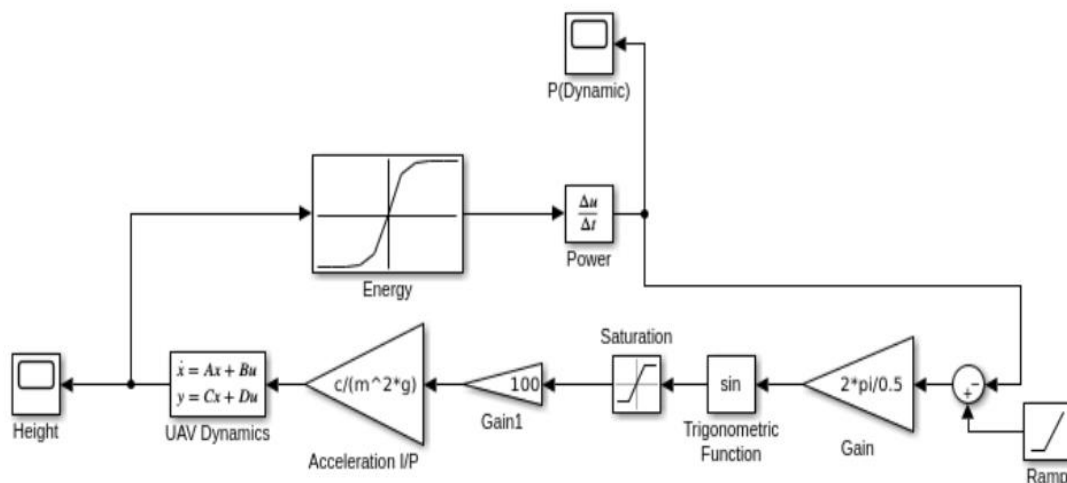


Figure 5.15: Simulink model for optimum height using sliding mode

It was possible for the height to be optimized for algorithm parameters, gain ( $k$ ) = 100, coefficient ( $\alpha$ ) = 0.5 and ramp ( $r$ ) = 0.01t. Larger values of  $k$  require greater control effort for no real improvement in convergence time. The case studies of Chapter 6 will show Tables of optimized altitudes in terms of convergence times for an exhaustive range of clustering scenarios. Nevertheless, it is not possible to optimize the height in real time because of longer convergence time and this optimization can only be performed offline as represented in Figure 5.16. However, the optimized height is identical to that for the extremum seeking control of Figure 5.9 for the same initial condition,  $h_0$ .

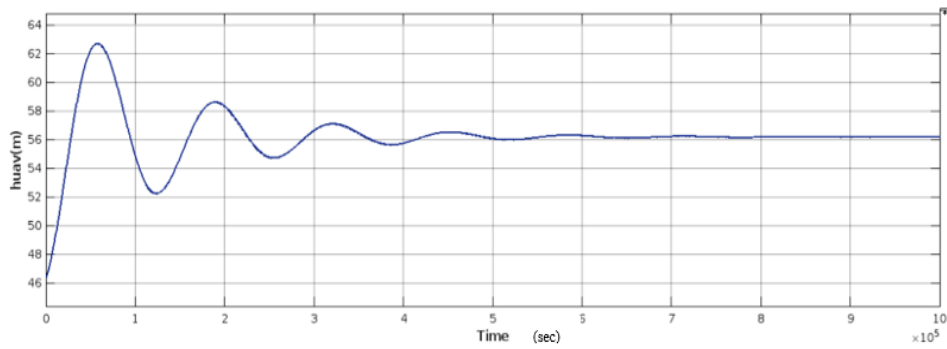


Figure 5.16: Optimized height value using sliding mode

When taking into account the instantaneous static power (Figure 5.17) at each height,  $h$ , the same optimized height is achieved but at the cost of a much longer convergence time. Also, the controller gain had to be reduced in order to achieve convergence at all. The optimized height and zero-power responses are shown in Figure 5.18 and Figure 5.19, respectively.

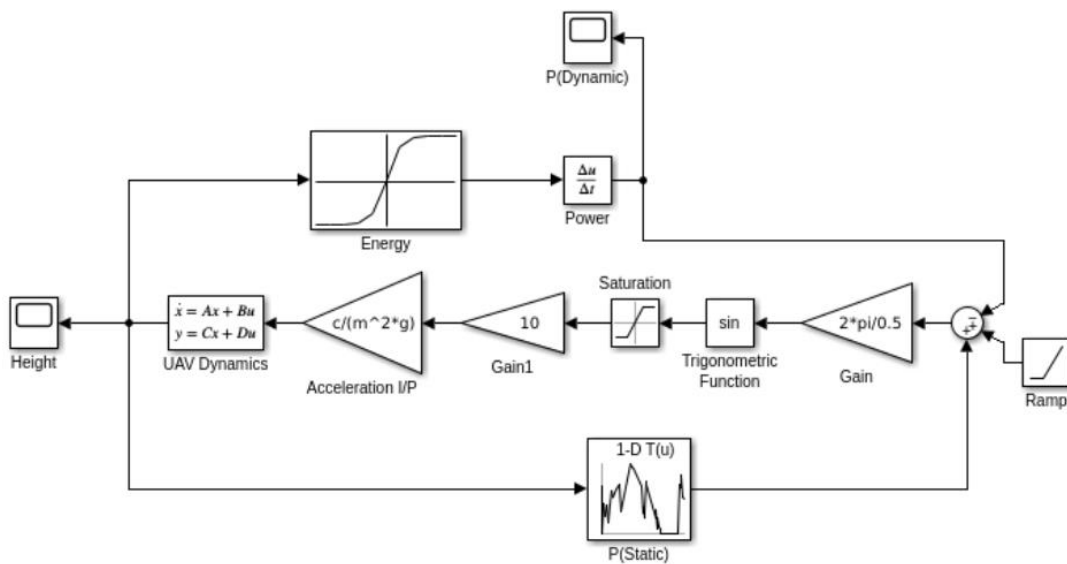


Figure 5.17: Simulink model for sliding mode optimization including static power

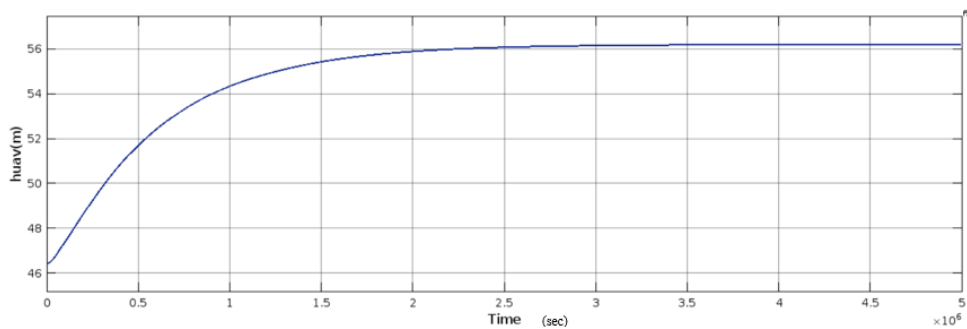


Figure 5.18: Optimized height using sliding mode with static power

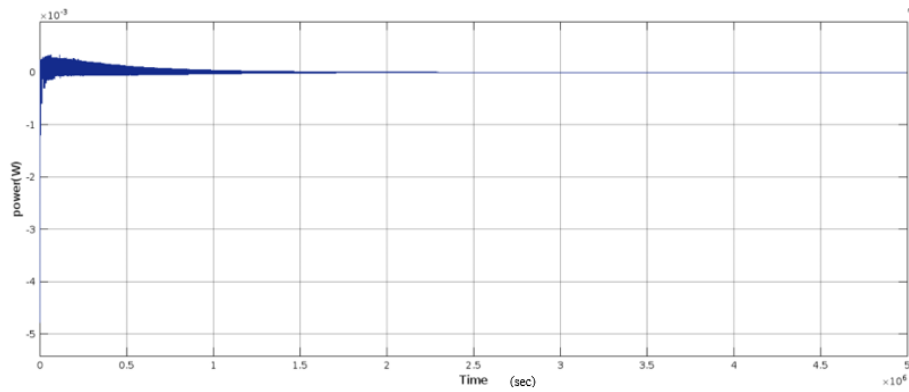


Figure 5.19: Zero power for reaching the optimal height with static power

Figure 5.20 provides a visual representation of the various optimized heights that are achieved. These values were found by using the sliding mode optimal trajectory approach while experimenting with different values for the initial  $h_0$  parameter calculated from the static optimization Table 5.1 of Section 5.2. and all the simulation results other than Figure 5.18 are in Appendix C.2.

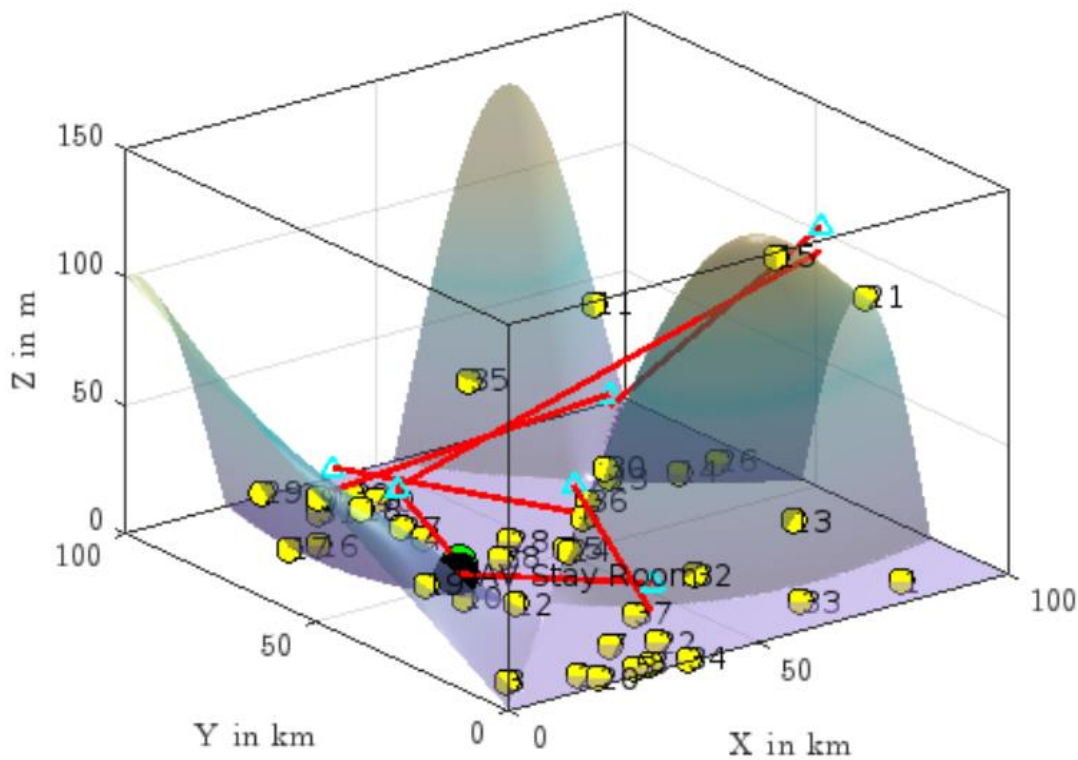


Figure 5.20: New optimized trajectory using sliding mode optimization

The optimal trajectory is designed by applying a hybrid approach which is a combination of static and dynamic optimization methods. The static optimization is implemented by reducing

the recycle time between the UAV rounds and then calculating the height of the UAV at each cluster centroids as represented in Table 5.1. The outputs from static optimization were used as inputs to dynamic optimization to calculate further optimized heights by taking into consider the UAV dynamics by designing a dynamic state model. An extremum seeking method is used to optimize the energy consumption of the UAV and it is clearly analysed from the Figure 5.7 and Figure 5.9 where the heights optimizing to a specific value. A zero-power performance is also verified to confirm the energy optimization where the power is settling to zero in few seconds as in Figure 5.10. In order to validate the results from extremum seeking, a sliding mode method is applied and it is observed that both provide with same result optimizing at a height of 56 m for one of the clusters as presented in Figure 5.12 and Figure 5.18 with zero-power performance.

#### **5.4. Summary**

An ideal trajectory for the UAV was designed using a combination of both static and dynamic optimization approaches, which have been discussed in this Chapter. To begin, in Chapter 5 a dome packing approach is developed in order to locate the most energy-efficient placements for the ground nodes and the UAV in a WPCN. Second, the amount of time spent recycling is improved so that an ideal trajectory can be designed for the UAV. As a consequence of this, static optimization is used to determine the best height by including the UAV dynamics while flying through the cluster centroids. These positions become the initial conditions for dynamic optimization. During the process of dynamic optimization, two techniques, namely extremum seeking and optimal sliding were used to further calculate the optimal height of the UAV, taking into account UAV dynamics and energy consumption. It is also interesting to note that these two approaches yield identical results in terms of optimal height value, even though they use different optimization approaches; the one applies the Theorem of Averages while the other derives and optimises Lyapunov functions. These results served to validate the two approaches against each other. The inclusion of static instantaneous power within the dynamic models made little or no difference to the results of the optimization, only to the time to convergence of the algorithms. In summary, the methodologies of both static and dynamic optimization formulated in Chapter 3 have been successfully implemented in this and the previous chapter, respectively.

# CHAPTER 6

## ANALYSIS AND DISCUSSION OF SIMULATION RESULTS

### USING CASE STUDY

#### 6.1. Introduction

In this chapter, an analysis of the simulation findings using ten distinct case studies is undertaken. Out of these, four will be presented: a variety of GN locations are considered in differing cluster formations. Then, both the static and the dynamic optimization techniques developed in Chapters 4 and 5 are applied. The static optimization comprises Dome packing, which is used both to cluster GNs and for beamforming to optimize charging and data transfer. This allows trajectory design in order to compute the initial height of the UAV to facilitate effective wireless charging and data transfer. This is because the energy term  $E_{Tot}$  is included in the cost function to be optimized. This is practically realised by equally distributing the probabilities between charging and data transfer (much like phone charging being faster and more efficient while simultaneously transmitting data to another device). The static optimization provides a starting point for dynamic optimization utilising extremum seeking and sliding mode optimal trajectory design to compute optimised heights for efficient system performance in terms of energy utilization, charging and data transfer.

#### 6.2. Case Study Design

The case study consists of positioning 40 GNs in three-dimensional space at random positions. Space packing is a formal method for the best utilization of space. However, in this application, it is not space but distance which is to be optimized between GN's and UAV in order to optimize energy and data transmission between them. Therefore, the randomly placed GNs must be clustered so that this can be achieved with respect to beaming range. Four random placements (case studies) of the 40 GNs have been selected so that clustering and UAV trajectory optimization can be demonstrated, and these are shown in Figure 6.1.

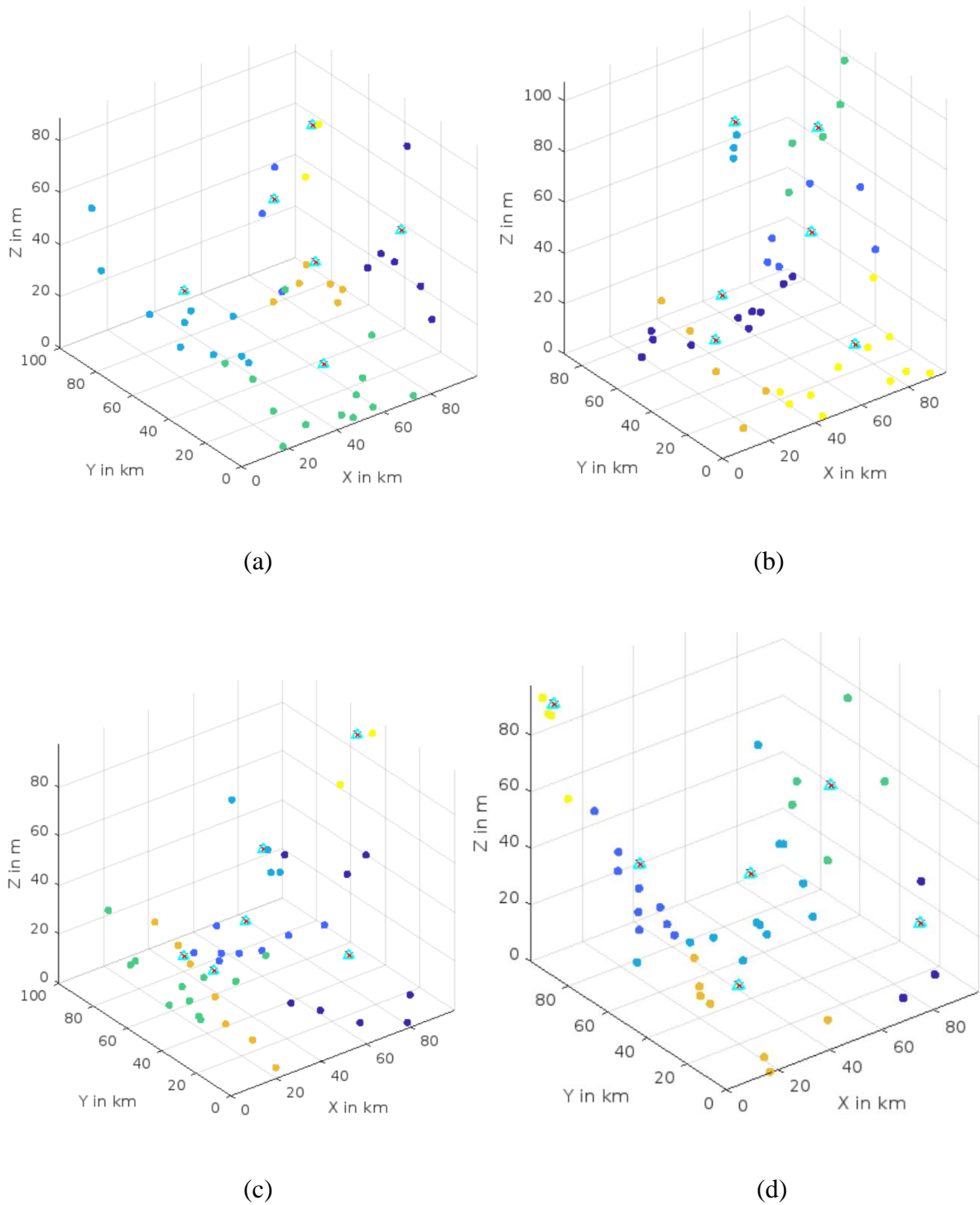


Figure 6.1 (a-d): Selected GN locations for application of the proposed approaches

Using the selected GN locations, the proposed Dome packing method is applied, whereby clustering of the GNs is simulated. Figure 6.1 (a-d) shows how the different clusters are represented as different coloured dots. A centroid can be calculated for each cluster which

determines the best position of the UAV to take up for the purposes of energy and data transfer between the GNs of that cluster. The beaming range determines the initial height values of the UAV, represented as light blue triangles with a red cross for each cluster. Figure 6.2 (a-d) also provides a picture of the different stages of the trajectories as the dome packing calculation proceeds and so illustrates the optimized trajectory of the UAV through the calculated height values.

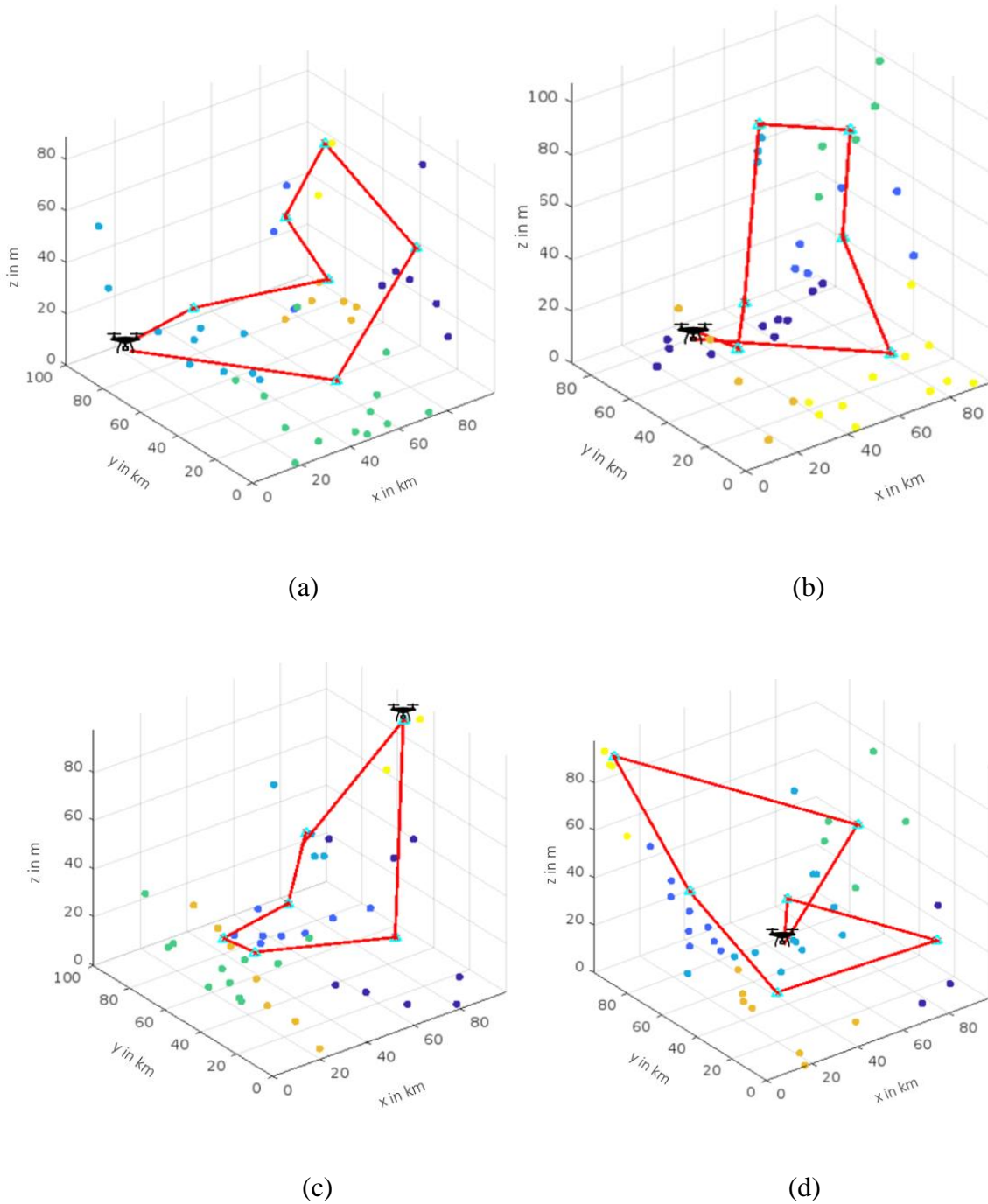
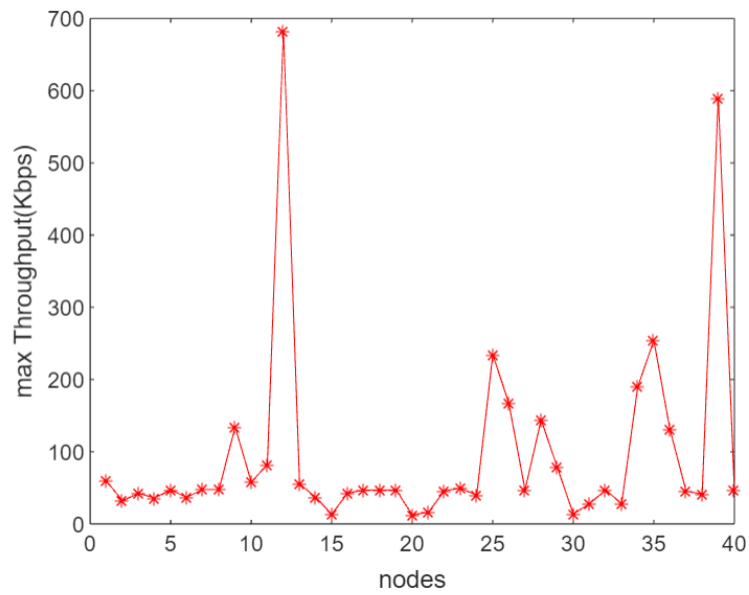


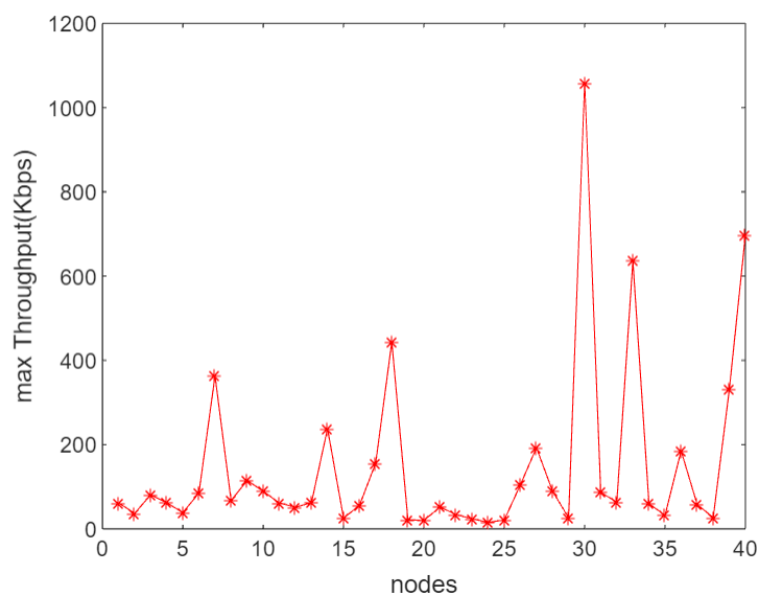
Figure 6.2 (a-d): UAV trajectories calculated for selected case studies

### 6.3. Analysis and Discussion

In order to verify the effectiveness of the proposed Dome packing method, the throughput received based on the energy collected by the nodes is represented in Figure 6.3 (a-d) and to be analysed. It is clear from Figure 6.3 that at some of the points the throughput is at its maximum, which is based on the lesser distance between the UAV and the GN's as well as the transmission time, since distance affects the time required for charging and data transfer.

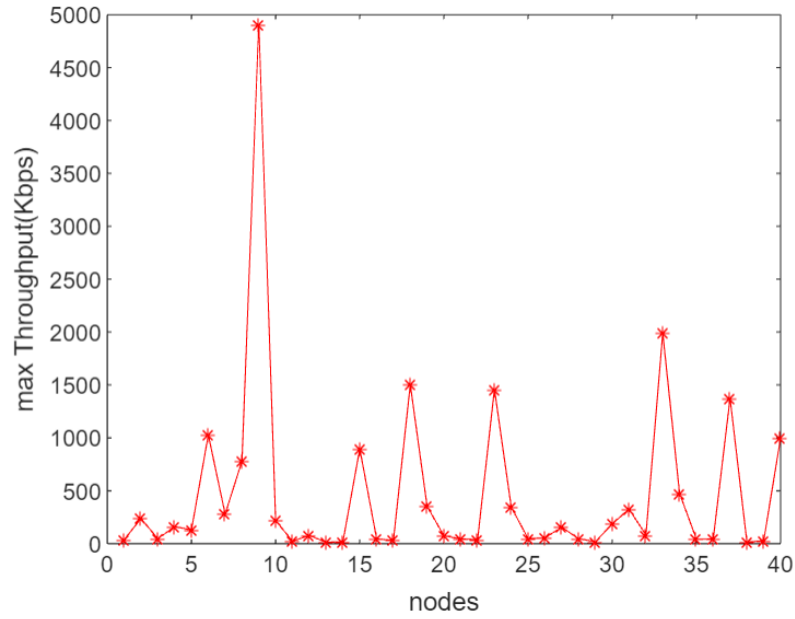


a)

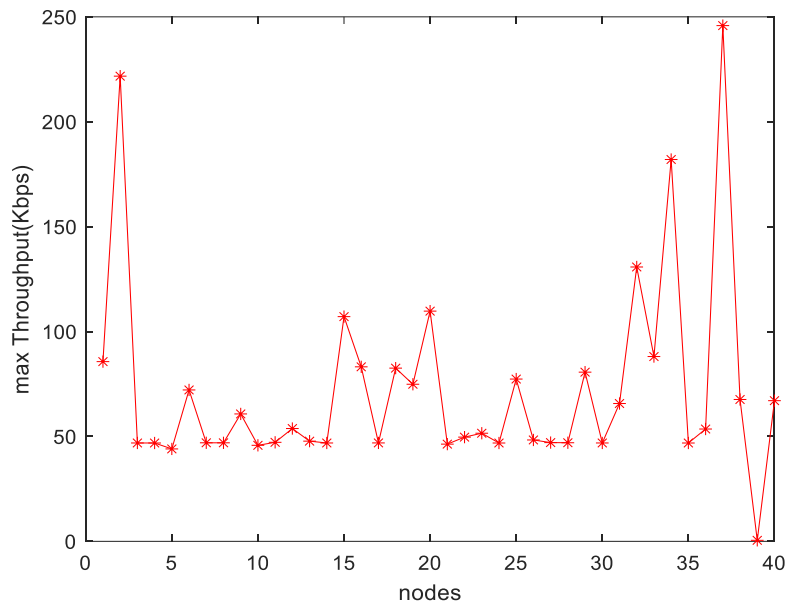


b)





c)



d)

Figure 6.3 (a-d): The throughput of the system for the proposed Dome packing method

The comparison between the proposed Dome packing approach and the default positioning of the GNs without any form of clustering is shown in Figure 6.4, from which it is abundantly evident that the suggested dome packing approach, in conjunction with trajectory planning, produces more effective outcomes by lowering the amount of energy that the UAV needs to function to around 15 percentage. The variations of the outliers at each round with UAV power

consumption due to the number of GNs in each cluster based on the different case studies. In a similar manner, Figure 6.5 presents a visual representation of the wireless power transfer from the UAVs to the GNs for all 10 different topologies (rounds). The outliers at some rounds in the graph is due to the random positioning of the UAV during WET. The wireless power transfer rate is proportional to the flighttimeunit or the amount of time needed to charge the GNs, and that this, in turn, affects the amount of energy that the UAV as a whole consumes. This is something that will be taken into consideration later via dynamic optimization.

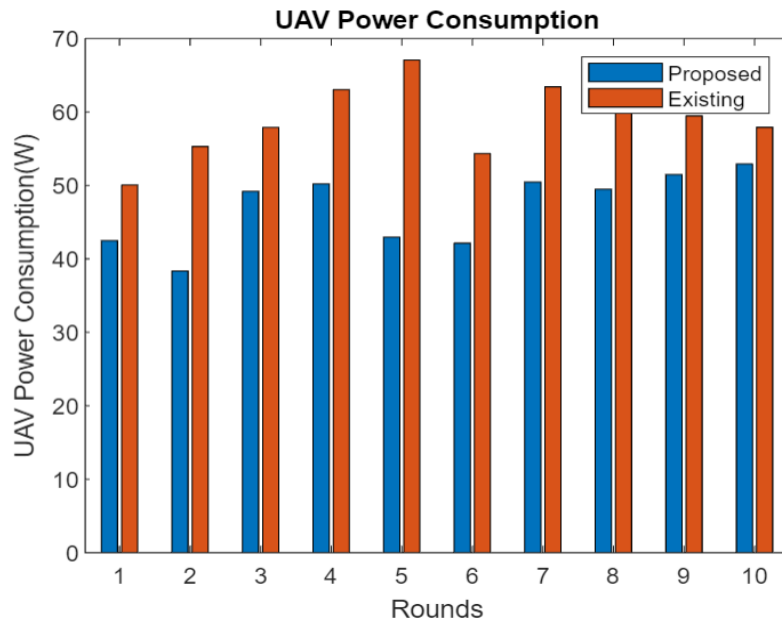


Figure 6.4: Energy consumed by the UAV with existing and proposed methods

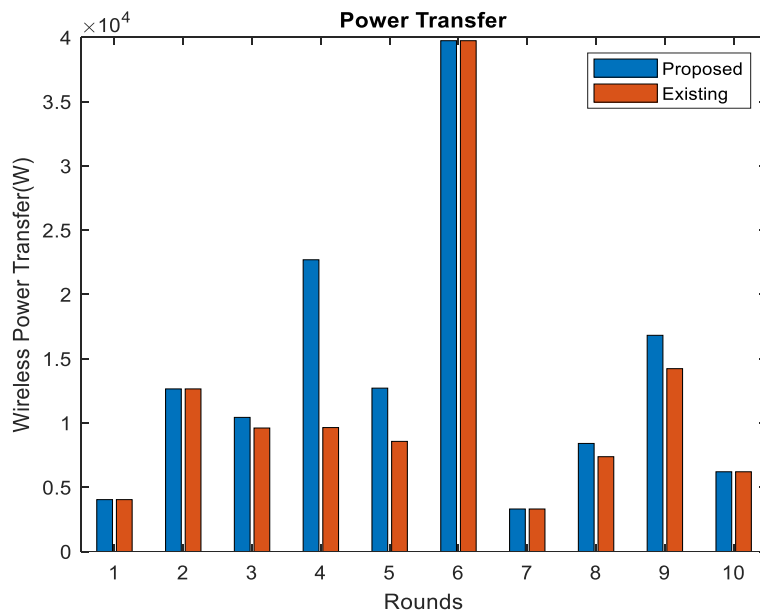


Figure 6.5: Comparison of wireless power transfer from UAV to GN's

The power consumption of the UAV and flying duration for each of the clusters is depicted in Figure 6.6 and 6.7, respectively. These indicate, as expected that the UAV would demand more energy with respect to the number of clusters/nodes traversed and flight time. However, it is equally clear that power consumption is lower around 16 percentage for dome packing than for non dome packing.

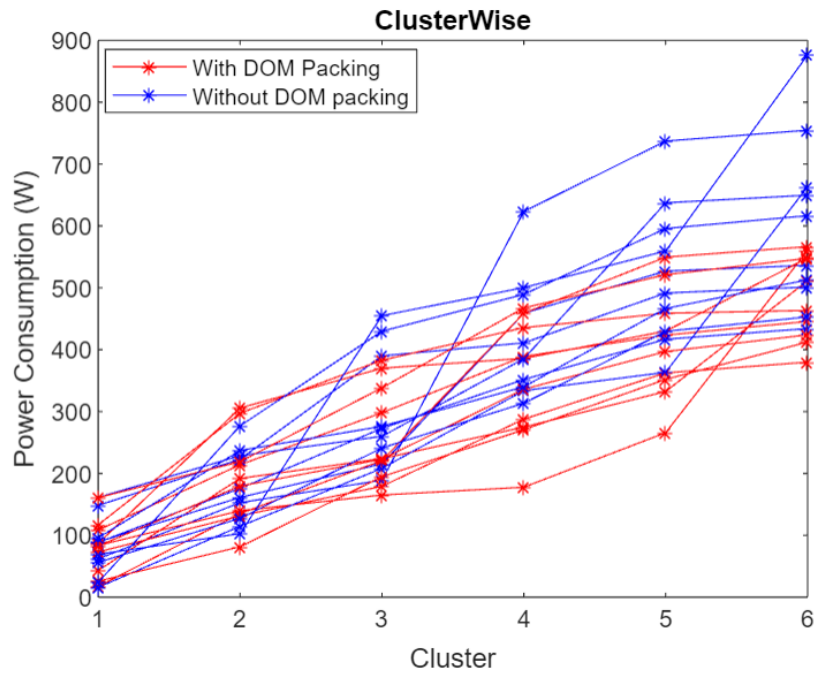


Figure 6.6: Comparison of UAV power consumption based on cluster

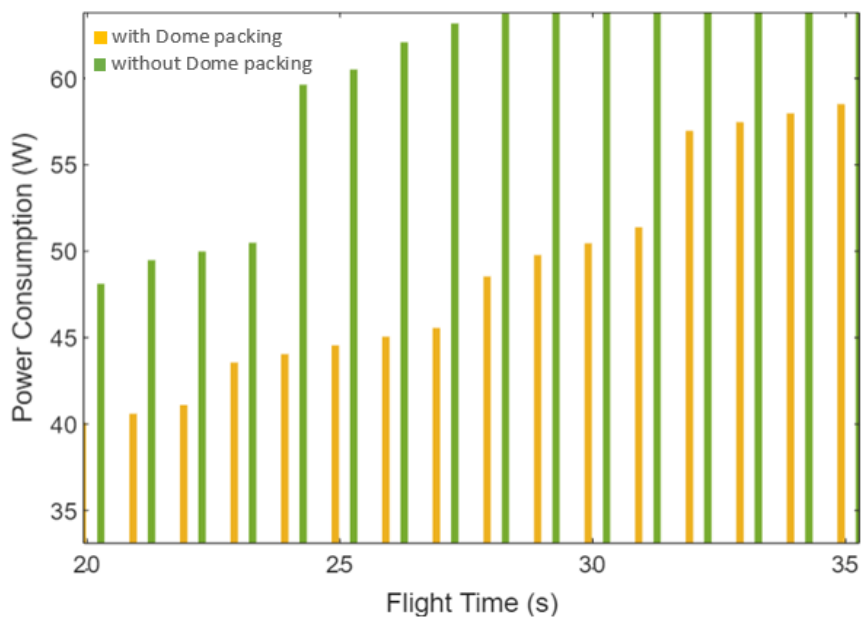


Figure 6.7: Comparison of UAV power consumption based on the flight time

In chapter 5, one example was presented ( $h_0 = 46.4073$  m) for which the static optimization had been achieved using the Dome packing technique. Here, the results of four of the ten case studies will be presented over a range of different topologies, resulting in different values of  $h_0$ . Table 6.1 summarizes the results of static optimization for four case studies over six clusters.

Table 6.1: Height of the UAV at each cluster centroid using Dome packing

	<b>Cluster 1</b>	<b>Cluster 2</b>	<b>Cluster 3</b>	<b>Cluster 4</b>	<b>Cluster 5</b>	<b>Cluster 6</b>
<b><math>h_0</math> Case 1</b>	10.3844	44.0529	66.4556	87.9171	26.6012	15.1577
<b><math>h_0</math> Case 2</b>	50.9126	44.2011	17.4232	15.3343	12.9443	87.2014
<b><math>h_0</math> Case 3</b>	22.4445	10.8931	28.9041	14.3083	29.7003	95.7170
<b><math>h_0</math> Case 4</b>	20.3241	51.3543	16.2861	67.0070	15.6760	90.393

These results for  $h_0$  now become the initial conditions for the dynamic optimization problem. The extremum seeking technique was one of the approaches used and demonstrated in section 5.3.2 for the initial condition  $h_0 = 46.4073$  m.

As for the static optimization, Table 6.2 presents the results of dynamic optimization using extremum seeking optimal trajectory method for the initial conditions of Table 6.1 over the same four selected case studies and six clusters.

It can be seen that convergence for extremum seeking optimization is achievable in real time (Table 6.3) whereas sliding mode takes longer convergence (simulation) time to reach optimal height . The improved convergence times are as a result of larger perturbation amplitudes, which also result in a larger discrepancy between optimal heights from optimal sliding mode.

Table 6.2: Optimized heights (m) of the UAV using extremum seeking

	<b>Cluster 1</b>	<b>Cluster 2</b>	<b>Cluster 3</b>	<b>Cluster 4</b>	<b>Cluster 5</b>	<b>Cluster 6</b>
<b>h ES Case 1</b>	20.2	53.85	76.30	97.57	36.20	24.34
<b>h ES Case 2</b>	59.04	54.0	26.8	27.45	25.0	97.10
<b>h ES Case 3</b>	32.30	20.5	39.0	23.90	39.60	105.0
<b>h ES Case 4</b>	30.20	61.50	25.80	76.80	25.20	100.0

Table 6.3: Real time convergence (s) of the UAV to reach optimum using extremum seeking

	<b>Cluster 1(s)</b>	<b>Cluster 2(s)</b>	<b>Cluster 3(s)</b>	<b>Cluster 4(s)</b>	<b>Cluster 5(s)</b>	<b>Cluster 6(s)</b>
<b>h ESOT Case 1</b>	60	60	70	60	130	55
<b>h ESOT Case 2</b>	130	50	60	50	50	48
<b>h ESOT Case 3</b>	70	40	60	60	60	30
<b>h ESOT Case 4</b>	60	75	70	50	60	40

In contrast to the extremum seeking method, dynamic optimization using the sliding mode optimal trajectory approach was also applied, firstly, to verify that the same optimum heights

were predicted, and as a secondary consideration, to see if an improved convergence time could be achieved.

Using the same initial conditions (Table 6.1), the optimal heights of Table 6.4 are presented for the sliding mode optimal trajectory method.

Table 6.4: Optimized heights (m) of the UAV using sliding mode

	<b>Cluster 1</b>	<b>Cluster 2</b>	<b>Cluster 3</b>	<b>Cluster 4</b>	<b>Cluster 5</b>	<b>Cluster 6</b>
<b>h SMOT Case 1</b>	21.42	53.853	76.40	97.85	36.94	24.67
<b>h SMOT Case 2</b>	61.40	53.86	26.6	25.0	22.7	97.155
<b>h SMOT Case 3</b>	30.90	20.7	39.6	23.80	39.76	105.6
<b>h SMOT Case 4</b>	30.5	61.6	25.94	77.12	25.22	100.32

As can be seen in Table 6.2, the sliding mode and extremum seeking both generate outcomes that are very similar to one another, within about 1min or so. The amount of time required for convergence of the extremum seeking method is significantly less than the amount of time required by the sliding mode optimal trajectory design of the UAV. This is not surprising considering the example of Section 5.3.3. One reason for this is that the size of switching gain, ‘k’, was limited by the rate of switching. Therefore, the sine (sgn) function was replaced by a saturation function in the hope of alleviating this issue. However, this was successful to a limited extent only. The ‘hard’ discontinuity is replaced by a ‘boundary layer’ or ‘soft’ discontinuity at the expense of accuracy. This also accounts for the slight difference in the optimized heights between the extremum seeking and sliding mode optimal trajectory approaches.

## 6.4. Summary

This chapter presents the results of four of the ten case studies that were undertaken across six clusters to calculate optimal trajectories of the UAV using both static and dynamic optimization methods. Whereas the results of the previous chapters demonstrated the efficacy of the method for one particular example only, the purpose of the case study was to show that the method was applicable across all topologies and initial conditions. As for the results of Chapter 5, the results for the two dynamic optimization results were verified against each other. The extremum seeking method proved to be the more effective and rapidly convergent of the two, while the sliding mode optimal trajectory only served to confirm its results. The simulations of each dynamic optimization approach were conducted under identical initial conditions, which themselves were derived using the Dome packing method for each of the topologies.

The case studies serve to verify and validate, not only the three static algorithms of Chapters 4 and 5, but also the two different dynamic optimization strategies developed in Chapter 3 and applied in Chapter 5.

## CHAPTER 7

### CONCLUSION AND FUTURE WORK

As per the aim of this thesis stated in Chapter 1, energy harvesting methods have been reviewed for the purposes of near real time monitoring and control of WDS and, as a result, it was confirmed that utilization of a UAV would provide a novel and suitable method for charging and communicating between GNs in a WDS, using the UAV as a mobile base station.

The key motivation of this research was to use a UAV as a flying base station for the charging and data collection from GNs within a WPCN for optimal energy management in a WDS. A variety of techniques were employed, not only for the modelling of the UAV but also for statically designing its trajectory using 3D dome packing and then dynamically optimizing its altitude based on energy cost functions.

A key consideration in addressing the second objective of optimizing energy usage was to resolve the so-called doubly-near-far problem, anticipated in Chapter 3, whereby nodes near to the energy transmitter receive the majority of energy, whereas the far away nodes that are starved, actually require more energy for data transmission due to their further distance from the transmitter. This problem is not solved merely by deploying a UAV, though it may alleviate LOS issues because the UAV does not have an unlimited store of energy to move to energy starved GNs. A mathematical optimization problem known as space-packing was therefore adapted to optimize distances between GNs and the UAV in 3D space to facilitate energy and information transmission, instead of optimally packing space. As this process traced out ellipsoids between GNs and UAV, this new method was termed ‘Dome packing’ by the author. Algorithms were derived to optimize UAV location with respect to charging and transmission efficiency using this static optimization approach.

The successful resolution of static problems through the implementation of static optimization methods, as discussed previously, has greatly improved the overall efficiency. However, one crucial aspect that has not been adequately addressed in these solutions is the energy consumption of UAV’s during their operation. The development of a dynamic model of the UAV enabled, in turn, the formulation of a dynamic optimization problem, which was then



solved using two separate approaches, i.e., extremum seeking and optimal sliding mode trajectory design. Both methods not only resulted in zero-power behaviour of the UAV, but also produced near identical optimal solutions for UAV altitude, thus mutually validating these solutions. The static solution was used as the initial condition of the dynamic optimization problem.

Finally, the combined strategies of static and dynamic optimization were proposed, designed, tested and verified across a range of GN cluster formations and proved to be robust and effective in terms of energy optimization and data transfer, resulting in estimated energy savings of 15 percent.

## **7.1. Theoretical Justification and Achievements**

A detailed literature review (Chapters 1 and 2) identified both, the variables of the WDS that needed to be monitored, and also the means by which this could be undertaken, using existing sensor technologies. One particular device was identified (Libelium, 2015), which sufficiently integrated water quality measurements (pH, ORP, DO, BOD etc.), solar self-charging and efficient data acquisition using universal data transmission protocols. However, it required adaptation for the purposes of optimized near real-time continuous monitoring using the techniques developed later in the thesis. As discussed in Chapter 2, the smart water monitoring system has several layers of design, but the emphasis of this thesis was to investigate the sensing and communication components of the system. In particular, the strategies that may be used to maximise their efficiency in the management of energy during communication in a real-time water monitoring system. The low power LoRa protocol was identified as the most suitable for the purposes of communication between GNs and the UAV.

The development of an energy optimization approach applicable to near real-time monitoring inside a WDS requires the formulation of a static energy cost or objective function. In chapter 3, the distances between GNs and UAV were calculated to determine the energy that the UAV would need to supply to the GNs via a beam by LOS. Additionally, the uplink and downlink communication energies were taken into consideration to form this cost function (3.15). The static optimization procedure places the UAV at the centroid of a cluster of GNs. This location enabled optimized data and energy transfer through beamforming. Clusters are formed by proximity to a centroid iteratively, through consideration of beamforming range (threshold for sensor operation). The Algorithms 4.1a and 4.1b achieved static optimization with respect to

both energy and data transfer using a Dome packing method, while Algorithm 5.1 optimized flight time between all cluster centroids. These algorithms were created using the K-means clustering method and verified by calculating precision, recall and F score criteria.

The successful static optimization of the UAV's flight path does not take into consideration the energy used by the motion of the UAV itself. To remedy this, a dynamic model of the UAV was developed as part of dynamic optimization problem formulation (5.1-5.5). Standard dynamic optimization procedures assume linear dynamics and quadratic cost functions (LQR). However, the optimization methods adopted in Chapter 3 have required neither of these assumptions to be satisfied. The formulation of the Lagrangian of the UAV dynamics allows the design of a dynamic cost function, which though quadratic, is summed with the static cost function discussed above.. The same cost function could also be non-quadratic that also works with the designed cost function. Therefore, a non-quadratic overall cost function needed to be anticipated. The dynamic optimization approaches used were based on two different paradigms:

- The Theorem of Averaging
- Lyapunov Stability

The first of these generates an extremum seeking algorithm while the second, an optimal sliding mode. In the former, equilibrium of the UAV ( $\dot{h} = 0$ ) is only possible at the optimum of the cost function ( $E_h = 0$ ) while, for the latter, the energy in the Lyapunov function must always be decreasing (eventually to zero) so that the sliding mode,  $s = 0$ , remains stable. These methodologies are demonstrated in Chapter 3. However, in Chapter 5, using zero-power as the optimization criteria, both conditions, for equilibrium and an optimum, are satisfied simultaneously because  $P = dE/dt = E_h \dot{h} = 0$ . This further motivated adoption of  $P$  as a second order sliding mode, replacing  $s = 0$ . So, therefore, the simulations of Chapter 5 all converge to  $P = 0$ , satisfying conditions for both extremum seeking and sliding mode existence criteria, respectively, as well as zero-power performance of the UAV.

It is noteworthy that the two approaches converged to within 1 m of the same optimal height (where the algorithms converged to a legal requirement) therefore, verifying their results against each other. However, the superiority of the extremum seeking approach over the optimal sliding mode approach is demonstrated by its real time convergence. The latter was therefore only implementable offline in river water system where the degradation of the water quality parameters will be slower. In both cases, the outputs of the static optimization,  $h_0$ , were

used as initial conditions for dynamic optimization. In an additional step, both static and dynamic optimization was combined by adding static power to dynamic power in the formulation of the input to the UAV model. It is notable that, not only was there no change to the optimal height, but also that the zero-power performance of the UAV was maintained. The convergence time, however, was compromised by addition of static power. This was indicative of the overall mission flight time combining static and dynamic phases. Nevertheless, real time implementation was still demonstrated by extremum seeking optimization. The parametric study confirmed results of the combined static and dynamic optimization approaches over an exhaustive scenario of different clusters/initial conditions.

### **7.1.1 Significance of the Study**

A summary of the achievements of this thesis is itemized as below:

- To meet the goal of implementing an energy optimization scheme, a UAV was incorporated that acts as a flying base station in a novel approach for the uplink and downlink communication and energy transfer between the base station and the GNs in a WDS. Key sensor and communication protocols have been identified for this purpose.
- An integration of static and dynamic optimization methods along with a dynamic UAV model was proposed in which four novel algorithms were formulated, all of which were found to converge to an optimum:
  - A Dome packing algorithm to optimally cluster GNs within the UAVs range.
  - Additionally, a flight time optimization algorithm, verified by F-score.
  - An Extremum seeking algorithm to dynamically optimize UAV altitude.
  - An Optimal Sliding mode algorithm to confirm optimal UAV altitude.
- The UAV was shown to operate as a zero-power system while optimizing altitude and maintaining stable equilibrium.
- It was possible to tune the extremum seeking algorithm to converge in real-time.

## **7.2. Future Work**

While the application of the current work is intended for use with WDS, the focus remained entirely on energy optimization of its components. The future work would refocus on the application that initially motivated the study, i.e., water quality. There are several possible developments that may naturally arise from the present work, particularly in terms of

extending the use of a single UAV to multi-UAV approaches, and the application of dynamic optimization, not just to energy management, but also to water quality regulation and distribution. Before elaborating on this in detail, other aspects of possible future work that could follow on from this thesis are identified as below:

1. To investigate the possibility of tuning automatically, variations of algorithms, such as extremum seeking and optimum sliding that converge to optimum in real time.
2. The necessity of securing the proposed UAV enabled WPCN to protect it from attacks such as virus, worms, phishing etc in the physical and sensing layer; security of the network layer is another possible concern.

For the application of dynamic optimization, a dynamic model of the water distribution system will be required. Only then, dynamic optimization algorithms can be designed to regulate water quality. For this purpose, the following aspects of future work would be required to be undertaken:

3. A dynamic model of water quality parameters such as DO and BOD from the data collected by the UAV in the current project will need to be developed (see Appendix C).
4. By replacing the UAV dynamic model with the water quality model of 3, an extremum seeking method can be extended to optimize the DO and BOD of successive reaches of a river/pipeline/reservoir by perturbation of the fresh water and/or effluent supply to the WDS.
5. Use optimal sliding mode as an alternative algorithm to that in 4 above. It is plausible that this could operate in real time due to the larger time constants for water quality parameters than those of the UAV.
6. Apply linear quadratic regulation (LQR) instead of the methods in 4 and 5 above by using a linearized model of the water quality (Appendix C) and adopting a quadratic cost function.
7. Separate UAVs may be required to monitor separate sections or reaches of the WDS or river, respectively. The implementation of multi-UAV enabled WPCN by integrating the proposed methodologies using AI such as reinforcement learning methods could be another possible extension of the current work.

In this work, only a narrow scope of the multiple uses of UAV, WPCN technologies and optimization methodologies has been explored. However, it has been possible to apply a

significant depth of knowledge about the latter to the former, which has demonstrated to the author that the sky truly is the only limit of the application of UAVs in the solution of complex problems.

## REFERENCES

Aarsnes, U.J.F., Aamo, O.M. and Krstic, M. (2019) Extremum seeking for real-time optimal drilling control. In *2019 American Control Conference (ACC)*. July 2019. IEEE. pp. 5222–5227. doi:10.23919/ACC.2019.8815162.

Abdulkarim, H. and Alshammari, I. (2015) Comparison of Algorithms for Solving Traveling Salesman Problem. *International Journal of Engineering and Advanced Technology (IJEAT)*, 4 (6).

Abirami, K. and Karlmarx, L.R. (2013) A novel fault-tolerant control scheme for water distribution systems. In *2013 International Conference on Energy Efficient Technologies for Sustainability (EETS)*. April 2013. IEEE. pp. 848–852. doi:10.1109/ICEETS.2013.6533496.

Achtelik, M.C., Stumpf, J., Gurdan, D., et al. (2011) Design of a flexible high performance quadcopter platform breaking the MAV endurance record with laser power beaming. In *2011 IEEE International Conference on Intelligent Robots and Systems (IRAS)*. September 2011, 5166–5172. doi:10.1109/IROS.2011.6094731.

Aggarwal, S. and Kumar, N. (2020) Path planning techniques for unmanned aerial vehicles: A review, solutions, and challenges. *Computer Communications*, 149: 270–299. doi:10.1016/j.comcom.2019.10.014.

Alam, M.M. and Moh, S. (2022) Survey on Q-Learning-Based Position-Aware Routing Protocols in Flying Ad Hoc Networks. *Electronics*, 11 (7): 1099. doi:10.3390/electronics11071099.

Al-Fuqaha, A., Guizani, M., Mohammadi, M., et al. (2015) Internet of Things: A survey on enabling technologies, Protocols, and Applications. *IEEE Communications Surveys and Tutorials (IEEE Commun Surv Tutor)*, 17 (4): 2347–2376. doi:10.1109/COMST.2015.2444095.

Al-Janabi, T.A. and Al-Raweshidy, H.S. (2017) Optimised clustering algorithm-based centralised architecture for load balancing in IoT network. In *2017 International Symposium on Wireless Communication Systems (WCS)*. August 2017. IEEE. pp. 269–274. doi:10.1109/ISWCS.2017.8108123.

Almutairi, J., Aldossary, M., Alharbi, H.A., et al. (2022) Delay-Optimal Task Offloading for UAV-Enabled Edge-Cloud Computing Systems. *IEEE Access*, 10: 51575–51586. doi:10.1109/ACCESS.2022.3174127.

Alsaba, Y., Leow, C.Y. and Abdul Rahim, S.K. (2018) Full-Duplex Cooperative Non-Orthogonal Multiple Access with Beamforming and Energy Harvesting. *IEEE Access*, 6: 19726–19738. doi:10.1109/ACCESS.2018.2823723.

Alshattawi, S.K. (2017) Smart Water Distribution Management System Architecture Based on Internet of Things and Cloud Computing. In *2017 International Conference on New Trends in Computing Sciences (NTCS)*. October 2017. IEEE. pp. 289–294. doi:10.1109/ICTCS.2017.31.

- Angeletti, P. and Lisi, M. (2014) Multimode beamforming networks for space applications. *IEEE Antennas and Propagation Magazine*, 56 (1): 62–78. doi:10.1109/MAP.2014.6821760.
- Aquilina, J.P., Farrugia, R.N. and Sant, T. (2019) On the Energy Requirements of UAVs Used for Blade Inspection in Offshore Wind Farms. In *2019 Offshore Energy and Storage Summit*. July 2019. IEEE. pp. 1–7. doi:10.1109/OSES.2019.8867145.
- Balanis, C.A. (2016) *Antenna theory: Analysis and Design*. 4th ed. Hoboken, New Jersey: John Wiley & sons.
- Bevacqua, M.T., Bellizzi, G.G. and Merenda, M. (2021) An Efficient Far-Field Wireless Power Transfer via Field Intensity Shaping Techniques. *Electronics*, 10 (14): 1609. doi:10.3390/electronics10141609.
- Bhatti, N.A., Alizai, M.H., Syed, A.A., et al. (2016) Energy Harvesting and Wireless Transfer in Sensor Network Applications. *ACM Transactions on Sensor Networks*, 12 (3): 1–40. doi:10.1145/2915918.
- Bi, S., Ho, C.K. and Zhang, R. (2015) Wireless powered communication: opportunities and challenges. *IEEE Communications Magazine*, 53 (4): 117–125. doi:10.1109/MCOM.2015.7081084.
- Bi, Z., Kan, T., Mi, C.C., et al. (2016) A review of wireless power transfer for electric vehicles: Prospects to enhance sustainable mobility. *Applied Energy*, 179: 413–425. doi:10.1016/j.apenergy.2016.07.003.
- Bizon, N.T.N.F.E. (2017) *Energy Harvesting and Energy Efficiency*. Cham, Switzerland: Springer International Publishing. doi:10.1007/978-3-319-49875-1.
- Cahn, A. (2014) An overview of smart water networks. *Journal - American Water Works Association*, 106 (7): 68–74. doi:10.5942/jawwa.2014.106.0096.
- Cao, H., Guo, Z., Wang, S., et al. (2020) Intelligent Wide-Area Water Quality Monitoring and Analysis System Exploiting Unmanned Surface Vehicles and Ensemble Learning. *Water*, 12 (3): 681. doi:10.3390/w12030681.
- Caspari, A., Bremen, A.M., Faust, J.M.M., et al. (2019) *DyOS - A Framework for Optimization of Large-Scale Differential Algebraic Equation Systems*. In pp. 619–624. doi:10.1016/B978-0-12-818634-3.50104-1.
- Chen, J., Du, C., Zhang, Y., et al. (2021) A Clustering-Based Coverage Path Planning Method for Autonomous Heterogeneous UAVs. *IEEE Transactions on Intelligent Transportation Systems*, pp. 1–11. doi:10.1109/TITS.2021.3066240.
- Chen, Z., Chi, K., Zheng, K., et al. (2020) Minimization of Transmission Completion Time in UAV-Enabled Wireless Powered Communication Networks. *IEEE Internet of Things Journal*, 7 (2): 1245–1259. doi:10.1109/JIOT.2019.2953691.
- Cho, S., Lee, K., Kang, B., et al. (2018) Weighted Harvest-Then-Transmit: UAV-Enabled Wireless Powered Communication Networks. *IEEE Access*, 6: 72212–72224. doi:10.1109/ACCESS.2018.2882128.

- Choi, S.Y., Gu, B.W., Jeong, S.Y., et al. (2015) Advances in Wireless Power Transfer Systems for Roadway-Powered Electric Vehicles. *IEEE Journal of Emerging and Selected Topics in Power Electronics*, 3 (1): 18–36. doi:10.1109/JESTPE.2014.2343674.
- COMSOL. (n.d.). Modeling of a Phased Array Antenna. [online] Available at: <https://www.comsol.com/model/modeling-of-a-phased-array-antenna-88011>. Danancier, K., Ruvio, D., Sung, I., et al. (2019) Comparison of path planning algorithms for an unmanned aerial vehicle deployment under threats. In *IFAC-PapersOnLine*. 1 September 2019. Elsevier B.V. pp. 1978–1983. doi:10.1016/j.ifacol.2019.11.493.
- Danish, M., Ansari, K.B., Aftab, R.A., et al. (2021) gPROMS-driven modeling and simulation of fixed bed adsorption of heavy metals on a biosorbent: benchmarking and case study. *Environmental Science and Pollution Research*. doi:10.1007/s11356-021-13207-y.
- Dong, Z. and Liu, C. (2021) Collaborative Coverage Path Planning of UAV Cluster based on Deep Reinforcement Learning. In *2021 IEEE 3rd International Conference on Frontiers Technology of Information and Computer (FTIC)*. 12 November 2021. IEEE. pp. 201–207. doi:10.1109/ICFTIC54370.2021.9647298.
- Downey, C. (2013, April 3). Understanding Wireless Range Calculations. *Electronic Design*. [online] Available at: <https://www.electronicdesign.com/technologies/communications/article/21796484/understanding-wireless-range-calculations>.
- Ejaz, W., Naeem, M., Basharat, M., et al. (2016) Efficient Wireless Power Transfer in Software-Defined Wireless Sensor Networks. *IEEE Sensors Journal*, 16 (20): 7409–7420. doi:10.1109/JSEN.2016.2588282.
- Farooq, W., Ur-Rehman, M., Abbassi, Q.H., et al. (2016) Design of a finger ring antenna for wireless sensor networks. In *2016 10th European Conference on Antennas and Propagation (AAP)*. pp. 1–4. doi:10.1109/EuCAP.2016.7481827.
- Fotouhi, A., Qiang, H., Ding, M., Hassan, M., Giordano, L.G., Garcia-Rodriguez, A. and Yuan, J. (2019). *Survey on UAV Cellular Communications: Practical Aspects, Standardization Advancements, Regulation, and Security Challenges*. *IEEE Communications Surveys Tutorials*, 21(4): 3417–3442. doi:https://doi.org/10.1109/COMST.2019.2906228.
- Geelen, C.V.C., Yntema, D.R., Molenaar, J., et al. (2021) Optimal Sensor Placement in Hydraulic Conduit Networks: A State-Space Approach. *Water*, 13 (21): 3105. doi:10.3390/w13213105.
- He, J., Wen, T., Qian, S., et al. (2018) Triboelectric-piezoelectric-electromagnetic hybrid nanogenerator for high-efficient vibration energy harvesting and self-powered wireless monitoring system. *Nano Energy*, 43: 326–339. doi:10.1016/j.nanoen.2017.11.039.
- Hossein, M. N., Taleb, T. and Arouk, O. (2016) Low-Altitude Unmanned Aerial Vehicles-Based Internet of Things Services: Comprehensive Survey and Future Perspectives. *IEEE Internet of Things Journal (IoT)*, 3 (6): 899–922. doi:10.1109/IIOT.2016.2612119.
- Hua, M., Li, C., Huang, Y., et al. (2017) Throughput maximization for UAV-enabled wireless power transfer in relaying system. In *2017 9th International Conference on*



- Wireless Communications and Signal Processing (WCSP)*. IEEE. pp. 1–5.  
doi:10.1109/WCSP.2017.8170970.
- Huan, J., Li, H., Wu, F., et al. (2020) Design of water quality monitoring system for aquaculture ponds based on NB-IoT. *Aquacultural Engineering*, 90: 102088.  
doi:10.1016/j.aquaeng.2020.102088.
- Izydorczyk, T., Ginard, M.M., Svendsen, S., et al. (2020) Experimental evaluation of beamforming on UAVs in cellular systems. Available at: <http://arxiv.org/abs/2003.12010>.
- Jo, S., Yang, W., Choi, H.K., et al. (2022) Deep Q-Learning-Based Transmission Power Control of a High Altitude Platform Station with Spectrum Sharing. *Sensors*, 22 (4): 1630.  
doi:10.3390/s22041630.
- Jushi, A., Pegatoquet, A. and Le, T.N. (2016) Wind Energy Harvesting for Autonomous Wireless Sensor Networks. In *2016 Euromicro Conference on Digital System Design (EDSD)*. August 2016. IEEE. pp. 301–308. doi:10.1109/DSD.2016.43.
- Kalantari, E., Yanikomeroğlu, H. and Yongacoglu, A. (2016) On the Number and 3D Placement of Drone Base Stations in Wireless Cellular Networks. In *2016 IEEE 84th Vehicular Technology Conference (VTC)*. September 2016. IEEE. pp. 1–6.  
doi:10.1109/VTCFall.2016.7881122.
- Kamalinejad, P., Mahapatra, C., Sheng, Z., et al. (2015) Wireless energy harvesting for the Internet of Things. *IEEE Communications Magazine*, 53 (6): 102–108.  
doi:10.1109/MCOM.2015.7120024.
- Karagianni, E., Rigas, E.S. and Bassiliades, N. (2022). Scheduling Drones to Recharge Electric Vehicles. doi:<https://doi.org/10.1145/3549737.3549763>.
- Kosunalp, S. (2016) A New Energy Prediction Algorithm for Energy-Harvesting Wireless Sensor Networks With Q-Learning. *IEEE Access*, 4: 5755–5763.  
doi:10.1109/ACCESS.2016.2606541.
- Krstić, M. and Wang, H.-H. (2000) Stability of extremum seeking feedback for general nonlinear dynamic systems. *Automatica*, 36 (4): 595–601. doi:10.1016/S0005-1098(99)00183-1.
- Kumar, P.M. and Hong, C.S. (2022) Internet of things for secure surveillance for sewage wastewater treatment systems. *Environmental Research*, 203: 111899.  
doi:10.1016/j.envres.2021.111899.
- Lambrinos, L. (2019) Internet of Things in Agriculture: A Decision Support System for Precision Farming. In *2019 IEEE Intl Conf on Dependable, Autonomic and Secure Computing, Intl Conf on Pervasive Intelligence and Computing, Intl Conf on Cloud and Big Data Computing, Intl Conf on Cyber Science and Technology Congress*. August 2019. IEEE. pp. 889–892. doi:10.1109/DASC/PiCom/CBDCCom/CyberSciTech.2019.00163.
- Lehman, B. and Weibel, S.P. (1999) Fundamental Theorems of Averaging for Functional Differential Equations. *Journal of Differential Equations*, 152 (1): 160–190.  
doi:10.1006/jdeq.1998.3523.

- Li, B., Qi, X., Yu, B., et al. (2020) Trajectory Planning for UAV Based on Improved ACO Algorithm. *IEEE Access*, 8: 2995–3006. doi:10.1109/ACCESS.2019.2962340.
- Liang, Y., Juntong, Q., Xiao, J., et al. (2014) A literature review of UAV 3D path planning. In *Proceeding of the 11th World Congress on Intelligent Control and Automation (WCICA)*. June 2014. IEEE. pp. 2376–2381. doi:10.1109/WCICA.2014.7053093.
- Libelium (2015) Waspote LoRa SX1272 Networking guide. *Libelium communication distributions*. 4.2.
- Libelium.com. (2022). Initial page - Smart Water Sensor Guide. [online] Available at: [https://development.libelium.com/smart\\_water\\_sensor\\_guide/](https://development.libelium.com/smart_water_sensor_guide/) [Accessed 16 Jan. 2022].
- Liu, Y., Dai, H.-N., Wang, H., et al. (2020) UAV-enabled data acquisition scheme with directional wireless energy transfer for Internet of Things. *Computer Communications*, 155: 184–196. doi:10.1016/j.comcom.2020.03.020.
- Lu, M., Bagheri, M., James, A.P., et al. (2018) Wireless Charging Techniques for UAVs: A Review, Reconceptualization, and Extension. *IEEE Access*, 6: 29865–29884. doi:10.1109/ACCESS.2018.2841376.
- Lu, X., Wang, P., Niyato, D., et al. (2016) Wireless Charging Technologies: Fundamentals, Standards, and Network Applications. *IEEE Communications Surveys and Tutorials*, 18 (2): 1413–1452. doi:10.1109/COMST.2015.2499783.
- M Series Mobile, radiodetermination, amateur and related satellite services (2017) *Guidelines for evaluation of radio interface technologies for IMT-2020*. Geneva.
- Madridano, Á., Al-Kaff, A., Martín, D., et al. (2021) Trajectory planning for multi-robot systems: Methods and applications. *Expert Systems with Applications*, 173: 114660. doi:10.1016/j.eswa.2021.114660.
- Magnusson, F. and Åkesson, J. (2015a) Dynamic Optimization in JModelica.org. *Processes*, 3 (2): 471–496. doi:10.3390/pr3020471.
- Majeed, A. and Oun Hwang, S. (2022) Recent Developments in Path Planning for Unmanned Aerial Vehicles. In *Motion Planning*. IntechOpen. doi:10.5772/intechopen.99576.
- Mallawaarachchi, V. (2020) *Evaluating Clustering Results*. [online] Medium.
- Mandloi, D., Arya, R. and Verma, A.K. (2021) Unmanned aerial vehicle path planning based on A\* algorithm and its variants in 3d environment. *International Journal of System Assurance Engineering and Management*, 12 (5): 990–1000. doi:10.1007/s13198-021-01186-9.
- Mandow, L. and de La Cruz, José.L.P. (2010) Multiobjective A\* search with consistent heuristics. *Journal of the ACM*, 57 (5): 1–25. doi:10.1145/1754399.1754400.
- Martin, R.A., Gates, N.S., Ning, A., et al. (2019) Dynamic Optimization of High-Altitude Solar Aircraft Trajectories Under Station-Keeping Constraints. *Journal of Guidance, Control, and Dynamics (GCD)*, 42 (3): 538–552. doi:10.2514/1.G003737.

MATLAB and Phased Antenna Array Toolbox Release 2012b, The MathWorks, Inc., Natick, Massachusetts, United States.

Menon, G.S., Ramesh, M.V. and Divya, P. (2017) A low cost wireless sensor network for water quality monitoring in natural water bodies. In *2017 IEEE Global Humanitarian Technology Conference (GHTC)*. October 2017. IEEE. pp. 1–8. doi:10.1109/GHTC.2017.8239341.

Miao, W., Ting-Jie, L., Fei-Yang, L., et al. (2010) Research on the architecture of Internet of Things. In *2010 3rd International Conference on Advanced Computer Theory and Engineering (ICACTE)*. August 2010. IEEE. pp. V5-484-V5-487. doi:10.1109/ICACTE.2010.5579493.

Miller, B., Stepanyan, K., Miller, A., et al. (2011) 3D path planning in a threat environment. In *IEEE Conference on Decision and Control and European Control Conference (DCECC)*. December 2011. IEEE. pp. 6864–6869. doi:10.1109/CDC.2011.6160385.

Mozaffari, M., Saad, W., Bennis, M., et al. (2017) Performance Optimization for UAV-Enabled Wireless Communications under Flight Time Constraints. In *2017 IEEE Global Communications Conference (GLOBECOM)*. December 2017. IEEE. pp. 1–6. doi:10.1109/GLOCOM.2017.8254660.

Mutiara, G.A., Herman, N.S. and Mohd, O. (2020). Using Long-Range Wireless Sensor Network to Track the Illegal Cutting Log. *Applied Sciences*, 10(19), pp. 6992. doi:10.3390/app10196992.

Na, Z., Liu, Y., Shi, J., et al. (2021) UAV-Supported Clustered NOMA for 6G-Enabled Internet of Things: Trajectory Planning and Resource Allocation. *IEEE Internet of Things Journal (IoT)*, 8 (20): 15041–15048. doi:10.1109/JIOT.2020.3004432.

Nie, X., Fan, T., Wang, B., et al. (2020) Big Data analytics and IoT in Operation safety management in Under Water Management. *Computer Communications*, 154: 188–196. doi:10.1016/j.comcom.2020.02.052.

Nikolteas, S., Raptis, T., Souroulagkas, A., et al. (2017) Wireless Power Transfer Protocols in Sensor Networks: Experiments and Simulations. *Journal of Sensor and Actuator Networks (SAN)*, 6 (2): 4. doi:10.3390/jsan6020004.

Nordrum, A. (2016) The internet of fewer things [News]. *IEEE Spectrum*, 53 (10): 12–13. doi:10.1109/MSPEC.2016.7572524.

Pacheco, J., Ibarra, D., Vijay, A., et al. (2017) IoT Security Framework for Smart Water System. In *2017 IEEE/ACS 14th International Conference on Computer Systems and Applications (AICCSA)*. October 2017. IEEE. pp. 1285–1292. doi:10.1109/AICCSA.2017.85.

Papas, I., Estivals, B., Ecrepont, C., et al. (2018) Energy Consumption Optimization through Dynamic Simulations for an Intelligent Energy Management of a BIPV Building. In *2018 7th International Conference on Renewable Energy Research and Applications (ICRERA)*. October 2018. IEEE. pp. 853–857. doi:10.1109/ICRERA.2018.8566915.

Philipp Hohenblum (2014) *Workshop on early warning systems*. Arona (Italy). Available at: [https://ercncip-project.jrc.ec.europa.eu/sites/default/files/reqno\\_jrc94436\\_workshop\\_on\\_early\\_warning\\_systems.pdf](https://ercncip-project.jrc.ec.europa.eu/sites/default/files/reqno_jrc94436_workshop_on_early_warning_systems.pdf) (Accessed: 5 July 2022).

Pi, W. and Zhou, J. (2021) Multi-uav enabled data collection with efficient joint adaptive interference management and trajectory design. *Electronics (Switzerland)*, 10 (5): 1–37. doi:10.3390/electronics10050547.

Pukrongta, N. and Kumkhet, B. (2019) The relation of LoRaWAN efficiency with energy consumption of sensor node. In *2019 International Conference on Power, Energy and Innovations (ICPEI)*. October 2019. IEEE. pp. 90–93. doi:10.1109/ICPEI47862.2019.8945016.

Radhakrishnan, V. and Wu, W. (2019) IoT Technology for Smart Water System. In *Proceedings - 20th International Conference on High Performance Computing and Communications, 16th International Conference on Smart City and 4th International Conference on Data Science and Systems, (HPCC/SmartCity/DSS)*. doi:10.1109/HPCC/SmartCity/DSS.2018.00246.

Radhakrishnan, V. and Wu, W. (2022) Energy Efficient Communication Design in UAV Enabled WPCN Using Dome Packing Method in Water Distribution System. *Energies*, 15 (10): 3844. doi:10.3390/en15103844.

Radhakrishnan, V., Wu, W. and Wu, T. (2021) A Dome packing method for UAV positioning using 3D Beamforming in WPCN for water distribution network. In *2021 26th International Conference on Automation and Computing: System Intelligence through Automation and Computing, (ICAC)*. 2021. doi:10.23919/ICAC50006.2021.9594179.

Saadi, A., Soukane, A., Meraihi, Y., et al. (2022) UAV Path Planning Using Optimization Approaches: A Survey. *Archives of Computational Methods in Engineering*, 29: 4233–4284, doi:10.1007/s11831-022-09742-7.

Safyanu, B.D., Abdullah, M.N. and Omar, Z. (2019) Review of Power Device for Solar-Powered Aircraft Applications. *Journal of Aerospace Technology and Management (ATAM)*. doi:10.5028/jatm.v11.1077.

Said, M., E., Belal, AA., Kotb Abd-Elmabod, S., et al. (2021) Smart farming for improving agricultural management. *The Egyptian Journal of Remote Sensing and Space Science (RSSS)*, 24 (3): 971–981. doi:10.1016/j.ejrs.2021.08.007.

Sanna, G., Godio, S. and Guglieri, G. (2021) Neural Network Based Algorithm for Multi-UAV Coverage Path Planning. In *2021 International Conference on Unmanned Aircraft Systems (ICUAS)*. 15 June 2021. IEEE. pp. 1210–1217. doi:10.1109/ICUAS51884.2021.9476864.

Sbarciog, M., vande Wouwer, A., van Impe, J., et al. (2020) Extremum Seeking Control of a Three-Stage Anaerobic Digestion Model. *IFAC-PapersOnLine*, 53 (2): 16773–16778. doi:10.1016/j.ifacol.2020.12.1142.

- Shahra, E.Q. and Wu, W. (2020) Water contaminants detection using sensor placement approach in smart water networks. *Journal of Ambient Intelligence and Humanized Computing (AIHC)*. doi:10.1007/s12652-020-02262-x.
- Shen, L., Wang, N., Zhu, Z., et al. (2022) UAV-Enabled Data Collection Over Clustered Machine-Type Communication Networks: AEM Modeling and Trajectory Planning. *IEEE Transactions on Vehicular Technology*, pp. 1–16. doi:10.1109/TVT.2022.3181158.
- Sun, Y., Xu, D., Ng, D.W.K., et al. (2019) Optimal 3D-Trajectory Design and Resource Allocation for Solar-Powered UAV Communication Systems. *IEEE Transactions on Communications*, 67 (6): 4281–4298. doi:10.1109/TCOMM.2019.2900630.
- Tang, J., Song, J., Ou, J., et al. (2020) Minimum Throughput Maximization for Multi-UAV Enabled WPCN: A Deep Reinforcement Learning Method. *IEEE Access*, 8: 9124–9132. doi:10.1109/ACCESS.2020.2964042.
- The UK Civil Aviation Authority (2019) *The Drone and Model Aircraft Code*.
- Timotheou, S., Krikidis, I., Gan, Z., et al. (2014) Beamforming for MISO Interference Channels with QoS and RF Energy Transfer. *IEEE Transactions on Wireless Communications*, 13 (5): 2646–2658. doi:10.1109/TWC.2014.032514.131199.
- Tong, P., Liu, J., Wang, X., et al. (2019) UAV-Enabled Age-Optimal Data Collection in Wireless Sensor Networks. In *2019 IEEE International Conference on Communications Workshops (ICC Workshops)*. May 2019. IEEE. pp. 1–6. doi:10.1109/ICCW.2019.8756665.
- Radhakrishnan, V. and Wu W. (2019) Wireless Powered Communication Network in Iot Enabled Water Distribution System. In *17th International Computing & Control for the Water Industry Conference (ICCWIC)*. Exeter, 4 September 2019.
- Viani, F., Bertolli, M., Salucci, M., et al. (2017) Low-Cost Wireless Monitoring and Decision Support for Water Saving in Agriculture. *IEEE Sensors Journal*, 17 (13): 4299–4309. doi:10.1109/JSEN.2017.2705043.
- Waen, D. J., Dinh, H.T., Cruz Torres, M.H., et al. (2017) Scalable multirotor UAV trajectory planning using mixed integer linear programming. In *2017 European Conference on Mobile Robots (ECMR)*. September 2017. IEEE. pp. 1–6. doi:10.1109/ECMR.2017.8098706.
- Wang, S., Zhao, L., Liang, K., et al. (2018) Energy beamforming for full-duplex wireless-powered communication networks. *Physical Communication*, 26: 134–140. doi:10.1016/j.phycom.2017.12.007.
- Wang, Z., Wen, M., Dang, S., et al. (2021a) Trajectory design and resource allocation for UAV energy minimization in a rotary-wing UAV-enabled WPCN. *Alexandria Engineering Journal*, 60 (1): 1787–1796. doi:10.1016/j.aej.2020.11.027.
- Wang, Z., Yang, H., Wu, Q., et al. (2021b) Fast Path Planning for Unmanned Aerial Vehicles by Self-Correction Based on Q-Learning. *Journal of Aerospace Information Systems*, 18 (4): 203–211. doi:10.2514/1.I010856.
- Wu, B., Guo, D., Zhang, B., et al. (2022) Completion time minimization for UAV enabled data collection with communication link constrained. *IET Communications*, 16 (10): 1025–1040. doi:10.1049/cmu2.12378.

- Wu, C., Huang, X., Luo, Y., et al. (2020) An Improved Sparse Hierarchical Lazy Theta Algorithm for UAV Real-Time Path Planning in Unknown Three-Dimensional Environment. In *2020 IEEE 20th International Conference on Communication Technology (ICCT)*. 28 October 2020. IEEE. pp. 673–677. doi:10.1109/ICCT50939.2020.9295690.
- Wu, Q., Zeng, Y. and Zhang, R. (2018) Joint Trajectory and Communication Design for Multi-UAV Enabled Wireless Networks. *IEEE Transactions on Wireless Communications*, 17 (3): 2109–2121. doi:10.1109/TWC.2017.2789293.
- Wu, Y., Kim, K., Henry, M.F., et al. (2017) Design of a leak sensor for operating water pipe systems. In *2017 IEEE/RSJ International Conference on Intelligent Robots and Systems (IROS)*. September 2017. IEEE. pp. 6075–6082. doi:10.1109/IROS.2017.8206506.
- Xu, J., Zeng, Y. and Zhang, R. (2018) UAV-Enabled Wireless Power Transfer: Trajectory Design and Energy Optimization. *IEEE Transactions on Wireless Communications*, 17 (8): 5092–5106. doi:10.1109/TWC.2018.2838134.
- Xu, L. da, He, W. and Li, S. (2014) Internet of Things in Industries: A Survey. *IEEE Transactions on Industrial Informatics*, 10 (4): 2233–2243. doi:10.1109/TII.2014.2300753.
- Yang, F., Xu, W., Zhang, Z., et al. (2018) Energy Efficiency Maximization for Relay-Assisted WPCN: Joint Time Duration and Power Allocation. *IEEE Access*, 6: 78297–78307. doi:10.1109/ACCESS.2018.2884953.
- Yang, S., Deng, Y., Tang, X., et al. (2019) Energy Efficiency Optimization for UAV-Assisted Backscatter Communications. *IEEE Communications Letters*, 23 (11): 2041–2045. doi:10.1109/LCOMM.2019.2931900.
- Yang, Z., Xu, W. and Shikh-Bahaei, M. (2020) Energy Efficient UAV Communication With Energy Harvesting. *IEEE Transactions on Vehicular Technology*, 69 (2): 1913–1927. doi:10.1109/TVT.2019.2961993.
- Yoo, J., Kim, H.J. and Johansson, K.H. (2017) Path planning for remotely controlled UAVs using Gaussian process filter. In *2017 17th International Conference on Control, Automation and Systems (ICCAS)*. October 2017. IEEE. pp. 477–482. doi:10.23919/ICCAS.2017.8204486.
- Yue, L. and Chen, H. (2019) Unmanned vehicle path planning using a novel ant colony algorithm. *EURASIP Journal on Wireless Communications and Networking*, 2019 (1): 136. doi:10.1186/s13638-019-1474-5.
- Zeng, F., Hu, Z., Xiao, Z., et al. (2020) Resource Allocation and Trajectory Optimization for QoE Provisioning in Energy-Efficient UAV-Enabled Wireless Networks. *IEEE Transactions on Vehicular Technology*, 69 (7): 7634–7647. doi:10.1109/TVT.2020.2986776.
- Zeng, Y., Xu, J. and Zhang, R. (2019) Energy Minimization for Wireless Communication With Rotary-Wing UAV. *IEEE Transactions on Wireless Communications*, 18 (4): 2329–2345. doi:10.1109/TWC.2019.2902559.
- Zeng, Y. and Zhang, R. (2017) Energy-Efficient UAV Communication With Trajectory Optimization. *IEEE Transactions on Wireless Communications*, 16 (6): 3747–3760. doi:10.1109/TWC.2017.2688328.

Zhan, C., Zeng, Y. and Zhang, R. (2018) Energy-Efficient Data Collection in UAV Enabled Wireless Sensor Network. *IEEE Wireless Communications Letters*, 7 (3): 328–331. doi:10.1109/LWC.2017.2776922.

Zhang, N., Zhang, M. and Low, K.H. (2021) 3D path planning and real-time collision resolution of multirotor drone operations in complex urban low-altitude airspace. *Transportation Research Part C: Emerging Technologies*, 129: 103123. doi:10.1016/j.trc.2021.103123.

Zhang, R. and Ho, C.K. (2013) MIMO Broadcasting for Simultaneous Wireless Information and Power Transfer. *IEEE Transactions on Wireless Communications*, 12 (5): 1989–2001. doi:10.1109/TWC.2013.031813.120224.

Zhao, W., Qiu, W., Zhou, T., et al. (2019) Sarsa-based Trajectory Planning of Multi-UAVs in Dense Mesh Router Networks. In *2019 International Conference on Wireless and Mobile Computing, Networking and Communications (WiMob)*. October 2019. IEEE. pp. 1–5. doi:10.1109/WiMOB.2019.8923410.

Zhou, B., Bian, C., Tong, J., et al. (2017) Fabrication of a Miniature Multi-Parameter Sensor Chip for Water Quality Assessment. *Sensors*, 17 (12): 157. doi:10.3390/s17010157.

Zhou, Z., Liu, Q., Ai, Q., et al. (2011) Intelligent monitoring and diagnosis for modern mechanical equipment based on the integration of embedded technology and FBGS technology. *Measurement*, 44 (9): 1499–1511. doi:10.1016/j.measurement.2011.05.018.

Zulkifli, C.Z. and Noor, N. (2017) Wireless sensor network and internet of things (IoT) solution in agriculture. *Pertanika journal of science and technology(PJST)*, 25.

# APPENDIX A

## Publications

### List of Publications

1. Radhakrishnan, V. and Wu, W. (2018). IoT Technology for Smart Water System. [online] IEEE Xplore. Available at: <https://ieeexplore.ieee.org/document/8622984>
2. Radhakrishnan, V. and Wu, W. (2019). Wireless powered communication network in IoT enabled water distribution system. Submitted for the Proceedings in 17<sup>th</sup> International Computing & Control for the water industry conference. 4 September. Available at: <http://www.open-access.bcu.ac.uk/7829>
3. Radhakrishnan, V., Wu, W. and Wu, T. (2021). Dome packing method for UAV positioning using 3D Beamforming in WPCN for water distribution network. Published in 2021 26th International Conference on Automation and Computing (ICAC), Doi: <https://doi.org/10.23919/ICAC50006.2021.9594179>.
4. Radhakrishnan, V. and Wu, W. (2022). Energy Efficient Communication Design in UAV Enabled WPCN Using Dome Packing Method in Water Distribution System. *Energies*, 15(10), p.3844. Doi: <https://doi.org/10.3390/en15103844>.
5. Radhakrishnan, V., Wu, W. and Jabbar, W. A. (2023) A Hybrid Approach for Energy optimization of UAV enabled WPCN in Water Distribution Systems. Submitted to *IEEE Internet of Things Journal*.



# IoT technology for Smart water system

Varsha Radhakrishnan and Wenyan Wu

Varsha Radhakrishnan  
Faculty of Computing,  
Engineering and Built  
Environment  
Birmingham City University  
Birmingham, United Kingdom  
varsha.radhakrishnan@mail.bcu.ac.uk

Wenyan Wu  
Faculty of Computing,  
Engineering and Built  
Environment  
Birmingham City University  
Birmingham, United  
Kingdom  
wenyan.wu@bcu.ac.uk

**Abstract**— A serious drop in ensuring the water quality in the distribution system is a factor that affects public health. This could lead to increase in biological and non-biological contents, change in colour and odour of the water. These contaminants cause a serious threat to the whole water ecosystem. The conventional methods of analyzing the water quality require much time and labour. So there is a need to monitor and protect the water with a real time water quality monitoring system in order to make active measurements to reduce contamination. The growth of the technology had helped in developing efficient methods to solve many serious issues in real-time. Internet of things (IoT) has achieved a great focus due to its faster processing and intelligence. This paper focuses on discussing the architecture, applications and need of IoT in water management system.

**Keywords**— Internet of Things, WSN, RFID, AI, Water distribution system.

## I. INTRODUCTION

Intelligent monitoring is defined as a method which is used to monitor, control, manage and optimize the network by using different computational methods that will provide customers with relevant tools and information [1]. The internet of things (IoT) forms an important part of intelligent monitoring which connects people and devices using wireless sensor technology. It is a fast growing research area in the military, energy management, healthcare and many more.

The concept of IoT was proposed by Kevin Ashton to demonstrate a set of interconnected devices [1]. IoT makes it possible to transfer information between different electronic devices embedded with new technology. The energy management is possible using energy harvesting mechanisms, which is a method of collecting energy from natural sources such as light, vibration, pressure etc. The combination of technologies such as Wireless sensor network (WSN), Radio frequency identification (RFID), Energy harvesting (EH) and Artificial Intelligence (AI) helps IoT to flourish widely.

Water distribution system (WDS) is a very important research area that affects the economic growth of our country. WDS mainly have two issues, first is the water loss due to leakage and the second is that it is prone to contamination. It is affecting the health and safety of the people. According to the report of world health organization (WHO) in 2017, around 2.1 billion people around the world lack safe drinking water. So there is a need to ensure the water quality and wastage by using IoT to reduce such issue.

There are different traditional methods to collect water datasets to measure its quality, but managing and monitoring the data from WDS in real time is challenging as the data is heterogeneous, data collection is time-consuming, energy required for processing, coverage and connectivity of the nodes in the network. By using IoT and combining technologies such as WSN, AI and EH can be used to ensure the water quality in real time and alerts the users to take remedial measures.

In this survey, we look at the need of IoT in smart water system. In the first step, a basic architecture is selected and applied in WDS by analysing and comparing different technologies, equipment, cost and methods to build a smart water system. It reveals the need for an IoT architecture with technologies combined for water distribution system. It also takes into account of its advantages and disadvantages based on the literature review. The selection of the best choice can be identified for smart water system at the end of this step. The next step involves selection of the parameters required using IoT for water distribution. At this step, the current issues during the selection of parameters and some suitable suggestions are provided. Finally, an overview of the benefits which is necessary to implement IoT in smart water system is discussed.

The survey structure is organized as follows. Section 2 explains the basic architecture and technologies applied at each layer in IoT for water management and section 3 specifies the parameters required to identify water quality, section 4 provides the applications of IoT in water and section 5 explains the benefits of IoT in smart water system based on the architecture and concluding with section 6.

## II. ARCHITECTURE

There are different architectures proposed by different authors based on the type and level of security required by each application. A six layered architecture has been proposed in [2] by combining Web services, RFID and WSN whereas a five level architecture has been mentioned in [4] based on telecommunication management network. The basic and simple architecture [3] consists of three layers which are perception, network and application layer. This architecture will be used in the review paper focusing on WDS.

### A. Perception Layer

The main use of the perception layer is to connect devices and collect data for processing from the IoT network. This layer consists of sensors, EH devices when applied to WDS.

Different types of sensors are available commercially which is used to detect water monitoring in real time. A sensor network using electrochemical optical sensors [7] is one among the sensors to identify temperature, water flow, pH etc. Another one is kapta 3000 AC4 to measure chlorine, temperature, pressure and conductivity of the water and it costs around 3200 pounds whereas spectro:lyser is another one to monitor colour, turbidity, COD, BTX O3 etc. with a longer range and costs about 11000 pounds. Smart water solution by libelium is another sensor in identifying water contaminants and costs around 5000 pounds [5], [6]. The choice of the water quality sensor depends upon the cost, efficiency and the selection of the water quality attributes.

Energy harvesting is a method of collecting energy from different natural sources such as light, wind, vibration etc. and converting it into electricity to power up a device or extend its battery life.

TABLE I. COMMERCIALY AVAILABLE WATER QUALITY SENSORS AND THE MEASURING PARAMETERS

Sensor	Water quality parameter	Source
Spectro:lyser	Turbidity, temperature, pressure, colour, dissolved ions, UV254	Broeke(2005)[9]
SmartCoast	pH, dissolved oxygen(DO), conductivity, temperature, turbidity, phosphate, water level	O'Flynn et al., 2007[10]
Kapta 3000 AC4	Chlorine, temperature, pressure, conductivity	McDougle et al., 2012[11]
Smart water(Libelium)	pH, dissolved oxygen(DO), conductivity, temperature, oxidation-reduction potential(ORP), turbidity, dissolved ions	Libelium(2014)[12]
Lab-on-chip	Any specific bio-chemical	Tsopela et al., 2016[13]
I::scan	Colour, turbidity, UV254	S::can(2017)[8]

Energy harvesting module is an electronic device used to generate energy and manage it for the working of its connected sensors, processing and communication units [14]. Energy harvesting methods are gaining more research interest each year due to their different properties. The new energy harvesting methods and their desirable properties such as low cost, efficiency, availability and high robustness could benefit the water management system [15].

TABLE II. HARVESTING TECHNIQUES AGAINST ENERGY PRODUCED AND COST

Harvesting technique	Power generated	Cost
Light (solar cell)	15mW/cm <sup>2</sup>	Low
Vibration	116μW/cm <sup>3</sup>	Low
RF	~100μW/cm <sup>3</sup>	Medium
Thermoelectric	40μw/cm <sup>3</sup>	Low
Electro-magnetic	18mW/cm <sup>3</sup>	High
Piezo-electric	330μW/cm <sup>3</sup>	High

The selection of the energy harvesting method is based on the type and location of the application. Kinetic, radiant, thermal and biochemical are the sources used to generate energy. The amount of energy produced by energy harvesting depends upon the pressure, flow rate and structure of the pipelines. Table 1 provides a list of the available harvesting techniques and the amount of power and cost involved in each method [15], [16], [17].

The energy harvesting methods suitable for water monitoring are the solar cell, piezo electric, electro-magnetic, fuel cell and thermo-electric. The practical implementation of solar cell seems to be difficult as the transferring of energy to underground water pipelines will be difficult whereas the fuel cell uses a chemical reaction to generate power which will be a slow process. The piezoelectric, electromagnetic and thermoelectric are the other three methods which are used widely for monitoring water pipelines [18], [19], [20]. Table 2 provides a comparison of these three techniques in the wireless network. The selection of the harvesting method was based on considering its advantages and disadvantages that were analysed during the literature [21], [22], [23].

TABLE III. COMPARISON OF HARVESTING TECHNIQUES USED IN WATER PIPELINES[20], [21], [22], [23]

Harvesting technique	Advantages	Disadvantages
Piezo-electric	High efficiency, easy to design, No need of external voltage source	Small leakage of charge due to polarization
Electromagnetic	Reliable, No need of external voltage source	Size bigger compared to other methods, low voltage load
Thermoelectric	Lightweight, Reliable	Difficult to design due to maintain optimal thermal conduction coefficient, low power generated

## B. Network Layer

The network layer of IoT in WDS combines processing, managing and transmission of the data passed from the perception layer. This layer also helps in managing the network devices and communication technologies for transmission.

The communication technology is classified into two based on the range of transmission. The cellular technology is used when long-distance transmission is required by using 2G, 3G, 4G [26]. The GSM, GPRS are some of the protocols used for long distance transmission. It requires more power consumption which makes them not much feasible for WDN. The short range protocols include Zigbee, 6lowpan, Radio frequency identification (RFID). The RFID uses an electronically programmed tag that is used to collect data [27].

The need of a programmed static tag makes it unreliable to use for measurement. The 6lowpan is an IP based protocol which can be easily connected to another IP network without any gateways. Another advantage is its low cost and power consumption. It supports both star and mesh topology. LoRa (Low Power Wide Area Network) is another protocol which gained public interest due to its low power consumption, cost and high data rate when applied in IoT and it uses the star topology. Zigbee is a widely used low power wireless

protocol that provides low cost, security during communication. It also supports star, mesh and tree topology [26]. The advantages of flowpan, LoRa and Zigbee make the best choices to be used in WDS.

Another technology that could be integrated with WDS is Artificial intelligence(AI). It is defined as a system that helps in problem-solving, decision-making, data identification, processing. Adaptive Neuro fuzzy inference system is one among the new AI method to predict the wastewater quality from industries [28] whereas an adaptive network based fuzzy system is used in [29] to detect the water quality from a paper mill. Artificial neural networks (ANN) and AI algorithms are also used in the water industry to monitor and predict the water quality which provides accurate results [30].

### C. Application Layer

The application layer manages the applications that will be used in WDS. This layer also provides user's security and privacy.

Cloud computing is one of the upcoming technology that could be used in the application layer of the WDS. Cloud computing is a solution for the storage, processing and management of heterogeneous data from different wireless devices and the cost of the service is based on the usage [31]. It can be considered as a separate layer between network and application layer. It helps IoT in storing backup data's, analysis and prediction of the received data based on each application.

## III. PARAMETERS IN SMART WATER SYSTEM

The parameters to detect the water quality depends on the property they exhibit and where it is applied. There are a number of parameters to detect the water quality, but monitoring all the parameters will affect the increase in workload and thereby affecting the quality of analysis. The parameters that are usually used to detect water quality in the pipeline include chemical, physical and biological properties.

### A. Quality Factors

The chemical properties include pH, dissolved oxygen and oxidation-reduction potential. The amount of acidity or alkalinity of a solution is determined using pH. In WDS, a pH between 6 and 9 is considered normal. The ability of the water to remove the impurities by itself is called oxidation-reduction potential and a high value of oxidation-reduction potential represents the good quality of water. The dissolved oxygen is the amount of oxygen dissolved in water and it should be 0.5mg/L for WDS [24].

The physical factors include temperature, turbidity and conductivity of water. Turbidity is the opacity or cloudiness due to the microscopic materials dissolved in the solution and it should not be less than 1NTU in WDS. High temperature affects the amount of oxygen in the water and disturbing the water quality [25].

The presence of bacteria, virus, algae and pesticides forms the biological factors affecting the water quality [25].

These are included in the basic category to determine the water quality. It is rather confusing as there aren't any international standard methods from any professional bodies for the selection of water quality parameters.

### B. Quantity Factors

The water level, pressure of flow and velocity are the quantity factors that should be considered when collecting the water data. The ultrasonic sensors and flow sensors can be used to detect the velocity and identify the change in water flow [32], [33], [34].

The management of sensor data in real-time is difficult as centralized or distributed approach is used to handle them. A hybrid approach with an efficient compression technology could be used to handle and filter the real-time data based on the necessity and to reduce the cost of transmission in the network layer.

### C. Technological Factors

The self-adapting network technology is a technological factor supporting the smart water system. The intelligent selection of stations, data fusion and forecasting to provide water quality information based on an emergency situation and make a rapid decision-making is essential for a smart water system. This could be integrated with the network layer of the architecture to achieve a more accurate real time monitoring [35].

### D. Topological Factors

The topological factor consists of active and passive elements that form the network. The active element consists of valves, turbines and pumps through which water flow and pressure can be controlled whereas the passive element consists of pipes and reservoirs which depends on the active elements. Real-time monitoring and controlling the operations from different water sources and managing the operational cost is a major factor affecting the water system. The recent researches of different optimization methods on dynamic topology using convex programming, clustering etc. could be an added advantage to the smart water system [36].

## IV. APPLICATIONS OF IOT IN WATER

### A. Smart Water System

The smart water applications include water pipeline monitoring, water quality in open water source, smart water meter reading, IoT security for smart water system(SWS) etc. In order to ensure the integrity of customer information, security of the devices and data passed through the network, a framework and methodology were developed [37]. Water quality monitoring of open water sources was another application that was implemented using IoT devices. It helps to preserve the water quality and protect the health of the economy using low-cost devices and network virtualization [38], [39]. Another application developed due to the growth of IoT was pipe leakage detection. Different IoT devices, WSN and cloud service were used to detect and alerts the user about the pipe leakage because a good amount of water wastage is occurring through leakage [40]. Wastewater monitoring and treatment is another upcoming application in IoT to treat the wastewater and use it for household activities and thereby saving the amount of water to a great extent [41], [42].

### B. Smart Irrigation

IoT based mobile applications have developed in farming to control the amount of water for crops based on the

surrounding temperature. It also manages the whole irrigation system by smartly monitoring the soil and growth of the crops and the irrigation sprinkler will get activated whenever necessary thereby reducing the water wastage and workload [43], [44].

#### C. Smart Gardening

The smart gardening application was focused on improving the mental health of the elderly people interested in gardening which uses IoT for its implementation. It uses a set of sensors to detect the temperature, light, water, soil moisture and a mobile application to remind the need and amount of water and nutrients for the plants [45].

#### D. Aquaculture System

The aquaculture is a technique of determining and alerting users about the water quality for culturing of aquatic organisms using IoT. This application is also used to monitor the plant's environment in aquariums. It helped the aquatic farmers to recycle the water whenever they receive user alerts on their mobile devices and results in increased productivity [46].

Most of the applications mentioned above are developed in the last year which clearly depicts the growth of IoT, especially in water. There is a need for more research in water with the growth of new technologies such as IoT.

### V. BENEFITS OF IoT ARCHITECTURE IN WATER MANAGEMENT

The following benefits of IoT help to expand the research into WDS.

#### A. Integration of Technologies

The integration of different technology has taken water management research to a new level. The combination of energy harvesting into IoT could resolve the energy management issues in the water distribution system. The solar cell, piezoelectric, electromagnetic and thermoelectric harvesting are the methods that could be integrated with the perception layer to enhance the smart water system. The upcoming research in micro-electro-mechanical systems (MEMS) such as piezoelectric nanowires, Lead zirconate titanate (PZT) films and multi-parameter sensor chip using iridium oxide film and X-ray photoelectron spectroscopy (XPS) analysis could also improve the research in water [47].

#### B. Data storage, Management and Computation

A solution to the storage issue of the wireless sensor network has been made possible by IoT-cloud combination. The use of cellular protocols, interaction aware schemes and clustering methods were used to store and manage sensor data using the cloud. Using these methods, the sensor data will be transferred into the cloud using specific algorithms and thereby provide network stability [48], [49].

Data fusion is another method to manage data in WSN. It is a method of automatically combining data from different sources that helps users to make decisions in many complicated situations. The most widely used model is Joint Director of Laboratories (JDL) which was developed to improve the cooperation and carry technological data within a group [50]. This concept has been implemented using the least square technique to identify the quality of water usage

in houses. It requires more computational power and cost. The data storage and management are applied in the network layer of IoT architecture.

#### C. Energy Management

The power transfer between the sensor nodes is another technological advancement to manage energy in IoT for water distribution system. The thermal or magnetic field will be suitable for the power transfer in determining the water quality in pipelines. An energy efficient scheduling scheme for power transfer and a wireless power transfer protocol were some of the recent developments in energy management [51], [52]. The wireless power transfer protocol consists of two protocols, one for balancing the energy and the other one for checking the power of each sensor nodes for energy transfer. The research on scheduling is to reduce the energy consumption of the transmitters in software-defined wireless sensor network [51]. This technique could be implemented in the network layer to manage energy in water distribution system.

As the growth IoT is rapidly increasing every year and several IoT architectures has been introduced based on the application. The current water distribution system now uses smart devices, artificial intelligent methods and MEMS which later on could be integrated with energy harvesting methods and more IoT devices, the basic architecture seems to be inefficient to be used in water distribution system with new technologies integrated. So there is a need for more research in creating an IoT architecture to be used in water distribution system.

### VI. CONCLUSION

Water quality is a serious factor that affects the health of the economy. The increase in the number of IoT devices and the development of new technology requires a standard IoT architecture which could help the clients to create a low cost and efficient system. This paper discusses about the implementation of IoT in water distribution system on the basis of IoT architecture, upcoming technologies such as cloud computing, Artificial intelligence, transmission techniques etc.; applications and the advantage of IoT in water distribution. The paper reveals some of the current issues when selecting parameters for the smart water system. The paper also suggests some solutions by referring to the recent or upcoming researches which could resolve the issues and integrate them to produce a more cost and energy efficient smart water system. The paper also provides a comparison of energy harvesting methods and water quality sensors used in the current water pipelines to select the best method suitable for the application. The basic architecture of IoT lacks a proper structure and requires more research for developing and implementing an architecture and integrate it into the water distribution system.

### VII. CHALLENGES AND FUTURE WORK

As IoT is growing every day with new technologies involved, new challenges arise. The IoT has encouraged people to connect to devices using the internet and the increase in the use of IoT devices motivated people to use smart technologies. The water quality in the distribution system is a serious factor that affects public health and smart water

system provides a user-friendly interface to monitor the water quality in houses and take remedial measurements if necessary. One of the main challenges in smart water system is managing the cost, energy and efficiency required for water distribution system. The selection of water quality, quantity and topological parameters is another challenge in the smart water system. So there is in need of research about these challenges to provide a new cost and energy efficient solution to the smart water system. The future work will focus on developing an IoT architecture in water distribution system with integration of new technologies such as cloud, energy harvesting etc.

#### ACKNOWLEDGMENT

This research is supported by European Union's Horizon 2020 research and innovation programme under the Marie Skłodowska-Curie-Innovative Training Networks (ITN)-IoT4Win (765921).

#### REFERENCES

- [1] Z. Zude, L. Qian, A. Qingsong, & X. Cheng, "Intelligent monitoring and diagnosis for modern mechanical equipment based on the integration of embedded technology and FBGS technology", pp. 1499-1511, 12 Nov. 2011. <https://doi.org/10.1016/j.measurement.2011.05.018>
- [2] J.M.P. Martinez, R.B. Llavori, M.J.A. Cabo, and T.B. Pedersen, "Integrating Data Warehouses with Web Data: A Survey," *IEEE Trans. Knowledge and Data Eng.*, preprint, 21 Dec. 2007, doi:10.1109/TKDE.2007.190746.
- [3] M. Zhang, F. Sun and X. Cheng, "Architecture of Internet of Things and Its Key Technology Integration Based-On RFID", *Proc IEEE Fifth International Symp. on computational intelligence and design*, Oct. 2012, doi:10.1109/ISCID.2012.81.
- [4] J. Lin, W. Yu, N. Zhang, X. Yang, H. Zhang, W. Zhao, "A survey on internet of things: Architecture enabling technologies security and privacy and applications", *IEEE Internet of Things Journal*, vol.4 (5), pp. 1125-1142, Oct. 2017.
- [5] M. Wu, T. Lu, F. Ling, L. Sun, H. Du, "Research on the architecture of Internet of things", *Advanced Computer Theory and Engineering (ICACTE)*, pp. 484-487, 2010.
- [6] P. Hohenblum, "Workshop on early warning systems" (2014). *Report of ERNCIP thematic area Chemical & Biological Risks in the Water Sector Deliverable D1 -Task 1*. Retrieved from [https://erncip-project.jrc.ec.europa.eu/sites/default/files/Review\\_of\\_sensors\\_to\\_monitor\\_water\\_quality.pdf](https://erncip-project.jrc.ec.europa.eu/sites/default/files/Review_of_sensors_to_monitor_water_quality.pdf), 26 Jun. 2014.
- [7] K. Abhirami and L.R. Karlmarx, "A novel fault-tolerant control scheme for water distribution systems", *Proc. IEEE Conference on Energy Efficient Technologies for Sustainability*, Apr. 2013, doi:10.1109/ICEETS.2013.6533496.
- [8] T. P. Lambrou, C. C. Anastasiou, C. G. Panayiotou and M. M. Polycarpou, "A Low-Cost Sensor Network for Real-Time Monitoring and Contamination Detection in Drinking Water Distribution Systems". *IEEE Sensors Journal*, 14(8), 2765-2772, 2014.
- [9] J. V.D. Broeke, "A short evaluation of the S:can Spectro:lyser", *Evaluation Report project number111508.030*, Kiwa, Netherlands, Jan. 2005.
- [10] B. O'Flynn, R. Martinez, J. Cleary, C. Slater, F. Regan, D. Diamond, H. Murphy, "SmartCoast: A wireless sensor network for water quality monitoring", *32nd IEEE Conference on Local Computer Networks*, Dublin, 15 Oct. 2007.
- [11] T. McDougale, M. Maurel, C. Lemoine, "Smart sensor network case study for drinking water quality monitoring", *Researchgate, Conference of International water association*, Korea, Jan. 2012.
- [12] Libelium, "Smart water sensors to monitor water quality in rivers, lakes and the sea", Retrieved March 26, 2018, <http://www.libelium.com/smart-water-sensors-to-monitor-water-quality-in-rivers-lakes-and-the-sea/>
- [13] A. Tsopele, A. Laborde, I. Salvagnac, V. Ventalon, E. Bedel-Pereira, I. Seguy, P. Temple-Boyer, P. Juneau, R. Izquierdo, J. Launay, "Development of a lab-on-chip electrochemical biosensor for water quality analysis based on microalgal photosynthesis", *Journal of Biosensors and Bioelectronics, ScienceDirect*, vol.79, pp. 568-573, Dec. 2015.
- [14] S. Kosunalp, "A New Energy Prediction Algorithm for Energy-Harvesting Wireless Sensor Networks with Q-Learning", *In IEEE Access*, vol. 4(1), 7 Sept. 2016
- [15] N. A. Bhatti, M. H. Alizai, A. A. Syed & L. Mottola, "Energy Harvesting and Wireless Transfer in Sensor Network Applications". *ACM Transactions on Sensor Networks*, 12(3), 1-40, 15Nov. 2015. <https://doi.org/10.1145/2915918>
- [16] P. K. Sharma and P. V. Baredar, "Analysis on piezoelectric energy harvesting small scale device- a review", *Journal of king saud university, ScienceDirect*, 22 Nov. 2017.
- [17] K Chang J Gao WY Wu, "Water quality comprehensive evaluation method for large distribution network based on clustering analysis". *International Journal of Hydroinformatics* 13(3) 2011 p390-400 doi: 10.2166/hydro.2011.021
- [18] M. I. Mohamed, W. Y. Wu; M. Moniri, Adaptive data compression for energy harvesting wireless sensor nodes, *10th IEEE International Conference On Networking, Sensing And Control (ICNSC)*, Pages: 633 - 638, France 2013
- [19] M. I. Mohamed, W. Wu & M. Moniri, "Power harvesting wireless sensor node framework for monitoring water distribution systems". *In eleventh international conference on computing and control for water industry CCWI 2011 Exeter UK*
- [20] [21] F. Yang, W. Y. Wenyuan, "An IoTs enabled Framework for Urban water system". *In E-proceedings of the 36th IAHR World Congress 28 June - 3 July, 2015*(id: 87075)IAHR2015.
- [21] M. I. Mohamed, W. Y. Wu, & M. Moniri, "Power harvesting for smart sensor networks in monitoring water distribution system". *In 2011 International Conference on Networking, Sensing and Control*, IEEE, pp. 393-398. 16 Nov. 2011.
- [22] F. U. Qureshi, A. Muhtaroglu, & K. Tuncay, "A method to integrate energy harvesters into wireless sensor nodes for embedded in-pipe monitoring applications". *In 5th International Conference on Energy Aware Computing Systems & Applications*, IEEE, pp. 1-4. 18 Oct. 2015.
- [23] F. U. Qureshi, A. Muhtaroglu, & K. Tuncay, "Near-Optimal Design of Scalable Energy Harvester for Underwater Pipeline Monitoring Applications with Consideration of Impact to Pipeline Performance". *IEEE Sensors Journal*, 17(7), pp.1981-1991. 1 Apr. 2017.
- [24] M. Jurian, C. Panait, V. Daniel, C. Bogdan, "Monitoring drinking water quality and wireless transmission of parameters", *Proc IEEE International Spring Seminar on Electronics Technology*, 12 Aug. 2010, doi: 10.1109/ISSE.2010.5547352.
- [25] M. Pale, A. Yahya, J. Chuma, "Wireless Sensor Network: A survey on monitoring water quality", *J. Applied Research and Technology*, vol.15(6), pp.562-570, Dec. 2017.
- [26] S. A. Sarawi, M. Anbar, K. Alieyan, M. Alzubaidi, "Internet of Things(IoT) communication protocols: Review", *Proc. IEEE International conf. on Information Technology*, 23 Oct. 2017.
- [27] M. U. Farooq, M. Waseem, S. Mazhar, A. Khairi, T. Kamal, "A Review on Internet of Things (IoT)", *International journal of Computer Applications*, vol.113(1), March 2015.
- [28] Z. Fu, J. Cheng, M. Yeng, J. Batists, "Prediction of industrial wastewater quality parameters based on wavelet de-noised ANFIS model", *Proc of IEEE 2018 Annual computing and communication workshop and conference (CCWC '08)*, 27 Feb. 2018.
- [29] J. Wan, M. Huang, Y. Ma, W. Guo, Y. Wang, H. Zhang, W. Li, X. Sun, "Prediction of effluent quality of a paper mill wastewater treatment using an adaptive network-based fuzzy inference system", *Applied Soft Computing*, vol. 11, no. 3, pp. 3238-3246, 2011.
- [30] A. H. Zare, "Evaluation of multivariate linear regression and artificial neural networks in prediction of water quality parameters", *Journal of Environmental Health Science & Engineering*, vol. 12, no. 1, pp. 1-8, 2014.
- [31] S. K. Alshattawi, "Smart Water Distribution Management System Architecture Based on Internet of Things and Cloud Computing", *IEEE International conference on new trends in computing sciences*, pp. 289-294, 11 Jan. 2018.

- [32] A. C. Niel, M. Reza, N. Lakshmi, "Design of Smart Sensors for Real-Time Water Quality Monitoring". *J IEEE Access* 4: 3975–3990, 2016.
- [33] P. Thinakaran, S. Nasir, C. Y. Leong, "Internet of Things (IoT) enabled water monitoring system". In: 4 IEEE global conference on consumer electronics, 27–30 Oct. 2015.
- [34] P. Yang, Hanneghan, M., Qi, J., Deng, Z., Dong, F. and Fan, D., 2015, October. "Improving the validity of lifelogging physical activity measures in an internet of things environment". In *Computer and Information Technology; Ubiquitous Computing and Communications; Dependable, Autonomic and Secure Computing; Pervasive Intelligence and Computing (CIT/IUCC/DASC/PICOM)*, 2015 IEEE International Conference on (pp. 2309-2314). IEEE.
- [35] Y. Ye, L. Liang, H. Zhao, Y. Jiang, "The system architecture of Smart Water grid for Water security". In *Elsevier 12<sup>th</sup> International Conference on Hydroinformatics (IHC)*, December 2016.
- [36] R. Wright, E. Abraham, P. Parpas and I. Stoianov, "Control of water distribution networks with dynamic DMA topology using strictly feasible sequential convex programming". In *Water resource research AGU journal*, 51(12), pp.9925-9941, December 2015.
- [37] J. Pacheco, D. Ibarra, A. Vijay, S. Hariri, "IoT security framework for Smart Water System". *Proc. of IEEE International conference on Computer Systems and Applications*, Tunisia, 12 Mar. 2018.
- [38] A. N. Prasad, K. A. Mamun, F. R. Islam, H. Haqva, "Smart water quality monitoring system". *Proc. of IEEE Asia-Pacific World Congress on Computer Science and Engineering*, Fiji, 23 May 2016.
- [39] G. S. Menon, M. V. Ramesh, P. Divya, "A low cost wireless sensor network for water quality monitoring in natural water bodies". In *IEEE Global Humanitarian Technology Conference*, USA, 25 Dec. 2017.
- [40] Y. Wu, K. Kim, M. F. Henry, K.Y. Toumi, "Design of a leak sensor for operating water pipe systems". In *IEEE International Conference on Intelligent Robots and Systems*, Canada, 14 Dec. 2017.
- [41] M.V. Ramesh, K.V. Nibi, A. Kurup, R. Mohan, A. Aiswarya, A. Arsha, P.R. Sarang, "Water quality monitoring and waste management using IoT". In *IEEE Global Humanitarian Technology Conference*, USA, 25 Dec. 2017.
- [42] J. Qi, P. Yang, G. Min, O. Amft, F. Dong and L. Xu. "Advanced internet of things for personalised healthcare systems: A survey". *Pervasive and Mobile Computing*, 41, pp.132-149. 2017.
- [43] O. Pandithurai, S. Aishwarya, B. Aparna, K. Kavitha, "Agro-tech: A digital model for monitoring soil and crops using internet of things (IOT)". *Proc. of IEEE International conference on Science, Technology, Engineering and Management*, India, 18 Jan. 2018.
- [44] S. Vaishali, S. Suraj, G. Vignesh, S. Dhivya, S. Udhayakumar, "Mobile integrated smart irrigation management and monitoring system using IOT". *Proc. of IEEE International conference on Communication and Signal Processing*, India, 08 Feb. 2018.
- [45] K. Lekjaroen, R. Pongnantayotin, A. Charoenrat, S. Funikul, U. Supasithimethee, T. Triyason, "IoT Planting: Watering system using mobile application for the elderly". *Proc. IEEE International Computer science and Engineering Conference*, Thailand, 23 Feb. 2017. doi:10.1109/ICSEC.2016.7859873.
- [46] M. Manju, V. Karthik, S. Hariharan, B. Sreekar, "Real time monitoring of the environmental parameters of an aquaponic system based on Internet of Things". *Proc. of IEEE International conference on Science, Technology, Engineering and Management*, India, 18 Jan. 2018.
- [47] B. Zhou, C. Bian, J. Tong, S. Xia, "Fabrication of a miniature multi-parameter sensor chip for water quality assessment". *Journal of Sensors*, vol. 17(1), 14 Jan. 2017.
- [48] D. Nguyen, & P. H. Phung, "A Reliable and Efficient Wireless Sensor Network System for Water Quality Monitoring". In *IEEE 2017 International Conference on Intelligent Environments (IE)*, pp. 84-91. <https://doi.org/10.1109/IE.2017.34>
- [49] T. A. Janabi and H. S. Al-Raweshdy, "Optimised clustering algorithm based centralised architecture for load balancing in IoT network". In *IEEE 2017 International symposium on Wireless Communication Systems*, Italy, 16 Nov. 2017.
- [50] D. Macci, A. Boni, M. De Cecco, D. Petri, Tutorial 14: Multisensor Data Fusion. *IEEE Instrum. Meas. Mag.* vol. 11 pp.24-33, Jun. 2008.
- [51] W. Ejaz, M. Naeem, M. Basharat, A. Anpalagan, & S. Kandeepan, "Efficient Wireless Power Transfer in Software-Defined Wireless Sensor Networks". In *IEEE Sensors Journal*, 16(20), 7409–7420, 12 Nov. 2016. <https://doi.org/10.1109/Jsen.2016.2588282>
- [52] S. Nikoletteas, T. Raptis, A. Sourologkias, & D. Tsolovos, "Wireless Power Transfer Protocols in Sensor Networks: Experiments and Simulations". In *Journal of Sensor and Actuator Networks*, 6(2), 4, 1 Apr. 2017. <https://doi.org/10.3390/jsan6020004>.



## WIRELESS POWERED COMMUNICATION NETWORK IN IOT ENABLED WATER DISTRIBUTION SYSTEM

R. Varsha<sup>1</sup>, W. Wu<sup>2</sup>

<sup>1</sup> Faculty of Computing Engineering and Built environment, Birmingham City University, United Kingdom

<sup>2</sup> Faculty of Computing Engineering and Built environment, Birmingham City University, United Kingdom  
<sup>1</sup>varsha.radhakrishnan@mail.bcu.ac.uk, <sup>2</sup>wenyan.wu@bcu.ac.uk

**Keywords:** IoT; Energy harvesting; water quality monitoring; WPCN

### EXTENDED ABSTRACT

#### INTRODUCTION

Water distribution system (WDS) is a very important research area that affects the economic growth of our country and requires a great amount of energy for monitoring and management. Many routing protocols has been developed to conserve energy and extend the battery life. In spite of considering the energy conservation, it results in performance degradations. So there is a need to ensure the water quality and wastage in real time by integrating new technologies such as wireless powered communication network (WPCN), Energy harvesting (EH) and AI methods to reduce such issues. In WPCN, the wireless devices first harvest energy from the RF source signals and then manage this energy for its processing. The research in the area of WPCN is leading more ways in energy harvesting and management due to charging over air when compared to the conventional battery charging system. Therefore, its free from battery replacement issues which results in low operational cost and increase in performance. Another advantage of WPCN is its stable and controlled power supply under different requirements and physical conditions. All these advantage makes WPCN a better choice in wireless energy transfer [2]. To extend WPCN into IoT, the designing of resource allocation schemes, interference management etc is considered carefully [1][3].

This research paper focusses on optimizing the energy used in the WPCN with multiple energy sources and multiple sensors in order to achieve zero power state where the the amount of energy produced and consumed reaches to a constant value. The problem of unfair information transmission and EH in a dynamic environment is planned to solve by implementing an energy management scheme where important decisions are taken using artificial intelligence methods.

#### METHODS

The representation of system model is as in figure 1 which consists of multiple RF energy sources and multiple sensors where different water quality data will be collected and transmitted to the base station from the pipeline. The model consists of three group of sensors which will be collecting different types of water quality parameters. The energy will be harvested and transmitted to the sensors by considering the issues such as EH fairness, doubly near far problem etc using the controller. Every process will be controlled and monitored by the controller where the energy management scheme using AI methods will be implemented. The energy and data transfer will be based on TDMA using a dynamic allocation scheme. A mathematical model is derived from to achieve zero power energy in the system.

#### RESULTS AND DISCUSSION

This paper makes a novel contribution to achieve energy optimization using WPCN for real time monitoring in water distribution system. The paper also extends WPCN by considering all the design considerations such as resource deployment, energy allocation, self-interference etc. The simulation is deployed in a 20 by 20 m environment by referring to a previous model [3] and the channel model position is calculated by subtracting the path loss along with the distance of the sensor node from the energy node from a constant value which dependshhbb on the assigned deploying environment space. In this model one of the node is chosen as a base node for data transmission based on the equal distance from the networks to the energy node. The table1 provides the assumptions that are used for simulation.

Parameter	Value
Transmission energy for RF nodes	3000 mA
RF frequency	915MHz
Medium Access control	802.15.4

Table 1. Assumptions considered for simulation

There are a few parameters that should be considered when setting up the model. One of them is the energy consumption of the sensor nodes which varies depending on the type and manufacturer of the sensors, energy



consumption of the energy harvesting nodes, setting the distance for the transmission and finally, the selection of frequency for transmission. The energy consumption of the nodes vary based on the amount of data to be sent, transmission distance etc. In this experiment, plug and sense by libelium has been used which consumes the power as in table 1.

State	Power Consumption
On	17mA
Sleep	30 $\mu$ A
Hibernate	7 $\mu$ A

Table2. Energy consumption of Libelium plug and sense

In this model three different groups of sensors are used to collect data. The first group is used to detect the water quality ions and the second to find the physical parameters such as temperature, pressure and third group to calculate pH, DO and turbidity. These values which are sent to the remote station will provide a clear picture about the quality of water in real time to the clients based on the energy produced by the energy sources and managing the energy using the algorithms implemented in the controller.

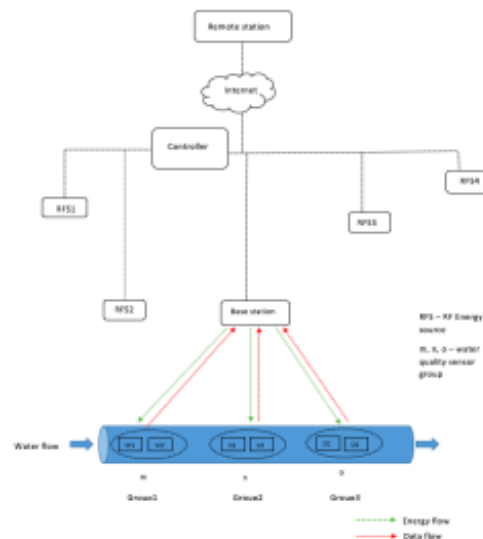


Figure 1. The System Model

The result of this model depends on how the energy is managed to achieve zero power by considering the fairness issues of the energy source and data transmission. The selection of the energy source is based on clustering by calculating the distance of the sensors from the energy source and every operation including the energy consumption will be monitored and controlled by the controller to achieve the desired result.

## CONCLUSIONS

The water quality has always been a serious issue and intelligent monitoring of the water is a powerful process that combines computing, engineering and environmental factors for ensuring the water quality and thereby protecting the water ecosystem. The upcoming WPCN technology with IoT helps to build an energy efficient and self-sustainable system that helps to reduce the energy scarcity issue without performance degradations.

## REFERENCES

- [1] P. Ramezani and A. Jamalipour, "Toward the evolution of wireless powered communication networks for the future internet of things". *IEEE Journals & Magazine*. vol. 31(6) July 2017, pp.62-69.
- [2] B. Suzhu, Z. Yong and Z. Rui, "Wireless powered communication networks: an overview". *IEEE Wireless Communications*. vol. 23(2), April 2016, pp.10-18.
- [3] Olatinwo, S. and Joubert, T. "Optimizing the Energy and Throughput of a Water-Quality Monitoring System". *Sensors Journal*, 18(4), April 2018, p.1198.



# *A Dome packing method for UAV positioning using 3D Beamforming in WPCN for water distribution network*

Varsha Radhakrishnan

*Faculty of Computing,*

*Engineering and Built Environment*

Birmingham City University

Birmingham, United Kingdom

varsha.radhakrishnan@mail.bcu.ac.uk

Wenyan Wu

*Faculty of Computing,*

*Engineering and Built  
Environment*

Birmingham City University

Birmingham, United Kingdom

wenyan.wu@u.ac.uk

Tianmeng Wu

*Department of Electrical*

*Engineering*

NorthEast Agriculture

University

Harbin, China

hrbwym@163.com

**Abstract**— In the practical implementation of wireless powered communication network (WPCN) project, the energy consumption is an important factor to evaluate the performance and efficiency of the communication. In this project, a UAV enabled WPCN acts as a hybrid access point to handle multiple ground terminals (GT's) in an uneven plane. The ground terminals will harvest radio frequency (RF) energy from the RF signals directed by the UAV and these terminal uses this harvested energy to send information to the uplink. The objective of the paper is to find an optimal position of UAV using a proposed dome packing method to navigate the UAV, thus UAV will be able to charge the GTs within the cluster using 3D beamforming method where the beam will be focusing to a particular terminal rather than broadcasting the signals everywhere and thereby minimize the total energy consumption and mission completion time.

**Keywords**— *Wireless powered communication network, Water distribution network, Unmanned aerial vehicle, 3D Beamforming, optimization.*

## I. INTRODUCTION

The water distribution network (WDN) is an important research area that focus on different issues such as intelligent monitoring for water quality, leakage etc and integrates new technologies for better and easier use. The WDN in the urban terrain covers wider area with pipes, sensors (nodes) and other components. Continuous monitoring requires communication between nodes and pipelines and these nodes send information to the control station and hence the power and its usage during communication is important for continuous monitoring [1-2]. Currently these components are powered by battery, however compared to the traditional battery charging technology, WPCN research is leading to new techniques in energy harvesting and management due to wireless charging. As a result, it does not require battery replacement, resulting in lower operating costs and improved performance. Another use of WPCN is its consistent and controlled power delivery under various

application specific demands that makes it best suited for low powered IoT devices. All these makes WPCN a preferable choice in wireless energy transfer (WET) for low operational cost, higher range and small form factor [3].

It is been past few decades that the UAV were developed for different applications such as military and emergency situations like flood [4]. In a UAV enabled WPCN, the UAV can act as an energy provider, data access point or as a hybrid access point depending on its purpose or application. In traditional fixed base station, much cost was involved in the maintenance, networking and resources which lead to use UAV as a flying base station. It is widely used recently because of the advantage in electronics such as high-speed microprocessors, sensors and new type of antennas etc. To increase the coverage, performance and operation, the UAV can act as a flying base station to work effectively that suits the application scenario as in figure 1.

In the past, sensors deployed in the ground needs to be recharged by replacing the battery after a fixed time-period which requires time and labour. This issue could be solved by combining WPCN and UAV which uses energy harvesting methods to harvest radio frequency (RF) energy from the RF waves directed by the UAV and the sensors uses this energy to transmit information to the uplink. Hence, the development of research in UAV enabled WPCN and its energy consumption is of great importance. There are huge benefits of using UAV as aerial base station such as the flexibility to move around and deployment helps rapid communication and a better line of sight (LoS) [5]. Even though the UAV creates huge benefits, there are some technical challenges which require some serious concerns such as battery life, energy consumption, 3D placement of UAV, trajectory planning which evaluates the performance of the communication.

The UAV helps to provide a constant LoS communication and different methods and architectures were recommended to increase the energy efficiency during communication by optimizing the trajectory path while acting as a flying base

station [6]. A trajectory based on time discretized approach with an assumed mission completion time to maximize the minimum harvested energy were used in one of the researches whereas another approach is used to maximize the average performance and minimum throughput to all devices [6]. A framework to optimize the trajectory in two-dimensional space has been introduced with single ground user and a UAV with constant speed is studied [7]. However, the ground users were considered uniformly in a two-dimensional plane for simplicity, but it may affect the applicability during implementation if it is considered in an uneven plane. The placement of the sensors is based on the work of [8]

The limited capacity and availability using a single UAV leads to its enhancement to use of multi UAV enabled communication system to handle different groups of ground terminal in large area. It helps to achieve higher throughput and lower delay. The research on improving the energy by focussing on throughput gained much attention.

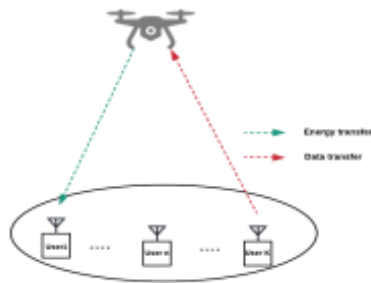


Fig 1: UAV as a flying base station

The deployment of UAV's in 2D space, the optimal altitude to achieve better coverage, finding the minimum number of drones also were studied in [9]. The energy efficiency is still a major factor during practical implementation in wireless powered networks. Some research assumed that the UAV would have surplus energy for its operation and some used methods like successive convex approximation for solving non-convex optimization problems, scheduling to manage the energy used by UAV [10].

The innovation in the field of antenna design by developing Beamforming method attracted more researchers to integrate it and implement in different scenarios such as mobile communication, energy harvesting etc. It is a method which uses multiple antennas to focus the waveform to a specific direction and alleviate the coverage issues as well as interference issues. For example, when moving a laptop from one place to another using a beamforming router, it recalculates the energy and the beam moves along with the movement of the laptop. A review of the implementation of beamforming in energy harvesting wireless networks summarize the concepts, architectures and different approaches [11]. This method has also been applied in full-duplex wireless powered communication to curtail self-interference and improve the throughput among the users [12]. In [13] and [14], a review of the beamforming methods and the factors which affects beamforming were discussed. The first factor which affects

beamforming is the array design which focus on the array configuration used in the design of the antenna as its ability to scan the main beam in three-dimensional space based on the elevation and azimuth angle. The second factor is the beaming period which depends on the network throughput and delay, and throughput drops and delay increases with increasing beaming time. Finally, the third factor is the range and it is used in wireless networks at medium and small ranges to provide a better signal to noise ratio. So, all these factors need to be considered while designing a beam. This paper focus on optimizing of the third factor which is the optimal position of the UAV which is required to minimize the energy during the communication by assuming some of the beaming factors as constant. In the practical application, the energy consumption affects the efficiency of wireless communication and the energy consumption of network which depends on the UAV's optimal position and time for moving and hovering. Hence this paper develops a algorithm for optimal position of the UAV to reduce the energy consumption and communication time for its operation.

To extend UAV enabled WPCN into water distribution network (WDN) application, the major factor that require a serious concern is minimizing the usage of energy during communication due to large scale of WDN. The optimization of unmanned aerial vehicle (UAV) positioning, height, throughput and time are the factors that should considered carefully while the minimizing the energy usage [15]. This case study is to apply on a water distribution system where a terrain is considered, which consists of surface with various elevations and hence a three-dimensional perspective of the ground nodes and the UAV is essential for delivering energy and communication services to the ground nodes. Therefore, a dome could be the perfect geometrical shape that could be applied to the considered model. As mentioned above, the altitude or height of the UAV is one of the aspects influencing the energy and time of the flight and this paper targets to optimize the position to efficiently use the power for UAV communication later in the research. Hence, a dome packing method with 3-dimensional beamforming method will be used to implement this work. The three-dimensional beamforming method is used to direct the energy signals to a destined ground terminal for an efficient communication compared to the traditional broadcasting method. The antenna arrays will be integrated with the UAV in this model to implement beamforming which will improve the coverage and efficiency of energy during communication.

In this paper, the remaining sections are organised as follows. Section 2 explains the related works and motivation for the project and section 3 specifies the model of the system, section 4 provides the proposed dome packing method and section 5 explains the simulation results and concluding with section 6.

## II. RELATED WORK AND MOTIVATION

Beamforming uses multiple radiating elements integrated into the antenna and phase shift them by adjusting the magnitude to point at different directions to reach the ground sensors. The main advantage is to gain more energy at the destination compared to the traditional antennas. The

direction of arrival is calculated using adaptive algorithms processed by the digital signal processor. For example, in order to change the direction of the active main lobe of the beam, an  $n$ -element phased array with variable delays can be used.

#### A. Beamforming using UAV

The Beamforming used in UAV for wireless communication to direct a signal/beam to an intended receiver. Beamforming is applied in some research where uplink has higher throughput for on board UAV [11][14]. The benefits of implementing beamforming include increased coverage since the beam is directed to a destination, higher data rate and quality of service, high security since the beams are not broadcasted in all the directions and less interference.

A two-dimensional (2-D) beamforming is mostly applicable in cellular communication or networks where the nodes to be accessed are placed in the horizontal axis of the antenna and it uses beamforming to control the beam pattern. Each of the sectors in cellular communication used a one-dimensional array of antenna elements to provide a circular shaped radiation pattern [16]. In [17], a 2-dimensional beaming algorithm is used in imaging using microwaves to detect the target behind the wall by reconstructing the images whereas [18] used for millimetre wave communication to attain high throughput in mobile communication. Even though 2D beamforming is widely used in different mobile communication network, it will not be an ideal fit in this paper as the scenario is considered on a three-dimensional perspective and hence a 2d approach will not be applicable.

A 3-D beamforming design with mm wave is used to identify beam coverage of the target area with fixed height in a plane whereas 3-D beamforming design for 5G cellular communication with fixed base station is used to study the impact of beaming [19][20]. Most of the previous literature focus on the coverage radius with less focus on the height of the UAV[19][21] whereas a 2-D (two-dimensional) trajectory planning, energy optimization and throughput maximization were investigated assuming it in an even plane[18][22]. One of the main attributes to optimize is the height of the UAV in a downlink communication while considering an uneven plane from a three-dimensional perspective of the UAV and ground node.

The tangential line method is used to find the trajectory of the UAV while collecting the energy or data. The research work in [23] uses tangential line method for path designing and broadcast energy to the ground nodes to achieve minimum throughput maximization. Whereas, [24] uses it for trajectory planning and trajectory optimization. The UAV requires much energy to fly higher to collect data and then lower the height to be available near the sensors to transfer energy. This time and energy loss can be reduced by using 3-dimensional beamforming.

The optimization is often performed in UAV to manage the time, energy, performance and throughput during the communication. In [25], the UAV acts as a flying base station and the performance optimization of the UAV to ground communication under time constraints using a cell

partitioning approach is implemented. In [26] and [27], energy efficiency is optimized by considering the hardware components such as landing gear, blades etc that constitute the weight of the UAV. Whereas [28],[29] used an iterative algorithm for optimizing the energy transfer and power and thereby increasing the energy efficiency in relay assisted WPCN and UAV enabled sensor network. In [30] where UAV acts as an aerial base station, energy efficiency is maximized by optimizing power allocation, trajectory, user scheduling and bandwidth in wireless mobile communication. The optimization of trajectory, routing or path are common in most of the UAV communication design for improving energy efficiency, performance and throughput. The authors of [9] proposed a model and a design for energy efficiency by considering the trajectory path, speed and time of a fixed wing UAV. Whereas, [31] used 3d trajectory and resource allocation for sum throughput maximization in solar powered UAV communication. Most of the research work focus n energy optimization in an even plane and the height of the UAV is assumed to be a constant. Based on the literature [25]-[31] there are no relevant research in minimizing the total energy of the UAV in a terrain. The authors in [32] proposed a multiantenna beamforming to maximize the minimum throughput performance on an even plane, but this work will focus on optimizing the altitude on a terrain by considering the maximum coverage of the GT's and planning to extend later towards increasing the energy efficiency by considering trajectory and time constraints.

This research focus to find the 3D position of the UAV to achieve the optimal altitude using beamforming in the wireless powered communication network in application of WDS. A beamforming model of UAV is proposed in this work, where the algorithm named dome packing to group and pack the sensors based on the beamforming range/coverage will find the optimal height of the UAV to charge the sensors on the ground. This paper also proposes a theoretical model to optimize the energy used in UAV enabled WPCN by optimizing the position of the UAV in the terrain.

### III. SYSTEM MODEL

A system model is proposed to optimize the position of the UAV and thereby reducing the time and energy of the flight shown in figure 2. In this model, a WPCN system with rotary wing-based UAVs which will be in line of sight (LoS) communication with the ground terminal nodes (GT's) connected to a rechargeable battery will be used. The GT's are positioned with  $x,y,h$  values to get a 3D perspective of the GT points. The UAV collects energy from an RF energy charging point and broadcast energy to GTs through WET using beamforming on board. The elliptical shape in the figure 2 represents the area where the ground sensors are placed with in the radius of  $R_c$ . Since a three-dimensional perspective of both the UAV and the ground nodes are considered, dome will be the ideal shape to represent clustering of the GT's in the terrain area. The radius of the clusters is represented using  $r$ . The initial position of the UAV will be calculated by using a 3D K-means clustering algorithm using the GT points  $(x_n, y_n, h_n)$  to calculate the clusters and its centroids. It is also considered

that the energy will also be received by the nodes during beamforming which is on the same line of sight as that of the nodes while charging.

This work will be using rotary wing UAV with Beamforming on board as it requires up, down motions and hovering positions. It will be using a three-dimensional perspective of the ground users which is assumed to be on an uneven plane with a downlink channel model.

Let the GT's be  $k \in \{1, 2, \dots, N\}$  will be on the ground and the UAV at position P at precalculated height H with a line of sight (LOS) communication path. The height is calculated after the initial clustering by using the mean progression of the different heights of the GT's in a cluster. A Uniform rectangular array (URA) with  $M \times N$  antenna array elements with half wavelength spacing which will be integrated in the UAV to implement 3D beamforming and the GT's with a single receiving antenna.

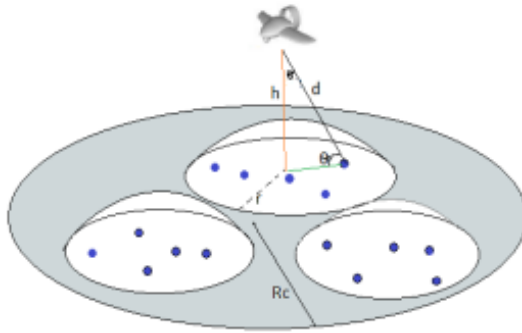


Figure 2: Representation of UAV enabled WPCN with 3d beamforming

The beam receiving area is assumed to be an ellipse of area 'Rc'. The channel vector can be represented as  $(M, N, \theta, \phi)$  where  $\theta$  and  $\phi$  are the azimuth and elevation angles. The antenna radiation pattern in GT's direction is formulated by

$$A(\theta, \phi) = A_H(\theta) + A_V(\phi) \quad (1)$$

And the antenna gains in horizontal and vertical planes ( $A_H, A_V$ ) is calculated as

$$A_H(\theta) = \min\left[12\left(\frac{\theta}{\theta_{3dB}}\right)^2, A_m\right] \quad (2)$$

$$A_V(\phi) = \min\left[12\left(\frac{\phi - \phi_{tilt}}{\phi_{3dB}}\right)^2, A_m\right] \quad (3)$$

where  $\theta_{3dB}$  and  $\phi_{3dB}$  represents the 3dB beamwidth of the horizontal and vertical patterns, and  $A_m$  is the side lobe level attenuation, and  $\phi_{tilt}$  represents the beam tilting angle [13][33]. The angles to steer the beam towards the GT direction is calculated by  $\tan^{-1}(H/d)$  where d is the distance (horizontal and vertical) from the cluster center to the ground terminal k. The half power beamwidth is also calculated to find the range of the beam created using  $\text{dsin}(\alpha)$  where  $\alpha$  is the beamwidth.

#### IV. PROPOSED DOME PACKING METHOD

In the proposed dome packing method, the ground terminal devices are randomly distributed at an area represented by radius  $R_c$ , which can be partitioned into  $K$  master clusters  $c = \{c_1 \dots c_K\}$  by 3D clustering using K-means [34] and a cluster center ' $\tau$ ' for each cluster is calculated. The UAV is positioned at  $c$  and 3D beamforming is applied at the precalculated height  $H$ . A heuristic approach will be used so that the UAV will not perform any height calculation operations at child nodes to save energy during recalculations. If any of the GT's are not reachable or the strength of the beam is less than -30 dB power (stronger the beam, less charging time), then the UAV should be adjusted to calculate the optimal position. The new position ( $\Delta x, \Delta y, \Delta h$ ) of the UAV will be calculated where  $\Delta x, \Delta y, \Delta h$  are the change in  $x, y$  and  $H$ . It is calculated on the basis of the position of the GT and the coverage of the beam. If the GT is not in the coverage, a re-clustering with child clusters will be performed followed using 3D beamforming.

Algorithm: Proposed Dome packing Method  
Finding the Optimal position of UAV for a single dome

- 1: Initialize target network and the UAV;
- 2: Initialize UAVs' initial position P and IoT ground terminal (GT)' positions
- 3: for GT  $k = 1, \dots, N$ , do
- 4:     Perform initial clustering of the IoT devices.
- 5: end for
- 6: As a result  $c_1, \dots, c_K$  master clusters will be formed
- 7: Calculate centroid of each master cluster  $\tau$
- 8:     for  $c = c_1 \dots c_K$
- 9:     do
- 10:         Position the UAV to the cluster  $c$ 's centroid at a precalculated position  $(x, y, H)$ ;
- 11:         Apply 3D Beamforming at the current UAV's location
- 12:         if any GT's in the cluster is not reachable and strength of beams is less than -30db power
- 13:             then a delta value will be calculated for a new position of UAV with  $\Delta x, \Delta y, \Delta h$
- 14:             if the new position is within the coverage
- 15:             then, apply 3D Beamforming at the new position
- 16:             else, based on optimal position, perform re-clustering (child cluster) at  $h$  value to cover the GT's
- 17:             Apply 3D Beamforming at the new position
- 18:             else the precalculated position  $(x, y, H)$  will be the same
- 19:         end for

#### V. SIMULATION RESULTS

Based on the model and simulation, the numerical results are used to validate the effectiveness of the proposed approach in optimizing the position of the UAV for energy minimization.

In the simulation, it's assumed that 8 ground terminal nodes were placed at predefined positions at varying height from the ground and the UAV is positioned at an altitude of  $H$  metres from the ground. The transmission power of the UAV to communicate with the GT's is 25dBm, frequency  $f=1 \times 10^6$ ,  $c=3 \times 10^8$  and the pathloss in the channel is  $\mu$ . The UAV and the GT's have a line of sight (LOS) communication. Initially, a 3D clustering is applied to all the GT's and the clusters with their centroids are fed to the UAV.



Figure 3: 3D Beamforming in UAV enabled WPCN

At the next step the optimal position of the UAV ( $x, y, H$ ) is calculated using the proposed algorithm and 3D beamforming is performed with vertical and horizontal angles with the GT nodes as represented in Figure 3. After calculating the optimal position, the beam will be steered towards each GT's to charge it effectively. Based on the model, the results are represented as in Figure 4, 5 and 6.

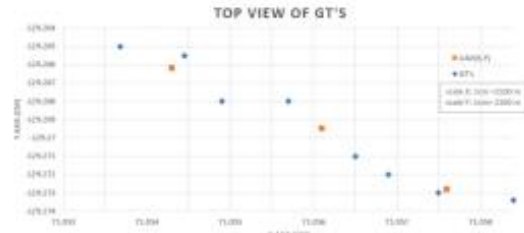


Figure 4: Position of GT's vs UAV position

The figure 4 represents a top view of the model with the position of the UAV and the GT's in the coordinates of the  $x, y$  axis. A side view of the GT's is represented as in figure 5, since it depicts a 3D view of the model and the  $x, y, H$  axis were scaled down to 1:20. From the simulation results on Figure 5, the optimal position of the UAV for charging of the GT's is calculated and a comparison of the model with an existing model [27] (represented as UAV charging) is performed to compare its rate of change. In the figure 6, a mathematical calculation of the energy used by the UAV (moving, hovering and beaming) is computed [35-36] after energizing each GT's and a comparison of the total energy consumed by the UAV against the GT's with and without using DOM packing is represented.

To calculate the energy consumption of the UAV the model proposed in [36] is used for this work. From the simulation

results on figure 6, it is evident that the proposed dome packing method provides better energy consumption than the compared method.

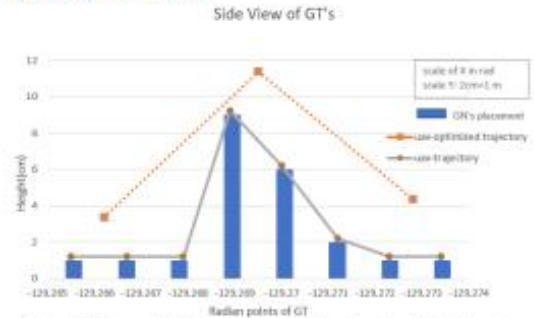
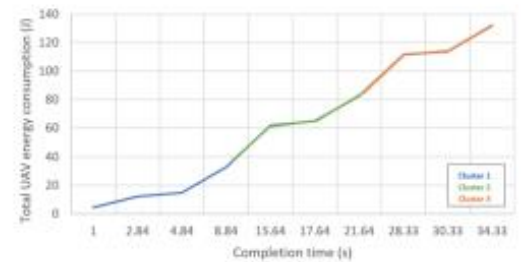


Figure 5: The optimal positions of UAV for charging the GT's using DOM packing and without DOM packing method



(a) Without using DOM packing method



(b) Using DOM packing method

Figure 6: Total energy consumption of the UAV vs completion time with and without DOM packing method

## VI. CONCLUSION AND FUTURE WORK

The research in WPCN is fast growing, combining with computing, beamforming and energy harvesting could lead new way of communication. In this work, a UAV enabled wireless powered communication network is used as a flying base station to provide energy to the ground sensor nodes in an uneven plane using 3D beamforming technique and this energy will be used to send information to the uplink. The total energy consumed by the UAV could be reduced by optimizing different factors and in this work, the position of the UAV is optimized by applying a dome packing algorithm. The future work is planned to extend the scenario to multi-UAV deployment and energy efficient trajectory design of UAV by considering the time factor. Later, the total combined energy consumption for the

communication is calculated against the energy received using artificial intelligent methods to reach a constant value to achieve energy efficiency in the wireless powered communication network.

#### REFERENCES

- [1] Radhakrishnan, V. and Wu, W., IoT technology for Smart water system, IEEE Smart city, 28-30 June 2018 Exeter UK.
- [2] Radhakrishnan, Varsha and Wu, W., (2019) Wireless Powered Communication Network In IoT Enabled Water Distribution System. In: 17th International Computing & Control for the Water Industry Conference, 1-4 September, Exeter UK
- [3] Bi, S., Zeng, Y. and Zhang, R. (2016). Wireless powered communication networks: an overview. *IEEE Wireless Communications*, 23(2), pp.10–18.
- [4] Karamuz, E., Romanowicz, R.J. and Doroszkiewicz, J. (2020). The use of unmanned aerial vehicles in flood hazard assessment. *Journal of Flood Risk Management*, 13(4).
- [5] Mozaffari, M., Saad, W., Bennis, M. and Debbah, M. (2016). Efficient Deployment of Multiple Unmanned Aerial Vehicles for Optimal Wireless Coverage. *IEEE Communications Letters*, 20(8), pp.1647–1650.
- [6] Xu, J., Zeng, Y., and Zhang, R., "UAV-enabled wireless power transfer: Trajectory design and energy optimization," *IEEE Trans. Wireless Communications*, vol. 17, no. 8, pp. 5092–5106, Aug. 2018.
- [7] Zeng, Y. and Zhang, R., "Energy-efficient UAV communication with trajectory optimization," *IEEE Trans. Wireless Communications*, vol. 16, no. 6, pp. 3747–3760, Jun. 2017.
- [8] Shahra Essa and Wenyan Wu (2020) Water contaminants detection using sensor placement approach in smart water networks, *Journal of Ambient Intelligence and Humanized Computing* (2020), <https://doi.org/10.1007/s12652-020-02262-x>, Springer 25 June 2020
- [9] Kalantari, E., Yanikomeroglu, H. and Yongacoglu, A., "On the number and 3D placement of drone base stations in wireless cellular networks," in *Proc. IEEE 84th Veh. Technol. Conf. (VTC-Fall)*, Sep. 2016, pp. 1–6.
- [10] Chen, Q. (2020). Joint Trajectory and Resource Optimization for UAV-Enabled Relaying Systems. *IEEE Access*, 8, pp.24108–24119.
- [11] Alsaba, Y., Rahim, S.K.A. and Leow, C.Y. (2018). Beamforming in Wireless Energy Harvesting Communications Systems: A Survey. *IEEE Communications Surveys Tutorials*, [online] 20(2), pp.1329–1360. Available at: <https://ieeexplore.ieee.org/document/8269301>.
- [12] Wang, S., Zhao, L., Liang, K., Chu, X. and Jiao, B. (2018). Energy beamforming for full-duplex wireless-powered communication networks. *Physical Communication*, [online] 26, pp.134–140. Available at: <https://www.sciencedirect.com/science/article/abs/pii/S187449071730455X>
- [13] Balanis, C. (2016). *Antenna Theory: Analysis and Design*, 4th Edition | Wiley. [online] Wiley.com, ISBN: 978-1-118-64206-1 Available at: <https://www.wiley.com/en-us/Antenna+Theory%3A+Analysis+and+Design%2C+4th+Edition-p-9781118642061>
- [14] Zydorczyk, T., Ginard, M., Svendsen, S., Berardinelli, G. and Mogensen, P. (2020). Experimental evaluation of beamforming on UAVs in cellular systems. [online] Available at: <https://arxiv.org/pdf/2003.12010.pdf>
- [15] Olatinwo, S. and Joubert, T.-H. (2018). Optimizing the Energy and Throughput of a Water-Quality Monitoring System. *Sensors*, 18(4), p.1198.
- [16] Razavizadeh, S.M., Ahn, M. and Lee, I. (2014). Three-Dimensional Beamforming: A new enabling technology for 5G wireless networks. *IEEE Signal Processing Magazine*, 31(6), pp.94–101.
- [17] Aamna, M., Ammar, S., Rameez, T., Shabeeb, S., Naveed, I.R. and Safwat, I. (2010). *2D Beamforming for Through-the-Wall Microwave Imaging applications*. [online] IEEE Xplore. Available at: <https://ieeexplore.ieee.org/abstract/document/5625725>.
- [18] Zhang, W., Li, B., Liu, Y. and Zhao, C. (2013). Hybrid Beamforming Technology in 60 GHz Millimeter Wave Uplink Communication System. *Journal of Electronics & Information Technology*, 34(11), pp.2728–2733.
- [19] L. Zhu, J. Zhang, Z. Xiao, X. Cao, D. O. Wu and X. Xia, "3-D Beamforming for Flexible Coverage in Millimeter-Wave UAV Communications," in *IEEE Wireless Communications Letters*, vol. 8, no. 3, pp. 837-840, June 2019, doi: 10.1109/LWC.2019.2895597.
- [20] J. Kelif, M. Coupechoux and M. Mansanarez, "A 3D beamforming analytical model for 5G wireless networks," 2016 14th International Symposium on Modeling and Optimization in Mobile, Ad Hoc, and Wireless Networks (WiOpt), Tempe, AZ, USA, 2016, pp. 1-8, doi: 10.1109/WIOPT.2016.7492925.
- [21] Yuan, Q., Hu, Y., Wang, C. and Li, Y. (2019). Joint 3D Beamforming and Trajectory Design for UAV-Enabled Mobile Relaying System. *IEEE Access*, 7, pp.26488–26496.
- [22] J. Xu, Y. Zeng, and R. Zhang, "UAV-enabled wireless power transfer: Trajectory design and energy optimization," *IEEE Trans. Wireless Commun.*, vol. 17, no. 8, pp. 5092–5106, Aug. 2018.
- [23] Tang, J., Song, J., Ou, J., Luo, J., Zhang, X. and Wong, K.-K. (2020). Minimum Throughput Maximization for Multi-UAV Enabled WPCN: A Deep Reinforcement Learning Method. *IEEE Access*, 8, pp.9124–9132.
- [24] Zeng, Y. and Zhang, R. (2017). Energy-Efficient UAV Communication with Trajectory Optimization. *IEEE Transactions on Wireless Communications*, 16(6), pp.3747–3760.
- [25] Mozaffari, M., Saad, W., Bennis, M. and Debbah, M. (2017). Performance Optimization for UAV-Enabled Wireless Communications under Flight Time Constraints. [online] IEEE Xplore. Available at: <https://ieeexplore.ieee.org/document/8254660>.
- [26] Yang, S., Deng, Y., Tang, X., Ding, Y. and Zhou, J. (2019). Energy Efficiency Optimization for UAV-Assisted Backscatter Communications. *IEEE Communications Letters*, 23(11), pp.2041–2045.
- [27] Wu, F., Yang, D., Xiao, L. and Cuthbert, L. (2019). Energy Consumption and Completion Time Tradeoff in Rotary-Wing UAV Enabled WPCN. *IEEE Access*, [online] 7, pp.79617–79635. Available at: <https://ieeexplore.ieee.org/document/8736248>.
- [28] Yang, F., Xu, W., Zhang, Z., Guo, L. and Lin, J. (2018). Energy Efficiency Maximization for Relay-Assisted WPCN: Joint Time Duration and Power Allocation. *IEEE Access*, 6, pp.78297–78307.
- [29] C. Zhan, Y. Zeng and R. Zhang, "Energy-efficient data collection in UAV enabled wireless sensor network", *IEEE Wireless Commun. Lett.*, vol. 7, no. 3, pp. 328-331, Jun. 2018.
- [30] Zeng, F., Hu, Z., Xiao, Z., Jiang, H., Zhou, S., Liu, W. and Liu, D. (2020). Resource Allocation and Trajectory Optimization for QoS Provisioning in Energy-Efficient UAV-Enabled Wireless Networks. *IEEE Transactions on Vehicular Technology*, 69(7), pp.7634–7647.
- [31] Sun, Y., Xu, D., Ng, D.W.K., Dai, L. and Schober, R. (2019). Optimal 3D-Trajectory Design and Resource Allocation for Solar-Powered UAV Communication Systems. *IEEE Transactions on Communications*, 67(6), pp.4281–4298.
- [32] L. Liu, R. Zhang and K.-C. Chua, "Multi-antenna wireless powered communication with energy beamforming", *IEEE Trans. Commun.*, vol. 62, no. 12, pp. 4349-4361, Dec. 2014.
- [33] Guidelines for evaluation of radio interface technologies for IMT-2020 M Series Mobile, radiodetermination, amateur and related satellite services. (n.d.). [online] Available at: [https://www.itu.int/dms\\_pub/itu-r/opb/rep/R-REP-M.2412-2017-PDF-E.pdf](https://www.itu.int/dms_pub/itu-r/opb/rep/R-REP-M.2412-2017-PDF-E.pdf)
- [34] A. K. Jain, "Data clustering: 50 years beyond K-means," *Pattern Recognit. Lett.*, vol. 31, no. 8, pp. 651–666, Jun. 2010.
- [35] Wang, Y., Giordani, M. and Zorzi, M. (2020). On the Beamforming Design of Millimeter Wave UAV Networks: Power vs. Capacity Trade-Offs. *ArXiv*. [online] Available at: <https://www.semanticscholar.org/paper/On-the-Beamforming-Design-of-Millimeter-Wave-UAV-Wang-Giordani/557df22d86af194f989f8b31430611f7c0784350>.
- [36] Zeng, Y., Xu, J. and Zhang, R. (2019). Energy Minimization for Wireless Communication With Rotary-Wing UAV. *IEEE Transactions on Wireless Communications*, 18(4), pp.2329–2345.

## APPENDIX B

### The Implementation Source Code

The B1 Block consists of code required to set up the scenario to create a terrain for the placement of the GN's and the initial position for the UAV to start the mission.

#### **B1. Blocks of code to set up the scenario and position GN's and initial position of the UAV**

---

```
global xmin xmax xres ymin ymax yres X Y Z Pl
rng(15,'twister')
%% Create un-even surface
xmin=0;ymin=0;
xmax=100;ymax=100;
xres=0.5; yres=0.5;
[X,Y] = meshgrid(xmin:xres:xmax,ymin:yres:ymax);
Z = Y.*cos(X/12) - X.*cos(Y/12);
Z(Z<0)=0;
% %% Charging % %% New
itr=10;
PrecisionH=zeros(1,itr);
RecallH=zeros(1,itr);
F1H=zeros(1,itr);
for i1=1:itr
    h0=figure(1);
    clf;
    h1 = surf(X,Y,Z,'FaceAlpha',0.5)
```

```

camlight(110,70)
brighten(0.6)
h1.EdgeColor = 'none';
h1.AmbientStrength = 0.4;
a = gca;
a.TickLabelInterpreter = 'latex';
a.Box = 'on';
a.BoxStyle = 'full';
xlabel('$x$', 'Interpreter', 'latex')
ylabel('$y$', 'Interpreter', 'latex')
zlabel('$z$', 'Interpreter', 'latex')
hold on
%% Node placement
nk=40; % No of nodes
% Emax=1000; % max Energy of nodes
% Emin=5; % min Energy of nodes
% V=20;
ReqPower=5;
%% UAV
c = 3e8;
fc = 1.5e9;
lamda = c/fc;
h_rec = phased.URA('Size',[16 16], 'ElementSpacing', lamda/2, 'Lattice', 'Rectangular')
Ptx=40 ; %40dBm --> 10Watts
noOfNodes=nk;
R =4.8; %node transmission range in km
a=1;
b=noOfNodes;
X0 = xmin+(xmax-xmin)*rand(1,nk);
Y0 = ymin+(ymax-ymin)*rand(1,nk);

```



```

x=X0;
y=Y0;
[u, v]=getgrid(x, y, xmin, xmax, xres, ymin, ymax, yres);
for ik=1:nk
    Xc=X(v(ik),u(ik));
    Yc=Y(v(ik),u(ik));
    Zc=Z(v(ik),u(ik));

    plot3(Xc,Yc,Zc,'o','LineWidth',1,...
'MarkerEdgeColor','k',...
'MarkerFaceColor','y',...
'MarkerSize',8');
    text(Xc, Yc,Zc, num2str(ik),'FontSize',10);
end
hold on
% UAV position
X1= xmin+(xmax-xmin)*rand(1,1);
Y1= ymin+(ymax-ymin)*rand(1,1);
[u1, v1]=getgrid(X1, Y1, xmin, xmax, xres, ymin, ymax, yres);
plot3(X(v1,u1)+2,Y(v1,u1)+2,Z(v1,u1)+2,'o','LineWidth',1,...
'MarkerEdgeColor','k',...
'MarkerFaceColor','g',...
'MarkerSize',12');
hold on
plot3(X(v1,u1),Y(v1,u1),Z(v1,u1),'o','LineWidth',1,...
'MarkerEdgeColor','k',...
'MarkerFaceColor','k',...
'MarkerSize',14');
xlabel('X in m')
ylabel('Y in m')

```

```

hold on

text(X(v1,u1),Y(v1,u1),Z(v1,u1),'UAV Stay Room','FontSize',10);

%% 3D Clustering

%% Input arguments (and print them)

k = 6; % number of clusters

numP = nk; % number of points

fprintf('k-Means will run with %d clusters and %d data points.\n', k, numP);

%% Create random data points

% Create a random matrix of size 2-by-numP

% With row 1/2 (x/y coordinate) ranging in [minX, maxX]/[minY, maxY]

for ik=1:nk

    xP(ik) = X(v(ik),u(ik));% xMax * rand(1,numP);

    yP(ik) = Y(v(ik),u(ik));% yMax * rand(1,numP);

    zP(ik) = Z(v(ik),u(ik));% zMax * rand(1,numP);

end

xMax = max(xP); % x between 0 and xMax

yMax = max(yP); % y between 0 and yMax

zMax = max(zP);

points = [xP; yP; zP];

%% Beam strength calculation with 3D K-means

tic;

[cluster,

centr,TotalbeamStrengthPr,TotalbeamStrengthEx,k,RxPower1,flighttime_unit,height,

Rb] = 3DkMeans(k, points,Ptx,ReqPower); % my k-means

myPerform = toc;

[Precision,Recall,F1]= measurement(cluster,points,k,nk);

PrecisionH(i1)=Precision;

RecallH(i1)=Recall;

F1H(i1)=F1;

fprintf('Computation time for kMeans.m: %d seconds.\n', myPerform);

```

```

%% Show Centroid Regions
hold on;
scatter3(centr(1,:),centr(2,:),centr(3,:),'^c','LineWidth',1.5);
axis([0 xMax 0 yMax 0 zMax]);
%% Optimization of Recycle Time
iv=1;
distF=inf;
while(iv<5000)
    seq=randperm(k);
    dist=0;
    for ic=0:k
        if(ic==0)
            dist=dist+norm([X(v1,u1)+2,Y(v1,u1)+2,Z(v1,u1)+2] -
centr(:,seq(ic+1)));
        elseif(ic==k)
            dist=dist+norm(centr(:,seq(ic)) -
[X(v1,u1)+2,Y(v1,u1)+2,Z(v1,u1)+2]);
        else
            dist=dist+norm(centr(:,seq(ic)) - centr(:,seq(ic+1)));
        end
    end
    if(dist<distF)
        distF=dist;
        bestseq=seq;
    end
    iv=iv+1;
end
%% Show Routing
for ic=0:k
    if(ic==0)

```

```

        line([X(v1,u1)+2 centr(1,bestseq(ic+1))],[ Y(v1,u1)+2
        centr(2,bestseq(ic+1))],[Z(v1,u1)+2 centr(3,bestseq(ic+1))],
        'Color','r','LineWidth',2, 'LineStyle','-')
    elseif(ic==k)
        line([centr(1,bestseq(ic)) X(v1,u1)],[centr(2,bestseq(ic))
        Y(v1,u1)],[centr(3,bestseq(ic)) Z(v1,u1)], 'Color','r','LineWidth',2,
        'LineStyle','-')
    else
        line([centr(1,bestseq(ic)) centr(1,bestseq(ic+1))],[ centr(2,bestseq(ic))
        centr(2,bestseq(ic+1))],[centr(3,bestseq(ic)) centr(3,bestseq(ic+1))],
        'Color','r','LineWidth',2, 'LineStyle','-')
    end
end
end
%% Flight Time
RxPowerH=[];
powercoeff=10;
Power=0;
flighttime=0;
RbCluster=zeros(1,numel(bestseq));
ab=1;
Pcluster=[];
Ftcluster=[];
Pc=[];
Ftc=[];
for ij=1:numel(bestseq)
    ind=find(bestseq(ij)==cluster);
    if(ij<numel(bestseq))
        dist1=norm(centr(:,bestseq(ij)) - centr(:,bestseq(ij+1)));
        Power=Power+dist1.*powercoeff/100;
    end
    if(~isempty(ind))
        for k=1:numel(ind)
            Power = Power +(flighttime_unit(ind(k))).*powercoeff;

```

```

        flighttime=flighttime+fligttime_unit(ind(k));
        hoveringtime(ab)=fligttime_unit(ind(k));
        RxPower(ab)=RxPower1(ind(k));
        Height(ab)=height(ind(k));
        P(ab)=Power;
        Ft(ab)=flighttime;

        Pc(k)=Power;
        Ftc(k)=flighttime;
        ab=ab+1;
    end

    RbCluster(ij)=sum(Rb(ind));
    RxPowerH(ij)=max(RxPower1(ind));
    Pcluster(ij)=sum(Pc);
    Ftcluster(ij)=sum(Ftc);
end

end

%% Existing Method

RxPowerHex=[];
powercoeffex=10;
Powerex=0;
flighttimeex=0;
RbClusterex=zeros(1,numel(seq));
ab=1;
Pclusterex=[];
Ftclusterex=[];
Pc=[];
Ftc=[];
for ij=1:numel(seq)
    ind=find(seq(ij)==cluster);

```

```

if(ij<numel(seq))
    dist1=norm(centr(:,seq(ij)) - centr(:,seq(ij+1)));
    Powerex=Powerex+dist1.*powercoeffex/100;
end
if(~isempty(ind))
    for k=1:numel(ind)
        Powerex = Powerex +(flighttime_unit(ind(k))).*powercoeffex;
        flighttimeex=flighttimeex+flighttime_unit(ind(k));
        Pex(ab)=Powerex;
        Ftex(ab)=flighttimeex;
        Pc(k)=Powerex;
        Ftc(k)=flighttimeex;
        ab=ab+1;
    end
    RbClusterex(ij)=sum(Rb(ind));
    RxPowerHex(ij)=max(RxPower1(ind));
    Pclusterex(ij)=sum(Pc);
    Ftclusterex(ij)=sum(Ftc);
end
end
ac=[Ft ;P;Ftex;Pex;]';
figure(2),
bar(ac)
hold on
xlabel('Flight Time (s)')
ylabel('Power Consumption (W)')
axis([0 40 0 75]);
figure(3),
plot(1:numel(bestseq),Pcluster,'-*r')
hold on

```

```

plot(1:numel(bestseq),Pclusterex,'-*b')
xlabel('Cluster')
ylabel('Power Consumption (W)')
legend('With DOM Packing','Without DOM packing')
title('ClusterWise')
figure(31),
plot(Rb/1000,'-*r')
xlabel('nodes')
ylabel('max Throughput(Kbps)')
figure(4),
plot(1:numel(bestseq),RbCluster(bestseq)/1000,'-*r')
xlabel('Cluster')
ylabel('max Throughput(Kbps)')
figure(5),
plot(1:numel(bestseq),RxPowerH(bestseq),'-*r')
xlabel('Cluster')
ylabel('max Rx-Power')
[val,inds]=sort(Height);
figure(6),
plot(Height(inds),hoveringtime(inds),'-*r')
xlabel('Height')
ylabel('Hovering Time')
figure(7),plot(Height(inds),RxPower(inds),'-*r')
xlabel('Height')
ylabel('RxPower')
%% Compute Energy
Energycoeff=0.1;
EnergyPr(i1)=distF.*Energycoeff;
EnergyEx(i1)=dist.*Energycoeff;
% Save Result

```

```

        TotBSPr(i1)=TotalbeamStrengthPr;
        TotBSEx(i1)=TotalbeamStrengthEx;
        pause(1);
end

%% Plot Result
%% Performance
figure,
bar([EnergyPr; EnergyEx])
xlabel('Rounds')
ylabel('UAV PowerConsumption(w)')
legend('Proposed','Existing')
figure,
bar([TotBSPr;TotBSEx])
xlabel('Rounds')
ylabel('Wireless Power Transfer(w)')
legend('Proposed','Existing')
title('Power Transfer')
%% Performance
ac=[PrecisionH ;RecallH;F1H];
figure,
bar(ac.*100)
xlabel('Iteration')
ylabel('% Value')
legend('Precision','Recall','Fmeasure')
title('Cluster Performance')

```



The B2 Block consists of implementation of three-dimensional clustering algorithm by computing the cluster centroids as well as calculating the throughput from the GN's.

## **B2. Blocks of code to perform 3D clustering using K-Means**

---

```
function [ cluster, centr, TotalbeamStrengthPr, TotalbeamStrengthEx , k, RxPower,  
fligtime_unit,height, Rb] = 3DkMeans( k, P, Ptx, ReqPower)
```

```
global xmin xmax xres ymin ymax yres X Y Z Pl
```

```
% 3D K-Means Clusters data points into k clusters.
```

```
% Input args: k: number of clusters.
```

```
% Points: m-by-n matrix of n m-dimensional data points.
```

```
% Output args: cluster: 1-by-n array with values of 0, ..., k-1
```

```
% Representing in which cluster the corresponding point lies in
```

```
% centr: m-by-k matrix of the m-dimensional centroids of the k clusters
```

```
numP = size(P,2); % number of points
```

```
dimP = size(P,1); % dimension of points
```

```
%% Choose k data points as initial centroids
```

```
% Choose k unique random indices between 1 and size(P,2) (number of points)
```

```
randIdx = randperm(numP,k);
```

```
% Initial centroids
```

```
centr = P(:,randIdx);
```

```
%% Repeat until stopping criterion is met
```

```
% init cluster array
```

```
cluster = zeros(1,numP);
```

```
% Initialize previous cluster array clusterPrev (for stopping criterion)
```

```
clusterPrev = cluster;
```

```

% For reference: count the iterations

iterations = 0;

% Initialize stopping criterion

stop = false; % if stopping criterion met, it changes to true

TotalbeamStrengthPr=0;

while stop == false

    % For each data point

    for idxP = 1:numP

        % init distance array dist

        dist = zeros(1,k);

        % Compute distance to each centroid

        for idxC=1:k

            dist(idxC) = norm(P(:,idxP)-centr(:,idxC));

        end

        % find index of closest centroid (= find the cluster)

        [~, clusterP] = min(dist);

        cluster(idxP) = clusterP;

    end

    % Recompute centroids using current cluster memberships:

    % init centroid array centr

    centr = zeros(dimP,k);

    % For every cluster compute new centroid

    for idxC = 1:k

        % Find the points in cluster number idxC and compute row-wise mean

```

```

        centr(:,idxC) = mean(P(:,cluster==idxC),2);

end

%% Check condition

% Verify UAV's minimum 10 m above to earth centroid value

flag=0;

for ab=1:k

    [u, v]=getgrid(centr(1,ab) ,centr(2,ab) , xmin, xmax, xres, ymin, ymax, yres);

    ab;

    if(Z(v,u) < centr(3,ab)+10)

        centr(3,ab) = centr(3,ab)+10;

    end

end

end

TotalbeamStrength=0;

for ik=1:numP

    H=abs(centr(1,k)-P(1,ik)); % X

    V=abs(centr(2,k)-P(2,ik)); % Y

    d=sqrt(H^2 + V^2);

    theta=acos(V/d);

    phi=atan(H/V);

    % assign constants

    theta3db=-30;

    phi3db=-30;

    Am=1000;

    HP_BeamW=Rxpowercompute(H,V,theta,phi,theta3db,phi3db,Am);%-

    Pl(d)/100;

```

```

    if(HP_BeamW <-30)

        flag=1;

    end

    TotalbeamStrength=TotalbeamStrength+db2mag(HP_BeamW)*db2mag(Ptx);

    RxPower(ik)=HP_BeamW;

    % Assign min height to 30 m

    d(d<=30)=30;

    height(ik)=d;

    fligtime_unit(ik)=ReqPower./(db2mag(HP_BeamW)*db2mag(Ptx));

    %% Maximum Throughput

    SF=6; % spreading factor

    CR=4; % code rate

    BW=50;% bandwidth in KHz

    Rb(ik)=SF*(4/(4+CR))/(2^SF/BW) * 1000 ./ fligtime_unit(ik);

    end

    % Checking for stopping criterion: Clusters do not change anymore

    if ((TotalbeamStrengthPr< TotalbeamStrength) & (flag ~= 1))

        TotalbeamStrengthPr=TotalbeamStrength;

    end

    % Update previous cluster clusterPrev

    clusterPrev = cluster;

    if(iterations==1)

        TotalbeamStrengthEx=TotalbeamStrength;

    end

```

```

iterations = iterations + 1;

if(mod(iterations,1000)==0)

    if(TotalbeamStrengthPr ==0)

        TotalbeamStrengthPr=TotalbeamStrengthEx;

    end

end

break;

end

end

% For reference: print number of iterations

fprintf('kMeans.m used %d iterations of changing centroids.\n',iterations);

end

```

---

The A3 Block consists of codes required to implement three-dimensional beamforming method.

### **A3. Blocks of code to perform beaming calculations**

---

```

function HP_BeamW=Rxpowercompute (H,V, theta, phi, theta3db, phi3db, Am)

d=sqrt(H.^2 + V.^2);

phitilt= atan(H/d);

A_H=@(theta) min([12*(theta/theta3db).^2; Am]);

A_V=@(phi) min([12*(phi-phitilt)./phi3db; Am]);

A=A_H(theta) + A_V(phi);

alpha= A/2;%beamwidth(A);

HP_BeamW=d.*sin(alpha);

end

```

---

## APPENDIX C

### Matlab script of setting the parameters for dynamic optimization methods to find optimal height of the UAV

---

```

a=1; % Reciprocal of time constant

c=1.5e-5; % Drag Coefficient

g=9.8; % Acceleration

m=1; % Mass of UAV

A=[0 1;0 -c/m]; % State model values A,B,C,D

B=[0;1];

C=[1 0];

h0= Dcentr; % Height values from static optimization

h=0:.001:120; % Height variation from 0 to 120 maximum

E= m*g*(h-h0)-0.5*m*a^2*(h-h0).^2; % Energy Equation

plot (h,E)

% Power and Height values from Dome packing Method

P = [8.1884 8.7458 9.7211 10.5155 11.3031 12.0327 13.0276
14.1735 15.6767 17.596 19.6626 20.3271 27.4831
28.3072 28.971 34.3243 34.83 35.3301 35.8512 36.3613
36.8616 37.4125 43.5545 44.0545 44.5549 45.0552
45.5552 46.0553 46.5563 47.0563 47.5563 56.9637
57.464 57.9698 58.5097 59.2119 59.822 60.564 61.3353
61.9872];

Height=[90.0161 30 67.0812 51.2056 66.359 43.5117 66.6128
84.1629 75.2106 86.0262 91.5452 58.4894 117.6356
113.2675 110.0819 88.4068 55.4821 64.3604 50.4234
57.5306 95.7589 92.0904 50.2147 60.6271 36.5413

```

49.5532	40.2028	37.246	35.3255	30	30	30	30	30
30	90.9829	86.9311	102.3359	74.9568	73.9874];			

```

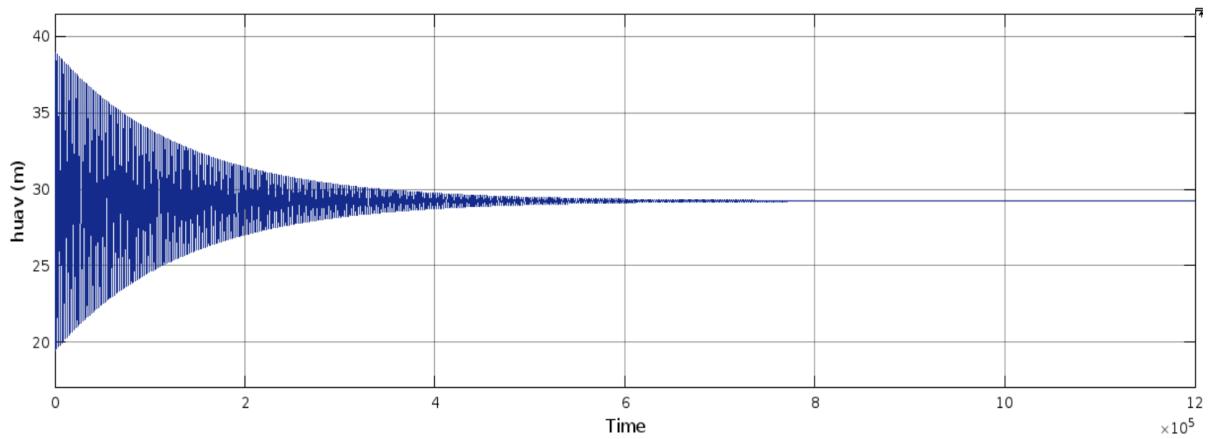
plot (P, Height, '-r');
xlabel ('UAV Power Consumption P (W)');
ylabel ('Height (m)');

```

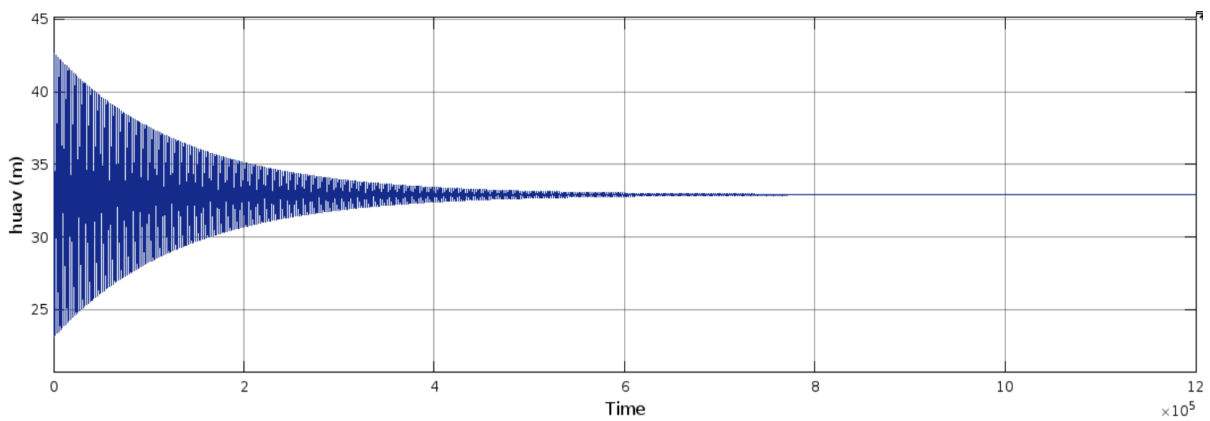
---

### C.1. Extremum Seeking Trajectories

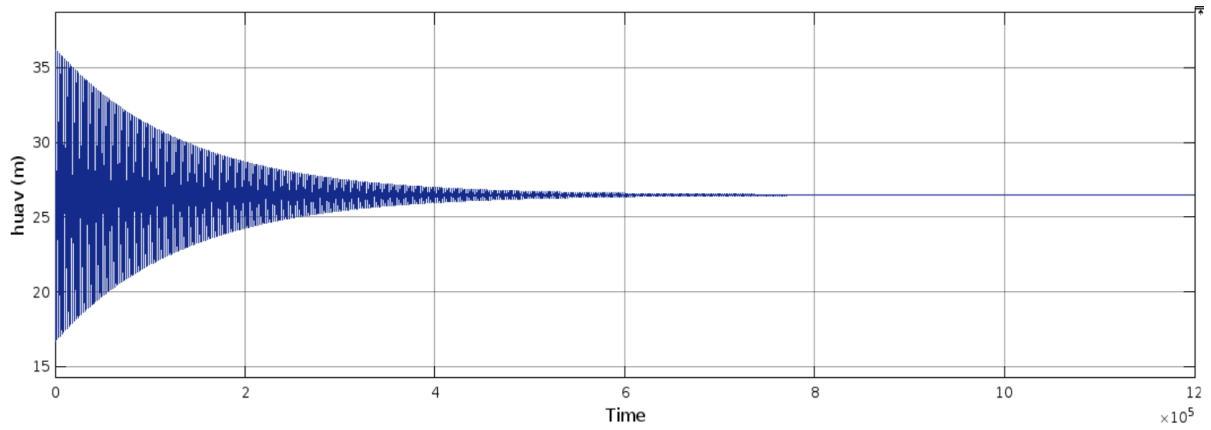
The optimal height values that were calculated based on the initial height values from static optimization is represented as in Figure C1.



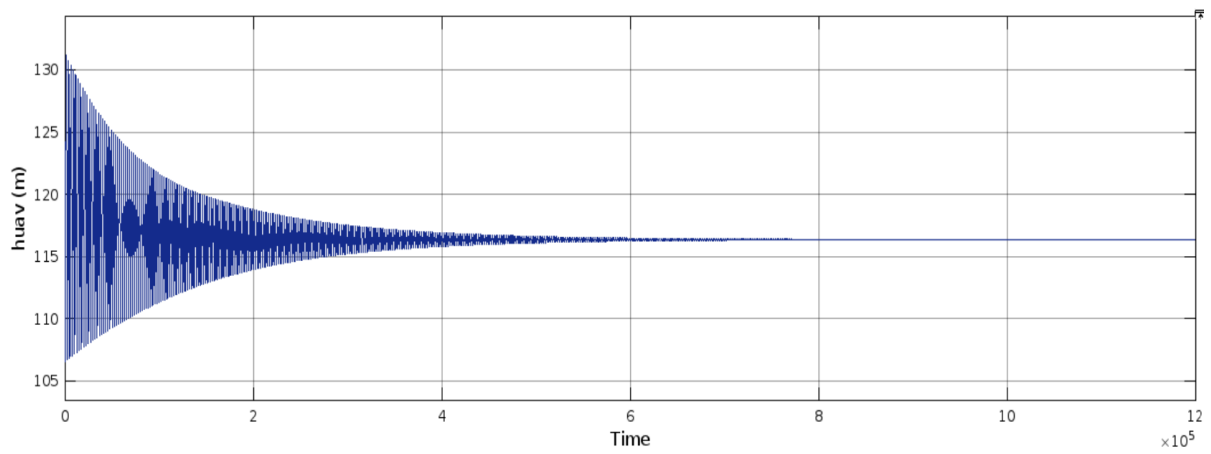
a)



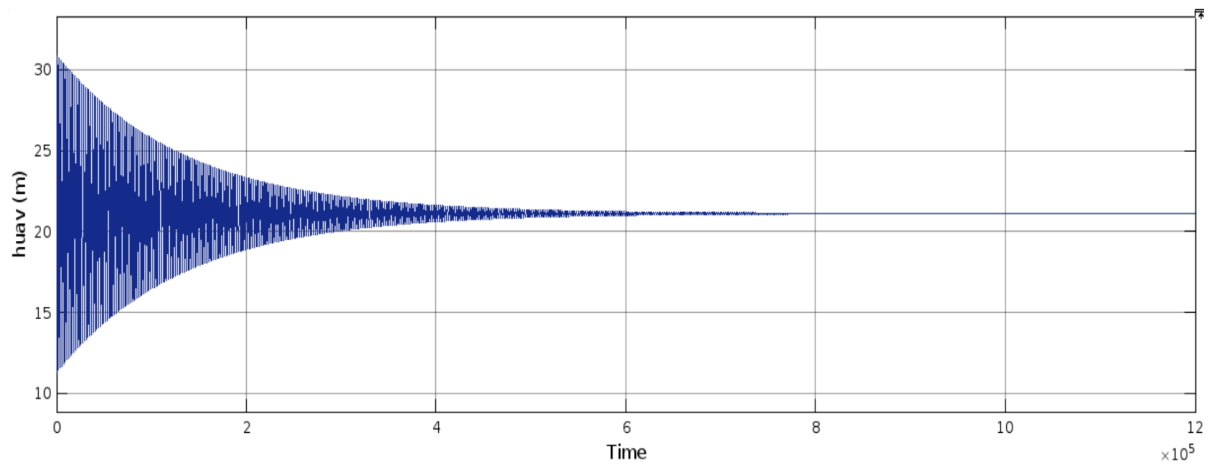
b)



c)



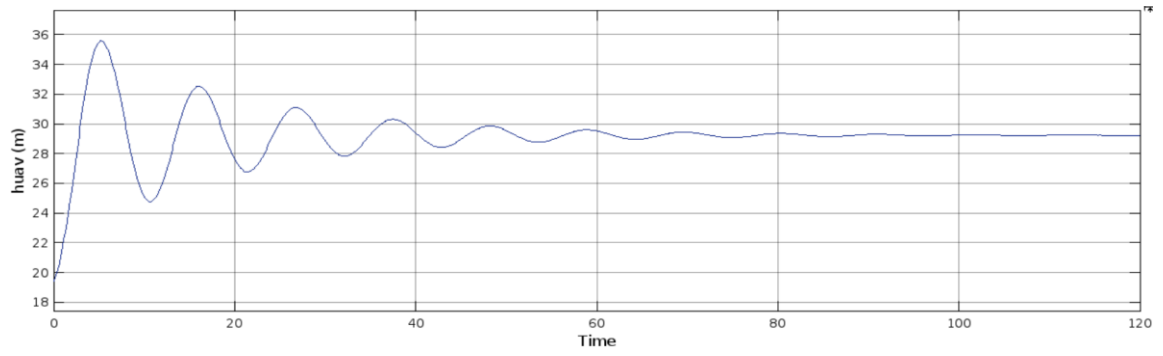
d)



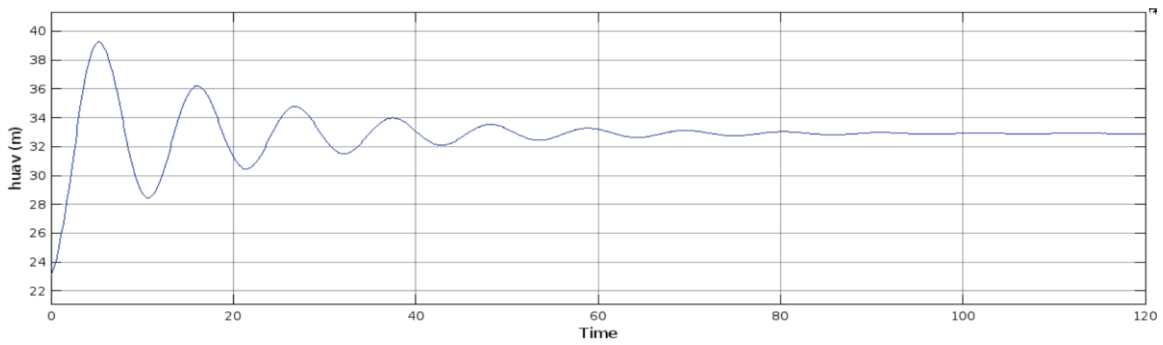
e)

Figure C1 (a-e): The optimized height values using Extremum seeking based on different clusters values as input from the static model a)  $h = 29.86$  b)  $h = 33.47$  c)  $h = 26.78$  d)  $h = 116.42$  e)  $h = 21.93$

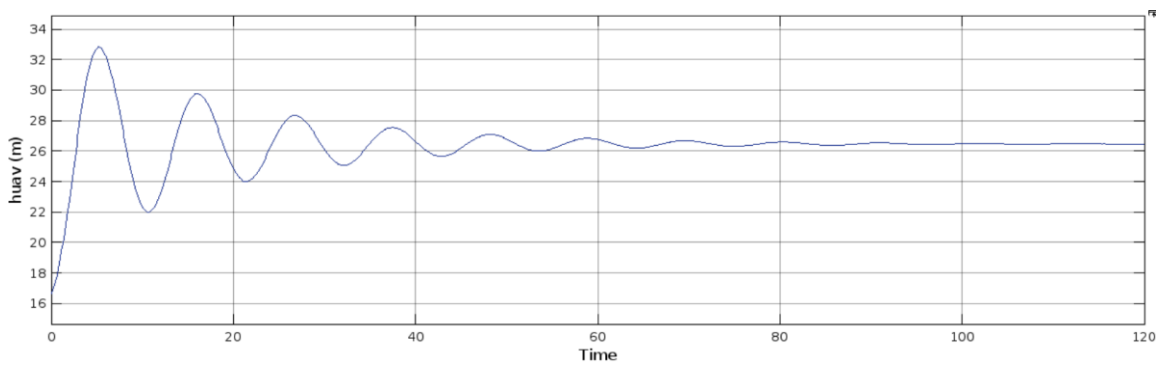




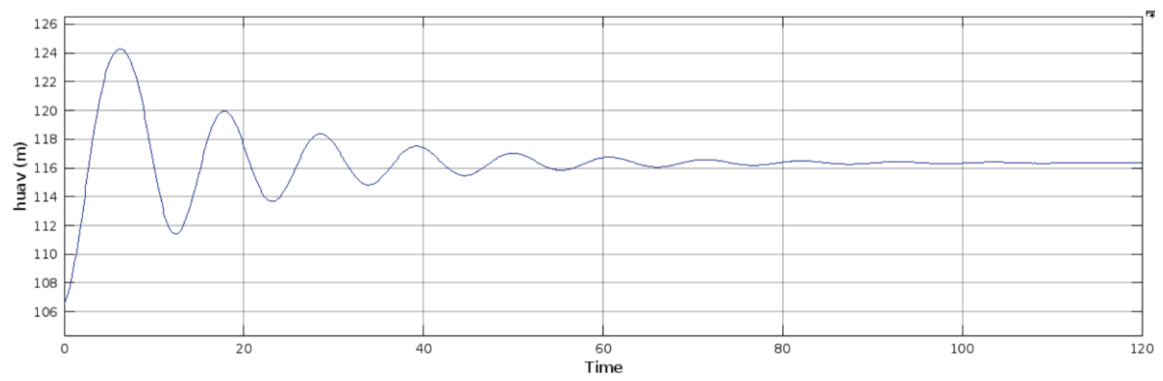
a)



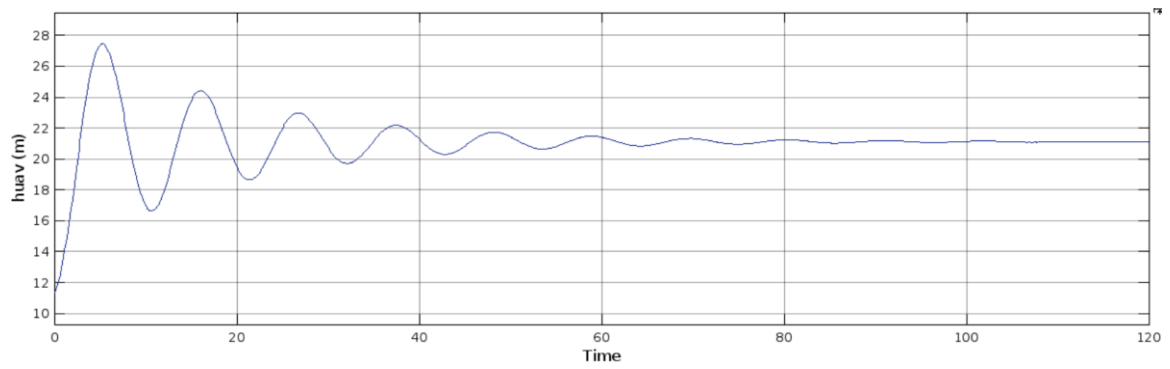
b)



c)

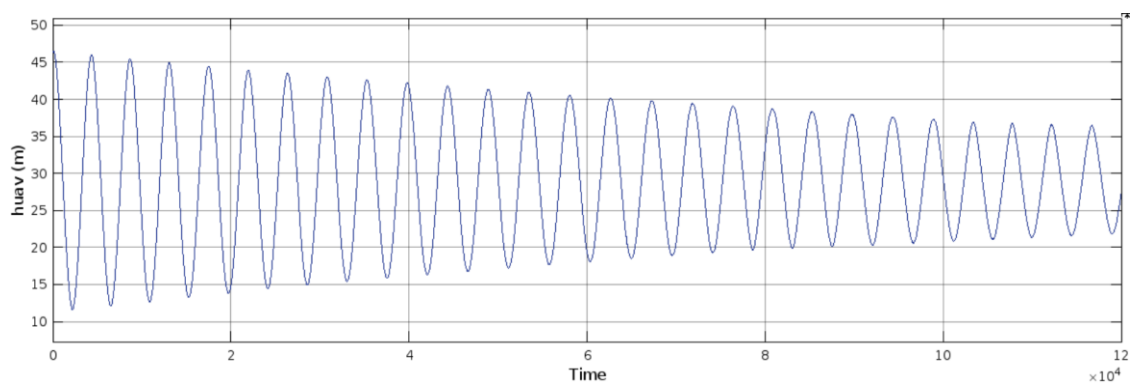


d)

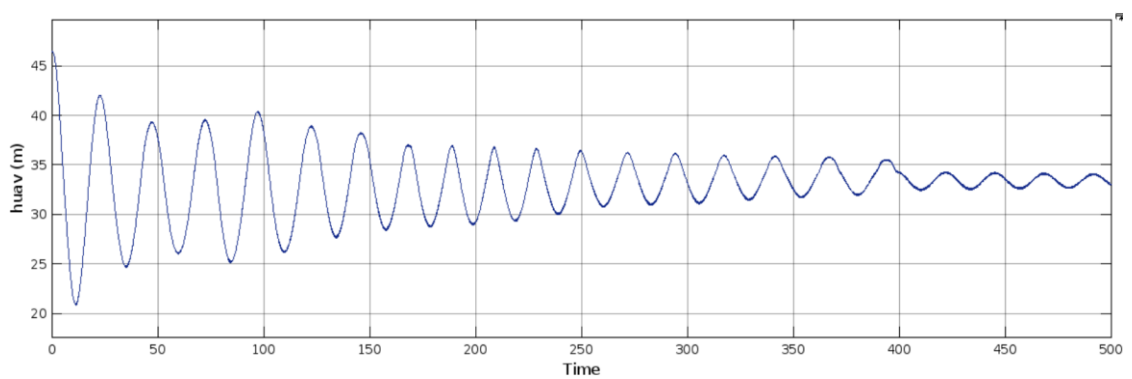


e)

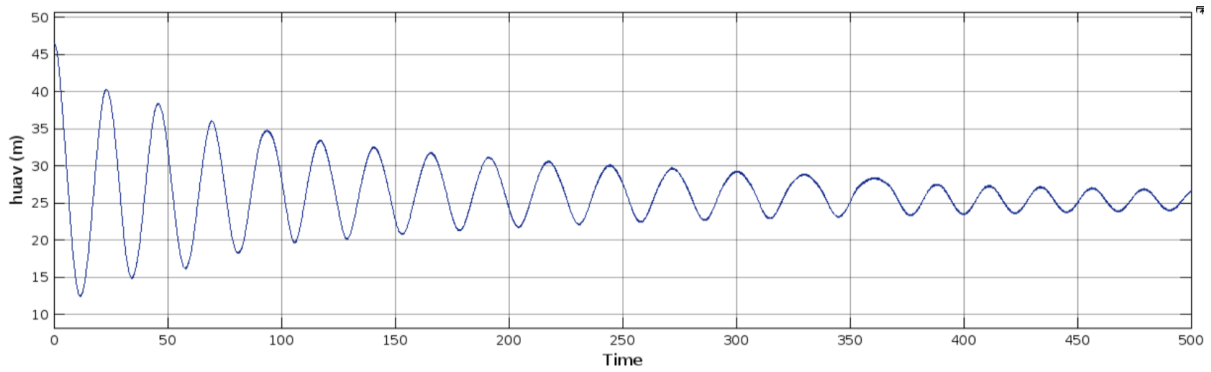
Figure C2 (a-e): The optimized height values using Extremum seeking based on different clusters values as input from the static model after tuning a)  $h = 29.53$  b)  $h = 33.52$  c)  $h = 26.82$  d)  $h = 116.36$  e)  $h = 21.68$



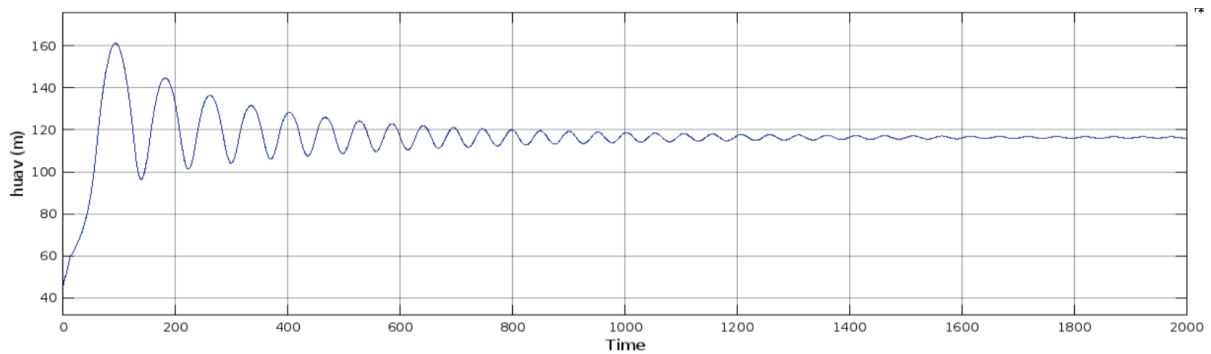
a)



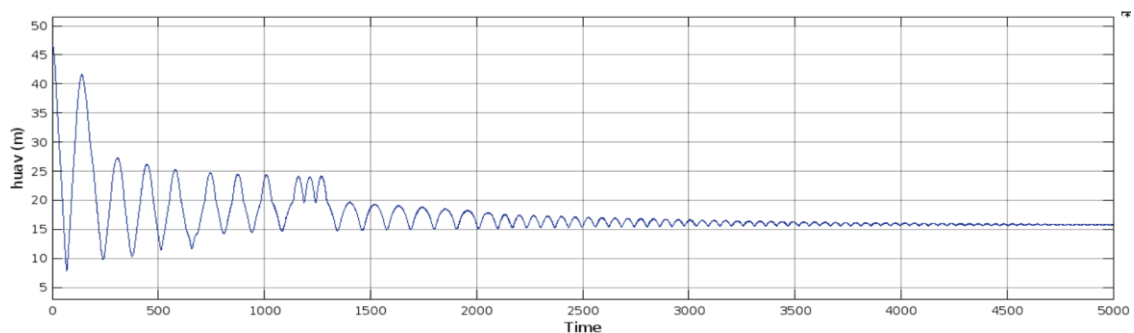
b)



c)



d)



e)

Figure C3 (a-e): The optimized height values using Extremum seeking based on different clusters values using initial condition and  $P(\text{static})$  as input a)  $h = 29.13$  b)  $h = 33.42$  c)  $h = 26.11$  d)  $h = 118.21$  e)  $h = 21.68$

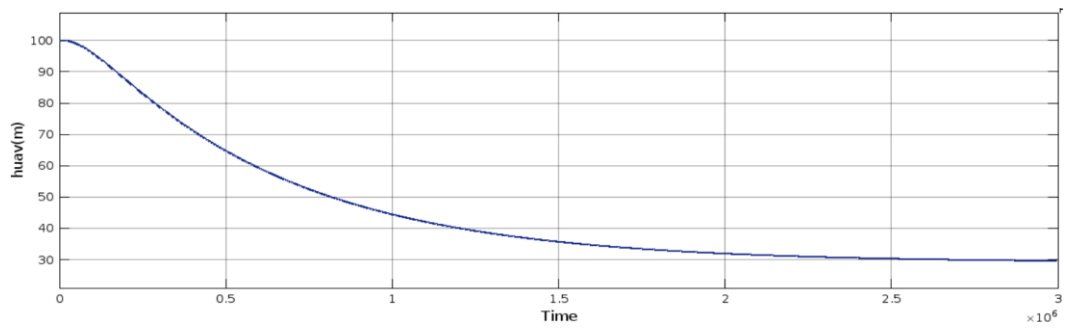
The different optimized height values are presented in Figure C3. These values were determined by applying the extremum seeking technique to the physical model with varying initial conditions ( $h_0$ ). When the UAV reaches an optimum height value by applying the optimization, a zero-power system is forced to be maintained because the energy is optimized (output of differentiator block approaches zero).

Table C.1 contains a listing of the height values that were calculated and optimised with the help of extremum seeking optimal trajectory.

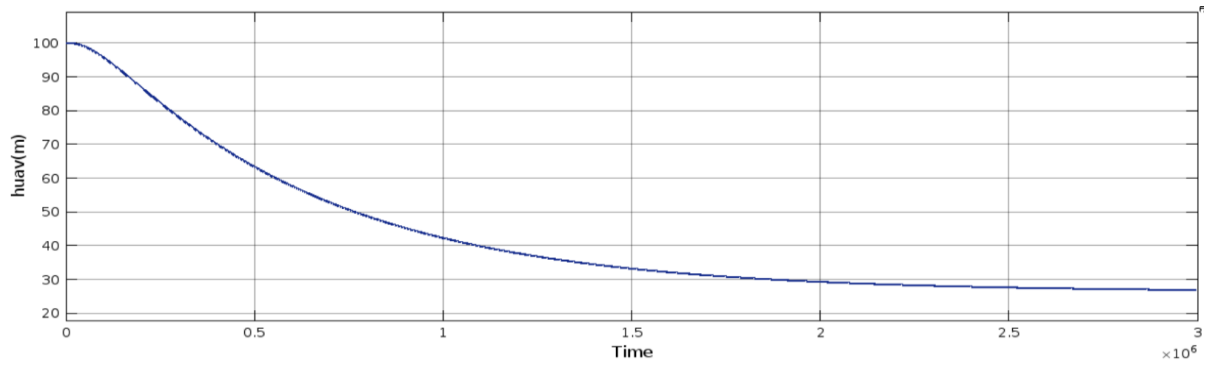
Table C.1: Optimized heights of the UAV using Extremum seeking

<b>ESOT h (m)</b>	29.13	33.42	26.11	118.21	21.68	56.2
-----------------------	-------	-------	-------	--------	-------	------

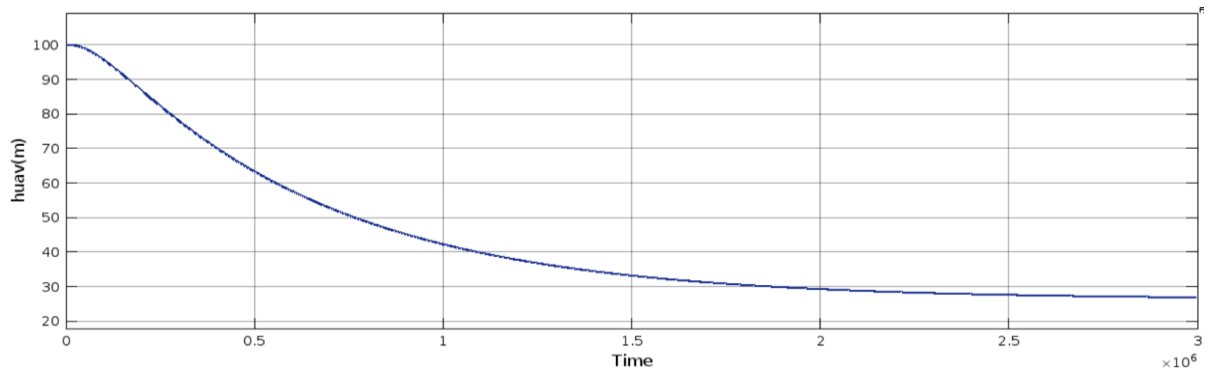
## C.2. Sliding Mode Optimal Trajectories



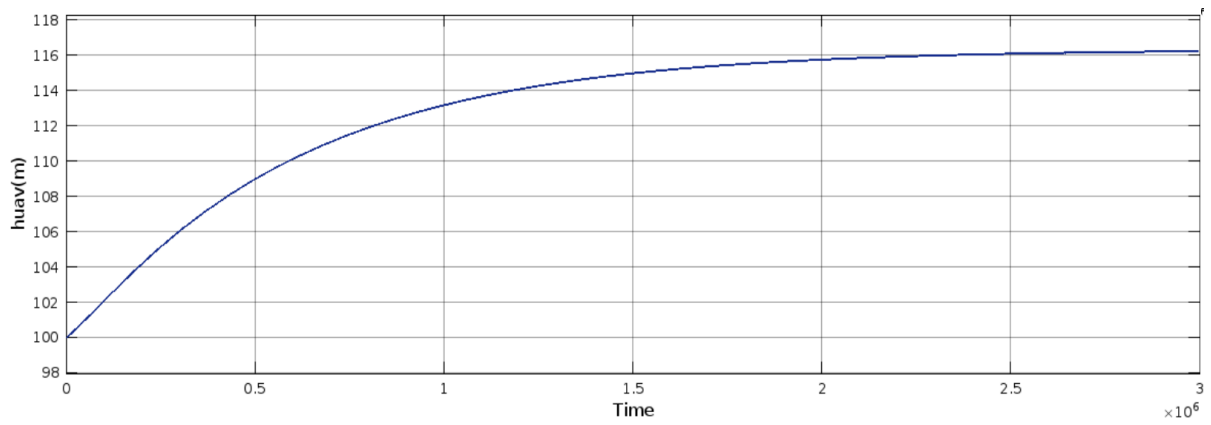
a)



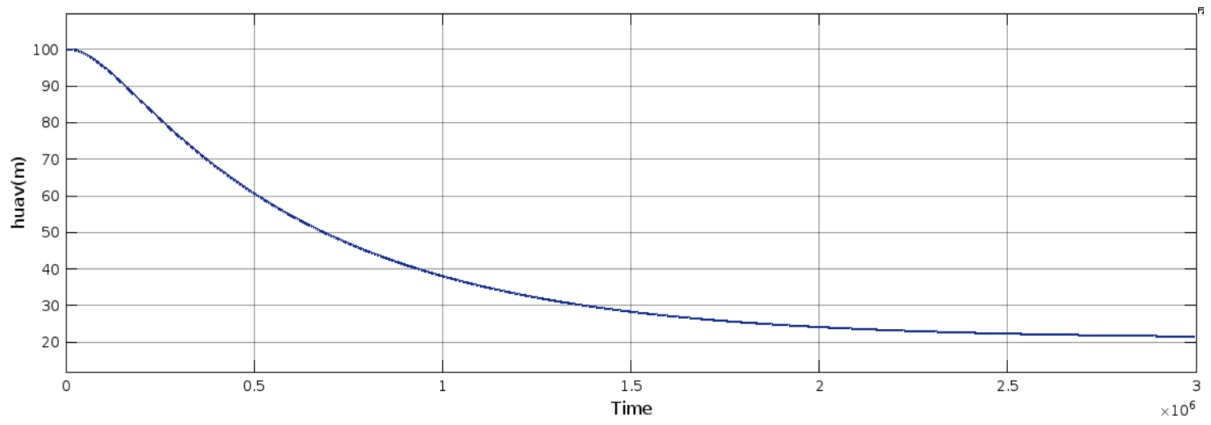
b)



c)

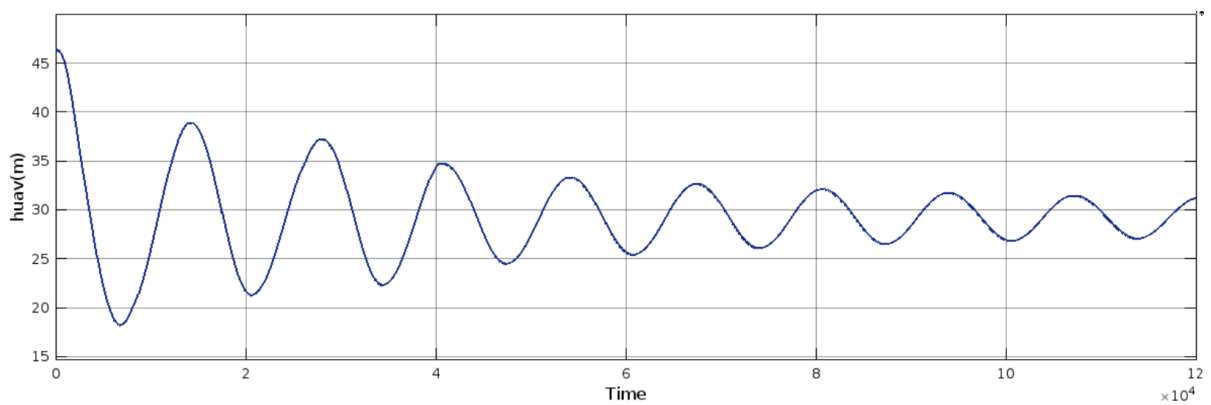


d)

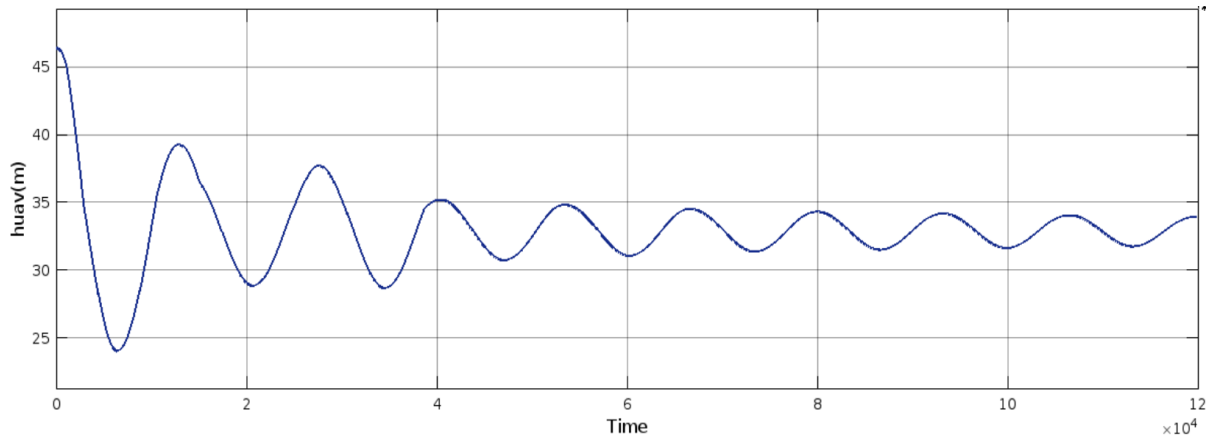


e)

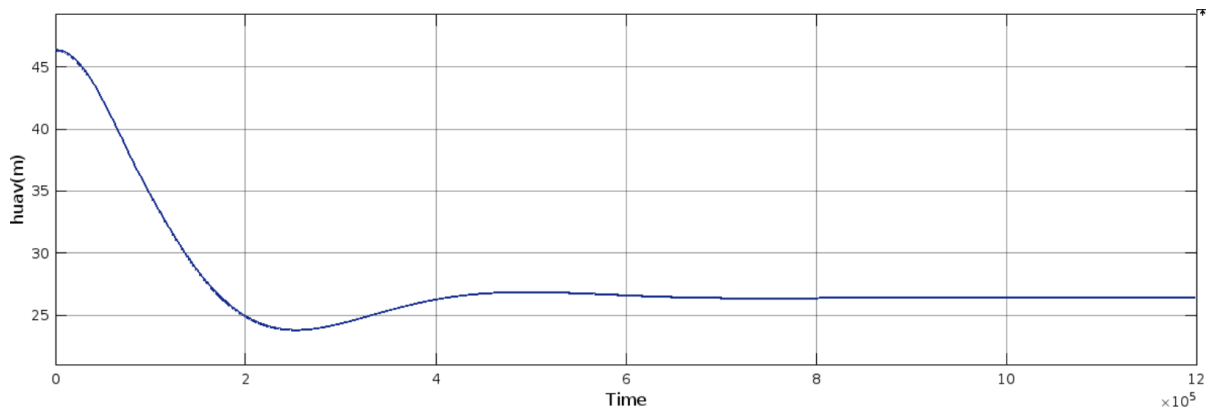
Figure C4 (a-e): The optimized height values using Sliding mode based on different clusters values as input from the static model a)  $h = 29.86$  b)  $h = 33.47$  c)  $h = 27.08$  d)  $h = 116.25$  e)  $h = 21.80$



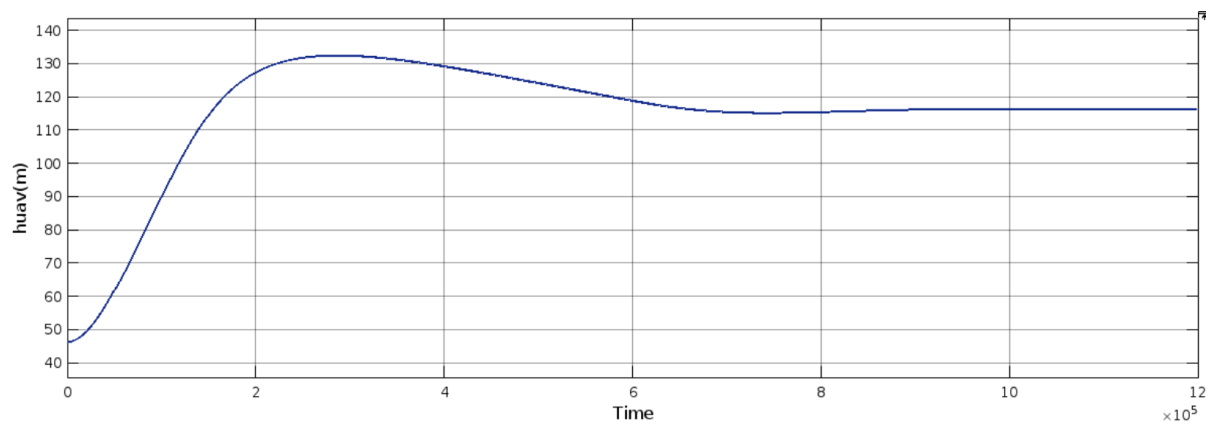
a)



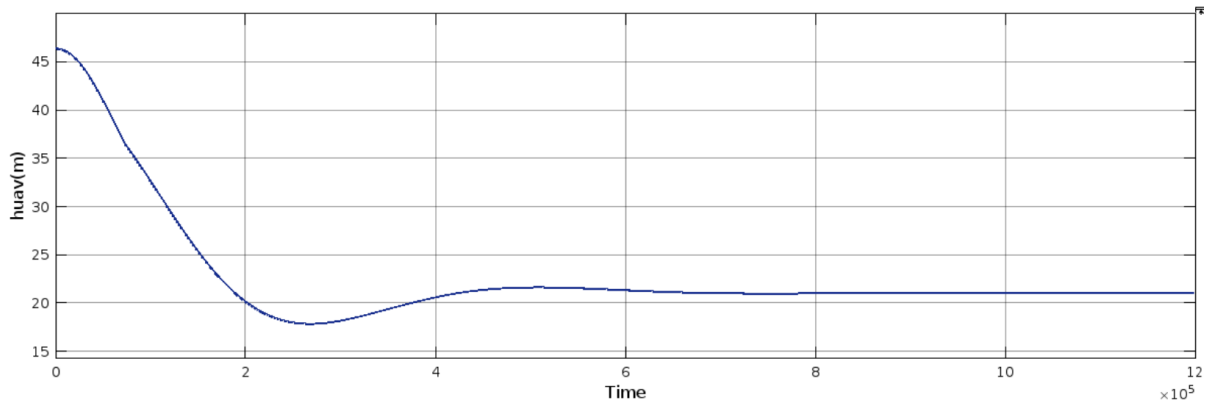
b)



c)



d)



e)

Figure C5 (a-e): The optimized height values using Sliding mode based on initial conditions (h0) and P(static) as input a) h = 28.93 b) h = 32.68 c) h = 26.12 d) h = 118.31 e) h = 21.32

The optimal height values calculated using extremum seeking algorithm, the newly optimised height values, which were determined through sliding mode optimization, will be utilised in conjunction with the reasoning that is given in Section 5.2 on methods of static optimization confirms this. Table C.2 contains a listing of the height values that were calculated and optimised with the help of the sliding mode optimal trajectory model.

Table C.2: Optimized heights of the UAV using Sliding mode

<b>SMOT h (m)</b>	29.93	32.68	26.12	118.31	21.32	56.12
-----------------------	-------	-------	-------	--------	-------	-------

### C.3. WDS Model for Dynamic Optimization

To apply the dynamic optimization methodologies of the future works (4-6) in Chapter 7 to the regulation as well as monitoring of water quality, a dynamic WDS model may be developed as follows:

$$\text{For B.O.D.: } db_i/dt = -D_{1i} b_i + (Q_{i-1}/V_i) b_{i-1} - (Q_i + Q_E)/V_i + e_i Q_E/V_i$$

$$\text{For D.O.: } do_i/dt = -D_{2i} o_i + (Q_{i-1}/V_i) o_{i-1} - (Q_i + Q_E)/V_i o_i - D_{1i} b_i$$

where, for a stirred tank reactor model for each reach i,

B.O.D. = Biochemical oxygen demand

D.O. = Dissolved oxygen

$D_{1i}$  = B.O.D. decay rate

$D_{2i}$  = D. O. reaeration rate

$Q_i/V_i$  = rate of stream flow per unit volume for reach  $i$  at a particular point

$Q_E/V_i$  = rate of effluent flow per unit volume in reach  $i$  at a particular point

$e_i$  = effluent input concentration for BOD

If this model replaces the UAV dynamics model of earlier chapters, a cost function can also be constructed for optimization of the water quality parameters (BOD and DO). The extremum seeking and sliding mode algorithms above could then readily be employed. For the LQR algorithm, the following cost function may be constructed:

$$J = \frac{1}{2} \int_0^{\infty} x' Q x + u' R u dt$$

where

$$x = \begin{bmatrix} \Delta b_i \\ \Delta o_{i-1} \\ \Delta o_i \\ \Delta b_{i-1} \end{bmatrix}$$

and,

$$u = \begin{bmatrix} \Delta(Q_i + Q_E)/V_i \\ e_i \Delta Q_E/V_i \end{bmatrix}$$

For the linearized state model, the  $x_2 u_1$  cross term can either be neglected or included using a separate weighting matrix,  $N$ .

The changes  $\Delta$  represent deviations in the values of states BOD, DO from predetermined benchmark criteria and flow rates  $u$ , from steady state values.

$Q$  and  $R$  are symmetric weighting matrices which emphasize the relative importance of either the states  $x$ , or the inputs  $u$ , in the optimization. e.g.,  $Q$ ,  $R$ , are fourth and second order identity matrices respectively, for equal weightings.

As a result, the LQR control law can be calculated from the well-known Riccati equation as  $u = -Kx$ , where  $K$  is the optimal gain that minimizes cost  $J$ .

It is possible to decentralize the model in several ways. The two reaches may be separated and interconnected, thereby making the multivariable problem single-input-single-output. Each of

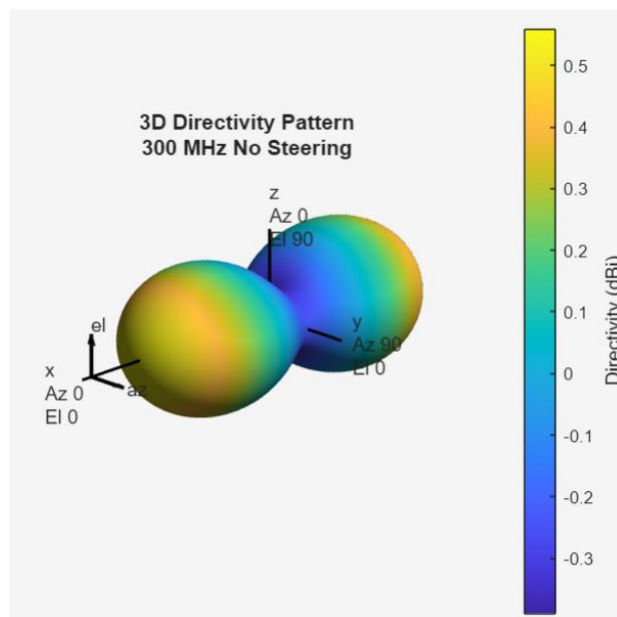


these sub systems can then be optimized with respect to BOD and DO successively, using any of the three algorithms, 4-6. There would be an added advantage if the extremum seeking and optimal sliding mode were used because the neglected cross term above could be reincorporated as both of these algorithms do not require a linear model.

Alternatively, the multi-input-multi-output optimization,  $u = -Kx$ , could be simplified as two single-input-single-output problems. These could then be augmented with an error state in order to drive the error to zero using integral action.

If separate UAVs are used for each decentralized zone to monitor water quality parameters in neighbouring reaches, then multiple UAVs would need to be coordinated within the WPCN.

#### C.4. Beam analysis at different frequencies

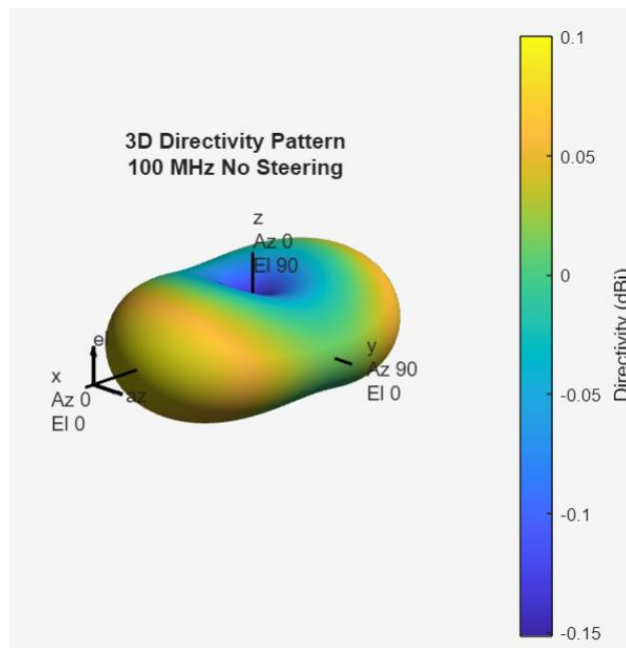


a)

Array Characteristics	
	<b>@ 300 MHz</b>
Array Directivity	0.57 dBi at 0 Az; 0 EI
Array Span	x=0 m y=250 mm z=350 mm
Number of Elements	48
HPBW	360.00° Az / 360.00° EI
FNBW	-° Az / -° EI
SLL	- dB Az / - dB EI
Element Polarization	None

b)

Figure C6 (a,b): Beam analysis at 300MHz



a)

Array Characteristics	
	@ 100 MHz
Array Directivity	0.11 dBi at 0 Az; 0 EI
Array Span	x=0 m y=250 mm z=350 mm
Number of Elements	48
HPBW	360.00° Az / 360.00° EI
FNBW	-° Az / -° EI
SLL	- dB Az / - dB EI
Element Polarization	None

b)

Figure C7 (a,b): Beam analysis at 100 MHz